From river valley to estuary

Nederlandse Geografische Studies / Netherlands Geographical Studies

From river valley to estuary
The early-mid Holocene transgression of the Rhine-Meuse valley, The Netherlands

Marc Hijma

This publication has been submitted as a Ph.D.-thesis in partial fulfilment of the requirements for the degree of Doctor at Utrecht University, The Netherlands. The public defence of this thesis took place on December 23, 2009.

Graphic design, cartography and figures: M.P. Hijma
Cover: Paraná delta, Argentina. It shows how the early-mid Holocene landscape in the Rotterdam area could have been. Photo by M.P. Hijma.

Contents

Figures

Tables

Voorwoord van dank

Wat is er lekkerder dan vier jaar lang je tanden te zetten in de ondergrond van West-Nederland? Soms had ik een stevig stuk te pakken, soms ook verkruimelde het al snel. Zo gaat onderzoek doen ook. Soms maak je een flinke stap voorwaarts, soms verkruimeld een ingeving al voordat het een idee geworden is. Het onderzoek smaakte goed en vele mensen hebben het diner voorbereid, opgegeten of meegeholpen met de afwas. Ik ben hen daarom veel dank verschuldigd.

Allereerst mijn promotor en co-promotoren: Piet Hoekstra, Ad van der Spek en Kim Cohen. Piet, ondanks dat jouw onderzoeksveld meer gericht is op actuele dan op vroegere kustontwikkeling heb je, wellicht juist daardoor, inhoudelijk mij meerdere malen op het juiste spoor gezet. Bedankt voor de goede samenwerking en alle ruimte die ik vier jaar lang gekregen heb. Ad en Kim, jullie hebben mij meer dan wie ook begeleid en ik heb veel van jullie geleerd. Ad, wellicht zal ik altijd meer een rivierenman dan een kustenman blijven, maar ik weet bij wie ik moet zijn voor advies als ik vastloop. Bedankt voor het regelen van dateringen, je commentaar op mijn stukken en je ongezouten mening. Kim, ik kan je met recht mijn dagelijks begeleider noemen. Elke dag kwam je wel even langs om te kijken hoe het ging. Ik bewonder je grote kennis van fluviatiele systemen en landschapsontwikkeling, maar bovenal je creativiteit (op vele gebieden). Je becommentarieerde scherp en met grote snelheid, wat bij mij de vaart erin hield. Ik heb al je hulp zeer gewaardeerd, ook bij het verkrijgen van mijn huidige baan in Leiden.

Naast mijn promotor en co-promotoren had ik nog drie mensen in mijn begeleidingscommissie zitten: Esther Stouthamer, Sytze van Heteren en Henk Berendsen. Henk Berendsen overleed helaas veel te vroeg. Verderop in dit dankwoord kom ik hier nog op terug. Esther en Sytze, bij elk overleg waren jullie aanwezig en jullie hebben dan ook veel bijgedragen aan de lijn van het project. Esther, je hebt daarnaast een belangrijke rol gespeeld bij het opzetten van het project. Vriendelijk dank! Daarnaast vond ik het erg gezellig om twee jaar met je een camping vol studenten te begeleiden. Sytze, samen met Ad vorm je een mooie tandem en je hebt me thuisgemaakt in de wondere wereld van de seismiek. Voor je commentaar gold: je moet even wachten, maar dan heb je ook wat!

Tijdens dit proefschrift heb ik heel veel data gebruikt die deels zelf in het veld verzameld zijn en deels uit reeds bestaande archieven verkregen zijn. In het veld heb ik gelukkig veel hulp gekregen, niet in de laatste plaats van alle boeren en landeigenaren die vrijwel altijd toestemming gaven om hun land te betreden. Thijs, John, Ingwer, Kim, Gilles, Wim, Joachim, Sanneke, Nelleke, Willem, Rens en Menno: veel dank!, zonder jullie had ik die

880.6 m nooit gehaald. Chris Roosendaal bedankt voor alle ondersteuning. But the most persistant field partner was without a doubt Gösta Hoffmann. Gösta, I really enjoyed our partnership. Thanks for all the conversations and your relativation skills. You played an excellent role as the "German idiot" when I knocked a farmer's door. Good luck in Oman with Anne and Mathea.

De grootste hoeveelheid gegevens was echter afkomstig uit bestaande databases. Verschillende gemeenten en organisaties hebben deze belangeloos gedeeld en, wellicht onbewust, een groot aandeel gehad in dit proefschrift. Hartelijk dank dus: Rien de Rijke (gemeente Zoetermeer), Wim Nohl (Fugro Ingenieursbureau B.V.), alle mensen van de Projectorganisatie HSL-Zuid, Boskalis en Puma voor de Maasvlakte-2 gegevens, maar vooral het Ingenieursbureau en het Bureau Oudheidkundig Onderzoek Rotterdam (BOOR) van de gemeente Rotterdam. Robert Berkelaar, Freyre Hechavarria (beiden Ingenieursbureau), Ton Guiran, Jurrien Moree en Ruben Lelivelt (BOOR): de bezoeken aan de bouwputten van de RandstadRail waren zeer leerzaam en van grote waarde. Veel dank voor het toelaten van een stel aardwetenschappers en de hulp bij de interpretatie. Ik hoop in de toekomst nog vaker bij jullie aan te kunnen kloppen! Ook dank voor alle andere gegevens die ik mocht gebruiken. Ruben, veel succes als zzp-er.

Quirijn en Ingwer, mijn waarde paranimfen. Quirijn, het blijft bijzonder hoe lang studie, werk en vriendschap al door elkaar heen lopen. Ik hoop dat dit nog heel lang zo doorgaat! Ingwer, mijn trouwe kamergenoot, enig in zijn soort. Bedankt voor alle gesprekken, het meedenken, het lachen en het drinken van de ultieme mix van cappuccino/espresso. Het was goed om te zien hoe je het laatste jaar je proefschrift helemaal voor je begon te zien en het nu zo goed afrond. Klasse!

De Zonneveldvleugel was vier jaar lang een warm nest onder de hoede van Juul. In de benedengang zorgden Sanneke en Nelleke ervoor dat er altijd iets te lachen was (in ieder geval voor hun!), maar ook voor de nodige frisse lucht tijdens de vele wandelingen in de Botanische Tuin samen met Joachim. Wim hield als nestor een oogje op ons allen en was altijd in voor goede raad. Gilles is Gilles en Ingwer heb ik al vaak genoeg genoemd. Dank aan alle andere collega's voor het gezellig maken van alle lunches en koffiepauzes.

Tijdens de afgelopen vier jaar was ik ook vaak te vinden in het gebouw van Deltares / TNO *Geological Survey of the Netherlands*. Heel veel mensen hebben mij daar geholpen met uiteenlopende zaken als data ontsluiten, access-queries verzinnen, boringen interpreteren, lakprofielen maken, pollen of diatomeen analyseren, maar ook met het betalen van dateringen en mechanische boringen. Dus, dank aan: Deltares/TNO, Wim Booltink, Frans Bunnik, Freek Busschers, Holger Cremer, Thaienne van Dijk, Serge van Gessel, Jenny Hettelaar, Denise Maljers, Hennie Mensink, Ruud Mutsaers, Jan Peeters, Hennie van der Putten, Jan Stafleu en Peter Vos.

Vele nieuwe dateringen van schelpen, zand en organisch materiaal waren nodig om de ontwikkeling van de Rijn-Maasmond te begrijpen. Uit de grote hoeveelheid veenmonsters pikten Hanneke Bos en Nelleke van Asch de beste macrofossielen die bij Klaas van der Borg van het R.J. van de Graaf laboratorium gedateerd werden. Van zand werd de ouderdom bepaald bij Jakob Wallinga en Alice Versendaal van het Netherlands Centre for Luminescence dating. Allen vriendelijk bedankt!

Als wetenschapper sta je vaak op de schouders van reuzen. Tijdens mijn promotie-onderzoek zijn helaas vier van 'mijn' reuzen overleden: Dirk Beets, Henk Berendsen, Orson van de Plassche en Leen Pons. Hun werk heeft veel voor mij betekend. Henk ben ik daarnaast veel dank verschuldigd voor het opzetten van het promotie-onderzoek en zijn hulp en advies tijdens de eerste 1.5 jaar.

Het zijn er inmiddels teveel om op te noemen: alle spelers van Rivierwijkers Zaterdag 3, bedankt voor de heerlijke potten voetbal. Over een veld draven en tegen een bal trappen blijft toch de beste manier van ontspanning!

Edward, John, Michiel, Quirijn, Thijs, Robbert, Stefan. Bedankt voor alle zin en onzin. Want zonder vrienden kan ik niet. Dank ook aan Trans(porting) Cactus, de leukste band ter wereld. Dat ene optreden heeft er flink ingehakt. Het schijnt dat Mexico aan onze voeten ligt.

Ik heb het geluk een hele fijne familie te hebben, die ook nog eens steeds groter en leuker wordt! Pa, Ma, John, Marjan, Karin, Pieter, Ruben, Timon, Julie, Michel, Jeanne en Joost: bedankt voor al jullie interesse, het grote vertrouwen, alle leuke momenten en er altijd voor me zijn. We houden contact.

Als laatste wil ik de persoon bedanken waarmee ik de meeste maaltijden gedeeld heb. Marieke, mijn lieve vrouw, wat is het toch leuk om met je samen te leven en te reizen. Hoe volgend jaar verloopt weten we nog niet, maar dat maakt niks uit. Bedankt voor alles, maar vooral voor de Blijdorp-put! Ja, voor altijd de jouwe.

<div style="text-align: right">Utrecht, november 2009</div>

Groeten,

Marc

1 General introduction

Data are as important as an open mind.
O. Catuneanu (2007), Principles of Sequence Stratigraphy. Elsevier, Oxford, UK.

An estuary is the seaward portion of a river system which receives sediments from both fluvial and marine sources and which contains facies influenced by tidal, wave and fluvial processes. It extends from the landward limit of tidal facies at its head to the seaward limit of coastal facies at is mouth (Dalrymple et al., 1992). Most of the present estuaries formed within incised fluvial valleys of the last glacial. When the ice sheets started to melt at the end of the glacial, these valleys drowned due to rapid sea-level rise. Estuaries are transgressive by nature, meaning that fluvial sediment supply is not sufficient to balance drowning and to form shoreline promontories (deltas). Still, sediment delivery by tidal processes in addition to fluvial sediment supply often results in relative thick packages of deposits within the incised-fluvial valleys. In the near future, many of these already low-lying areas are thought to face (increased) drowning as a consequence of mainly rapidly rising sea levels and increased rates of delta subsidence (e.g. due to groundwater extraction). River-mouth areas are among the most densely populated areas of the world and include valuable harbours and other infrastructure. Other, more natural river-mouth areas host important coastal-wetland ecosystems. Ambitious plans for coastal protection and mitigation of expected sea-level rise are therefore being developed.

The sedimentary archives of the river-mouth areas contain important information on estuarine evolution under different rates of sea-level rise. By studying the associated deposits, our understanding of natural river-mouth development will increase. Such understanding aids delta management in general and flood protection in particular. Moreover, it provides insight to the build-up of other Quaternary as well as ancient incised-valley fills (reservoir geology, sequence stratigraphy). The latter deposits have drawn attention in petroleum exploration as they host and cap considerable hydrocarbon reservoirs. In a more direct and practical manner, understanding the build-up of the subsurface of a river-mouth area is crucial for the foundation of infrastructure (i.e. engineering geology). Detailed understanding of the build-up of an incised-valley fill for a completely covered case, this thesis, thus serves the general understanding of transgressive fluvial-coastal sequences in modern and ancient settings around the world. This thesis

presents a study on the development of the mouth of the Rhine-Meuse system in the western Netherlands, between 12000-6000 yr ago (Fig. 1.1). Extensive data sets of the Holocene evolution of both the upstream fluvial area as well as in non-fluvial coastal region provide an excellent framework for this study. In the following paragraphs, a historical perspective of the research regarding river-mouth areas, sea-level rise and sequence stratigraphy is presented. It starts with a wide, global view, followed by a closer look at the Rhine-Meuse system. Identified gaps in the understanding of the seaward part of the alluvial system give rise to the thesis' problem definition and objectives. The introduction further includes a thesis outline. But first the Holocene geological setting and used terminology will be introduced.

1.1   Holocene geological setting and terminology

In a geological context, The Netherlands are commonly referred to as the Rhine-Meuse delta. During the Holocene the Rhine and Meuse shared a back-barrier delta in the central Netherlands, filling a back-barrier basin that trapped most riverine sediments before they could reach open sea. The individual branches reach the sea via estuaries. Back-barrier
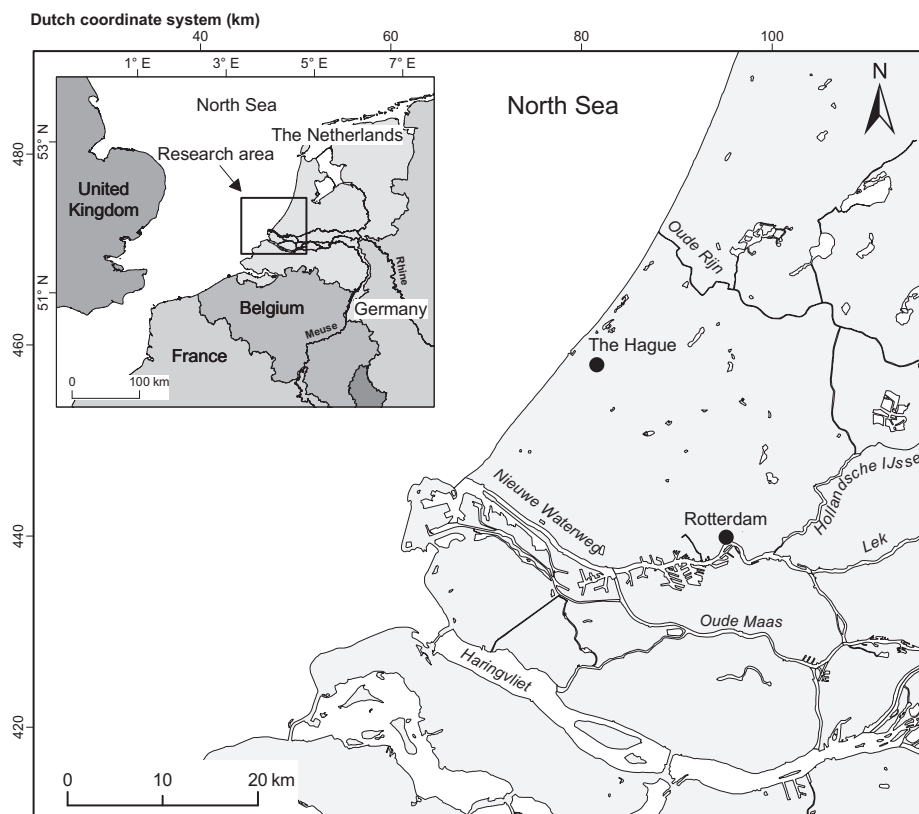
Figure 1.1 The location of the study area.

delta formation started 7000-6000 years BP (Before Present), but more importantly was preceded by a few millennia of rapid coastal and fluvial change during the early Holocene. During the early Holocene, the area experienced progressive coastal retrogradation and inland shifting of tidally influenced areas.

In a strict sense, the term 'delta' is not applicable for such a situation, since depositional progradation is characteristic for a delta. A better label for the early Holocene transgressive situation of the study area as-a-whole is 'Rhine-Meuse estuary' or 'submerged Rhine-Meuse incised-valley system'. To avoid terminological confusion associated with 'delta' and 'estuary', this thesis uses the term 'Rhine-Meuse river-mouth area' for the study area as a whole, and reserves the terms 'estuary' and 'delta' to smaller-scale features (e.g. wide tidal channels, mouth bar complexes) mapped within the area.

The Holocene period started ~11700 yr BP (Rasmussen et al., 2006) and is divided in five pollen-based subdivisions (Fig. 1.2). In this thesis, the early Holocene includes the Preboreal and Boreal, the middle Holocene the Atlantic and the late Holocene the Subboreal and Subatlantic subdivisions.

1.2 Historical perspectives

1.2.1 River-mouth areas, with emphasis on the Rhine-Meuse system

River-mouth areas have been sites of human habitation since the dawn of man. The earliest descriptions date from Greek and Roman times. These authors were already aware of fluvial sedimentation processes (e.g. Plato and Homer; op. cit. Boyd et al., 2006) and the connection between a river, its valley and sedimentation at its seaward end (Herodotus, who applied the term 'delta' to the mouth of the river Nile). Also the word estuary dates from these times. It is derived from the Latin word 'aestus', originally meaning 'heat'. Most likely, the word was used for estuaries as well, because due to the tides the water seemed to boil (Jay, 2004).

Deltaic and estuarine research remained descriptive until the 19th century when concepts such as long-term fluvial erosion and deposition, base level and fluvial equilibrium were developed (e.g. Lyell, 1830; Gilbert, 1880). In the middle of the 20th century detailed research further increased our understanding of rivers, deltas and estuaries (Fisk, 1944; Mackin, 1948; Preddy, 1954; Hughes, 1958). Van Straaten (1952; 1954a; b; 1961; 1965) and Terwindt c.s. (Oomkens and Terwindt, 1960; Terwindt et al., 1963) published the results of important estuarine studies in The Netherlands. Advancements culminated in two dedicated conferences: in 1967 (Lauff) and in 1975 (Cronin). Resulting papers defined many aspects of estuaries, both on short and geological time scales. Detailed reviews of estuarine research can be found in Reinson (1992), Dalrymple (1992), Perillo (1995), Fitzgerald and Knight (2005) and Boyd et al. (2006).

In The Netherlands, research on Holocene estuarine/deltaic developments has been carried out for a long time by groups and individuals as two relatively separated communities: coastal researchers and fluvial researchers. Research on the 'fluvial dominated' central and eastern part of the Rhine-Meuse delta was started by important mapping and research campaigns of the famous Wageningen school of C.H. Edelman (e.g. Bennema and Pons, 1952; Pons, 1957; Pons and Bennema, 1958; Sonneveld, 1958). This was followed up by research of the Geological Survey of The Netherlands (Verbraeck, 1970; Van de Meene, 1977; Verbraeck, 1984; Bosch and Kok, 1994) and Leiden University (Louwe Kooijmans, 1974; Van der Woude, 1983). From the 1980s onward research in the Rhine-Meuse delta was mainly conducted by the Utrecht school of Henk Berendsen.

A
CHRONOSTRATIGRAPHY

^{14}C ka BP			Continental	Regional	cal ka BP
	HOLOCENE	Flandrian	Late Holocene	Subatlantic	
2.5					2.6
			Middle Holocene	Subboreal	
5					5.7
				Atlantic	
7.9			Early Holocene	Boreal	8.7
9.15				Preboreal	10.25
10.15					11.65
10.95	PLEISTOCENE	Weichselian	Late Glacial	Younger Dryas	12.85
11.7				Allerød	13.90
12.1				Older Dryas	14.03
12.5				Bølling	14.64
			Pleniglacial	Late Pleniglacial LGM	21
					30
				Middle Pleniglacial	60
				Early Pleniglacial	75
			Early Glacial		117

Figure 1.2 Radiocarbon ages and inferred calibrated ages for the Holocene follow Van Geel et al. (1980/1981). Late Glacial ^{14}C ages follow Hoek (2001; 2008), while the Late Glacial calendar ages follow Rasmussen et al. (2006). Remaining Pleistocene chronostratigraphy according to Vandenberghe (1985) and Van Huissteden and Kasse (2001).

A series of Ph.D.-theses on a wide range of related subjects resulted in detailed palaeogeographic reconstructions and thorough understanding of fluvial behaviour (amongst others Berendsen, 1982; Törnqvist, 1993; Weerts, 1996; Makaske, 1998; Stouthamer, 2001; Cohen, 2003; Gouw, 2007b; Erkens, 2009). The research up to 2001 is exemplified by the publication of Berendsen and Stouthamer (2001). A short overview of the developments is provided in Chapter 2.2. The early Holocene in general and the thick stacks of estuarine deposits in the western Netherlands in particular however, remained hardly studied and poorly mapped. Researchers working in this area mainly provided detailed information on Holocene deposits (off- and onshore) younger than 6000 years such as the beach-barrier/coastal dune system and the tidal inlets and flood basins (e.g. Zonneveld, 1960; Pons et al., 1963; Van Straaten, 1965; Verbraeck and Bisschops, 1971; Van Staalduinen, 1979; Kok, 1987; De Groot and De Gans, 1996; Van der Valk, 1996b; Cleveringa, 2000; Van Heteren et al., 2002; Rieu et al., 2005; Van den Berg et al., 2007). The older Holocene sediments lack direct surface expression, are very heterogenic and occur several meters below polder surface or are located offshore. Data collection is time-consuming and expensive, and detailed mapping required a dedicated effort. This thesis aims to overcome this gap in knowledge of the subsurface of The Netherlands. It will link the development of the fluvial and coastal systems by studying them as a coherent unit.

1.2.2 Sea-level rise, with emphasis on the southern North Sea

The idea that sea level is not constant, but can vary significantly was already suggested by Leonardo da Vinci in the early 16th century as a mechanism to explain the presence of marine shells on high mountain tops (Richter, 1939). He believed that the sea once covered the mountains and afterwards dropped in level, hereby exposing the mountain tops. Later, in the 18th century, it was suggested and soon accepted that sea level had not dropped, but instead the mountains had risen to explain the high elevation of marine shells (Hutton, 1788). Still, the concept of fluctuating sea levels was not abandoned. The changes could either be caused by a deformation of oceanic basins (tectono-eustasy), an addition of sediments to the ocean (sedimento-eustasy) or the addition or removal of water during glaciations and deglaciations (glacio-eustasy). The development of the different theories was extensively described by Fairbridge (1961). The glacio-eustatic concept was developed by McLaren (1842) who calculated a possible drop of ~100-200 m during ice ages. For the last ice age, this number was later refined by e.g Woldstedt (1954) to 115-120 m. By coring and dating coral reefs, Fairbanks (1989) pin-pointed the last glacial sea-level lowstand to be 121 ± 5 m below the present level, since then reproduced at various locations around the world. This lowstand marks the Last Glacial Maximum (LGM; somewhere between 26-19 ka BP) when global ice volume reached its maximum. After the LGM, global eustatic sea level rose with strong variations in rate to the present level that was reached some seven to six thousand years ago (e.g. Fairbanks, 1989;

Chappell and Polach, 1991; Bard et al., 1996; Fleming et al., 1998; Hanebuth et al., 2000; Lambeck et al., 2002; Peltier and Fairbanks, 2006; Hanebuth et al., 2009).

On a more regional scale, such as the North Sea Basin and the study area within it, the global eustatic signal is modified by many factors such as tidal range, long-term background tectonics and shorter-term glacio/hydro-isostatic adjustment and gravimetric effects. This results in regional, relative sea-level patterns that can be the opposite from the global, eustatic pattern. Sea-level research in The Netherlands was pioneered in the early 1950's by Bennema (1954a; b) and Van Straaten (1954), but took a giant leap with the work of Jelgersma (1961; 1966; 1979) that would heavily influence subsequent research, both in The Netherlands and abroad. The next benchmark work was completed two decades later when Van de Plassche (1982) applied and further refined Jelgersma's basal-peat method, leading to an exceptionally well constrained sea-level curve for the period 7500-4000 yr ago. Sea-level reconstructions from beach-barrier deposits (Roep and Beets, 1988) supported this curve. Van de Plassche's work, including later refinements (Van de Plassche and Roep, 1989; Van de Plassche, 1995; Van de Plassche et al., 2005; Berendsen et al., 2007b), still is the blueprint for the relative sea-level curve and inland groundwater rise of the last 7500 years in the Rhine-Meuse delta, with contributions by other workers as well (Van Dijk et al., 1991; Cohen, 2005). In the last 7500 years sea level rose approximately 11 m with a gently decreasing rate of 0.6 m/100 yr (7 ka BP) to 0.2-0.1 m/100 yr (last 3 ka). Hardly any sea-level data exists for the period before 7,500 years. Relevant deposits are deeply buried or located offshore and therefore harder to study. The absence of a reliable early Holocene sea-level curve hinders understanding early Holocene fluvial and marine behaviour.

Jelgersma (1961) already noted differences in Holocene time-depth position of sea-level curves along the shore of the southern North Sea basin (see also Kiden, 1995). This is primarily explained by differential glacio/hydro-isostatic adjustments (GIA) and related to the final phase of peripheral forebulge collapse under The Netherlands and the German and Dutch sectors of the North Sea (Lambeck, 1995; Kiden et al., 2002; Vink et al., 2007). A single curve can therefore never represent the entire southern North Sea sea-level history. Time-depth differences in the southern North Sea decreased during the Holocene as the GIA-effect became less pronounced. The effect has been modelled recently (Vink et al., 2007) and the spatial and temporal GIA-effects reveal important information on the position of ice sheets in time and space. These models are calibrated using amongst other sea-level data. As indicated, these data are scarce for the early Holocene, a period when GIA-effects were strong. To further improve the existing models, accurate early Holocene sea-level data are needed. The western Netherlands is an excellent study area for gathering such data as sea-level rise affected the incised Rhine-Meuse valley relatively early.

20

This thesis presents the results of a reconstruction of early-mid Holocene sea levels that in summary are relevant in two ways: 1) to understand early-mid Holocene fluvial and coastal development and 2) to validate and improve GIA-models.

1.2.3 Sequence stratigraphy

In the last three decades, the concepts of sequence stratigraphy have been increasingly used in sedimentary geology. Sequence stratigraphy was developed as an interdisciplinary method that merged allogenic (from outside the system) with autogenic (from within the system) processes into a conceptual model to explain the evolution and stratigraphic architecture of sedimentary basins based on changes in depositional trends (Miall, 1995; Catuneanu, 2007). It is defined as "*the analysis of cyclic sedimentation patterns that are present in stratigraphic successions, as they develop in response to variations in sediment supply and space availability for sediment to accumulate*" (Posamentier and Allen, 1999). Although some of the concepts date to the early 20th century, sequence stratigraphy fully emerged in the 1970's (Vail, 1975; Vail et al., 1977). Stacked deposits are divided into units or systems tracts. A systems tract includes "*all strata accumulated across the basin during a particular stage of shoreline shifts*" (Catuneanu, 2007). This is a fundamentally different approach of analyzing sedimentary successions than the other widely used approach of lithostratigraphy. The latter deals with the lithology of the sediments and their organization into units based on their lithological character and is more static (Hedberg, 1976). Sequence stratigraphy on the other hand deals "*with the correlation of coeval stratal units, irrespective of the lateral changes of facies that commonly occur across a basin*" (Catuneanu, 2007)

In The Netherlands, sequence stratigraphic concepts have not been used widely to describe the development of the Rhine-Meuse system. Papers that do address these concepts focus on the last glacial (Törnqvist et al., 2003; Wallinga et al., 2004; Törnqvist et al., 2006). In this thesis, the presented palaeogeographic development of the Rhine-Meuse system will subsequently be described using sequence stratigraphic terminology.

1.3 Problem definition and objectives

Previous research on the Holocene geological record of the Rhine-Meuse system in the western Netherlands mainly focused on the last 6000 years, despite the presence of thick accumulations of older Holocene tidal and tidal-fluvial deposits buried at depth. Yet, the first half of the Holocene appears to be the period in which the Rhine-Meuse palaeovalley drowned during rapid sea-level rise and transformed into the broad estuary that set the scene for the build-out of the later back-barrier delta. Through studying the deposits of this essential period at an adequate level of detail, we can learn how and how fast rivers responded to sea-level rise and coastal transgression. Detailed descriptions of the

transgressive deposits allow recognising key palaeoenvironments from them (e.g. upper estuary, intertidal flat) and to reconstruct palaeogeographic developments influenced by river, wave and tidal processes (Fig. 1.3). This will increase our understanding of sedimentary successions of both recent and ancient estuarine and deltaic systems elsewhere in the world. The drowning was induced by rising sea levels, but these and the rate of sea-level rise are not well constrained for the period before 7500 years. The area appears to contain a depositional record from which sea-level data for the early Holocene may be extracted. Depositional trends within this record can further be used to test sequence stratigraphic concepts. The main research objectives of this Ph.D.-study are therefore to analyze and explain:

1. The early-mid Holocene sedimentary succession of the Rhine-Meuse river-mouth area;
2. The development of the river-mouth area in the early-mid Holocene in response to rapid sea-level rise;
3. The interaction of the fluvial and coastal systems during the early-mid Holocene transgression.
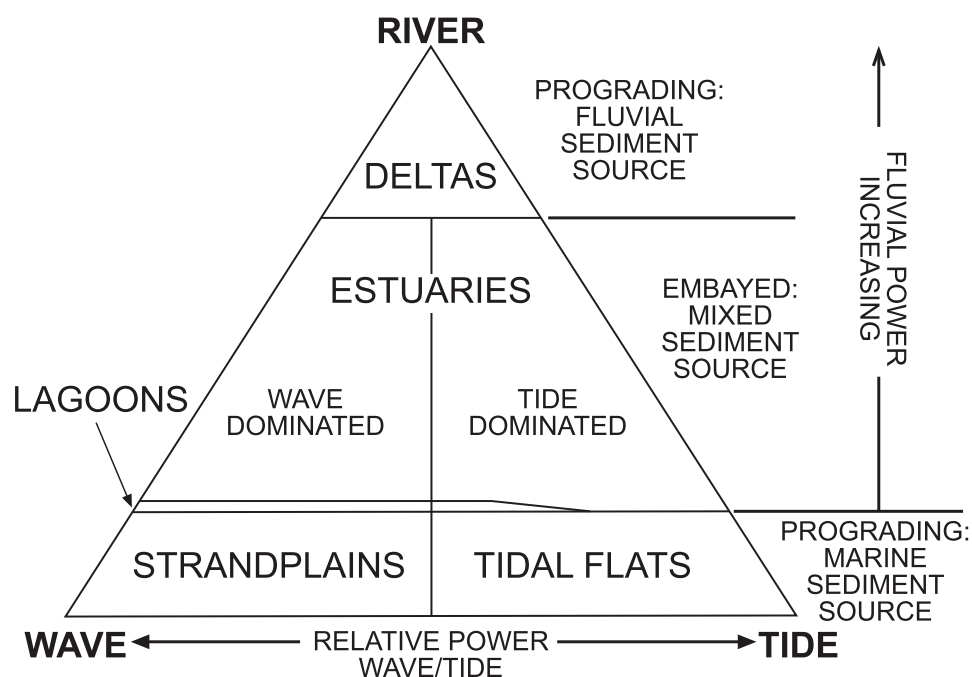
Figure 1.3 Triangular coastal classification using the three parameters of river, wave and tidal processes respectively, together with direction of sediment supply (After Boyd et al., 2006).

To satisfy these objects, the following research tasks were formulated:

- To merge the large amount of available data (core descriptions, radiocarbon dates, pollen analyses, seismic data, etc.) concerning the subsurface of the study area into one database (Chapter 2);
- To use this database to document the sedimentological architecture of the study area and to understand the spatial and temporal changes in facies (Chapters 2 and 4);
- To reconstruct Holocene sea levels for the period before 7500 years ago (Chapter 3);
- To reconstruct the early-mid Holocene evolution of the study area, to decipher fluvial-marine interactions and to describe the evolution in sequence stratigraphic terminology (Chapter 5).

1.4　Thesis outline

Chapter 2 contains a detailed documentation of the Holocene deposits in the lower Rhine-Meuse delta. It describes the evolution of the Rhine-Meuse river mouths between 12000 and 6000 years ago and the transition from a fluvial to an estuarine system. The driving mechanism behind the observed changes is rapid sea-level rise. Using newly obtained sea-level index points, the existing sea-level curve for the western Netherlands has been reliably extended to 9000 years ago (Chapter 3). Offshore, seismic data has been used to reconstruct Holocene geological history and the behaviour of tidal channels in an estuarine setting (Chapter 4). Chapter 5 presents the palaeogeography of the Rhine-Meuse river-mouth area in six maps. It also addresses the sequence stratigraphic subdivision of the succession. Finally, in chapter 6 the main conclusions of this thesis are synthesised. In addition, the applications of this study and recommendations for future research are discussed.

The four main chapters (2-5) of this thesis were written as journal papers. This inevitably means that some repetition occurs in the description of the study area, geological setting, etc. The reference lists of the journal papers have been merged into a single reference section.

2 From river valley to estuary: the evolution of the Rhine mouth in the early to middle Holocene

Abstract

The aim of this chapter is to reconstruct the evolution of the early to middle Holocene Rhine-Meuse river mouths in the western Netherlands and to understand the observed spatial and temporal changes in facies. This is achieved by constructing three delta wide cross sections using a newly accumulated database with thousands of core descriptions and cone penetration test results, together with a large set of pollen/diatom analyses and OSL/^{14}C-dates. Most of the studied deposits accumulated in the fluvial-to-marine transition zone, a highly complex area due to the interaction of terrestrial and marine processes. Understanding how the facies change within this zone is necessary to make correct palaeogeographic interpretations. We find a well preserved early to middle Holocene coastal prism resting on lowstand valley floors. Aggradation started after 9 ka cal BP as a result of rapid sea-level rise. Around 8 ka most parts of the study area were permanently flooded and under tidal influence. After 8 ka a bay-head delta was formed near Delft, meaning that little sand could reach the North Sea. Several subsequent avulsions resulted in a shift from the constantly retreating Rhine river mouth to the north. When after 6.5 ka the most northerly river course was formed (Oude Rijn), the central part of the palaeovalley was quickly transgressed and transformed into a large tidal basin. Shortly before 6 ka retrogradation of the coastline halted and tidal inlets began to close, marking the end of the early-middle Holocene transgression.

This chapter describes the transition from a fluvial valley to an estuary in unprecedented detail and enables more precise palaeo/reconstructions, evaluation of relative importance of fluvial and coastal processes in rapidly transgressed river mouths, and more accurate sediment-budget calculations. The described and well illustrated (changes in) facies are coupled to lithogenetic units. This will aid detailed palaeogeographic interpretations from sedimentary successions, not only in The Netherlands, but also in other estuarine and deltaic regions.

2.1   Introduction

In the early to middle Holocene, low-lying areas (particularly fluvial plains) were transgressed during the post-glacial period of sea-level rise (SLR). Fluvial valleys transformed into estuaries and subsequently into deltas after sea-level rise decelerated in the late Atlantic (Stanley and Warne, 1994). Globally, extensive research has been performed on the development of estuaries within fluvial valleys during the Holocene transgression (e.g. Allen, 1990; Dalrymple et al., 1994; Dalrymple and Choi, 2007; Frouin et al., 2007). In the central and eastern part of The Netherlands, the adaptation of the Rhine-Meuse system to the transgression has been documented in great detail for the entire Holocene (e.g. Pons, 1957; Verbraeck, 1984; Törnqvist, 1993; Berendsen and Stouthamer, 2000; Cohen, 2003). Middle to late Holocene coastal response has also been studied intensively (e.g. Beets et al., 1992; Van der Spek and Beets, 1992; Van der Valk, 1996b; Beets and Van der Spek, 2000; Cleveringa, 2000). However, knowledge of sediment response to SLR near the Rhine-Meuse mouths in the preceding early-middle Holocene is still limited. The facies distribution and sedimentary architecture of early-middle Holocene deposits near the mouths are therefore poorly understood. This is partly due to the depth of the associated deposits: the sediments lie more than 10 m below mean sea level (MSL) and hence data accumulation is difficult and time consuming. Understanding is also poor, because the coastal-deltaic setting of the last 6000 years is quite different than in the first part of the Holocene, making it hard to find modern analogues for early-mid Holocene depositional environments. In particular, the difference in relative SLR (from 8-10 mm/a in the early-mid Holocene to nearly zero in the late Holocene; Jelgersma, 1961; Van de Plassche, 1982; Hijma and Cohen, In press: Chap. 3) provide major differences in boundary conditions. Understanding the driving mechanisms behind facies changes during the transition from a Late Glacial fluvial valley to an estuarine system is important for applications involving the subsurface of subrecent coastal plains (e.g. palaeo-reconstructions, construction works, water management) and ancient coastal-plain deposits (mining, oil, hydrocarbon exploration, palaeo-reconstructions).

The aim of this chapter is to reconstruct the evolution of the early-mid Holocene Rhine-Meuse river mouth area in the western Netherlands (Fig. 2.1) and to understand the observed changes in facies through time, as preserved at the base of the coastal prism. This is achieved by constructing three delta-wide cross sections using a newly accumulated database with thousands of core descriptions and cone penetration test results, together with a large set of pollen/diatom analyses and OSL/^{14}C-dates. Cross sectional relationships and environmental indicators were used to identify sedimentary units marking stages of coastal-fluvial transition. Elaborate dating provides ages for these units. Combining age, depth and sedimentary relations gives insight in the timing and speed of SLR. This integrative, detailed documentation of the early to middle Holocene

deposits near the Rhine-Meuse river mouths is needed to address the driving mechanisms for changes in facies.

2.2 Geological setting and lithostratigraphy

This study comprises the area in the west-central Netherlands where the Rhine and Meuse debouched into the North Sea during the Holocene. The study area is located onshore and covers ~50x25 km (Fig. 2.1). For the larger part, the area is located within the West Netherlands Basin (WNB), an active depocentre of the North Sea Basin (e.g. Ziegler, 1994). The southwest of the study area is situated on a relatively stable shoulder block of the London-Brabant massif, the Campine High (Fig. 2.1; Kooi et al., 1998).
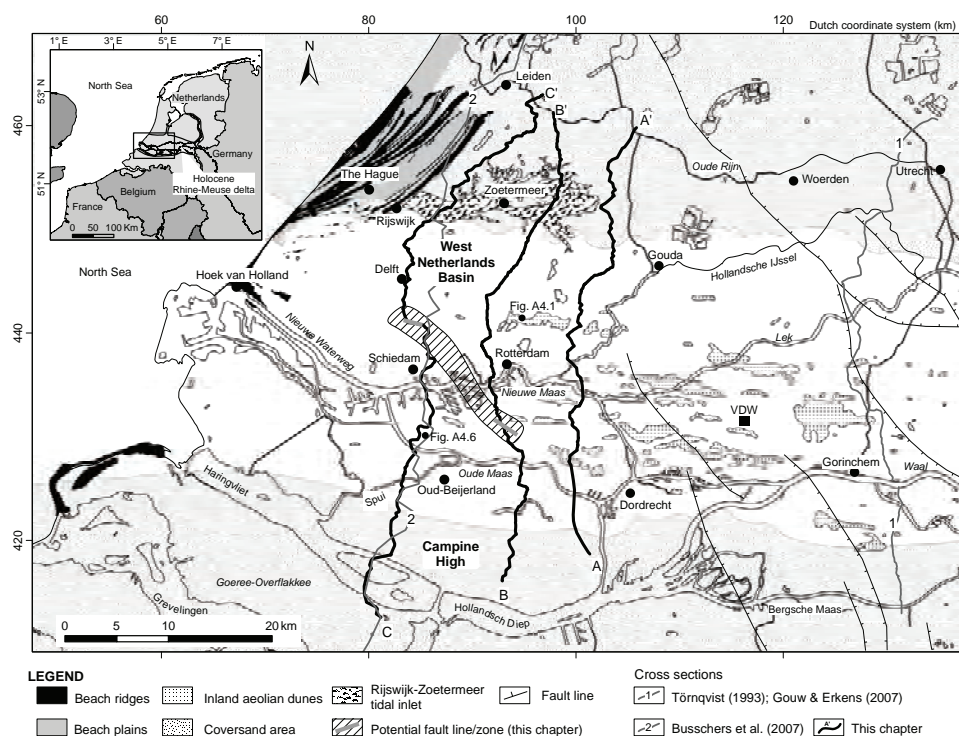
Figure 2.1 The outline of the study area and location of cross sections in the western part of the Rhine-Meuse delta, The Netherlands. Positions of inland aeolian dunes, beach ridges, beach plains and Quaternary-active faults according to the Geological Survey of The Netherlands (TNO, 2009). VDW = study area Molenaarsgraaf of Van der Woude (1983). The position of two cores that lie outside the line of the cross sections is indicated (Figures A4.1 and A4.6).

A fault zone separates this block from the WNB (Van Balen et al., 2000), but the exact position of active Quaternary faults in the study area is unknown. Differences in both observed and modelled SLR on either side of the fault zone suggest the fault zone to have displaced several metres in the last 20,000 years (Vink et al., 2007).

2.2.1   Pleistocene

The stage for Holocene sedimentation in the study area was constructed by Late Pleistocene Rhine and Meuse rivers. During the Early Glacial-Early Pleniglacial (117-60 ka; all ages in calendar years BP) only the Meuse was active in the study area, thereafter both the Rhine and the Meuse (Zagwijn, 1974; Verbraeck, 1984; Busschers et al., 2007). The Weichselian Rhine-Meuse deposits belong to the Kreftenheye Formation (KF, Fig. 2.2). The glacial to interglacial transition resulted in river style change from fully braided during the Last Glacial Maximum (LGM, 25 ka BP) to single meandering in the middle Holocene (Pons, 1957; Pons and Bennema, 1958; Berendsen et al., 1995; Schirmer, 1995). North and south of the LGM valley, aeolian sandsheets accumulated ('coversands'; Wierden Mb., Figs. 2.1-2). Between 14.5-9 ka channel belts developed that lowered the valley floor and are characterised by fining-upward successions. Climate-driven forcing is invoked to explain the incision and coeval change in fluvial style. In the central Netherlands, in areas of net tectonic subsidence, activity of these channel belts lowered the floodplain some 1-2 meters below the Late Pleniglacial surface (e.g. Pons, 1957; Törnqvist, 1998; Berendsen and Stouthamer, 2001). In the study area, elevation differences between Late Pleniglacial and Late Glacial-Early Holocene valley floors have not been resolved. The valley floors seem to converge near the present coastline (Pons, 1954; Törnqvist, 1998). During high discharges thin layers of silty clay loam overbank deposits were laid down (Wijchen Member cf. Törnqvist et al., 1994; Fig. 2.2, see also Autin, 2008). Deposition of the Wijchen Member (WM) increased in the early Holocene (EH) during the final full meandering phase when floodplain lowering had halted (Busschers et al., 2007). The Younger Dryas-earliest Holocene meandering channel belts are characterised by deeply scoured channels (Pons, 1957; Berendsen et al., 1995). An exceptionally deep residual channel fill (~19 m below floodplain) of EH age is known from Schiedam (De Groot and De Gans, 1996). On the north-eastern side of the incisive channel belts, inland aeolian dune fields (up to 15 m high) developed (Delwijnen Mb., Figs. 2.1 and 2.2), mainly fed by sand blown out of river beds during low stages of discharge (Pons and Bennema, 1958).

Apart from climatic forced transitions, glacio-isostatical forcing has been proposed to explain pre-LGM/post-LGM fluvial behaviour (Cohen, 2003; Busschers et al., 2007) and spatial differences in relative SLR (Kiden et al., 2002; Cohen, 2005; Vink et al., 2007). These papers as well as geophysical modelling studies (Lambeck et al., 1998; Peltier, 2004; Steffen, 2006) place the study area just south of a zone of maximum peripheral crustal upwarping towards and during the LGM ('forebulge crest'), and consequently in an area

of accelerated subsidence ('forebulge collapse') in Late Glacial, early and middle Holocene times.

A
CHRONOSTRATIGRAPHY

B
LITHOSTRATIGRAPHY

^{14}C ka BP

cal ka BP

		Continental	Regional	
HOLOCENE (Flandrian)		Late Holocene	Subatlantic	
		Middle Holocene	Subboreal	
			Atlantic	
		Early Holocene	Boreal	
			Preboreal	
PLEISTOCENE (Weichselian)		Late Glacial	Younger Dryas	
			Allerød	
			Older Dryas	
			Bølling	
		Pleniglacial	Late Pleniglacial (LGM)	
			Middle Pleniglacial	
			Early Pleniglacial	
		Early Glacial		

^{14}C ka BP values: 2.5, 5, 7.9, 9.15, 10.15, 10.95, 11.7, 12.1, 12.5

cal ka BP values: 2.6, 5.7, 8.7, 10.25, 11.65, 12.85, 13.90, 14.03, 14.64, 21, 30, 60, 75, 117

Lithostratigraphy (B): Nieuwkoop Formation; Echteld Formation (TM); Naaldwijk Formation (Walcheren Member, Wormer Member); Boxtel Formation (Delwijnen Member); Kreftenheye Formation (Wijchen Member)

Figure 2.2 Radiocarbon ages and inferred calibrated ages for the Holocene follow Van Geel et al. (1980/1981). Late Glacial ^{14}C ages follow Hoek (2001; 2008), while the Late Glacial calendar ages follow Rasmussen et al. (2006). Remaining Pleistocene chronostratigraphy according to Vandenberghe (1985) and Van Huissteden and Kasse (2001). Lithostratigraphy for the Rotterdam area cf. Westerhoff et al. (2003); Wijchen Member cf. Törnqvist et al. 1994; TM=Terbregge Member (this chapter).

2.2.2   Holocene

Globally, SLR had been ongoing since the end of the LGM (Fairbanks, 1989), but the location of the study area was only transgressed around the Boreal-Atlantic transition, ~9 ka. The Holocene transgression forced the Rhine-Meuse river system (Echteld Fm., Fig. 2.2) to change into a complex estuarine system with frequent river avulsions (Pons et al., 1963; De Groot and De Gans, 1996) and several large tidal inlets (Beets et al., 1992; Beets and Van der Spek, 2000). Associated tidal deposits belong to the Wormer Member (Fig. 2.2). Before ~7 ka the main Rhine-branches debouched in the Rotterdam area, but between 7-2 ka in the Leiden area. The Meuse debouched in the Rotterdam area throughout the Holocene (De Groot and De Gans, 1996; Berendsen and Stouthamer, 2000).

After the major landward shift of fluvial deposition in the late Boreal-middle Atlantic, relative SLR slowed down (Fig. 2.3; Jelgersma, 1961; Van de Plassche, 1982) and since then global sea level remained approximately constant (e.g. Peltier, 2002).
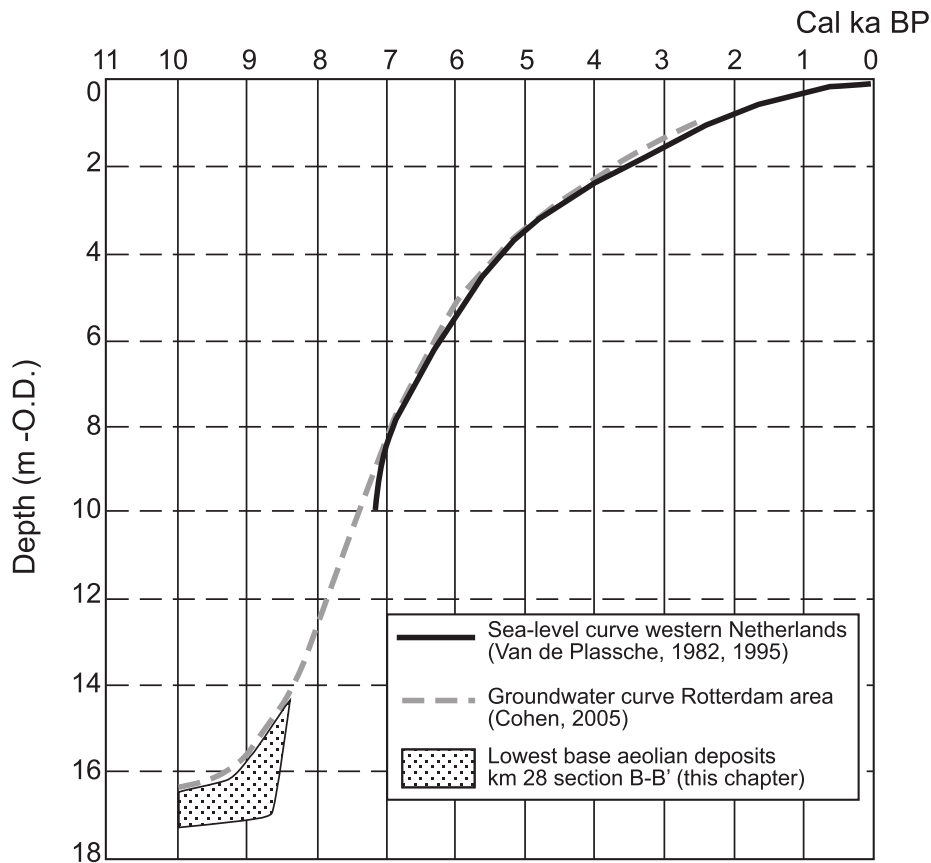
Figure 2.3 Relative sea-level curve for the western Netherlands (Van de Plassche, 1982) together with a groundwater curve for the Rotterdam area (Cohen, 2005; location Blijdorp: section B-B' km 28.5).

Hence it was predominantly ongoing subsidence that contributed to relative SLR in The Netherlands in post-Atlantic times (Jelgersma, 1961). After the middle Atlantic, the balance between the creation of accommodation space and sediment supply changed in favour of the latter and landward shifting of coastal depositional environments halted. This happened diachronously along the coast as a consequence of variations in sediment delivery. The tidal inlets closed one by one in the next millennia, leaving only the Rhine-estuary near Leiden and the Meuse-estuary near Rotterdam to interrupt the barrier ridges in the study area (Beets et al., 1992). During the Subboreal, laterally extensive peat-beds (Nieuwkoop Fm., Fig. 2.2) developed in between the river branches – locally as oligotrophic bogs. The largest peat volumes occur at the upstream limit of the study area. Since, the Subatlantic marine ingressions (Walcheren Mb., Fig. 2.2) increased coevally with human activities and reclamation such as peat mining (Pons et al., 1963; Beets et al., 1992; Vos and Van Heeringen, 1997).

From hydrodynamical modelling of palaeo-tides it is evident that after the southern North Sea was transgressed ~8 ka BP, the study area experienced very similar tides as today, with ranges in the order of 1.5-2 m. It is inferred that before that time, the Rhine-Meuse estuary in the Southern Bight and Strait of Dover experienced a different tidal regime with most likely microtidal conditions (Van der Molen and Van Dijck, 2000; Van der Molen and De Swart, 2001a, b).

2.3   Material and methods

To facilitate documentation and reconstruction of the build-up of the Holocene succession, three delta-wide cross sections were constructed. The distance between the cross sections is ~10 km and they are situated perpendicular to the valley axis (Fig. 2.1). The southern part of cross section A-A' was adopted from Gouw (2002) – all other parts are newly constructed.

2.3.1   Acquisition of corings and cone penetration tests

A total of 828 corings and 724 cone penetrations tests (CPTs; see below) have been used. Most of these reach the Pleistocene substrate. The spacing between data points varies considerably along the lines, but is on average ~110 m. Most data come from the database of TNO (2009). In addition, we used the databases of the municipalities of Rotterdam and Zoetermeer, from Utrecht University (Berendsen, 2005) and from railroad construction offices. At selected locations, we executed 74 hand corings to fill gaps in the available archived data set, to verify past observations and to sample for dating. The total dataset includes descriptions of corings, CPTs and rare outcrops in construction pits which are highly variable in quality and amount of detail. Higher quality corings with detailed descriptions were used for geological interpretations. Of lower quality data only straight

forward properties were used for correlation. Surface elevation was verified to ~10 cm accuracy using the AHN digital elevation model (Rijkswaterstaat-AGI, 2005). All borehole, CPT and other elevation data used relates to The Netherlands' Ordnance Datum (O.D. i.e. 'Normaal Amsterdams Peil'), which approximates present MSL. Due to topographic inversion (differential compaction), channel systems down to 4 m below the surface could be traced using the AHN digital elevation model and hence borehole placement strategy could be optimized (Berendsen and Volleberg, 2007; Berendsen et al., 2007a). Hand corings were carried out with various drilling devices: Edelman auger, gouge and Van der Staay suction corer (Oele et al., 1983). They were logged in the field at 10 cm intervals conform Berendsen and Stouthamer (2001). This included a description of texture, organic matter content, median grain size, colour, calcium carbonate content and other observations. In Rotterdam, two underground railway construction pits were visited in which EH sediments were inspected, logged and sampled. On occasion, we could observe and sample material from mechanically obtained cores at the facilities of the Bureau Oudheidkundig Onderzoek Rotterdam (BOOR) and TNO that were collected during various engineering projects between 2002-2007. At two locations mechanically-cored material was obtained for our mapping project specifically.

CPTs are used to identify different unconsolidated sediments and are routinely performed during the construction of roads and buildings in the western Netherlands. Resolution of the CPT-logs is in cm, as resistance to cone penetration (sleeve friction, pore pressure) is continuously measured while driving a rod into the ground at a constant rate. The technique and the usage for subsurface reconstruction has been described in detail by Coerts (1996). CPT-logged units can be converted to lithological units using geotechnical relationships, permitted that conversions are verified versus nearby lithological core data. Critical considerations are: (1) the relationship between resistance/friction and lithology is depth dependent, due to increasing weight of the overlying sediments, and (2) a sediment layer must have a certain minimum thickness to arrive at typical CPT-values for that type of sediment. A sand layer in clay has to be 15-20 cm thick, while a clay layer in sand has to be 40-50 cm thick to be distinctly visible in a CPT (Coerts, 1996).

2.3.2 Pollen and diatom analysis

At TNO, a library of internal reports provided data and interpretations of analyses performed between 1955 and 2008 (Appendix 1). Sixty-four pollen/diatoms samples from 7 sites were specifically analysed for this study (App. 1: H4-H6). Pollen preparation followed Faegri and Iversen (1975), while diatom preparation followed Cremer et al. (2001).

2.3.3 Age control

Proper age control is essential to determine the timing of developments in the study area. Relative ages are provided by lithostratigraphical, architectural and biostratigraphical relations in the cross sections, but absolute dates are necessary to assess diachronous deposition within identified units. All available early-mid Holocene radiocarbon and optically stimulated luminescence (OSL) dates within 3 km of the cross section were evaluated resulting in 88 ^{14}C and 18 OSL dates (Apps. 2 and 3). Old radiocarbon dates were often obtained from bulk samples which are prone to contamination and hard water effects and should be interpreted with care (Törnqvist et al., 1992). For this study a further 57 ^{14}C and 8 OSL dates were obtained (Apps. 2-3). For ^{14}C dating of organic samples, cm-thick slices of sediment were treated with a 5% KOH-solution and then washed and wet-sieved over a 150 μm mesh. From the residue, suitable terrestrial macrofossils were selected using a microscope and submitted for AMS-dating. OxCal 4.0 software (Bronk Ramsey, 1995; 2001) with the INTCAL04-curve (Reimer et al., 2004) was used to calibrate the radiocarbon dates. Radiocarbon ages of marine shells were corrected using the Marine04-curve (Hughen et al., 2004).

The principles of OSL-dating and its application to fluvial stratigraphy were described by Wallinga (2002). For this study eight samples were dated at The Netherlands Centre for Luminescence dating (www.lumid.nl). The dose rate was obtained from radionuclide concentrations determined by laboratory gamma ray spectrometry, assuming water saturation since the time of deposition (20% water by weight) and taking into account a contribution from cosmic rays. The equivalent dose was obtained from OSL measurements on small aliquots (2 mm diameter) of sand-sized quartz (180-212 μm), using the single aliquot regenerative dose procedure (Murray and Wintle, 2003). Following preheat plateau tests, a preheat of 240ºC combined with a cutheat of 220ºC was adopted. Net OSL signals were obtained through an early background subtraction method (Ballarini et al., 2007). With the adopted procedure a given laboratory dose could be accurately determined and recycling ratios were unity. For each sample at least 26 single aliquot equivalent dose estimates were obtained. Dose distributions indicated significant overdispersion, which is attributed to incomplete resetting of the OSL signal in some of the grains at the time of deposition and burial. Such heterogeneous bleaching is to be expected for the Holocene samples as the channels are incised in Pleistocene deposits and older sediments were likely redeposited with little light exposure. To obtain a burial dose from the dose distribution, the finite mixture model of Galbraith and Green (1990) was applied, using an overdispersion parameter of 10% (following Rodnight et al., 2006). OSL ages are obtained by dividing the burial dose by the dose rate; quoted uncertainties are the one sigma confidence interval and include all systematic and random errors. Additional

information on the OSL methods used and the results obtained is available in the OSL-lab report (www.njgonline.nl: online information with this published chapter).

2.3.4 Construction of cross sections

Each core description has been interpreted and divided into lithogenetic units (e.g. floodplain, levee, tidal flat) and key stratigraphic levels (e.g. peat layers, paleosols) were noted. By comparing neighbouring core descriptions, units were either connected or laterally bounded. CPTs were used as complementary data, since they provide indirect observations of lithology only. In the following section, we will describe the used lithogenetic units and applied criteria, followed by additional remarks about the usage of existing detailed data on the Rijswijk-Zoetermeer inlet (Fig. 2.1).
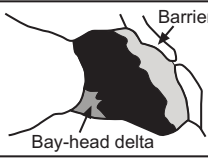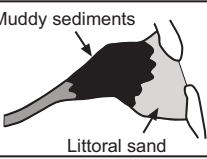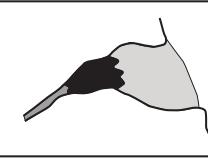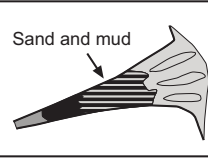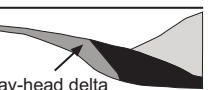
Fluvial deposits

For deposits of fluvial-deltaic origin with no tidal influence, their lithogenetic and architectural principles (summarised in Gouw & Erkens, 2007) were used as attribution rules during cross section construction. A channel belt is regarded as the body of sediment (mostly comprised of sand), deposited in a (former) river channel, irrespective of the type of fluvial system. Associated natural levee deposits (sandy/silty clay) of meandering/anastomosing systems normally grade as wings into clayey flood basin deposits. Consequently, each encountered meandering or anastomosing channel belt is assumed to have had a natural levee attached to it. Such levees may or may not have been preserved, and may or may not have been penetrated in neighbouring boreholes. The width of the channel belts and the relative size of accompanying levees varies between fluvial systems (e.g. meandering or anastomosing), but evidently also between individual distributaries (Makaske, 2001; Gouw, 2007a). Crevasse deposits share many lithological properties with natural levee deposits. The available information did often not allow distinguishing between these deposits and therefore they were merged into the same unit.

At the base of the Holocene succession, loamy overbank deposits are encountered (Wijchen Member: WM). This stiff, (blue)gray, silty clay loam (Törnqvist et al., 1994) is normally easily recognizable (Figs. A4.1-A4.4 in Appendix 4). However, from lesser quality core descriptions it is sometimes impossible to judge if the loam is present. In those cases the WM was not drawn. Early Holocene (EH) channel belts are thought to have deposited large parts of the WM (Berendsen and Stouthamer, 2000; Busschers et al., 2005) and the thickness of the WM was therefore used as an indicator for the location of EH channel belts (thickest close to the channels). In areas where EH channel belts were recognised in corings with nearby CPT-tests, the latter show distinct sediment characteristics: CPT-logs penetrating EH channel belts reveal more oscillations in grain size than Late Glacial channel belts. This knowledge was then subsequently used to further map EH channel belts with CPT-data.

Fluvial-tidal deposits

In the study area, the presence of wave-dominated estuaries is a-priori known (Fig. 2.4). An estuary is commonly defined as "*the seaward portion of a river system which receives sediments from both fluvial and marine sources and which contains facies influenced by tide, wave and fluvial processes and extends from the landward limit of tidal facies at its head to the seaward limit of coastal facies at is mouth*" (Dalrymple et al., 1992). In estuaries, a transition from predominantly fluvial to predominantly tidal deposits via fluvial-tidal deposits occurs (e.g. Terwindt et al., 1963; Van den Berg et al., 2007). In this study, fluvial-tidal deposits are defined as *deposits of a predominantly fluvial source with a tidal signature, but deposited under predominantly fresh conditions*. The fluvial-tidal zone in which they accumulate starts at the landward limit of the estuary and ends at a certain point in the estuary; obviously its limits constantly change through time. As such, the zone is less extensive on its seaward side than in the definition of Van den Berg et al. (2007) where it ends at "*the most seaward occurrence of a textural or structural fluvial signature at high river stage*", but similar to the combined fluvial-tidal and transition zone of Terwindt et al. (1963). The zone can have lengths of tens to hundreds of kilometres (Dalrymple and Choi, 2007).

	Wave-dominated			Tide-dominated
	Lagoonal	Partially-closed	Open-ended	Tidal
Morphological configuration	Closed, partially open, shore-parallel	Shore-parallel to shore-normal	Shore-normal	Shore-normal
Tidal range	Microtidal	Microtidal to mesotidal	Mesotidal to low macrotidal	High macrotidal (extreme tidal ranges)
Circulation pattern	Partially mixed	Partially mixed to well stratified (dependent on river discharge)		Homogenous (vertically and laterally)
Sediment distribution pattern	Barrier / Bay-head delta	Muddy sediments / Littoral sand		Sand and mud
Axial section	Bay-head delta	Sea level		
Example:	Great Sound, New Jersey	Miramichi, New Brunswick	Gironde	Broad Sound, Australia

Figure 2.4 Classification of several types of estuaries under different boundary conditions. Note the distinct central basin with muddy sediments in between fluvial-tidal and tidal (littoral) sandy deposits in the lagoonal and partially closed types of wave-dominated estuaries (After Reinson, 1992). A bay-head delta is formed where the river enters the central basin. The absence of high macrotidal conditions marks the Rhine-Meuse estuary as wave-dominated.

Pinpointing the landward limit of fluvial-tidal deposits in a succession is very important as they mark the most landward extent of marine influence during the turn-around from transgression to regression and also the location of river mouths in the estuarine basin. Developed diagnostic criteria for the fluvial-tidal zone are based on detailed sedimentary structures and sequences (Van den Berg et al., 2007) and are very useful when interpreting outcrops, or undisturbed mechanically obtained core material, but cannot be used when interpreting archived borehole-descriptions. These descriptions also do not allow distinguishing between predominantly fresh and predominantly brackish depositional environments. We applied various criteria to identify fluvial-tidal deposits in a systematic way (see below). The fluvial-tidal deposits are merged into the newly introduced Terbregge Member (TM) of the Echteld Formation.

Fluvial-tidal channels
Sandy channel deposits formed under predominantly freshwater conditions, but with mud drapes formed during tidally induced flow reversal (Fig. 2.5). They are indicated by the presence of freshwater shells or the mineral vivianite ($Fe_3^{2+}(PO_4)_2 \cdot 8H_2O$). Since it is very rare for vivianite to form under brackish/salt water conditions (Fagel et al., 2005), its presence strongly suggests a freshwater environment. An absence of shells is also an indicator for fluvial dominance as in tidal dominated deposits many shells are often present. Ichnology was seldomly used as an environmental discrimination tool, as in most cases it was not mentioned in borehole descriptions. Mapped channel systems with tidal signature that could be connected to fluvial channels upstream were regarded as fluvial-tidal channels. In these situations the sand bodies typically had no marked westward continuation: they grade into finer grained tidal deposits of a central area (Fig. 2.4), known as the 'poor in sand' zone (Van Veen, 1936; op. cit. Terwindt et al., 1963) that is similar to the central estuarine basin of Dalrymple et al. (1992).

Fluvial-tidal flood basins
The early to middle Atlantic fluvial flood basins were most likely permanently flooded (Van der Woude, 1983). In the fluvial-tidal zone, water levels in the flood basins were influenced by the tide. This is evident from the distinct layering in the deposits that is not observed in areas upstream. The deposits can be metres thick and are found over large areas. The silty to sandy clay contains large amounts of layered woody debris (i.e. leaves, twigs, branches; mainly from *Salix* subspecies; Figs. A4.1, A4.3, 2.5). Pollen and diatom analysis indicate predominantly freshwater conditions although with occasional input of brackish water. The excellent preservation of the organic material is also typical for a freshwater environment. The lack of soil formation and rooting suggests permanent flooding, subaqueous deposition and little vegetation. Therefore, flood basin forests within the study area cannot have produced the bulk of the encountered debris. We consider the

upstream fluvial-deltaic area as the main source area for the woody debris as large swamp forests were present there (Van der Woude, 1983).
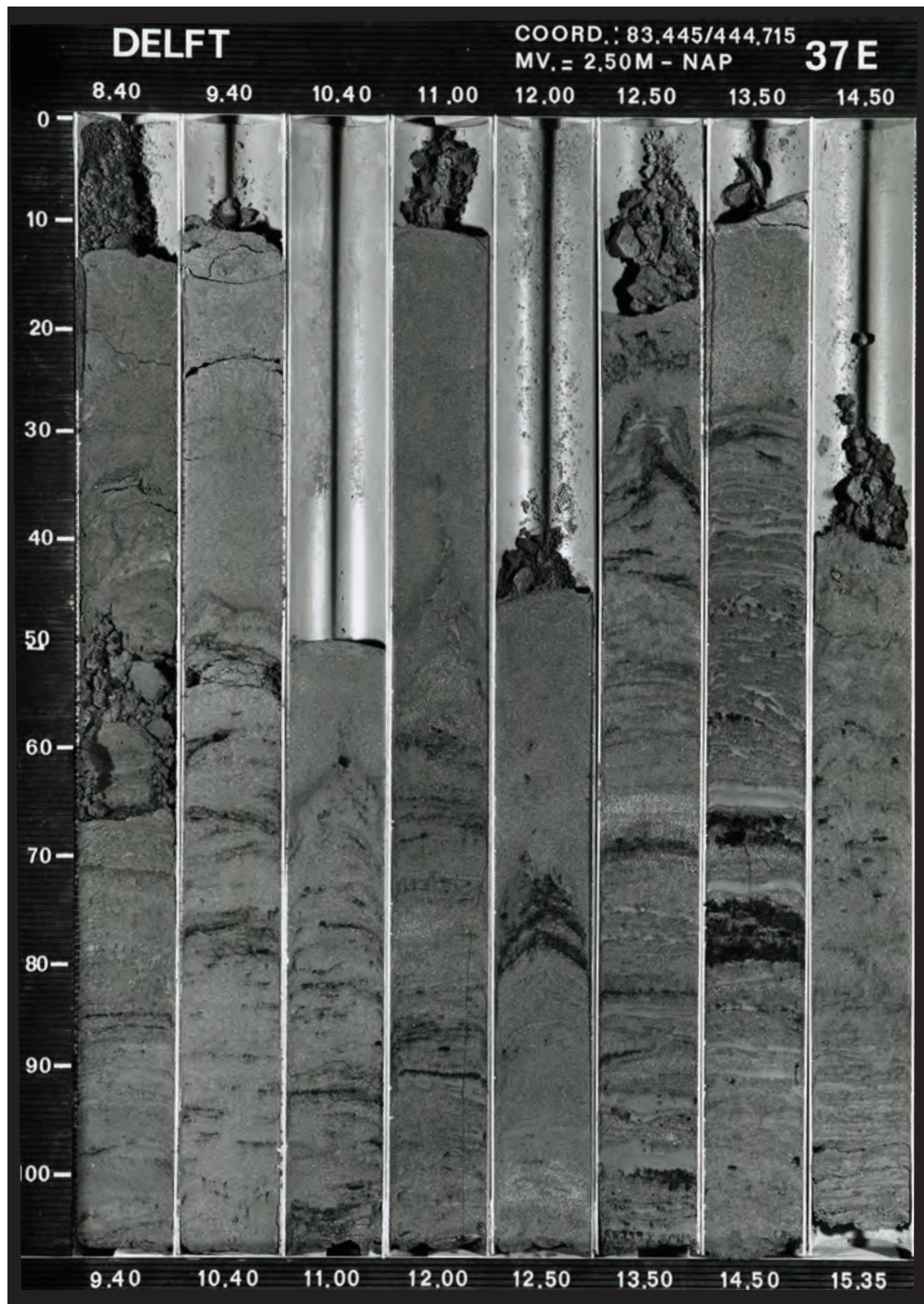
Figure 2.5 Core B37E0570 (Add. 1, section C-C', km 42). The sandy deposits most likely are part of a bay-head delta complex in the upper estuary. A fluvial source for the sand is evident from the absence of shells, the amount and composition of detritus and blue vivianite stains that are typically formed under fresh-water conditions.

River mouth: tidal deposits

We distinguished three tidal facies-units, namely tidal channels (predominantly sand, Fig. A4.6), sand dominated sub- or intertidal flats (predominantly flaser bedding) and mud dominated sub-, inter-, or supratidal areas (cf. Van der Spek and Beets, 1992; Fig. A4.7). Brackish conditions are dominant, indicated by pollen and diatom analysis and by the presence of brackish-water molluscs (e.g. *Hydrobia sp., Scrobicularia plana, Cerastoderma sp.*). Brackish-water molluscs are generally more robust than freshwater species, therefore better preserved and easy to recognize. The muddy tidal deposits consist of greyish blue, sandy clays with many molluscs, occasional yellow stains of jarosite ($KFe_3^{3+}(OH)_6(SO_4)_2$) and in more elevated parts numerous phragmites remains. Subtidally deposited silty clays are often clearly laminated and soft, while intertidal and especially supratidal deposits are stiffer due to periodic wetting and drying and may contain vegetation horizons. Intertidal deposits show strong bioturbation. The clays further contain admixed sea-salt that allows distinguishing it from similar-looking freshwater clays by its excellent, although arbitrary, taste.

The late Holocene marine deposits (Walcheren Mb.) at the top of the Holocene succession contain similar facies, but these deposits are treated as a single unit, because their details are not the topic of this chapter.

Peat

In the back-barrier area, organic deposits of various compositions formed. We chose to subdivide these deposits according to their main constituents. This reveals the vertical and lateral successions such as progressive drowning and progressive infilling. Gyttja indicates standing-water conditions that occur in lagoonal lakes. Peats indicate infilling of shallower standing water. We classified eutrophic fen-peat (*Phragmites, Carex*), fen-wood peat (*Alnus, Salix*) and oligotrophic peat (*Sphagnum, Erica*). All form under freshwater conditions, but *Phragmites* can also withstand mesohaline conditions (Chambers et al., 1999). However, salt marshes are normally dominated by *Spartina* (Silberhorn, 1999). In rare cases, swamp forests can grow under slightly brackish conditions (Stortelder et al., 1998). Fen-wood peat usually forms with mean annual groundwater levels varying between 10 cm above or below the surface (Stortelder et al., 1998). Fen-peat can form in water depths up to 2 m, but on average forms in mean annual water depths of ~0.5 m (Den Held et al., 1992).

The basal peat at the base of the Holocene transgression typically lies below fluvial-deltaic flood basin deposits (Figs. A4.2-A4.4). Dates from the top of this peat layer provide age control for the onset of fluvial-deltaic aggradation at that position in the Rhine-Meuse valley. Absence of basal peat can be explained by 1) later erosion or 2) the position of channel belts during peat formation. In the latter case, overbank deposition or river

discharge hindered peat formation. In other words: absence of basal peat is one of the indicators for the position of EH channel belts.

Rijswijk-Zoetermeer tidal inlet

In the study area, deposits marking or flanking the former Rijswijk-Zoetermeer tidal inlet (Fig. 2.1) have been studied in considerable detail, amongst others in temporary outcrops (Van der Valk, 1996b; Cleveringa, 2000; Van der Spek et al., 2007). The 2.5 km wide inlet had its maximum size between 6.8-6.4 ka, just before the transition from barrier retrogradation to barrier progradation. Detailed palaeo-ecological analyses near its landward boundary (Fig. A4.8) indicate that there was no connection to a river branch (Raven and Kuijper, 1981). The barrier behind which the Rijswijk-Zoetermeer deposits accumulated, runs northeast-southwest in the direction of Hoek van Holland (Fig. 2.1). Associated tidal inlet, washover, beach plain, shoreface and aeolian deposits have been described in detail (Van der Valk, 1996b; Cleveringa, 2000; Van der Spek et al., 2007). The scale of our cross sections did not allow distinguishing between these deposits.

Drawing of time lines

As an additional step, time lines were drawn in the cross sections as an exercise for verifying the lithostratigraphical correlations throughout the cross sections. The time lines will also aid future palaeogeographic and sediment budget reconstructions in papers to come. The method of Gouw and Erkens (2007) was used to time slice a cross section. Drawn time lines are primarily based on dated marker horizons within the flood basin deposits (e.g. peat beds, paleosols) and stratigraphical relationships dictated by the lithogenetic facies models (previous section). Parts of the cross section lack datings. In those areas, 3-D interpolations of Holocene palaeogroundwater tables were used (Cohen, 2005). For a given location in the delta, the interpolation provides maximum ages for the start of eutrophic peat formation at given depths, because the base of the peat marks past groundwater tables. Due to compaction, it is likely that observed peat at any given elevation is somewhat younger than the groundwater model predicts.

The oldest time line (9 ka) approximately marks first deltaic aggradation in the study area. Most vertical accommodation occurred in the early-mid Holocene and the developments during this phase of rapid transgression are the focus of this chapter. Therefore, we use a 500-yr interval for the time between 9000 and 7500 BP. Three additional time lines (6500, 5000 and 2500 BP) are provided for the upper part of the section. The reliability of the time lines depends on the quality of time control and stratigraphic relationships. Gouw and Erkens (2007) estimated the accuracy of time lines in their most downstream cross section (Fig. 2.1) to be ~1.0 m. Accuracy of the time lines in our cross sections varies largely as dates are unequally spread over the study area. In areas with limited time control, we estimate the time lines to be accurate within ~1.5 m.

Naming of fluvial channel belts and tidal inlet systems

To name the nested incisive channel belts recognised within the Late Glacial-EH valley, we partly adopted the convention of Cohen (2003; his App. 1). Identified channel belts are encoded after their presumed time of initiation (W=Late Weichselian, H=Early Holocene) and source (Rhine: R, Meuse: M) and inferred order of abandonment (a,b,c). Our naming of remaining architectural units comprising the Rhine-Meuse palaeovalley follows the subdivision of Busschers et al. (2007).

Berendsen & Stouthamer (2001; their App. 3) listed a series of fluvial channel belts, mainly upstream of the study area, named them and introduced numeric channel belt IDs for easy reference. Their identified channel belts connect to features in our cross sections and where these are simple downstream continuations of upstream channel belts, we adopted the naming and numbering. To name former tidal inlets and estuaries, we used topographical names of the villages above them.

2.4   Description of cross sections

2.4.1   Cross section A-A'

This most eastward cross section (Fig. 2.1, Addendum 1) is 51 km long and is based on 191 cores and 336 CPTs. The first 8.5 km in the south are based on Gouw (2002). The sections northern end is formed by the Oude Rijn channel belt. To the south it reaches into areas of marginal fluvial deposition only: the section stretches well south of the Late Pleistocene-EH palaeovalley. The key to the cross sections is shown in Addendum 1. In the text, the combination of 'H-' with a number refers to an internal report of TNO (App. 1). References to radiocarbon dates within the cross sections are indicated by italic numbers between brackets (App. 2); OSL-dates by italic letters between brackets (App. 3). The number sign (#) and accompanying number corresponds with the numbering of channel belts by Berendsen and Stouthamer (2001). Based on the cross sections, a schematic overview of channel belt positions is given in Figure A4.9. In chapter 5, the palaeogeography of the study area will be addressed in more detail. The younger strata are treated briefly, as they are not the focus of this chapter.

Late Glacial and early Holocene rivers

In section A-A', the sandy top of Late Glacial and earliest Holocene fluvial deposits is encountered at depths between 13 and 18 m -O.D. Between km 7-12, 15.5-20.5 and 22-28.3 it is capped by a silty clay loam, covered by the basal peat. Between km 8.5-22, inland aeolian dunes are occasionally present on and intercalated *within* the loam. In their direct vicinity, depressions mark channel beds that were the source areas for these dunes. The loam is 1 m thick on average, but thicknesses reach 2 m locally. The loam and basal peat

40

are absent between km 7.5-8.5, 12-15.5, km 20.5-22 and km 30-35.3. This marks the position of channel belts WM-b/HM-a, WR/HR-a and WR-b/HR-b/c, inferred to be active channels at the time basal-peat formation set on. Overbank sedimentation by these channels explains the local excess thickness of the WM in their immediate vicinity. The valley floor of HM-a, HR-a and HR-c is encountered at lower elevations than the surrounding older valley floors due to incision. Near km 8 a Late Glacial Meuse channel belt is assumed (WM-a), based on the absence of the Wijchen Member and the presence of aeolian dunes. The age of the basal peat overlying the WM (Fig. A4.2; *35-37*), shows activity of HR-a to have ended before 9.3 ka. A transported wood fragment at the top of HR-c channel deposits (16 m -O.D.) was dated ~9-8.6 ka (*42*) and two OSL-dates from this channel have an average age of 8.4 ± 0.5 ka (*a,b*). This means that the channel was still active at the time that HR-a had been abandoned. HR-c fringes the coversand area. The cross section cuts HR-c twice and at an angle, therefore in reality the channel is smaller. The oldest observed deltaic Rhine channel belts are restricted to km 29-34 area. They are the first Holocene channel belts that show to have raised their bed level in response to base-level rise and hence succeeded the HR-b/c channel belts.

Atlantic aggradation

Widespread, but diachronous, basal peat formation marks the transition to lagoonal-deltaic sedimentation in this area. Radiocarbon dates of the base of the basal peat fall within the range of 9.3-8.8 ka (*35-37, 139*), while the top has been dated at ~8.2 ka (*3, 34*). The latter dates provide a local maximum age for the onset of clastic aggradational deposits. Near channels, basal peats are covered by clayey, clastic deposits. Further away from the channels, basal peats grade into gyttja indicating peat formation could not keep up with groundwater-table rise. It suggests that large parts of the study area turned into permanently flooded flood basins, as suggested before by Van der Woude (1983) for an area ~15 km upstream (Fig. 2.1). At km 27 a sand sheet (105-150 μm; 14-12 m -O.D.) of ~1-2 m thick and ~1 km wide is interpreted as the infill of a flood basin lake. The clastic flood basin deposits often show a distinct light-dark banding (Fig. A4.2). The darker bands are relatively rich in diatoms and can be associated with spring bloom (App. 1, H-2). If true, it suggests rapid sedimentation. Segment 7-8 m in Figure A4.2 would have been deposited in only 24 years. Diatom species in this segment (*Cocconeis placentula*, *Cocconeis placentula var. lineate* and *Cymbella sinuate*; H-2) indicate shallow freshwater with little flow. To the south, near km 4 (core 02.05.002) scans of diatom content show a short period of predominantly brackish assemblages at that time (De Wolf, 2002). In contrast, in the northern half of section A-A', brackish conditions do not appear until ~6.4 ka (e.g. *38, 45, 48*). It indicates that northerly freshwater flood basins kept receiving steady input of river discharge throughout the early Atlantic.

The majority of the earliest aggrading Rhine-channels (~8.5-7.5 ka) is concentrated north of Rotterdam between km 24-34. Additional channels have been recognised at km 6.5 and between km 12-16. Considering their position, the three most southerly channel belts are attributed to the Meuse. Around 7.7 ka the main Rhine discharge shifted northwards due to an avulsion ~8 km upstream of section A-A' (Bosch and Kok, 1994). The new resulting channel belt was positioned within the coversand area (km 36-44; the three sand bodies between km 38-41 are the same winding channel belt). The area of the former main river system was left occupied by secondary channels only, and was fully abandoned around ~6.9 ka (channel belt at km 30.5). Widespread peat formation and humic clay deposition started in the flood basins between km 3-30, evident from a discontinuous organic bed at 10 m -O.D. The onset of this situation is dated ~7.5 ka (*15, 31, 41, 47, 49*) and is related to the abandonment of this area by the main Rhine-branches. The phase of organic bed formation lasted only a few centuries (*2, 18*). Above the organic bed, the fluvial-tidal flood basin deposits of the Terbregge Mb. (TM) are widespread (e.g. Fig. A4.1). They mark the landward end of the estuary after ~7.3 ka (*15, 18*). The start of deposition coincides with the establishment of one main Rhine branch (channel belt #177, km 43) that drained northwestwardly (Fig. A4.9), following a renewed avulsion just upstream (avulsion 74; Berendsen and Stouthamer, 2001). OSL dates from this channel (*d,e*) have an average of 7.6 ± 0.7 ka. The lower OSL date suggests the presence of fluvial activity before the channel became the main Rhine-branch, with seems valid because it is situated within a depression of the coversand. To the north of this channel, a tidal flood basin was present since ~7.5 ka (based on 50), indicated by the frequent occurrence of *Hydrobia* and *Cerastoderma* shells. The tidal flood basin was most likely connected to the same downstream tidal inlet as channel #177. After ~6.4 ka, following a third major avulsion some 40 km upstream section A-A' (Berendsen and Stouthamer, 2001), the main Rhine branch shifted north (#133, km 50) into the tidal flood basin that immediately freshened. The new branch possibly debouched into the North Sea through the same tidal inlet as its predecessor (#177). The tidal basin was gradually filled and after 5 ka the Rhine started to prograde through the basin and developed a 2 km wide meandering channel belt. Progradation of the river mouth is also indicated by the shape of surrounding barrier ridges (Beets et al., 1992). The avulsion left the area south of km 44 abandoned from steady fluvial sediment input after ~6.4 ka and peat formation started fairly synchronous over great distances (9-6 m -O.D., *17, 39, 144, 145*). South of km 24 mainly fen-wood peat was formed, while more to the north *Phragmites-Carex* peat dominates. Between km 28 and km 44 peat formation was quickly halted by marine ingressions. That region became the landward fringe of a tidal flood basin with shallow, brackish open water and tidal flats (H4-6). The associated, mainly clayey, transgressive deposits often erosively overlie the peat with a lag deposit of *Cerastoderma* and *Hydrobia* shells (Fig. A4.7). Wave-action within the tidal flood basin was most likely the erosive agent. The lag is widespread and

can be interpreted as a bay ravinement surface (cf. Reynaud et al., 1999). Dates from the shells and the underlying peat yield ages of 6.3-6.2 ka for this subregional ingression (*38, 43-46, 48, 141, 142*). The tidal deposits near km 43 accumulated on an intertidal flat (B31C1166, H-4; diatoms *Cymatosira belgica*, *Delphineis minutissima* and *Dryopteris/Chenopodiacaea* pollen assemblages). In core B38A1846 (km 35.5; Fig. A4.7), the base of the tidal sediments (~9 m -O.D.) was also deposited on an intertidal flat, while palaeo-ecological information from the top layers (~7 m -O.D.) indicate deeper water and a most likely permanently flooded area (H-4).

Small sandy tidal channels were encountered between km 31 and 34.5 that can be traced to a southwesterly source area in the digital elevation data (Fig. A4.8). These channels do not connect to the Rijswijk-Zoetermeer tidal system, but probably connect to a tidal inlet west of Rotterdam, i.e. the estuary of the Meuse. In between the two tidal inlet systems, a low tidal watershed must have been present (Fig. A4.8; further discussed below). In the late Atlantic, the tidal basins started to fill in and widespread peat formation started between 5.5-5 ka (Van der Valk, 1996).

Two channel belts at km 3 and 7.3 mark the position of Meuse-branches between 7.5 and 6.5 ka. The channel at km 7.3 is the downstream continuation of the Gorkum-Arkel (#52) channel belt, dated 7.4-6.4 cal ka BP ~30 km upstream (Törnqvist, 1993). The other channel presumably links up with the upstream Hill (#67) Meuse channel belt.

Younger strata (last 5.5 ka)
During the Subboreal, the position of the Rhine main outlet was very stable. The Meuse debouched into an estuary near Rotterdam, downstream of section A-A'. Outside the channel belts, virtually the whole area had turned into peat land. Peat formation continued until the Middle Ages, when humans started to lower groundwater tables to reclaim arable land and mined the peat for fuel. The latter activity is the cause for the near complete absence of peat between km 29-44.5 and surfacing of marine deposits of late Atlantic and early Subboreal age. The Rhine started a stepwise shift of its main discharge towards the Meuse-estuary after ~2 ka (Berendsen and Stouthamer, 2000).

The position of the Meuse during the Subboreal and Subatlantic is not obvious from section A-A'. At km 6 it appears that an older channel belt was eroded by the Oude Maas estuary. Also the exceptionally thick channel belt deposits of the Gedempte Devel at km 9 may indicate this channel to have reoccupied an older Meuse channel belt. Alternatively, the thick deposits can be the result of tidal influence or the cross section passes through a channel confluence or channel-bend scour where channel belts deposits are naturally anomalously thick (up to five times the average thickness; Ardies et al., 2002).

2.4.2 Cross section B-B'

This cross section (Fig. 2.1, Addendum 1) is ~57 km long and based on 236 cores and 270 CPTs. It extends well south of the Late Glacial Rhine-Meuse palaeovalley. The northern end is formed by the Oude Rijn channel belt.

Late Glacial and early Holocene rivers

South of km 5 and north of km 45, sandy aeolian deposits of Late Glacial age overlie Pleniglacial Rhine-Meuse deposits (Busschers et al., 2007). In between, the Late Glacial-EH palaeovalley surface occurs at depths of 17 to 14 m -O.D. North of km 14, it is overlain by the WM; to the south this member is absent. Between km 27-28, 29-32 and north of km 35 the WM is also absent. This marks the position of the Rhine channel belts during the Late Glacial-EH (HR-d; WR-a/HR-a; HR-b, WR-b, HR-c). At km 39.5, a dated peat bed provides a minimum age for abandonment of WR-b (~9.5 ka, *78*). Near km 18, a marked step in the elevation of the top of channel belts deposits (~16 m -O.D.) is visible, which is mimicked in overlying deposits. This step is a candidate marker of a neotectonically active fault, suspected to border the WNB (Fig. 2.1). The EH Meuse channel belt (HM-a) was most likely positioned near km 17, where the most southerly and earliest aggrading channel belts have been recognised.

At several locations aeolian river dunes were encountered. At km 1, an isolated dune is observed well within the coversand area. In the Rhine-Meuse palaeovalley, a dissected complex of relatively low dunes is present within the stretch km 17-29. Dated plant remains in cross-bedded deposits underneath an aeolian dune (*72*) give ages of 9.4-9.1 ka. A humic layer in a small residual channel that dissects the dune has an age of ~9.4-9.0 ka (*71*). This constrains the age of this particular dune to ~9.2 ka (Cohen and Hijma, 2008). Dates *57-60* constrain the formation of the dune near km 27 to the late Boreal–early Atlantic. Between km 41-42, fringing the HR-c channel belt, a flat sand body is present with a decalcified top. We interpret it as a dune, formed at the northern limit of Late Glacial/EH Rhine activity.

Evidence for earliest, slightly aggrading rivers was found in a construction pit in Rotterdam (km 27-29; Cohen and Hijma, 2008). The top of the channel belt deposits (HR-d) undulates irregularly in this area, but is on average somewhat higher than the older channel belt surfaces to the north. OSL (*f-h*) and radiocarbon (*72*) dates show the channel to have been active in the Boreal. To the south of HR-d, the thickness of the WM decreases significantly. A peat layer on top of a distal part of the WM has been dated ~9 ka (*55*), a terminus ante quem for the abandonment of HR-d. Given its northward position, HR-d probably belonged to the Rhine-system. Closer to the channel basal peat formation started at ~8.5 ka (*59, 69, 70*). Pollen and diatom analysis of this layer indicate shallow

standing water (epiphytic diatoms) with abundant water plants (*Nymphaeaceae*), no tidal and little fluvial influence (H-4).

Atlantic aggradation

Channel belts at km 30-32.5 and km 39-41 mark the position of the main Rhine-branches between 8.5-7.7 ka. The channel belt deposits are stacked and have thick natural levee deposits. Between the belts widespread peat formation started just before 8 ka (*53, 57, 64, 65, 77*). Upstream avulsions (see description 2.4.1) led to the formation of the channel belts (#204) at km 44.5 and gradual abandonment of channel belt #53 to the south; the avulsion was completed ~7.3 ka. Pollen and diatom analyses on core 07.09.036 (km 36; interval 13/10 m -O.D.) indicate a freshwater flood basin with some tidal influence towards the top (H-5, H-6). Near km 48.5 (core 07.09.034), diatom (*Cocconeis placentula*, planctic species) and pollen (*Nymphaeaceae*) analyses show that below ~11 m -O.D. deposits accumulated in a fresh, standing water environment (H-5, H-6). At 10.5 m -O.D., the abundance of river transported palynomorphs can be related to 7.7-7.3 ka avulsion events that routed river discharge into this area. Above 9.5 m -O.D., sedimentation occurred in a tidal environment, with initially still fresh, but increasingly more salt water environments (H-5, H-6). The small and heterolithic (sand-clay) channel belts at km 52-56 are most likely the downstream continuations of channel #177 in cross section A-A'. The initiation of channel #133 (Oude Rijn) and the abandonment of channel #177 seem to coincide with the formation of the Voorschoten tidal system (km 53, 134 in cross section C-C') within the former mouth of channel #177. Estuarine conditions near channel #133 are evident from diatom analysis (H-27; km 56; 9-5 m -O.D.), revealing sandy intertidal flat environments with a nearby estuary. After progradation of channel #133 had begun (see description 2.4.1), widespread peat formation started ~5.2 ka.

Between km 9.5-14 multiple small channels with top-of-channel deposits between 9 and 4.5 m -O.D. suggest this to have been an anastomosing part of the fluvial delta. Based on depth-position, three generations can be distinguished, that most likely are linked to the upstream Gorkum-Arkel (#52) channel belt system (Berendsen and Stouthamer, 2001). The main Meuse channel belt was situated at km 8-9. As in section A-A', flood basin deposits in between the Rhine-Meuse channels (km 6-36, around 9 m -O.D.) are strikingly homogenous in build-upl (Terbregge Mb., Fig. A4.3). They date to ~7.5-6.5 ka. Near the centre of Rotterdam and north of km 36, the presence of the TM is not clear due to a lack of detailed corings. North of km 36, *Phragmites* fragments seem to occur more frequently instead of woody debris. At km 26 a fluvial-tidal channel is present, analysed in detail in core 07.09.201, some 700 m upstream of the line of section. Diatom and pollen analyses (H-4, H-6) show that despite the tidal sedimentary signature, freshwater conditions prevailed. This is also evident from the composition of surrounding freshwater peats.

Younger strata (last 5.5 ka)

Besides a small corridor occupied by a main Meuse channel (km 8-9), widespread peat occurence over the southern 30-km of the section shows the existence of a large swamp after 6.5 ka. At km 8-9 a stacked channel belt complex marks the position of the main branch of the Meuse-estuary until the Oude Maas (#132) channel belt was formed in post-Roman times. The channel belt complex can be connected upstream to the severely eroded Meuse-system at km 6 in cross section A-A' and was most likely at some point also linked to channels at km 4 and km 7.5 in that same cross section. South of km 7, salt marshes were present. To the north, widespread peat formation started between 6.5-5.5 ka. Over most of the section peat formation appears to have started before 6 ka, simultaneous with the onset in cross section A-A'. North of km 18, *Phragmites* peat was formed instead of wood peat. See description 2.4.1 for further developments.

2.4.3   Cross section C-C'

This cross section (Fig. 2.1, Addendum 1) is 73.5 km long and is based on 401 cores and 118 CPTs. It runs from the former islands Goeree-Overflakkee in the south to the Oude Rijn channel belt in the north.

Late Glacial and early Holocene rivers

Between km 11 and 53, the Late Glacial-EH valley floor is situated at depths of 21 to 16 m -O.D. To the south and north, the Holocene succession overlies Pleniglacial deposits situated 3 to 5 m above the Late Glacial Rhine-Meuse palaeovalley. Near km 8-9 a depression is observed within the Pleniglacial deposits, filled with fluvial deposits with a more local signature (18-14 m -O.D.), which may indicate that the valley of a local tributary was crossed here (e.g. the Late Glacial river Mark). Over most of the section, the valley floor is capped by the WM. Where it is absent, the top of the channel belts shows undulations of 1-2 m amplitude, depicting the original river bed relief. Note that observation-density varies strongly along the section, allowing to resolve palaeovalley topography in detail for parts of the section only. Late Glacial–EH Meuse activity was concentrated between km 23-27.5 (WM-a/HM-a), while the Rhine was mainly active within two channel belts (km 29-32: WR-a/HR-a; km 36-41: WR-b/HR-b/c). A considerable part of the deposits mapped as the WM have been supplied by channel belts HM-a and HR-a/b/c.

Near km 37.5 a marked step in elevation is visible in the top of sandy channel-belt deposits (19 m -O.D.) and overlying deposits. The step is of similar magnitude as observed at km 18 in cross section B-B' and is a candidate marker of a neotectonically active fault running ESE-WNW. This direction matches that of faults bounding the WNB in the deeper subsurface. In Figure 2.1 the inferred fault zone is indicated.

At Schiedam (km 35) a remarkably deep (~19 m) and relatively narrow entrenchment is present below 18 m -O.D. The infill consists of late Preboreal-Boreal freshwater clays (De Groot and De Gans, 1996; Busschers et al., 2005), suggesting that the entrenchment occurred in the Preboreal. It probably represents a final phase of activity of channel belt HR-a, that in the Late Glacial had reworked the zone between km 29-31, while shifting northwards laterally. Channel belt activity between km 29-31 must have ended in the Preboreal, as the area was subsequently covered by thick WM deposits.

In the WNB the basal peat on top of the WM has been dated ~9.4-9.0 ka (*98, 111, 146*). On the southern block two dates south of km 29 give younger ages of ~8.8 ka (*92, 93*), suggesting that peat formation started earlier in the WNB than on the southern block due to lower elevations (relatively more subsidence). More dates are needed to resolve this issue. Buried inland dunes occur between km 27-33, adjacent to EH channel belts (HM-a and HR-a) and overlying the WM.

At km 23-27.5 a Meuse channel belt is present. About 500 m upstream of the line of section (core B37G0548), a clastic channel fill within this channel belt was described (H-1, see also Busschers et al., 2007). The base of the fill has been OSL-dated at 10-11 ka (*n, o*); a peat at the top of the fill at ~8.8 ka (*92, 93*). The youngest phase, HM-a, is probably situated at km 26-27.5, because there the WM appears absent.

Atlantic aggradation

In section C-C' aggradation started shortly after ~8.7 ka (*92, 93*). On the higher elevated coversand areas, aggradation did not start before 7.7 ka (*86, 136, 138*). The oldest aggrading Rhine channel belts are situated at km 30.8, km 36, km 44 and km 47 and have their top at 15 m -O.D. Their associated overbank deposits consist of sandy, light gray clays with horizontal layers of predominantly fine sand, possibly indicating tidal influence. Occasionally, layers of coarser sand are encountered (Fig. A4.4). Near km 37 a natural levee is capped by fen wood peat dated to ~8 ka (*103*). Several small channel belts near km 24 (15 m -O.D.) identify the earliest aggrading Meuse channel belts.

North of km 29, fluvial-tidal flood basin deposits (TM) are encountered between 12-9 m -O.D. An incorporated thin layer of clayey wood peat (possibly a strongly rooted soil horizon) between km 35-38 was dated ~7.3 ka (*102;* Fig. A4.5). Between km 26-29 the presence of the TM is not clear. Between km 29-31 the amount of wood fragments is lower than to the north, but still indicates steady fluvial supply. This changes abruptly south of km 26, where extensive laminated heterolithic bedding (clay-sand) is observed (Fig. A4.6), associated to the large estuarine Meuse channel system (km 16-20), that most likely was formed ~7.3 ka after a landward shift of the estuary due to the northward shift of the main Rhine-branches (see description 2.4.1). The channel belt at km 15 presumably positions the Meuse just before this occurred. To the south of the estuarine channel, extensive tidal flat deposits are present that overlie ~0.5-1 m of freshwater clay containing many *Salix*

leafs. The associated fresh flood basin first turned into a supratidal salt marsh (12 m -O.D) and then rapidly into an intertidal flat, amongst others supported by diatom assemblages (H-5) indicating a marine ingression. The intertidal/flat deposits consist of fining upward clay-sand alterations with *Hydrobia* and *Cerastoderma* shells. Median grain sizes are smaller than 100 μm. Towards the top (5 to 3 m -O.D.) marine influence decreased rapidly and fresh swamp vegetation returned (H-6) under the influence of nearby Meuse-branches (Verbraeck and Bisschops, 1971). The muddy intertidal flat deposits south of km 2 mark the edge of the Atlantic Meuse estuary.

Several Rhine-branches debouched in the Delft area in the early Atlantic (km 36-46). Overlying and underlying peat beds, as well as dates of upstream connections, constrain significant delivery of Rhine discharge to 8.0-7.3 ka. A 3-4 km wide and relatively thick sandy body (here after named Delft sands) is present between km 39 and 46 at depths of 15 to 9 m -O.D. (maximum thickness ~7 m; average thickness ~4-5 m, appears longer in cross section than in plan view). The top consists of very fine sands (110-150 μm) and the sands contain frequent clay laminations and organic detritus, occasional beds of coarser sand and shell fragments (Fig. 2.5). This sandbody is interpreted to represent a bay-head delta (as in Fig. 2.4, fully treated in the discussion section; for location see Fig. A4.9). The bay-head delta can be connected to upstream channel belts # 53/204 (km 32 and 41, cross section B-B'). Freshwater conditions at this position during this time are evident from vivianite stains and diatom analysis (H-3; below 10.5 m -O.D. at km 61). The bay-head delta was abandoned following the 7.3-ka avulsion that established channel belt #177 (see description 2.4.1). In the former bay-head delta area a shallow tidal basin existed afterwards that silted up rapidly and discontinuous peat formation started after ~6.9 ka (*110*).

Narrow tidal channel belts at km 65.5-68 (9 m -O.D.) presumably link up to channels at km 45-49 in cross section B-B' and if so were active after 7.3 ka. The sandy tidal channel deposits flanking the southern edge of channel belt #133 (km 72.5, 6-12 m -O.D.) suggest that channel belt connected to an existing tidal channel system. Between km 46-70 complex tidal systems developed, starting subsequently after 7.5 ka (*125*). The largest tidal inlet, the Rijswijk-Zoetermeer system at km 50-54, had its maximum size between ~6.8 and 6.4 ka and closed around ~6.1 ka (Van der Valk, 1996b; Cleveringa, 2000; see also 119, 120, 124, 125). Sandy deposition of the Stompwijk tidal system ended also around 6.1 ka (*131*). The sandy deposits between km 46-50 are part of the Rijswijk-Zoetermeer sandsheet (succession back-barrier to beach plain deposits) that formed between ~6.7-6.3 ka (Van der Valk, 1996b; Cleveringa, 2000; Van der Spek et al., 2007). Date *134* seems to indicate that the Voorschoten tidal system had its maximum activity after 6.4 ka. This is probably related to the disappearance of the Waddinxveen channel belt, allowing tidal channels to penetrate further landward. North of the Rijswijk-Zoetermeer tidal inlet, diatoms in core B30H0369 (km 62.4) indicate brackish lagoonal sedimentation for the 8

and 6 m -O.D. interval, dated at ~6.3-6 ka (*126-131*). After 6 ka (*126*), marine influence increased and the area became part of an intertidal zone (H-3) within the estuarine outlet of channel belt #133. The sandy deposits of the closed Rijswijk-inlet probably formed a modest topographic high for some time due to less compaction than surrounding peats and clays. This high might have separated the Oude Rijn and Meuse-estuaries (Fig. A4.8). Between km 34-45 mainly clay was deposited between 6.5-5 ka (*99-101, 104-106, 108-110*). The area was probably part of the Meuse-estuary. At the base, diatoms indicate sub- to intertidal conditions (species *Cyclotella striata, Cymatosira belgica, Cocconeis diminuta)* with fresh admixtures suggesting the presence of a nearby river mouth (H-30, H-31), possibly reflecting the Meuse to the south. To the top, the environment gradually changed to a supratidal salt marsh (*Diploneis interrupta, Nitzchia navilcularis, Rhoicosphenia curvata)* with occasional phases of freshening (H-30, H-31).

Younger strata (last 5.5 ka)

After ~5 ka peat formation started and continued until the Middle Ages. Between km 22-34 large scale peat formation already started ~6.5 ka (*91*). Between km 48-61 the peat was removed by humans. North of km 64 peat could not form due to sedimentation of the Oude Rijn. The Meuse shifted north to the area of the present Oude Maas. The abandoned Meuse-estuary (km 16-20) silted up above its surroundings. Consequently, peat formation started to bury this abandoned estuary relatively late, around ~4.5 ka (*90*). South of km 16 peat formation started after ~6.2 ka BP (*87*). Peat formation continued into Subboreal times and eventually caused oligotrophic raised bogs to develop on top of eutrophic peat in large parts south of km 16. Subatlantic developments match those described in 2.4.2.

2.5   Discussion

2.5.1   Earliest Holocene fluvial evolution

The Wijchen Member in the western Netherlands

The WM comprises overbank deposits of Late Glacial and in particular EH Rhine–Meuse channels (H- and R-channels, Add. 1). This is evident from its thickening in the vicinity of these channel belts. In the study area, the bulk of the WM was deposited during the EH (Busschers et al., 2007; this chapter). Dark floodplain paleosols occur in the top of the WM (e.g. Törnqvist et al., 1994; Autin, 2008). In some parts of the study area, especially in the NE near EH Rhine channels, additional paleosols (mostly one extra) are found within the WM. Berendsen and Stouthamer (2001; 2002) have hypothesized an Allerød age for the lower horizon in the western part of The Netherlands, extrapolating genetical models established for the Lower Meuse valley upstream of the study area (e.g. Berendsen et al., 1995). They used this hypothesis to map the extension of pre-Allerød braid plains: in areas

with two vegetation horizons, pre-Allerød braid plains must be present. Lithogenetical considerations (this chapter) and ^{14}C and OSL dating evidence from within and below the WM invalidate this hypothesis (*60*, this chapter; also Busschers et al., 2005). Paleosols that occur within the WM *in the western Netherlands* are by majority of EH age, just as the paleosol in its top. Rather than identifying patches of pre-Allerød braid belt surfaces, areas with double paleosols predominantly overly channel belts of Younger Dryas and Preboreal age. In the study area four vegetation horizons are indentified, each of subregional extent and of different EH age (compare dates *98*, *111* with dates *57-60)*. This indicates the EH in the western Netherlands to have been more dynamic regarding natural levee and overbank deposition history than previously realised. The temporal and spatial distribution of the WM thus reflects the complex avulsion history of EH-channels.

Cause for early Holocene entrenchments

Rhine discharge in our study area was split over two parallel running channel belts until the late Boreal (Fig. A4.9). Channel belts of Preboreal and Boreal age show deep scour. The scour depth observed at Schiedam (cross section C-C'; ~19 m below river plain; 37 m -O.D.) is enigmatically deep compared to scour features in Rhine channel belts of similar age in upstream reaches. Berendsen et al. (1995) and Cohen (2003) reported on deep residual channels in the upstream Rhine-Meuse delta, but none are deeper than 8 m below the contemporary floodplain. Van Heteren et al. (2002) described channel fills offshore the present coastline that reach depths of 35 m -O.D., similar to the scour at Schiedam. The top of the offshore channel fill deposits occurs between 19 and 23.5 -O.D. Most of them are partly embedded within (and sometimes topped by) a several metres thick, fine-grained unit that is comparable to the WM and thus mainly of (Pre)Boreal age. The similar age and scour depth of the offshore channels and the Schiedam channel suggests that they belong to the same channel belt and have incised this deep by one shared process. Van Heteren et al. (2002) interpreted the offshore fills as estuarine and suggested local scouring in tidal inlets as a possible mechanism for the deep thalweg of several channels. However, at the time of entrenchment (Preboreal-early Boreal, see description 2.4.3) relative sea level was well below 30 m -O.D. –based on eustatic levels from e.g. Fairbanks (1989) and modelled levels by Vink et al. (2007)-, excluding the possibility of nearby tidal inlets. Also, the entrenched channel at Schiedam and the entrenched channels offshore lie ~40 km apart, excluding local tidal inlet scour. The offshore *channel fills* can well be of estuarine nature, but the initial *entrenchment* cannot. De Groot and De Gans (1996) after Roep et al. (1975) and Smith (1985) suggested a relation with the breach of the Dover Strait, but this occurred during pre-Weichselian glacials (Gibbard et al., 1988; Gupta et al., 2007; Busschers et al., 2008). An interesting new finding is that the deeply entrenched systems are most likely all situated outside the West-Netherlands Basin on the southern slower subsiding area underlain by the London-Brabant massif (Fig. 2.1). This is

suggested by the presence of an active fault immediately upstream from the Schiedam entrenchment (Fig. 2.1, Addendum 1, see also 2.4.2/2.4.3). This would have led to more scour than in the WNB, although the differential scour depth can be at maximum the difference in subsidence, in this case only a few metres. It can therefore not explain the excessive scour completely. Another possibility is the difference in channel bank erodibility downstream of Schiedam due to the earlier start of aggradation and hence thicker fine grained overbank deposits than in areas upstream. This could have hindered lateral migration of EH channel belts, stimulating deeper scour than in areas upstream of Schiedam. A less likely option is the scouring effect of water confined under a frozen river surface during a period of sudden discharge increase. This effect could have been strongest in areas of low river gradient (i.e. downstream of the delta hinge line, in the late Preboreal situated close to Schiedam), as ice cover would have been thickest there due to lower flow velocities and hence less likely to break up during an increase of discharge.

Valley floor gradient
Younger Dryas and (Pre)Boreal channel belt surfaces occur in incised position. The cross sections allow determining their elevation relative to older and younger systems. The lowest recognised valley floors in the study area (e.g. km 30-31, cross section B-B'; km 46-48 cross section C-C') represent their youngest phase (see also Busschers et al., 2007). These valley floor levels lie on average ~1 m lower than the surrounding valley floors and the width over which they are lower excludes the possibility of locally encountered variability. Upstream, the lowest valley floor was named Terrace X and is situated up to 2 m lower than the surrounding valley floor or Lower Terrace. The lower gradient of Terrace X results in a downstream decrease in differential elevation (Pons, 1957). By extrapolating the gradient lines to the west, Pons (1957) suggested the terraces to merge somewhere offshore the present coast line. Based on extrapolating the Lower Terrace gradient of Pons (1954) and a newly constructed gradient for Terrace X, Törnqvist (1998) proposed a convergence near Rotterdam. The new data show that the intersection point between the two terraces is not situated near Rotterdam, but more to the west. It also shows that Terrace X represents a YD-EH valley floor and is not only of YD age. Future research on valley floor gradients should also include existing offshore seismic data (e.g. Van Heteren et al., 2002; Rieu et al., 2005; chapter 4 of this thesis).

It is important to realize that over large parts in the western Netherlands the upper few metres of the Late Glacial-EH sandy substrate consist of aeolian deposits. This has direct consequences for constructing longitudinal profiles for the Rhine-Meuse valley. This applies especially to the top of the YD-EH river plain which is overlain by many aeolian dunes and thus at a lower position than judged from merely mapping 'the top of sand' level.

The period of incision that started in the Allerød and culminated in early Boreal times (unit B6b; Busschers et al., 2007), shows that the western Netherlands was a net export area for sand. This material was transported towards present-day offshore areas. The study area likely was a net sink for flood basin sediments during this time, testified by the widespread occurrence of the WM, draped over considerable widths of Late Glacial and EH buried terraces and flanking (Pre)Boreal channel belts.

2.5.2 Boreal inland aeolian dune formation in the western Netherlands

The cross sections traverse several inland aeolian dune fields. Large aeolian sheets (~2 m thick), with an occasional higher dune, are present over considerable areas, which was not realised before. Past mapping restricted the extent of dune fields to the direct vicinity of known higher dunes and presumed Younger Dryas to earliest Holocene ages (e.g. Bosch and Kok, 1994). This study shows that some dune fields of modest height, but considerable extent, date from the late Boreal (reproducing a local observation of Pons and Bennema, 1958). This follows from date *72* (Oxcal mean 9306 BP; cross section B-B', km 28) below an observed dune in a construction pit and date *71* (OxCal mean 9175 BP) from a residual channel fill of a channel that dissects the same dune. Dune formation therefore occurred between 9.3 and 9.2 ka BP and is tentatively related to the 9.3 ka BP cooling event (Von Grafenstein et al., 1999; Marshall et al., 2007; Rasmussen et al., 2007). Boreal aeolian activity can also be inferred from the admixture of in-blown sand in Boreal deposited parts of the WM (Van der Woude, 1983). In the eastern part of The Netherlands several dunes were palynologically dated at the Younger Dryas (Pons, 1957) and we do not exclude older ages for adjacent dune fields of greater height in the Rotterdam area. Multiple OSL-dating on inland aeolian dunes is needed to constrain different periods of dune formation.

2.5.3 Estuarine evolution: bay-head delta formation

Between 8 and 7.3 ka, a 3-4 km wide and ~4-5 m thick sand body was deposited near Delft (Delft sands, km 39-46, cross section C-C') that can be connected to upstream fluvial channel belts, strongly suggesting a fluvial source for the sediment. This is also apparent from the predominantly freshwater depositional environment, evident from vivianite stains and diatom analysis. Based on the deltaic geometry (Fig. A4.9), the presence of tidal structures and brackish-water fauna, the fluvial source and the stratigraphic position between fluvial deposits below and tidal basin deposits above, we interpret the Delft sands as a bay-head delta deposit formed in the upper estuary (see also Fig. 2.4). Unfortunately, most cores end in the top of the sand body that is only fully penetrated by a few cores. The top of the sand body generally consists of very fine sands (110-150 μm). Too little information is available to describe the upward trend in grain size within the sand body, although core B37E570 (Fig. 2.5) seems to show a fining upward succession. Generally

though, bay-head deltas show an overall coarsening upward succession (Boyd et al., 2006). Possibly the fining-upward unit represents a bay-head delta distributary channel. However, during rapid SLR and continuous rapid landward migration of the whole estuarine system, it is possible that a bay-head delta succession may show a general fining-upward trend.

The formation of the delta means that little sand reached the open sea and hence hardly any fluvial sand was available for alongshore transport and barrier formation. Seaward of the bay-head delta and seaward of cross section C-C', a central basin must have been present. Water depths in this basin would have been shallow (maximum 5 m), as sea level was ~10 m -O.D. and the drowned EH surface is encountered at 15 m -O.D. The formation of mouth bars in the bay-head delta would have led to channel bifurcations. Such processes may have driven the avulsions that made the Rhine partially abandon the Delft area after 7.7 ka. It is striking that at the river mouths of the younger channel belts #177 and #133 no bay-head deltas have been recognised. If they existed, a lack of corings near the mouth of #177 is the most likely explanation for not encountering bay-head deltas. The bay-head delta of #133 would have been largely reworked during subsequent progradation of the channel belt and very poorly preserved and hard to recognize.

2.6 Conclusions

Our integrative approach allowed reconstructing the age, tidal and fluvial facies distribution and architecture of the deeper Holocene subsurface of the Rhine-Meuse delta. The main conclusions regard the transformation from fluvial valley to estuary:

- The Younger Dryas – (Pre)Boreal period is characterised by one major Meuse and two major Rhine channel belts that were reworking Late Glacial deposits while lowering their beds;
- Widespread inland aeolian activity along river beds occurred in the Younger Dryas and Preboreal, but also during the Boreal;
- Convergence of late Pleniglacial and Younger Dryas-early Holocene valley floors does not occur near Rotterdam, but more to the west;
- In the early Atlantic aggradation started and Rhine discharge began to concentrate in the northern part of the palaeovalley. Outside the channel-belt areas, widespread peat formation started ~9 ka and ended between 8.5 and 8 ka. By that time most parts of the study area were permanently flooded and tidally influenced. The central part of the valley remained fresh due to river discharge, while at the fringes slightly brackish environments existed;
- After 8 ka a bay-head delta formed near Delft. This means that almost all sandy sediment was trapped in the back-barrier basin and did not reach the North Sea and could not contribute to barrier formation. Several avulsions resulted in a

stepped northward shift of the constantly retreating Rhine river mouth into a tidal basin. The Meuse still debouched south of Rotterdam. In the upper estuary, woody debris containing silty clays, were rapidly deposited;

- After 6.5 ka the Oude Rijn-estuary formed and the central part of the palaeovalley was quickly transgressed and transformed into a large tidal basin. Shortly before 6 ka retrogradation of the coastline halted and tidal inlets began to close.

This chapter describes the transition from a river valley to an estuary in unprecedented detail and enables more detailed palaeo-reconstructions, evaluation of relative importance of fluvial and coastal processes in rapid transgressed river mouths, and more accurate sediment-budget calculations. The described and well illustrated (changes in) facies are linked to lithogenetic units. This will aid detailed palaeogeographic interpretations from sedimentary successions, not only in the Rhine-Meuse delta, but also in other estuarine and deltaic areas.

Acknowledgments

This chapter is dedicated to the late Henk Berendsen and Leen Pons, whose profound understanding of the evolution of the Rhine-Meuse delta is so much reflected in this chapter.

3 Timing and magnitude of the sea-level jump preluding the 8200 yr event

Abstract

Evidence from terrestrial, glacial, and global climate model reconstructions suggests that a sea-level jump caused by meltwater release was associated with the triggering of the 8.2 ka cooling event. However, there has been no direct measurement of this jump using precise sea-level data. In addition, the chronology of the meltwater pulse is based on marine data with limited dating accuracy. The most plausible mechanism for triggering the cooling event is the sudden, possibly multi-staged drainage of the Laurentide proglacial Lakes Agassiz and Ojibway through the Hudson Strait into the North Atlantic ca. 8470 ± 300 yr ago. Here we show with detailed sea-level data from Rotterdam, The Netherlands, that the sea-level rise commenced at 8450 ± 44 cal BP. Our timing considerably narrows the existing age of this drainage event and provides support for the hypothesis of a double-staged lake drainage. The jump in sea level reached a local magnitude of 2.11 ± 0.89 m within 200 yr, in addition to the ongoing background relative sea-level rise (1.95 ± 0.74 m). This magnitude, observed at considerable distance from the release site, points to a global-averaged eustatic sea-level jump which is double the size of previous estimates (3.0 ± 1.2 m versus 0.4 to 1.4 m). The discrepancy suggests either a coeval Antarctic contribution or more likely, a previous underestimate of the total American lake drainage.

3.1   Introduction

The period of abrupt cooling that started 8247 yr ago (Thomas et al., 2007) and was centred ca. 8.2 ka (all ages in calendar years) is the most pronounced Holocene climate excursion (Alley and Ágústsdóttir, 2005). There is general consensus that drainage of Laurentide proglacial Lakes Agassiz and Lake Ojibway was the driving mechanism for the 8.2 ka cooling. The event is often seen as an analogue for possible future freshening of the
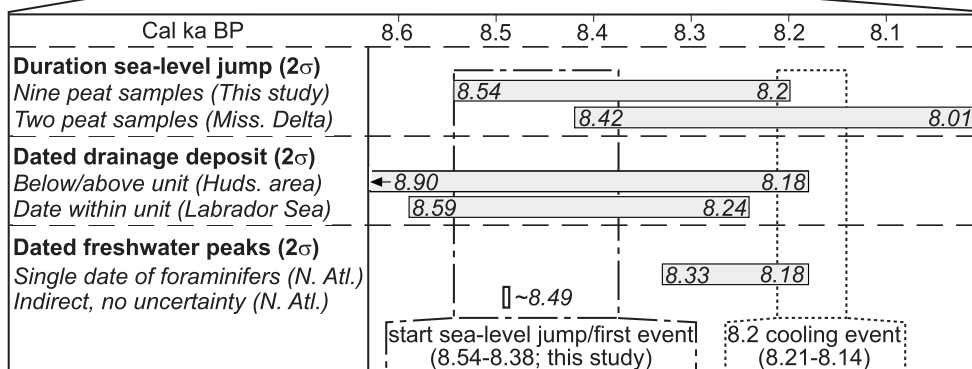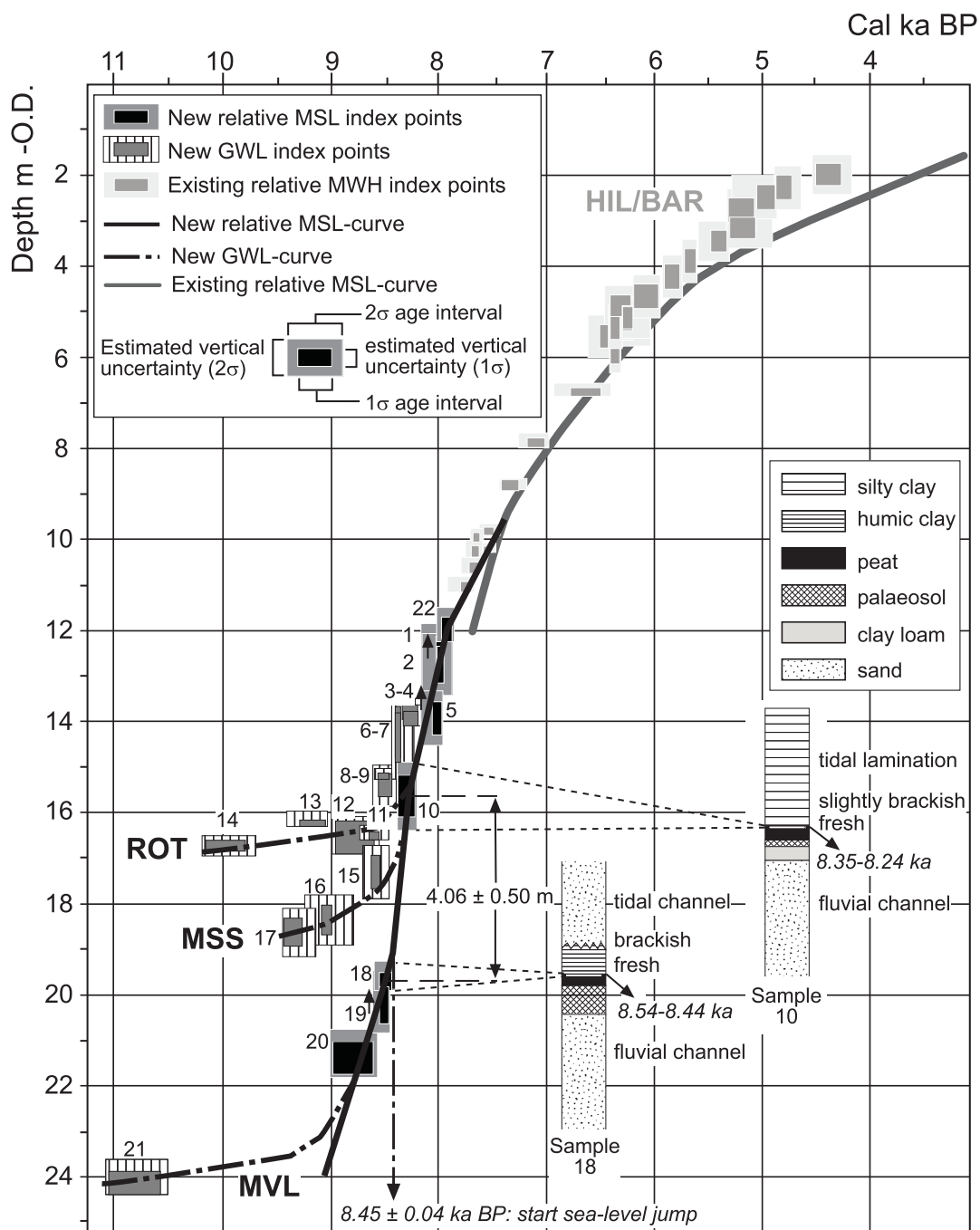
Figure 3.1 (opposite page) Relative sea-level rise in the western Netherlands based on geological data (9-7.5 ka: this study; 7.5-4 ka (Van de Plassche, 1982; Berendsen et al., 2007b)). The upper panel plots age-depth index-points and shows that the sea-level jump commenced at ca. 8.45 ka cal BP. Sedimentological (lithology, structure) and palaeo-environmental indicators (pollen, diatoms) are plotted as core logs for the two sites with transgressed basal peat that most closely bracket the jump magnitude. The groundwater-level (GWL) rise (depicted for ROT, MSS and MVL) is plotted as sigmoidal curves that show initial fluvial-controlled groundwater levels graded to palaeovalley floodplain level (dipping from -17 to -24 m between ROT and MVL), then gradual establishment of sea-level control in the coastal zone and eventual full pick-up of mean sea level (MSL) rise ('20-18', '10', '5', '1-2', '22'). Arrows above index-points indicate that their depths are possibly overestimated, because of uncertain amounts of compaction. The lower panel compares the timing of the Rotterdam jump with other published sites. The end of the jump coincides with the start of the 8.2 ka event, the onset appears to have been two centuries before. Dates from the Hudson (Huds.) area (Barber et al., 1999; post-date SE Hudson Bay and pre-date East Hudson Strait) were recalibrated using the Marine04-curve (Hughen et al., 2004) using reservoir effects defined in the original publications. The 2σ-interval of the Labrador Sea-date (Hillaire-Marcel et al., 2007) was obtained by calibrating the original radiocarbon date (7950 ± 80 14C yr BP). MHW—Mean high water; Miss.—Mississippi; N. Atl.—North Atlantic.

North Atlantic and serves as a test case for assessing the sensitivity of ocean circulation to freshwater perturbations in climate models. Accurate constraints on the timing and magnitude of the drainage event are essential for such applications.

The timing for the lake drainage was first established at 8470 ± 300 BP by dating bivalves above and below the preserved drainage deposit (Barber et al., 1999; 1σ). In the Labrador Sea the deposits associated with the lake drainage record two drainage events that post-date 8560 ± 70 BP (Hillaire-Marcel et al., 2007; 1σ). Foraminifers within the deposit are mostly older than this date, indicating settling of reworked material, with the youngest date from the unit being 8420 ± 80 BP (Hillaire-Marcel et al., 2007; 1σ). Evidence for two-stages of lake drainage is provided by other proximal marine and proglacial lake sites (Teller et al., 2002; Ellison et al., 2006), with the largest drop in lake volume being associated with the first event (Teller et al., 2002). A single age obtained from foraminifers in the North Atlantic dates the second freshwater event to 8343-8184 BP (Ellison et al., 2006; 2σ), while for the first event an age of ca. 8490 BP was indirectly derived (Ellison et al., 2006; no uncertainty given). All these calibrated ages are from radiocarbon dates and include marine reservoir age-corrections of uncertain accuracy. For this reason it is probable that the actual age uncertainty associated with these age estimates of the event exceeds the quoted interval limits.

There is considerable debate regarding the total volume of ice-lake freshwater that was released into the North Atlantic and to what extent decay of the Laurentide ice sheet (LIS) contributed in addition to lake drainage. Reconstructions of Lakes Agassiz and Ojibway (Leverington et al., 2002) suggest a volume of 163,000 km^3 or 0.46 m equivalent eustatic sea-level rise (SLR) for the most favoured ice configurations (earth radius 6370 km; 70% covered by oceans). However, coeval rapid disintegration of the LIS could have raised the total rise to a maximum of 1.4 m global SLR (Von Grafenstein et al., 1998). By shifting the ice margins 1° north or south, the lake volumes would be ~200% and 45% of the favoured volume (Leverington et al., 2002).

Pinpointing the sea-level jump using geological data from coastal settings has the potential to provide independent constraints on the total volume of freshwater released. A first attempt was made using data from the Mississippi delta where two vertically separated peat layers, pre- and post-dating the 8.2 ka event, were radiocarbon-dated (Törnqvist et al., 2004; Fig. 3.1). The 1.19 ± 0.2 m elevation difference constrains total relative SLR at the site, i.e. contributions by local subsidence and eustasy as well as the sea-level jump itself. Since then, geophysical modelling (Kendall et al., 2008) has indicated that the Mississippi-delta likely recorded only 20% of the eustatic value associated with the meltwater pulse due to its proximity to the source area. The documented 1.19 m rise is now considered to mainly reflect 'background' SLR (BSLR) due to local glacio-hydro-isostatic adjustment (GIA) (Kendall et al., 2008) and modest eustatic SLR caused by the steady melting of the remaining ice masses at this time. It is also clear that the duration of the Mississippi RSL jump extends well into and beyond the 8.2 ka cooling period (Fig. 3.1), thus including post-8.2 ka event SLR.

In summary, thus far the 8200 yr sea-level jump has not been directly measured and the existing 0.4 m to 1.4 m range is based on projection, source reconstruction and modelling. To properly constrain the magnitude of this event a distant site is required with series of highly resolved sea-level index points collected from a small area, ideally spanning a sufficiently long period of time to determine pre- and post-event rates of RSL change. The Rhine-Meuse delta in The Netherlands provides such a site, recording the abrupt rise within sediments that are preserved at depths of 13-25 m below present sea level (Hijma et al., 2009: Chap. 2). This paper details this evidence and provides the first calculation of magnitude and timing of the sea-level jump based on well-dated, precise palaeo-sea-level data.
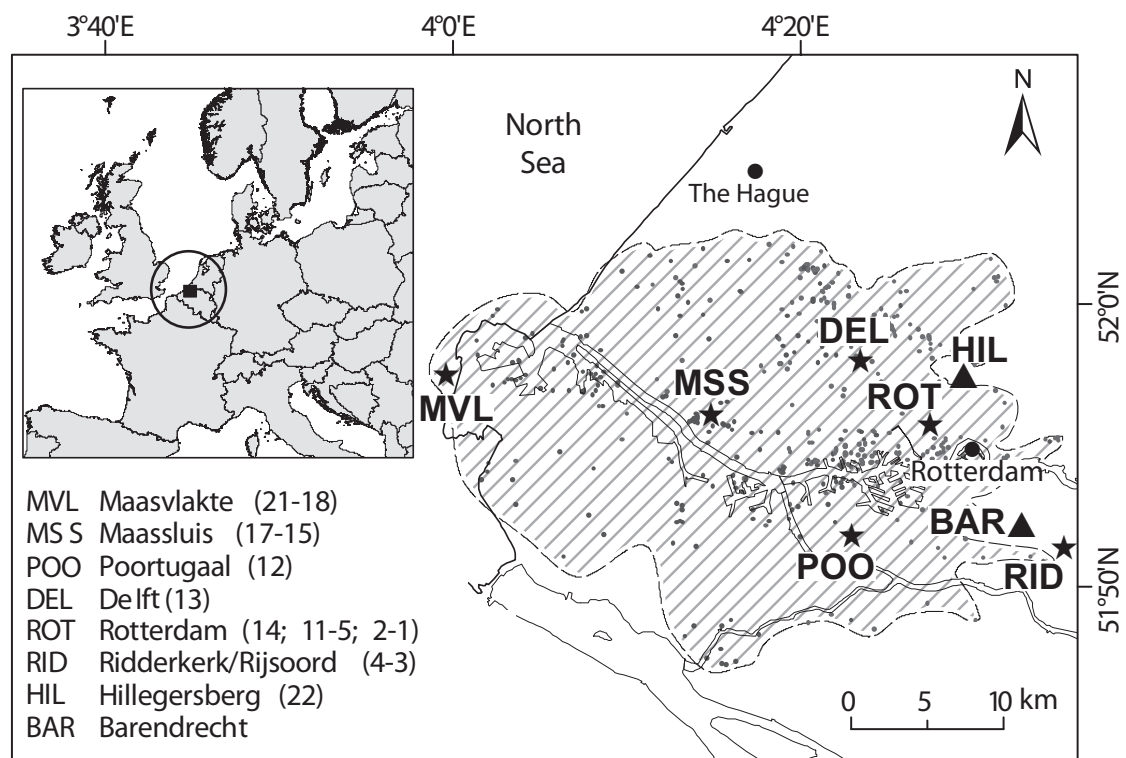
*Figure 3.*2 Location map of the study area and the research sites. Stars indicate sites used for constructing the pre-7.5 ka sea-level curve, triangles mark sites with post-7.5 ka data. The numbers between brackets refer to the numbers listed in Fig. 3.1. The hatched area (778 km2) indicates where the drainage event (drowned organic layer at relevant depth) is recognised in borehole descriptions (the dots).

3.2 Material and methods

We collected and dated (mainly basal) peat samples from within the Rhine-Meuse delta (Figs. 1, 2). Autochthonous terrestrial plant macrofossils were picked from sampled peats for radiocarbon dating (details in Suppl. Information [SI], Table S3.1). All radiocarbon ages were calibrated using OxCal 4.0.5 software (Bronk Ramsey, 2001). Following established methodologies developed in the study area (Jelgersma, 1961; Van de Plassche, 1982), and successfully applied globally since (Törnqvist et al., 2004), these coastal peats provide high quality sea-level index-points. The method relies on the notion that under conditions of forced transgression, coastal peat forms extensively around local mean high water level (MHW) in a landward shifting zone. Where peats are collected in densely sampled series (Fig. 3.1), palaeo-waterlevel history is pinpointed with a precision of <0.5 m and <100 yr. It is necessary to estimate the former tidal range in order to specify local mean sea levels (MSL) at the time of the event. Before 8 ka, the Rhine-Meuse delta was situated on the margins of a shallow basin (the southern North Sea) (Lambeck, 1995) with

microtidal conditions. MSL was probably <0.5 m below MHW at the Rhine river mouth (Van der Molen and De Swart, 2001a) (SI, Table S3.2). Height uncertainties defined at 1σ and 2σ ranges around local MSL (Fig. 3.1; SI, Table S3.2) include assessments of the water depth in which the peat formed, minor post-depositional compaction, tidal amplitude uncertainty and of errors arising from measuring surface elevation and sample depth.

3.3   Results

At sites MVL, MSS and ROT, five dates obtained from peat just below a regionally-traceable contact (Fig. 3.2) yielded 1σ-ages of 8512 ± 45, 8587 ± 50, 8490 ± 53, 8498 ± 43 and 8505 ± 45 cal BP (Samples '9', '15', '18', '19' and 'a', yielding a combined age of 8522 ± 37 cal BP; Figs. S3.2-3; A4.10-12). The stratigraphic contact records a sudden water-level rise that was caused by a sea-level jump at ~8.5 ka (the maximum date for the start of the event). Abrupt drowning transformed the former swamps (peats) into fluvial-tidal open-water environments (gyttja mud) throughout the river-mouth area (Hijma et al., 2009: Chap. 2) (Fig. 3.1). Radiocarbon-dated terrestrial plant macrofossils from the base of the gyttja-mud give a minimum age for the start of the event. At site ROT three dates from this layer (samples '6 and 7', both 8373 ± 34 cal BP, and sample 'b', 8421 ± 57 cal BP; SI, Table S3.1) have a combined average age of 8385 ± 16 cal BP (1σ; SI). These minimum and maximum ages narrowly bracket the start of the event to 8544-8375 cal BP (2σ) with a mean of 8450 ± 44 cal BP (1σ) (Figs. 3.1 and 3.3, details SI).

Samples '18-19' and '10' (Table 3.1, Fig. 3.1) pre and postdate the presumed sea-level jump in the study area. These samples were taken from basal freshwater peats that are non-erosively overlain by clastic subaqueous deposits. Sample '19' was taken from a peat layer at the same site as sample '18' (~5 km apart), from a similar sedimentary succession and a similar sample depth, yielding similar ages (Table 3.1; Fig. A4.12). Diatom analyses revealed a brackish assemblage for the clays overlying sample '19', clearly indicating that at site MVL the swamp environment was converted to estuarine conditions during the abrupt rise. As sample '19' has an uncertain compaction error (SI), this sample has not been used for calculating the magnitude of the event. At site ROT, diatom analyses around samples 'a' and 'b' (~1 km apart from sample '10') indicate a slightly brackish environment both before and after the event, while laminations within the overlying clays indicate increased tidal influence (Fig. A4.10). These transgressive palaeo-environmental and sedimentological data make the top-of-peat samples '18' and '10' excellent sea-level indicators. The difference in elevation and age between samples '18-19' and '10' is 4.06 ± 0.50 m and 195 ± 68 yr respectively (1σ). This height range includes the presumed sea-level jump, as well as background relative sea-level rise in the 195 ± 68 yr that separate the two samples.
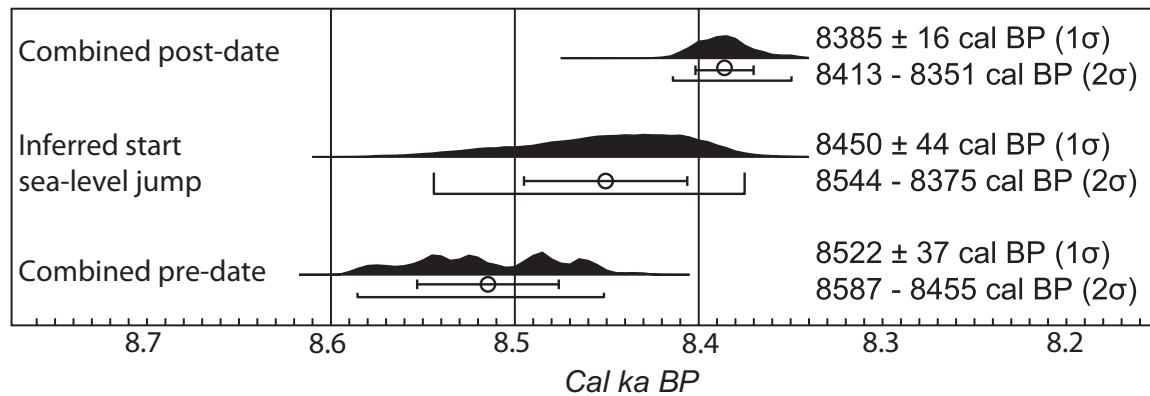
Figure 3.3 OxCal-plot (Bronk Ramsey, 2001) of the calculated timing of the sea-level jump. The calculation is based on the weighted average of five dated samples directly below ('9', '15', '18-19' and 'a') and three dated samples directly above ('6-7' and 'b') the drowning event layer.

BSLR at Rotterdam was relatively large due to its location in an area of long term tectonic subsidence, combined with additional post-glacial GIA-related subsidence (Kiden et al., 2002; Vink et al., 2007). Based on our sea-level index points for the centuries before and after the event, the rate of BSLR was 10 ± 1.5 mm/yr (1σ; SI, Table S3.3). This rate is supported by geophysical modelling (Vink et al., 2007) that predicts a BSLR of 9-10 mm/yr relative sea-level rise at the study site between 9-8 ka. The observed rise of 4.06 ± 0.50 can therefore be split into 1.95 ± 0.74 m of BSLR and a sea-level jump of 2.11 ± 0.89 m (1σ; SI, Table S3.4). Geophysical modelling of gravimetric effects indicates that the western Netherlands likely recorded ~70% of the global mean for a meltwater pulse released from a Laurentide source (Kendall et al., 2008). If this is correct, the global eustatic jump would be ~3 m ± 1.25 m (1σ) with an equivalent water volume of 10.7 ± 4.5 x 10^{14} m³. The probability that the full 4.06 ± 0.50 m rise is all due to BSLR is ~10% (t-test; SI, Table S3.4).

3.4   Discussion and conclusions

A sea-level jump of magnitude discussed above must have influenced marine deltas across the world, especially at far-field sites. Indeed, numerous delta-studies from Southeast Asia (Hori and Saito, 2007; Liu et al., 2007; Tamura et al., 2009) attribute drowning and back-stepping events observed in deltaic sedimentary archives to an abrupt sea-level rise. The jump is therefore of global significance, not just for the link to the 8200 climatic event, but also for its circumoceanic sedimentary imprint. Despite its importance, no other area than the Rhine-Meuse delta provides a self-consistent series of sea-level index-points of sufficient precision to quantify the jump as well as the BSLR. Our chronology suggests that

Table 3.1 Samples used for calculating sea-level jump magnitude.

ID[1]	Laboratory number	Lat., lon.[2] (°N, °E)	Depth[3] (m-O.D.)	Vertical error margin[4] (m-O.D.)	^{14}C yr BP (1σ)	Cal yr BP[5]	Cal age range (2σ) (cal yr BP; %)	Dated material	Reference
10	UtC-14940	51°55′25′′ 4°27′59′′	16.30	15.18-16.10	7486 ± 41	8298 ± 55	8383-8199; 95.4	Mainly *Alisma pl.* and *Scirpus lac.* (top fen peat)	Hijma et al. (2009: Chap. 2)
18	UtC-15344	51°57′22′′ 3°59′44′′	19.60	19.51-20.04	7700 ± 60	8490 ± 53	8591-8401; 95.4	*Alnus* fruit	Hijma and Cohen (In Press: Chap. 3)
19	GrN-21460	52°0′2.2′′ 3°59′21.5′′	20.65	19.82-20.63	7720 ± 40	8498 ± 43	8584-8422; 95.4	(top fen-wood peat)	Hijma and Cohen (In Press: Chap. 3)

1 - Identification number corresponds to Fig. 3.1

2 - Latitude, longitude in degrees, minutes, seconds (World Geodetic System 1984)

3 - O.D. = Dutch Ordnance Datum (~mean sea level)

4 - Details of error margin calculation in Table S3.2

5 - Mean of calibrated age (± 1σ)

the start of the jump occurred ~100 yr before it was recorded in the Mississippi delta (Fig. 3.1). Precise sea-level data from far-field sites is needed to further constrain the magnitude of this event.

Previous studies considered the global sea-level equivalent of the event to have been between 0.4 and 1.4 m (Von Grafenstein et al., 1998; Barber et al., 1999; Renssen et al., 2001; Leverington et al., 2002; Bauer et al., 2004; Clarke et al., 2004; Törnqvist et al., 2004; Wiersma et al., 2006; Kendall et al., 2008), which is considerably smaller compared with the magnitude recorded near Rotterdam. This discrepancy necessitates consideration of other potential contributions to this event, two of which are discussed here. (1) The Antarctic ice-sheet is a possible co-contributor to accelerated SLR in the centuries preceding the 8.2 ka climate event. As the Atlantic Meridional Overturning Circulation slowed down in the North Atlantic due to the meltwater release, this changed the meridional density gradient which may have led to increased Antarctic Intermediate Water Formation (Stocker, 1998) and warming of circum-Antarctic seas (the so-called bi-polar seesaw). This would have affected the coastal margins of the Antarctic ice sheet and, to a more limited extent, the Antarctic interior. At present however, there is no strong evidence for massive changes in Southern Ocean circulation around ca. 8.5-8.2 ka. Any significant increased SLR contribution from Antarctica would have been fully recorded in areas where the impact of the North American drainage event on relative SLR was limited, such as in the Mississippi delta, but so far no indications exist for this. (2) Underestimated Laurentide and Greenland contributions are a second possible source. The evidence for multi-staged lake drainage (Clarke et al., 2004; Ellison et al., 2006; Hillaire-Marcel et al., 2007) and the proposed timing for first and last events (Ellison et al., 2006; Hillaire-Marcel et al., 2007; Fig. 3.1) imply that at least two events produced the total jump of 2.11 ± 0.89 m at Rotterdam. The duration of the Rotterdam event matches a two-staged lake drainage scenario better than a single event model. The onset of accelerated transgression at Rotterdam likely coincides with the first event of lake drainage and partial Laurentide ice disintegration (Ellison et al., 2006; Fig. 3.1). Some 150-200 years of partial lake recharge later, a second drainage event caused the final collapse of the Hudson Bay ice-dam, with a more substantial reduction of ice volume (Ellison et al., 2006). The latter event preceded the peak of the 8.2 ka cold spell by just a few decades (Ellison et al., 2006; Fig. 3.1).

Considering all the available data, a two-staged lake drainage event together with rapid disintegration of affected parts of the LIS is the most probable explanation for the sea-level jump associated with the 8.2 ka event. Other high quality sea-level datasets from around the world are needed to further constrain the magnitude of the jump and its globally distributed eustatic fingerprint. If there was a significant Antarctic contribution, the fingerprint will differ strongly from one caused by the Laurentide lake drainage event alone (Kendall et al., 2008). Further resolving the details of the 8.2 ka event is vital if this

event is to be used to test the performance of climate models and to assess their capacity to simulate future climate response to the anticipated freshening of the North Atlantic ocean.

Acknowledgments

Supplementary information to chapter 3

This supplementary material covers: 1) Table S3.1 showing details of the samples used to construct Fig. 3.1, together with three photos of sedimentary successions associated to the sea-level jump; 2) Table S3.2 listing the vertical error calculations; 3) Table S3.3 showing the calculation of the rate of background sea-level rise (BSLR); 4) Table S3.4 containing magnitude of the sea-level jump error calculations and 5) details of used OxCal CQL-routines and plots regarding the timing of the start of the sea-level jump. We start with some remarks regarding robustness and remaining uncertainty and our definition of sea-level jump onset and completion as recorded at Rotterdam.

Robustness and remaining uncertainty

In the main text we calculated the timing and magnitude of the sea-level jump preceding the 8200 BP event, scrupulously accounting for the many uncertainties involved. Extracting a decent number of suitable index-points, from within a brief time interval and assessing associated time-depth errors was possible because for the study area and surroundings a much larger dataset exists that covers this interval and its bracketing intervals (recently integrated and documented; Hijma et al., 2009: Chap. 2). This provides geological context for the selected samples and secures the validity of their selection. Of particular importance is (i) that we were able to trace the sedimentary contact marking the change in depositional environment caused by accelerated sea-level rise for over 30 km inland transgressive distance and similar width (Fig. 3.1; Figs. A4.10-12), (ii) had the rare opportunity to see and sample key intervals in the sequence in building pit outcrops, (iii) the circumstances to sample vertical series of peats at various positions inland from the paleo-coastline, enabling robust selection of those index points that relate to sea-level (Fig. 3.1).

 As far as we are aware, the study presented here is the first to calculate sea-level jump magnitude separated from background rates accounting for all important sources of uncertainty (see Table S3.2). The relative large uncertainty in BSLR and jump magnitude (1.95 ± 0.75 m, 38% resp. 2.11 ± 0.89 m, 42%) is mainly due to propagation of age uncertainty in the BSLR calculation. A remaining age-uncertainty of ± 40/50 cal yr (1 sigma) for dates collected in series and known stratigraphical order is intrinsic to the AMS radiocarbon dating method and hard to avoid. This uncertainty strongly propagates in the calculation of background sea-level rise and hence also in the calculation of the magnitude of the jump. Proper calculation of background sea-level rise is however essential in defining magnitudes of sea-level jumps and for comparing derived magnitudes from different sites.

Defining sea-level jump onset and completion

Sudden accelerated SLR is evident to have started ~8450 yr BP through a marker sedimentary contact which defines the onset of the jump event and which our data pinpoints in time and depth. The moment that SLR returned to its background rate ('normal' melting of remaining ice sheets), however, is not associated to a regionally traceable sedimentary contact. The nature of impact on coastal environments of a metre-magnitude meltwater pulse is that it causes near-instantaneous drowning of considerable areas of former river mouth wetlands (testified by our study area). At downstream positions, change to open water was long lasting, but along the upstream fringe of the impact zone wetland environments naturally returned, implying that SLR had dropped back to background rates. At site ROT this happened ~8300 BP (sample '10'), but it may lag the actual completion of the melt water pulse by a few decades.

Table S3.1

Table S3.1 numbers the samples as in Fig. 3.1. We indicated whether a sample represents inland, local groundwater level or coastal groundwater level pinpointing past sea-level. That distinction follows from palaeo-environmental information obtained from the sampled material, position in the sedimentary succession (ideally: the top centimetre of relative thin transgressed basal peat bed), and from the break in water-level rise trends observed in age-depth plots of series of samples collected vertically from single sites (Fig. 3.1). The deepest-youngest basal peat samples are generally sea-level indicators – all others indicate slightly higher inland groundwater levels similar to what has been firmly established for post-7.5 ka data (Cohen, 2005). This supplement concentrates on the newly collected pre-7.5 ka data in the Rotterdam area (Fig. 3.2). For reference and to show consistency with established SLR for the post-7.5 ka BP interval, Fig. 3.1 includes the published HIL and BAR subsets (Van de Plassche, 1982; Berendsen et al., 2007b). HIL/BAR sample details can be found in the database that exists for the Rhine-Meuse delta in The Netherlands: http://www.geo.uu.nl/fg/palaeogeography/data/avulsions/radiocarbon_dates_Berendsen_&_Stouthamer_2001.pdf.

Collected geological materials were used to (i) construct coastal palaeo groundwater-levels and relative sea-level rise at the Rhine river mouth and (ii) to assess the timing of the sea-level jump, recorded as a regional drowning at the sites in the Rotterdam area (Figs. A4.10-12). Most new sampled material was seen in its original stratigraphical position between 2001 and 2007 by the authors in building-pit outcrops and high-quality cored material and in most cases also sampled by the authors. From our samples, macrofossils of terrestrial plant species were picked by specialists Hanneke Bos and Nelleke van Asch using Dept. of Physical Geography laboratory facilities and submitted for dating. Samples '1', '2', '6', '7' and '14' were sampled from the same building pit exposures as our samples '5', '10', '11', 'a' and 'b', and have been submitted for dating by

BOOR (Bureau Oudheidkundig Onderzoek Rotterdam—archaeological division of Rotterdam municipality). Details on the geology of the study area, such as elevation of the Rhine palaeovalley, are found elsewhere (Busschers et al., 2005; Busschers et al., 2007; Hijma et al., 2009: Chap. 2). These sources provide regional stratigraphical detail on the sampled material including hundreds of radiocarbon dates on overlying and underlying strata confirming the chronological integrity of the dataset presented and used in this paper.

Samples 'a' and 'b' have alternative labelling because they were taken from a local residual channel fill and the relation of their time-depth data to regional palaeo-water levels is not clear. Samples 'a' and 'b' bracket the sedimentary contact in the channel fill (Fig. A4.10). Progressive shallowing of the filling residual channel was interrupted, and replaced by gyttjaic deposition in regionally deepened waters, palynologically reflected as strongly raised concentrations of aquatic plant remnants (Geological Survey of The Netherlands internal reports (Bunnik, 2008; Cremer, 2008)). This gyttjaic-layer was traceable within and between building pits and at site ROT, and in cores downstream to MVL (Fig. 3.1; Figs. A4.10-12). This sedimentary change marks the ~8450 BP western Netherlands drowning event that is linked to the first drainage event. Pollen and diatom data (De Wolf, 1995; Cleveringa and Veldkamp, 1996; Bunnik, 2008; Cremer, 2008; De Wolf, Unpublished) reveal the environment to have become brackish right above the jump-contact at site MVL (Fig. A4.12). At more inland site MSS, sediments initially remained fresh, but record brackish spectra decimetres above (Fig. A4.11). At site ROT ('Blijdorp', Fig. A4.10) pollen indicate a freshwater environment in immediate surroundings, whereas residual channel diatoms indicate slightly brackish environment both before and after the event (*Planothidium delicatulum* and *Fragilarioid sp.*). The typical layering of the lagoonal clay overlying the gyttja at Rotterdam Blijdorp strongly suggests tidal influence. Due to compaction, the difference in elevation between sample 'a' and '2' is only ~1.5 m even though SLR rose >6 m between 8500 and 8000.

Table S3.1 Details of used samples to reconstruct groundwater-level and sea-level rise in the Rotterdam area.

ID[1]	Lab. Nr.[2]	Coord.[3] (X,Y)	Lat., lon.[4] (°N, °E)	Sample depth[5] (m -O.D.)	^{14}C yr BP (1σ)	δ^{13}C (p.mil)	Cal. age range (2σ) (cal. yr BP; %)	Cal yr BP[6] (1σ)	Name (location)	Material	GWL or SL- First index point[7]	Ref.[9]
1	GrA-32037	91078 438453	51°55'51'' 4°27'28''	13.39-13.40	7180±45		8156 8088 8.1 / 8063 7932 87 / 7886 7882 0.3	8001±50	Pit Blijdorp: 2nd pollenbin (ROT)	Top clayey reed peat	GWL	1
2	GrA-32101	91078 438453	51°55'51'' 4°27'28''	13.61-13.62	7160±45		8150 8144 0.4 / 8106 8094 0.8 / 8053 7925 89.8 / 7898 7868 4.4	7981±44	Pit Blijdorp: 2nd pollenbin (ROT)	Bott. clayey reed peat	GWL	1
3	UtC-15340	99670 428378	51°50'28'' 4°35'4''	13.91-13.96	7420±70	-27.4	8382 8153 87.4 / 8141 8131 0.9 / 8122 8104 1.7 / 8095 8049 5.4	8243±79	core 07.09.007 (RID)	*Alnus* fruit (bott. fen-wood peat)	GWL	1
4	UtC-15338	99632 431481	51°52'9'' 4°35'0''	14.05-14.10	7400±60	-26.3	8363 8152 83.9 / 8143 8130 1.3 / 8124 8047 10.2	8229±77	core 07.09.016 (RID)	21 *Populus* bud scales, *Frangula al.*, *Salix cal.* (bott. fen-wood peat)	GWL	1
5	UtC-14941	91671 437648	51°55'25'' 4°28'0''	14.30-14.31	7211±40	-26.1	8160 8084 20.8 / 8072 7955 74.6	8033±55	Pit CS: 12A (ROT)	Mainly *Alnus* fruits/branches (bott. fen-wood peat)	SL[8]	1
6	GrN-30066	91058 438530	51°55'54'' 4°27'27''	15.17-15.18	7560±40		8428 8315 94.9 / 8231 8224 0.5	8373±34	Pit Blijdorp: 1st pollenbin (ROT)	Gyttja/Organic clay	SL	1
7	GrN-30067	91058 438530	51°55'54'' 4°27'27''	15.21-15.22	7560±40		8428 8315 94.9 / 8231 8224 0.5	8373±34	Pit Blijdorp: 1st pollenbin (ROT)	Gyttja/Organic clay	SL	1
8	UtC-15339	92615 436111	51°54'36'' 4°28'50''	15.93-15.96	7710±70	-26.8	8608 8385 95.4	8499±63	core 07.09.201 (ROT)	*Linum usitatissimum* (top clayey fen peat)	GWL	1
9	GrN-30068	91058 438530	51°55'54'' 4°27'27''	15.26-15.27	7740±40		8591 8431 95.4	8512±45	Pit Blijdorp: 1st pollenbin (ROT)	Clayey fen-wood peat	GWL	1
10	UtC-14940	91671 437648	51°55'25'' 4°28'0''	16.30-16.31	7486±41	-25.4	8383 8199 95.4	8298±55	Pit CS: 11B (ROT)	Mainly *Alisma pl.* and *Scirpus lac.* (top fen peat)	SL	1
11	UtC-14939	91671 437648	51°55'25'' 4°28'0''	16.60-16.61	7817±43	-26.4	8724 8508 91.7 / 8499 8457 3.7	8599±60	Pit CS: 10B (ROT)	Mainly *Mentha* and *Carex* (bott. fen-wood peat)	GWL	1
12	UtC-14224	86218 430764	51°51'40'' 4°23'19''	16.71-16.89	7880±70	-26.2	8982 8548 95.4	8737±124	core B37G0548 (POO)	Terr. bot. macrofos. (bott. wood peat)	GWL	2
13	UtC-10757	86817 442257	51°57'52'' 4°23'42''	16.30-16.31	8220±60		9401 9348 6.7 / 9322 9021 88.7	9193±97	core B37E0586 (DEL)	Terr. bot. macrofos. (top loam layer)	GWL	3
14	GrN-29687	91585 439555	51°56'27'' 4°27'54''	17.24-17.25	8850±70		10184 9690 95.4	9942±144	Pit SF (ROT)	Bott. clayey fen-wood peat	GWL	1
15	GrN-21605	76955 438765	51°55'55'' 4°15'16''	18.12-18.16	7810±40		8700 8670 3.1 / 8658 8508 88 / 8499 8457 4.3	8587±50	core B37B0226 (MSS)	Bott. clayey fen peat	GWL	4

Table S3.1 (continued)

ID[1]	Lab. Nr.[2]	Coord.[3] (X,Y)	Lat, lon.[4] (°N, °E)	Sample depth[5] (m -O.D.)	14C yr BP (1σ)	δ13C (p.mil)	Cal. age range (2σ) (cal. yr BP; %)			Cal yr BP[6] (1σ)	Name (location)	Material	GWL or SL- First index point[7]	Ref.[9]
16	GrN-21606	76955 438765	51°55'55'' 4°15'16''	19.07-19.10	8090±40		9233 9133 8919 8885 8832	9228 8971 8893 8862 8782	0.2 87.9 1.4 1.7 4.2	9024±72	core B37B0226 (MSS)	Top clayey fen peat	GWL	4
17	GrN-21607	76955 438765	51°55'55'' 4°15'16''	19.15-19.20	8300±50		9442	9132	95.4	9306±87	core B37B0226 (MSS)	Bott. clayey fen peat	GWL	4
18	UtC-15344	59349 441772	51°57'22'' 3°59'44''	19.63-19.64	7700±60	-27.3	8591	8401	95.4	8490±53	B43 (MVL)	*Alnus* fruit (near top fen-wood peat)	SL	Ch. 3
19	GrN-21460	58991 446620	52°0'2.2'' 3°59'21.5''	20.65-20.68	7720±40		8584	8422	95.4	8498±43	core P18-313	Top fen-wood peat	SL	Ch. 3
20	UtC-15404	59681 442309	51°57'40'' 4°0'1''	21.43-21.46	7910±80	-26.6	8998 8570	8580 8559	94.5 0.9	8773±126	B13-1 (MVL)	*Mentha, Alisma, Carex, Typha* (bott. fen-wood peat)	SL	Ch. 3
21	UtC-15346	57801 439590	51°56'11'' 3°58'25''	24.32-24.39	9450±70	-25.1	11075 10875	10945 10510	16 79.4	10740±151	B68 (MVL)	Mainly *Scirpus, Carex* (bott. fen-wood peat)	GWL	Ch. 3
22	GrN-7859	93535 441250	51°57'23'' 4°29'35''	11.76-11.80	7105±40		8005 7907	7915 7850	64.2 31.2	7929±41	Hilleg. C.5 (HIL)	Bott. fen-wood peat	SL	5
a	UtC-14952	91087 438458	51°55'51'' 4°27'29''	15.12-15.14	7730±42	-28.0	8589	8425	95.4	8505±45	Pit Blijdorp: 4AB (ROT)	*Oenanthe, Alisma, Alnus, Carex* (top fen peat)	RCF	1
b	UtC-14953	91087 438458	51°55'51'' 4°27'29''	15.05-15.09	7610±60	-28.6	8545	8327	95.4	8421±57	Pit Blijdorp: 4C (ROT)	*Oenanthe, Alisma, Alnus, Salix* (bott. lagoonal gyttja)	RCF	1

1 - Number corresponds to number in Fig. 3.1, except 'a' and 'b', they were only used for calculation the timing of the event

2 - GrA- and GrN-samples were dated by the Centre for Isotopes, Groningen, the Netherlands; UtC-samples by R. van de Graaf-lab, Utrecht, the Netherlands

3 - Dutch coordinate system: Rijksdriehoekstelsel. Position in metres.

4 - Position in degrees, minutes, seconds (WGS 1984)

5 - O.D. = Dutch Ordnance Datum (~ mean sea level)

6 - Mean of calibrated age range as calculated by OxCal 4.0.5

7 - Groundwater-level (GWL), sea-level (SL) index point or taken from within a residual channel fill with unknown relation to local groundwater level (RCF)

8 - Relatively large compaction uncertainty

9 - References 1-5 are respectively Hijma et al. (2009), Busschers et al. (2007), Busschers et al. (2005), Cleveringa and Veldkamp (1995) and Van de Plassche et al. (1995). They provide additional sample information. Sample '19' was obtained from Ad van der Spek (pers. comm.)

Table S3.2

We here present our calculations regarding the *vertical* position of relative mean sea-level index points and their error margins. The section follows the methodology developed for sites HIL and BAR (Van de Plassche, 1982; Berendsen et al., 2007b) with the exception that we included tidal amplitudes as an additional error. It follows the numerical sequence used in Table S3.1:

1. *Estimation of upward/downward errors*
   a. Surface elevation: All HIL and BAR data were levelled and have an estimated error of 0.01-0.02 m following Berendsen et al. (2007b). Also samples '1', '2', '6-14' and '21' were levelled with an estimated error of 0.01 m. Sample 18-20 are from boreholes collected offshore. As a rule of thumb, the accuracy decreases with depth at a rate of 0.01 m/m (Pers. comm. with the engineering company Boskalis). Elevations were corrected for the height of the tide at the time of core collection. All other surface elevations were obtained using the AHN (Rijkswaterstaat-AGI, 2005) laser-altimetry digital elevation resource for The Netherlands (5x5 m grid and cm resolution) or the 1:10,000 height map of The Netherlands, both with an associated 0.1 m error (Berendsen and Volleberg, 2007).
   b. Sample depth in core or construction pit: In construction pits we used measuring tape and photographed scale-indicators to determine sample depth ('5' and '10-11') relative to a surface of known elevation (levelled for construction purpose). We set the associated error at 0.1 m. The depth of the samples taken by BOOR was levelled in the construction pit. In core segments, typical of metre length, we measured depth relative to base of core segment during sub-sampling. In the last two cases we used an associated error of 0.02 m.
   c. Palaeo-water depth uncertainty margin: Samples were upward corrected for palaeo-water depth based on peat type (see below). Here, an additional uncertainty around that estimation is included. For fen-wood peat samples we set it to 0.1 m, for fen-peat 0.2 m, for gyttja 0.5 m.
   d. Tidal amplitude: The dated peat layers formed at relative mean high water. Samples were downward corrected with the tidal amplitude to obtain relative mean sea level (see below). As uncertainties with inferring palaeo-tidal amplitudes are large (depth and age uncertainties of the palaeobathymetry of the transgressing southern North Sea, and choice of oceanic tide solution used as input for regional numerical tidal modelling), we set them to 75% of the estimated tidal amplitude.

The combined error follows from standard cumulative error propagation rules.

2. *Employed upward/downward corrections*

a. Correction for palaeo-water depth: Fen-wood peat is considered to form at the year-round mean (ground)water level. Ecological studies show fen-peat to form typically at 0.5 m of water depth (Den Held et al., 1992) in modern situations. The dominant botanical macrofossils in sample '10' (*Alisma plantago*, *Scirpus lacustris*) indicate year-round water depths < 0.5 m; water depth was estimated to be 0.3 m. Gyttja is arbitrarily assumed to have formed in water depths of ~0.75 (samples '6-7'). Sample '17' was taken from a very wet palaeosoil and estimated to have formed on average at 0.1 m *above* year-round mean water level. Sample '19' was taken from a peat layer of unknown botanical content. We therefore set the water depth at 0.25 m, right in between fen-wood and fen-peat.

b. Correction for palaeo-tidal amplitudes: Tidal amplitudes in the early Holocene were very low near the study area due to the configuration of the southern North Sea. Large parts still lay dry and full connection between the northern North Sea and the Strait of Dover comparable to today may have established as late as ~8000 BP (Conradsen and Heier-Nielsen, 1995; Lambeck, 1995; Jiang et al., 1997; Van der Molen and Van Dijck, 2000). Timing and configuration of the initial connection is not well established, however, and could have occurred earlier, e.g. during the jump. The establishment of an amphidromic system within the southern North Sea during the jump would have led to a slight drop (a few decimetres) of local MSL and a slight increase of tidal amplitudes that would have nearly balanced out (Van der Molen and De Swart, 2001a). Irrespective, tidal amplitudes at sea near the study area increased during the event due increasing water depths in the North Sea. They were modelled to be 0.3 m and 0.5 m for 8500 and 8000 BP respectively (Van der Molen, 2002). Mapping shows the early-middle Holocene Rhine-estuary to have been relative wide and to have hosted many storage basins (Hijma et al., 2009: Chap. 2). Such implies the incoming tidal wave to have diminished in amplitude in an upstream direction, known as the flood-basin effect (Zonneveld, 1960; Jelgersma, 1961). We therefore set the tidal amplitude for the sea-level index points at 0.15 m and 0.25 m for 'pre jump' and 'post jump' sea-level index- points respectively (Fig. S3.1). For groundwater-level index-points inland, no tidal amplitude is considered.

c. Correction for post-depositional compaction: Peats at the base of Holocene deltaic wedges typically are compacted considerably, the degree depending on peat-composition and thickness, weight and sedimentation history of the overburden. Vertical displacement for samples taken almost directly above consolidated substrate may range from centimetres to decimetres. Vertical correction was obtained by applying a factor of 2.5 to the height of the top and a factor of 1.5 to the height of the base of the sample above a consolidated substrate (e.g. sand). For example, from a peat layer of 0.20 m in thickness and situated above a consolidated substrate, a sample was

taken between 0.01 and 0.02 m below the top. This sample is 'decompacted' to have formed 0.27-0.48 m above the consolidated surface. The correction factors follow a study of Van de Plassche and co-workers (Van de Plassche et al., 2005). They based their maximum factor estimate on an age-depth analysis from the central Netherlands which indicated a compaction factor of slightly more than 2 (Gotjé, 1993). The factor for the base of the sample is arbitrarily derived. We collected basal peat overlying sands, and in some cases pedogenetically altered loams of Late Glacial-early Holocene age (Busschers et al., 2007; Hijma et al., 2009: Chap. 2). We consider the latter to have been subaerially consolidated to their stiffened state and thickness before peat formation set on (Cohen, 2005). Most peats were sampled very close to the consolidated substrate and upward correction due to 'decompaction' is up to a few decimetres. Samples '1', '2' and '5' are underlain by > 2 m of poorly consolidated freshwater-tidal clays (Hijma et al., 2009; Fig. A4.10) for which established compaction correction procedures are not applicable. We applied a correction of 0.75 m and 0.5 m for the top respectively bottom of the sample, which provides a minimum elevation only (arrows in Fig. 3.1). Sample '19' was taken from core P18-313 (Fig. A4.12) that does not reach a consolidated substrate. As basal peat layers in the study area seldom exceed a few decimetres thickness, we assumed the consolidated substrate to be just below core termination to assess compaction which may have led to underestimation (hence arrow-indication in Fig. 3.1).
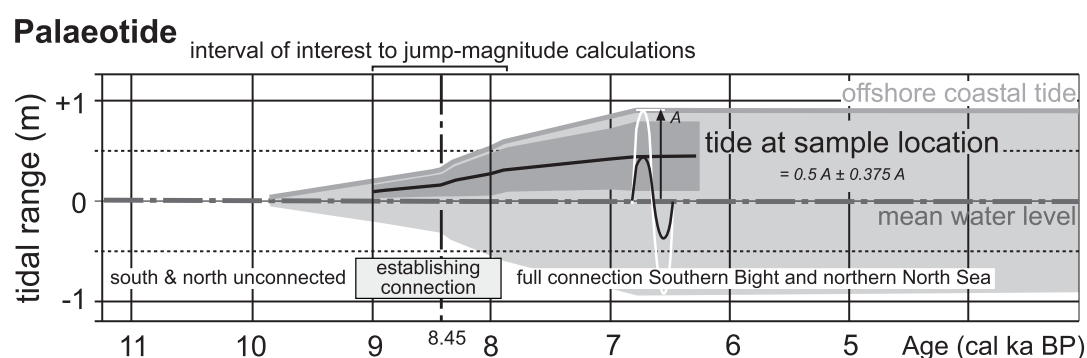
Figure S3.1 The offshore tidal amplitude throughout the Holocene along the coast near Hoek van Holland (upper grey line, based on Van der Molen and De Swart, 2001a). For the sample sites in the Rhine-Meuse estuary, we assumed the tidal amplitude (black line) to be half the offshore value due to the flood-basin effect and used that value in our calculations. Because of the many uncertainties involved, we set the uncertainty at 75% of the tidal amplitude at the sample location (or 37.5% of the offshore tidal amplitude). The development of the connection between the Southern Bight and the northern North Sea is based on a compilation of published articles Conradsen and Heier-Nielsen (1995), Lambeck (1995), Jiang et al. (1997) and Van der Molen and Van Dijck (2000).

Table S3.2 Error-margin calculations for used time-depth data. See Table S3.1 for details. For sea-level index points, calculated error margins represent relative MSL.

ID[4]		Upward/downward uncertainties							Upward/downward corrections					Total vertical error ranges				Lower compact. limit	Lower MSL limit	
	A Top depth (m -O.D.)[5]	B Bottom depth (m -O.D.)	C Surf. elevat. (m)	D Depth in core or pit (m)	E Water depth (m)	F Tid. ampl. (m)	G1 Total vertical error 1σ (m)	H=2xG Total vertical error 2σ (m)	I W[6]	J T[7]	K P[8]	L2 C1[9]	M3 C2[10]	N=A-G-I+J-L Min. depth top 1σ (m -O.D.)	O=B+G-I+J-L Max. depth base 1σ (m -O.D.)	P=A-H-I+J-L Min. depth top 2σ (m -O.D.)	Q=B+H-I+J-L Max. depth base 2σ (m -O.D.)	R=B+K Top consolid. substrate (m -O.D.)	S=R+F+J Lower MSL limit (m -O.D.)	Mat.
1	13.39	13.40	0.01	0.02	0.20	0.19	0.28	0.55	0.50	0.25	0.00	0.75	0.50	12.11	12.93	11.84	13.20	?	?	Fen peat
2	13.61	13.62	0.01	0.02	0.20	0.19	0.28	0.55	0.50	0.25	0.00	0.75	0.50	12.33	13.15	12.06	13.42	?	?	Fen peat
3	13.91	13.96	0.10	0.02	0.10	0.00	0.14	0.29	0.00	0.00	0.00	0.13	0.00	13.64	14.10	13.50	14.25	13.96	13.96	Fen-wood peat
4	14.05	14.10	0.10	0.02	0.10	0.00	0.14	0.29	0.00	0.00	0.00	0.12	0.00	13.78	14.24	13.64	14.39	14.10	14.10	Fen-wood peat
5	14.30	14.31	0.01	0.10	0.10	0.19	0.24	0.47	0.00	0.25	0.30	0.75	0.50	13.56	14.30	13.33	14.53	Same as '10'	Same as '10'	Fen-wood peat
6	15.17	15.18	0.01	0.02	0.50	0.00	0.50	1.00	0.75	0.00	0.09	0.25	0.14	13.67	14.80	13.17	15.30	15.27	15.27	Fen peat
7	15.21	15.22	0.01	0.02	0.50	0.00	0.50	1.00	0.75	0.00	0.05	0.15	0.08	13.81	14.90	13.31	15.40	15.27	15.27	Fen peat
8	15.93	15.96	0.01	0.02	0.20	0.00	0.20	0.40	0.50	0.00	0.00	0.08	0.00	15.15	15.66	14.95	15.86	15.96	15.96	Fen-wood peat
9	15.26	15.27	0.01	0.02	0.10	0.00	0.10	0.20	0.00	0.00	0.00	0.02	0.00	15.13	15.37	15.03	15.47	15.27	15.27	Fen peat
10	16.30	16.31	0.01	0.10	0.20	0.19	0.29	0.58	0.30	0.25	0.30	0.77	0.45	15.18	16.10	14.89	16.39	16.61	17.05	Fen peat
11	16.60	16.61	0.01	0.10	0.10	0.00	0.14	0.28	0.00	0.00	0.00	0.02	0.00	16.43	16.75	16.29	16.89	16.61	16.61	Fen-wood peat
12	16.71	16.89	0.01	0.02	0.10	0.00	0.10	0.20	0.00	0.00	0.00	0.45	0.00	16.16	16.99	16.06	17.09	16.89	16.89	Fen-wood peat
13	16.30	16.31	0.01	0.02	0.20	0.00	0.20	0.40	-0.10	0.00	0.00	0.02	0.00	16.17	16.61	15.97	16.81	16.31	16.31	Palaeo-soil
14	17.24	17.25	0.01	0.02	0.10	0.00	0.10	0.20	0.50	0.00	0.00	0.03	0.00	16.61	16.85	16.51	16.95	17.25	17.25	Fen peat
15	18.12	18.16	0.10	0.02	0.20	0.00	0.22	0.45	0.50	0.00	0.15	0.47	0.23	16.92	17.66	16.70	17.88	18.31	18.31	Fen peat
16	19.07	19.10	0.10	0.02	0.20	0.00	0.22	0.45	0.50	0.00	0.10	0.33	0.15	18.02	18.67	17.80	18.90	19.20	19.20	Fen peat
17	19.15	19.20	0.10	0.02	0.20	0.00	0.22	0.45	0.50	0.00	0.00	0.13	0.00	18.30	18.92	18.08	19.15	19.20	19.20	Fen peat
18	19.63	19.64	0.20	0.02	0.10	0.11	0.25	0.50	0.00	0.15	0.00	0.03	0.00	19.51	20.04	19.26	20.29	19.64	19.90	Fen-wood peat
19	20.65	20.68	0.21	0.02	0.15	0.11	0.28	0.56	0.25	0.15	0.15	0.45	0.23	19.82	20.63	19.54	20.91	20.83	21.09	Fen peat
20	21.43	21.46	0.21	0.02	0.10	0.11	0.26	0.53	0.00	0.15	0.09	0.30	0.14	21.02	21.74	20.75	22.00	21.55	21.81	Fen-wood peat
21	24.32	24.39	0.24	0.02	0.10	0.00	0.26	0.53	0.00	0.00	0.00	0.18	0.00	23.88	24.65	23.62	24.92	24.39	24.39	Fen-wood peat
22	11.76	11.80	0.01	0.02	0.10	0.19	0.21	0.43	0.00	0.25	0.00	0.10	0.00	11.70	12.26	11.48	12.48	11.80	12.24	Fen-wood peat

1 - G=$\sqrt{C^2+D^2+E^2+F^2}$; 2 - L=(B+K-A)*2.5; 3 - M=(K)*1.5; 4 - Number corresponds to number in Fig. 3.1

5 - O.D. = Dutch Ordnance Datum ~ mean sea level; 6 - Correction for water depth (m); 7 - Correction for tidal amplitude (m); 8 - Peat below sample (m)

9 - Correction compaction max. (top; m). For samples 1, 2, 5 formulae L and M were not used due their position high above a consolidated substrate which would have yielded unrealistic values. Instead, fixed correction values of 0.75 and 0.5 m were used for the top and base respectively.

10 - Correction compaction min. (base; m).

3. *Total vertical error (ranges displayed in Fig. 3.1)*

   a. <u>minimum depth top 1σ</u>: obtained by adding upward vertical error (1σ) and upward corrections for water level and compaction to the elevation of the top of the sample minus the downward correction for the tidal amplitude;

   b. <u>maximum depth base 1σ</u>: obtained by adding downward vertical error (1σ) and upward correction for water level and compaction to the elevation of the base of the sample minus the downward correction for the tidal amplitude. When used in calculations this value is not allowed to exceed the lower MSL limit;

   c. <u>minimum depth top 2σ</u>: obtained by adding upward vertical error (2σ) and upward corrections for water level and compaction to the elevation of the top of the sample minus the downward correction for the tidal amplitude;

   d. <u>maximum depth base 2σ</u>: obtained by adding downward vertical error (2σ) and upward correction for water level and compaction to the elevation of the base of the sample. When used in calculations this value is not allowed to exceed the lower MSL limit.

Table S3.3

Table S3.3 shows how the rate of BSLR was calculated. We calculated the rate both before and after the sea-level jump using the available index points. Before the jump, samples '18-20' were used, while after the jump samples '1-2', '5', '10' and '22' were used. Lines of maximum and minimum slope were manually fitted through the error boxes, while assuring each line crosses all 1-SIGMA boxes and touched one on its extreme left side and another on its extreme right side. The best fit is the average slope and the error the difference between the maximum and minimum slope. This yielded a BSLR rate of 10.3 mm/yr ± 76% before the jump and 11.5 mm/yr ± 42% after the jump. The latter high rate is primarily caused by 'sample 5'. Although error margins are inevitably relatively big, the average rates compare well with the results of a recent modelling study (Vink et al., 2007) that calculated a BGR of 9-10 mm/yr for the period 9000-8000 BP. We consider BSLR rates lower than 8.5 mm/yr and higher than 11.5 mm/yr highly unlikely (amongst others given the trends from regional data sets used in (Cohen, 2005)) and constrained BSLR to 10 mm/yr ± 15% and used that value and error in subsequent calculations.

For cross-validation, we fed the derived 2.11 ± 0.89 m (1σ) sea-level jump (Table S3, see below) to a linear regression analysis to calculate BSLR using samples '18-19' (pre-jump) and '1-2', '5', '10' and '22' (post-jump). The elevations of the latter were lowered with the magnitude of the sea-level jump to obtain a sample-elevation had the sea-level jump not occurred, and we did so for three scenarios with jumps of 1.22 m, 2.11 m and 3.00 m. Regression analysis on the result yields background rates of SLR between ~8.4-11.4 mm/yr, in good agreement with the *prior* defined range of 10 mm/yr ± 15%.

74

Table S3.3 Calculation of the background rates of sea-level rise.

Background rate of SLR after the sea-level jump

Input data

ID[1]	Lab. Nr.[2]	Mean age (Cal yr BP)	1σ error	Mean depth (m -O.D.)	1σ error	A Max slope (mm/yr)	B Min slope (mm/yr)	C=(A+B)/2 mean rate (mm/yr)	D=(A-B)/2 1s error (%)
22	GrN-7859	7929	41	11.97	0.27				
1	GrA-32037	8001	50	12.52	0.41				
2	GrA-32101	7981	44	12.74	0.41	16.4	6.6	11.5	42
5	UtC-14941	8033	55	13.93	0.37				
10	UtC-14940	8298	55	15.64	0.46				

Background rate of SLR before the sea-level jump

Input data

ID[1]	Lab. Nr.[2]	Mean age (Cal yr BP)	1σ error	Mean depth (m -O.D.)	1σ error	E Max slope (mm/yr)	F Min slope (mm/yr)	G=(E+F)/2 mean rate (mm/yr)	H=(E-F)/2 1s error (%)
18	UtC-15344	8490	53	19.70	0.20				
19	GrN-21460	8498	43	20.23	0.41	18.1	2.4	10.3	76
20	UtC-15404	8773	126	21.38	0.36				

Regression analysis of the background rate of SLR for the period ~8.5-8.0 kyr BP when substraction a sea-level jump with the range of 2.11 ± 0.89 m

Input data

ID[1]	Table nr.[3]	Lab. Nr.[2]	K Mean age (Cal yr BP)	L 1σ error	M Mean depth (m -O.D.)	N Range of sea-level jump (m)	O Elevation sample without 1.22 m jump	P Elevation sample without 2.11 m jump	Q Elevation sample without 3 m jump	R[4] BGR1.22 = slope (K1:K7,O1:O7)*1000 (mm/yr)	S BGR2.11 = slope (K1:K7,O1:O7)*1000 (mm/yr)	T BGR3 = slope (K1:K7,O1:O7)*1000 (mm/yr)
19	1	GrN-21460	8498	43	20.23	**min**	20.23	20.23	20.23			
18	2	UtC-15344	8490	53	19.57	1.22	19.57	19.57	19.57			
10	3	UtC-14940	8298	55	15.64	**mean**	16.86	17.75	18.64	11.43	9.89	8.35
5	4	UtC-14941	8033	55	13.93	2.11	15.15	16.04	16.93			
2	5	GrA-32101	7981	44	12.74	**max**	13.96	14.85	15.74			
1	6	GrA-32037	8001	50	12.52	3.00	13.74	14.63	15.52			
22	7	GrN-7859	7929	41	11.97		13.19	14.08	14.97			

1 - Number corresponds to number in Fig. 3.1

2 - For details: See Tables S3.1 and S3.2

3 - These cell numbers are used in the equations. 'A2' refers e.g. to the value in cell A2

4 - BGR = Background rate

This agreement is less good when a background rate of 9 or 11 mm/yr (and according magnitude and 1σ range) are explored, suggesting that BSLR indeed approximated 10 mm/yr.

Table S3.4

Table S3.4 shows how the magnitude of the sea-level jump was calculated using samples '10', '18' and '19'. As samples '18' and '19' are from the same area (~5 km apart) we combined their age with OxCal to a single date, 8493 ± 40 BP (column A/B). We then calculated the difference in age between this date and the date of sample '10' (columns E/F) to be 195 ± 68 yr. In this period sea-level rose 4.06 ± 0.50 m (columns G/H). We did not use index point '19''s vertical position, as its (de)compaction may be underestimated (see Table S2). Had no jump occurred, sea-level rise would have risen with 10 ± 1.5 mm/yr for this period, in total 1.95 ± 0.74 m (columns K/L). This means that an additional jump of 2.11 ± 0.89 m is needed to explain the observed sea-level rise (M/N).

We conservatively evaluated the statistical significance of observed SLR acceleration in the series of index-points. Using a t-test we estimate the chance that the observed rise of 4.06 ± 0.5 m resembles the independently predicted BSLR of 1.95 ± 0.74 m. We set the number of samples (n1, n2) at 2 (the minimum value, i.e. the most conservative). Using the below formulae, this yields a Students-t of 3.34 and a d.o.f. of 2 and a two-tailed probability of ~8%. (Excel-function TDIST). Soon as we weigh additional sedimentary information, such as the change from slowly accumulation of peat to rapidly aggrading gyttjaic mud and back to peat, that implies increased n (e.g. n1= 4) and the probability that all rise is BSLR drops to below 1%.

$$t = \frac{\overline{\chi}_1 - \overline{\chi}_2}{\sqrt{\dfrac{s_1^2}{n_1} + \dfrac{s_2^2}{n_2}}} \qquad\qquad d.o.f. = \frac{\left(\dfrac{s_1^2}{n_1} + \dfrac{s_2^2}{n_2}\right)^2}{\left(\dfrac{s_1^4}{n_1^2(n_1-1)} + \dfrac{s_2^4}{n_2^2(n_2-1)}\right)}$$

The fact that the key samples '10' and '18' are from sites ~30 km apart does not necessitate a correction for the river gradient effect. Prior to the sea-level jump, our inland sites such as (ROT) show a regional inland groundwater table raised above MSL due to the river gradient – but during the 4 meter of MSL rise towards sample '10' the water level became fully controlled y MSL. At the downstream site MVL, the transition from 'river gradient affected' groundwater tables above MSL/MHW to estuarine water tables at MSL/MHW is made prior to the jump event, as curves in Fig. 3.1 show. The river gradient effect does apply to samples of similar age taken at the respective sites. For example, samples '19' and '12' have similar ages, yet the sample at the Maasvlakte site is situated almost 4 m lower, implying a river gradient of ~0.12 m/km.

76

Table S3.4 Calculation of the magnitude of the sea-level jump.

Input data			Chronology (yr) Before present					Elevation (m) Relative MSL[1]			
			A	B	C[3]	D[4]	ID[6]	E	F	G = E1 - E2	H[5]
ID[6]	Table numbering[7]	Lab. Nr.[8]	Cal yr BP	1σ error (yr)	Time span (yr)	1σ error (yr)		Mean depth (m -O.D.)	1σ error (m)	Difference in elevation (m -O.D.)	1σ error (m)
18/19	1	UtC-15344 / GrN-21460	8493	40	195	68	18	19.70	0.20		
10	2	UtC-14940	8298	55			10	15.64	0.46	4.06	0.50

I = 10 mm/yr (background rate of SLR)   **J = ± 15% (1σ error background rate)**

Magnitude calculation

K=C*I	L[9]		M=G-K	N=√(H²+L²)

Background rise (m)	1σ error (m)	Magnitude jump (m)	1σ error (m)
1.95	0.74	**2.11**	**0.89**

1 - Derived from Table A4.2
3 - C=A1-A2
4 - D=√(B1²+B2²)
5 - H=√(F1²+F2²)
6 - Number corresponds to number in Fig. 3.1
7 - Cell numbers are used in the equations. 'A2' refers e.g. to the value in cell A2.
8 - For details: See Tables S3.1 and S3.2
9 - L=(√(J²+(D*100/C²))/100*K

Chronological Query Language (CQL) routines

This section provides OxCal 4.0.5 CQL-routines (Bronk Ramsey, 1995; 2001; using IntCal04 from Reimer et al., 2004) for calculation of event ages and associated uncertainty (1σ) based on the collected assemblage of dates in their sequential sedimentary context.

Dates immediately below the drowning event

Dates '9', '15', '18', '19' and 'a' were each sampled directly below non-erosive sedimentary contacts marking sudden accelerated transgression, i.e. transition to deeper water conditions (peat to gyttja). Dates '9' and 'a' are from samples taken from the same organic horizon, 80 m apart within construction pit ROT-Blijdorp. Dates '18' and 'a' were obtained from selected macrofossils. Dates '9', '15' and '19' are conventionally dated bulk material. The R_Combine statement below yields a combined age of 7746 ± 20 ^{14}C yr BP or 8522 ± 37 BP (1σ; Fig. S3.2):

```
R_Combine("")
 {
  R_Date("9",7740,40);
  R_Date("15",7810,40);
  R_Date("18",7700,60);
  R_Date("19",7720,40);
  R_Date("a",7730,42);
};
```
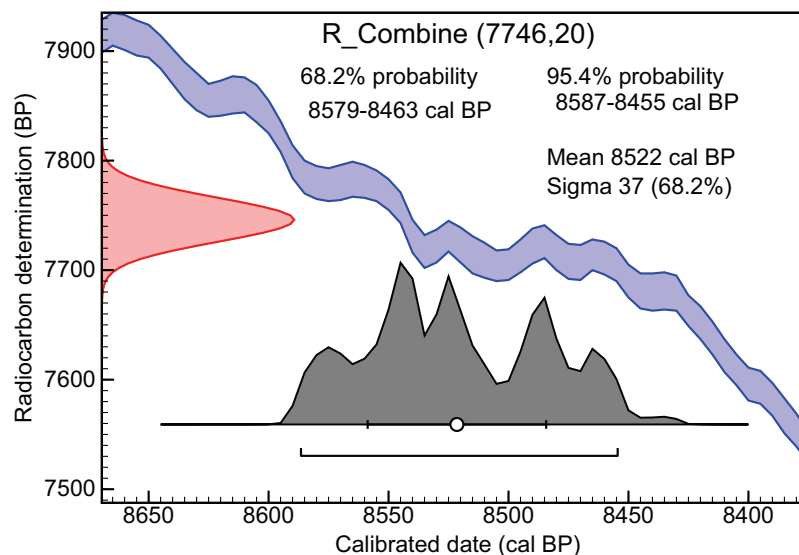

Figure S3.2 R_combine calculation of five radiocarbon dates just below the drowning event.

Dates immediately above the drowning event

Dates '6', '7' and 'b' were each sampled directly above a non-erosive sedimentary contact marking sudden transition to deeper water conditions. Dates '6' and '7' (both bulk samples) were obtained 4 cm above each other at the base of a detritus/organic clay layer, situated above wood peat from which date '9' was obtained.

The accumulation of detritus overlying wood peat indicates sudden drowning of the swamp forest.Sample 'b' was taken from a gyttja layer that immediately overlies a clayey peat layer from which date 'a' was obtained (Fig. A4.10). The R_Combine statement below yields a combined age at 7569 ± 26 ^{14}C yr BP or 8385 ± 16 BP (1σ; Fig. S3.3).

```
R_Combine("")
 {
  R_Date("6",7560,40);
  R_Date("7",7560,40);
  R_Date("b",7610,60);
 };
```
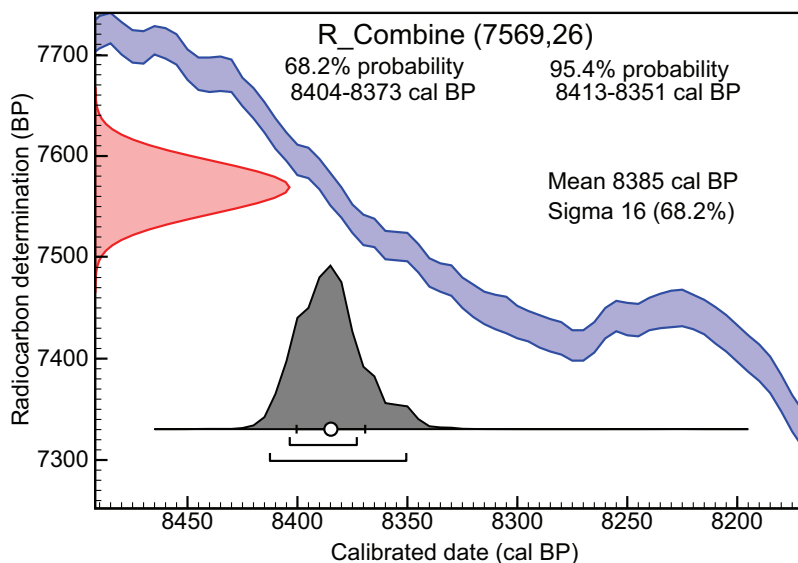

Figure S3.3 R_combine calculation of three radiocarbon dates from just above the drowning event.

Timing of the start of the sea-level jump event

The lateral continuity of the gyttja of site 'b' and the detritus of '6/7' is evident from tracing the outcrop along the building pit wall as well as tracing the gyttja layer across the entire study area (see Figs. A4.10-12 and accompanying text). This made the ROT Blijdorp building-pit dataset very suitable for constraining the timing of the drowning event. The event occurred between 7746 ± 20 and 7569 ± 26 ^{14}C yr BP and based on the CQL-routine below, most probably at 8450 ± 44 (1σ; results in Fig. 3.3 and Table S3.5).

```
Sequence()
{
 Boundary(R_Date("below drowning event",7746,20));
 Date("drowning event");
 Boundary (R_Date("above drowning event", 7569, 26));
};
```

Table S3.5 Oxcal-output of the calculated start of the sea-level jump.

Name	Unmodelled (BP)								Modelled (BP)							
	from	to	%	from	to	%	μ	1σ	from	to	%	from	to	%	μ	1σ
Boundary	8404	8373	68.2	8413	8351	95.4	8385	16	8405	8374	68.2	8415	8350	95.4	8386	16
R_Date above sea-level jump	8404	8373	68.2	8413	8351	95.4	8385	16								
start sea-level jump									8482	8394	68.2	8544	8375	95.4	**8450**	**44**
Boundary	8579	8463	68.3	8587	8455	95.4	8522	37	8555	8457	68.2	8586	8452	95.4	8515	39
R_Date below sea-level jump	8579	8463	68.3	8587	8455	95.4	8522	37								

4 Development of a mid-Holocene estuarine basin, Rhine-Meuse mouth area, offshore The Netherlands

Abstract

This study shows the response of a Holocene estuarine basin in The Netherlands to rapid rates of sea-level rise. High resolution seismic data, lithological information and ^{14}C-dates were collected offshore the western Netherlands on the lower shoreface. They reveal well preserved late Weichselian-early Holocene terrestrial and middle Holocene back-barrier deposits in an estuarine setting. They are overlain by subrecent lower shoreface deposits. Back-barrier tidal channels started to fill in between 8.3-7.4 cal ka BP. At that time, the main Rhine outlet shifted north to a position directly east of the study area and began dumping sediment into the tidal basin. Together with the ongoing decrease in both the rate of sea-level rise and tidal amplitude increase, the shift caused tidal-prism decrease and channel infilling. The tidal-channel fills and occasionally the terrestrial deposits are truncated due to wave-action during the landward migration of the coastline through the study area. This happened before 6.6 ka BP. At least one event of barrier overstepping occurred between 7.5 and 6.6 ka BP and was most likely governed by rapid sea-level rise. Barrier rollover could not keep up with back-barrier basin widening on the landward side and at a certain point the barrier was overstepped. The back-barrier channels migrated laterally only tens of metres in several hundreds of years and do not show a typical tidal channel configuration, but are rather straight. This was caused by the thick estuarine clays in which they were embedded, hindering lateral migration, and the pre-existing, straight estuarine channel pattern that they inherited.

The development of the study area shows that besides sea-level changes, river-mouth shifting, substrate gradient and type are important governing factors in the behaviour of back-barrier systems.

4.1   Introduction

Transgressive depositional sequences are highly variable (Cattaneo and Steel, 2003) and usually only their basal parts are preserved (Belknap and Kraft, 1981). As a result, using such sequences to reconstruct and understand past coastal behaviour is difficult. A proper understanding of this behaviour is critical however, because it is a prerequisite for the prediction of future coastal response to the expected acceleration in sea-level rise (SLR). Methods of investigation of Holocene transgressive sequences vary. Onshore, reconstructions are based on core descriptions, geomorphological mapping and/or ground-penetrating radar (e.g. Neal, 2004). Offshore, seismic data have been used successfully in combination with core descriptions to study Holocene transgressive deposits.

In the western Netherlands (Fig. 4.1), the Holocene transgressive sequence in the Rhine-Meuse river mouth area has been described in detail for the onshore part. During the Holocene, this area hosted a wide estuary in which several distributaries debouched. Before 7.2 ka BP (all ages in calendar years) and after 2 ka BP, this palaeo-estuary was situated in the Rotterdam area. In between, the estuary of the Rhine was situated in the Leiden area, while the Meuse-estuary remained near Rotterdam (e.g. Pons et al., 1963; De Groot and De Gans, 1996; Berendsen and Stouthamer, 2000; Hijma et al., 2009: Chap. 2; Fig. 4.1). North of the Rotterdam palaeo-estuary, offshore seismic data and corings showed that back-barrier tidal-channel systems existed before 7 ka BP. Their behaviour was governed by changing tidal amplitudes, rates of SLR and sediment supply (Rieu et al., 2005; Fig. 4.1). A second offshore study directly west of the present Rotterdam estuary proved the presence of river-mouth environments in that area before 7 ka BP. It also provided evidence for a strong link between shifting distributaries and coastal development (Van Heteren et al., 2002; Fig. 4.1). Both areas became located on the lower shoreface after 6.5 ka BP when the shoreline shifted to the east of these areas (Van Heteren et al., 2002; Rieu et al., 2005). This study aims (1) to determine how much of the Holocene transgressive record is preserved in the transitional zone between river-mouth and adjacent back-barrier areas and (2) to analyse the response of a Holocene estuarine basin in this zone to rapid rates of SLR. Using seismic data, core descriptions, radiocarbon ages and detailed onshore reconstructions made previously (Hijma et al., 2009: Chap. 2), we specifically study the influence of the nearby Rhine-Meuse palaeo-estuary on the coastal system.

The study area (Fig. 4.1) is part of the southern North Sea basin and lies 2-7 km offshore on the lower shoreface. Present water depths are in the order of 12-15 m. During the Last Glacial Maximum lowstand, large parts of the southern North Sea, including the study area, lay exposed. The southern North Sea was dissected by the Rhine-Meuse valley (Laban, 1995; Busschers et al., 2007). The terrestrial landscape was transgressed during the post-glacial SLR. The pace and nature of the transgression was controlled by the rate of

82

SLR, sediment supply, river-mouth position, tidal regime and antecedent morphology. As it was flooded, the terrestrial landscape was locally eroded by tidal channels, but primarily was buried by mud and peat in a back-barrier setting (Beets et al., 1995; Rieu et al., 2005). After the shoreline had bypassed the now offshore areas, the back-barrier deposits were truncated by shoreface erosion (Rieu et al., 2005). At present, a thin active layer covers an incomplete sequence of Holocene coastal sediments.

In the following part, the geology and palaeogeographical development of the western Netherlands and the study area will be shortly reviewed to provide a proper framework for this chapter.
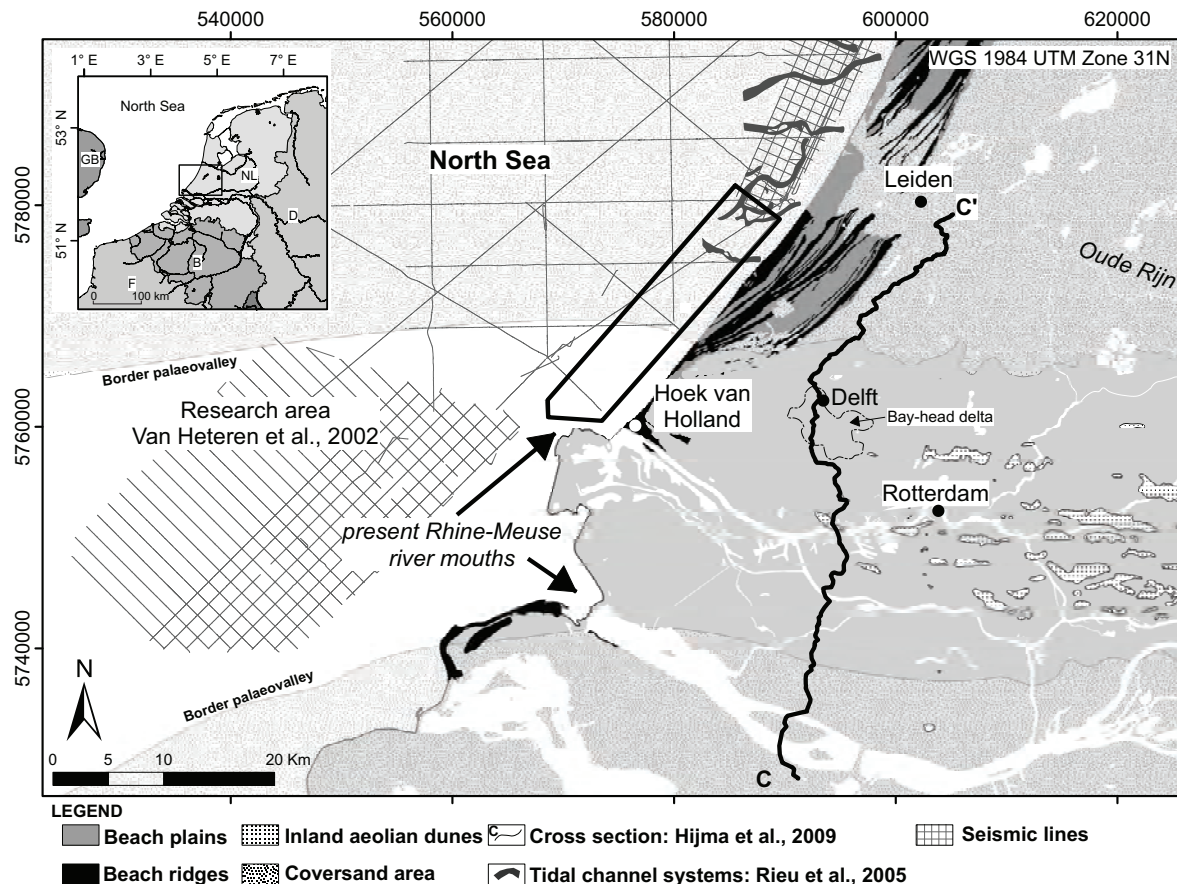
Figure 4.1 Position of the study area offshore The Netherlands (black rectangle). Also shown are mapped Atlantic tidal channels (Rieu et al., 2005), the study area of Van Heteren et al. (2002), the location of the westernmost cross section of Hijma et al. (2009: Chap. 2) as well as the position of a bay-head delta deposit (Hijma et al., 2009: Chap. 2), inland aeolian dunes and the coversand area that borders the palaeovalley. See text for further explanation.

4.1.1 Late Pleistocene and early-mid Holocene developments in the western Netherlands

At the end of the Pleistocene, the Rhine-Meuse system had formed an east-west trending valley that was 40 km wide at the present coastline and in which coarse, gravelly sands were deposited (e.g. Pons, 1957; Zagwijn, 1974; Törnqvist et al., 2003; Busschers et al., 2007). On both the north and south side it was flanked by 1-2 m higher areas that are Weichselian terraces covered by aeolian sand sheets (Fig. 4.1: coversand area). During the Younger Dryas-early Holocene (Fig. 2.2) the Rhine and Meuse contracted to a few incised channels and during high discharge events a loamy clay bed was deposited, covering large parts of the palaeovalley. Aeolian dunes (up to 15 m high) were blown out of seasonally dry riverbeds (Pons and Bennema, 1958; Berendsen and Stouthamer, 2000). At the onset of the Holocene, sea level in the southern North Sea was more than 60 m lower than today (Jelgersma, 1979) and the present-day southern North Sea was still land. At the end of the Atlantic (6 ka BP), sea level had risen to 5 m below present mean sea level (Fig. 4.2). The rapidly rising sea level forced the groundwater table up, stimulating widespread peat growth ('basal peat', starting ~11 ka BP) in a zone that shifted landward as groundwater continued to rise (Vermeer-Louman, 1934; Bennema, 1954b; Jelgersma, 1961).
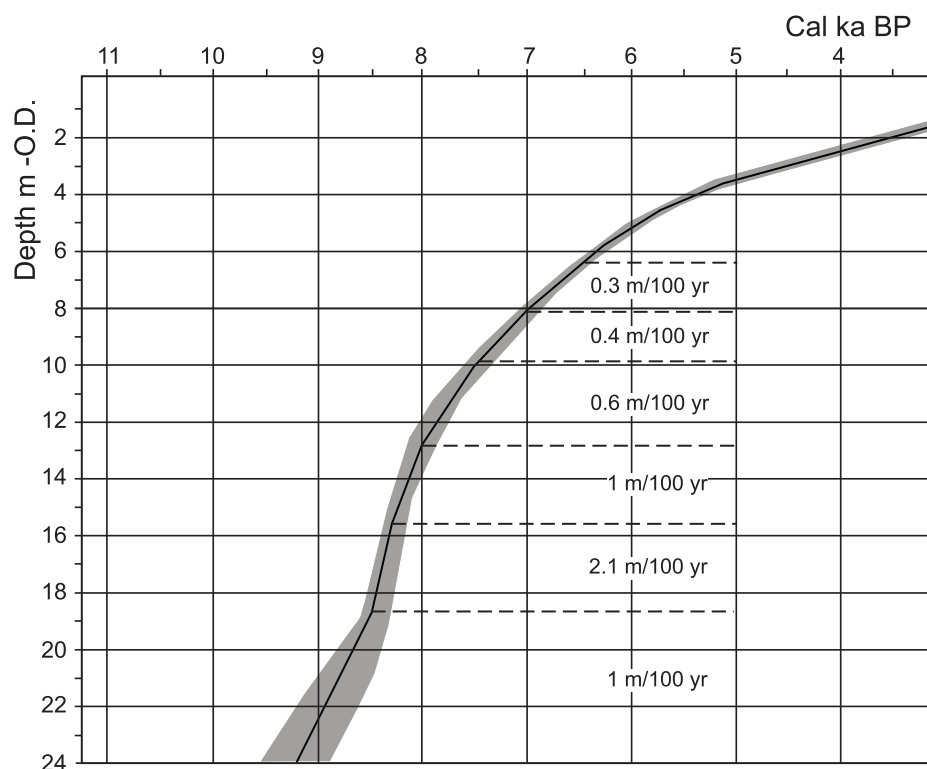
Figure 4.2 Sea-level curve for the western Netherlands, Rotterdam area based on Hijma and Cohen (In press: Chap. 3) and Van de Plassche (1995).

Coevally, rivers started raising their beds and aggradational overbank deposits accumulated in permanently flooded basins (Van der Woude, 1983) under increasing tidal influence (Hijma et al., 2009: Chap. 2). Most of the central western Netherlands was made up of back-barrier basins behind a series of inferred barrier islands (Beets and Van der Spek, 2000; Rieu et al., 2005). Constant coastal retrogradation occurred as sediment-supply rates were insufficient to keep up with the expanding tidal basins caused by SLR. Before 8 ka BP the Rhine-Meuse estuary was located south of or in the southern part of the study area (Pons et al., 1963; De Groot and De Gans, 1996; Van Heteren et al., 2002; Hijma et al., 2009: Chap. 2). After 8 ka BP the Rotterdam Rhine-Meuse estuary gradually started to lose discharge and ~7.2 ka BP, a new Rhine-estuary in the Leiden area had become the main Rhine outlet, while the Meuse remained in the Rotterdam area (Berendsen and Stouthamer, 2000; Hijma et al., 2009: Chap. 2). The relict promontory of the Rotterdam-estuary near Hoek van Holland (Fig. 4.1) was eroded and the sediment transported to the north by net longshore transport in the following centuries (Van Straaten, 1965; Van Heteren et al., 2002).

Model results show that by ~7 ka BP the present tidal motion in the North Sea had fully established (Van der Molen and De Swart, 2001a; Uehara et al., 2006). Since then, the tidal range along the central western Netherlands' coast has been ~1.8 m. Before 7 ka BP, tidal ranges were considerably lower, e.g. only 0.6 m 8.3 ka BP. The mean significant wave-height was 0.7-1.1 m (Van der Molen and De Swart, 2001b).

4.1.2 Holocene developments in the study area: shifting shorelines

The study area was transgressed ~8.5 ka BP during a period of increased rates of sea-level rise (sea-level jump; Hijma and Cohen, In press: Chap. 3). It was part of a back-barrier basin until 7.5-6.5 ka BP when the shoreline had migrated to a position further landward (based on Van der Valk, 1996a; b; Cleveringa, 2000; Rieu et al., 2005). North of the study area, coastline retrogradation was marked by at least one period of barrier overstepping as is suggested by the presence of tidal channels lacking evidence for systematic landward migration (Rieu et al., 2005). Coastal retreat was faster in the northern part of the study area than in the southern part, which was situated close to the Rotterdam Rhine-Meuse estuary. Thick stacks of older fluvial and estuarine deposits (mud and sand) slowed down retrogradation. At 6 ka BP, the shoreline of the northern part of the study area had receded to a position 5-10 km east of the present shoreline, while in the southern part the shoreline was still situated to the west of the present coastline (Beets and Van der Spek, 2000; see most landward beach ridge in Fig. 4.1), resulting in an west-east trending shoreline. Open-marine processes became dominant in a growing part of the study area, resulting in widespread erosion and only limited deposition. Retrogradation of the coastline halted ~6.3 ka BP (Van der Valk, 1996b; Cleveringa, 2000) and switched to progradation and closure of most tidal inlets (Beets and Van der Spek, 2000). Significant

deposition occurred during the Subboreal and Subatlantic progradation of the coastline. The sediment used for progradation was mainly sourced from the degrading promontory near Hoek van Holland (Cleveringa, 2000).

In the northern part of the study area, Atlantic back-barrier channel fills were recognised in seismic records and corings (Fig. 4.1; Beets et al., 1995; Rieu et al., 2005). These tidal channels were active in a 500-year timeframe between 8 and 6 ka BP. A gradual reduction in the rate of relative SLR during this time has been suggested (Rieu et al., 2005) as the initiator for the infilling of the channels: the basin deepened at a slower rate while total sediment delivery remained most likely fairly constant. This resulted in a reduction of the basin volume (initially mainly of the subtidal part) and, in the long run, a reduction of tidal amplitudes in the basin due to increased dampening (more friction) of the incoming tidal wave. Both effects lead to a decrease of tidal prism (the volume of water that the tide carries in and out a basin) that triggered infilling of the back-barrier channels and tidal inlets.

During the retreat of the coastline to a position landward of the early-mid Atlantic tidal basin, the upper part of the back-barrier sequence was truncated and only the deepest parts of the tidal-channel fills were preserved. The channels can be recognised in seismic data up to 12 km offshore the present coastline, are up to 1 km wide, have migrated in a variety of directions and show a predominant southwest-northeast orientation (Fig. 4.1; Rieu et al., 2005).

4.2   Materials and methods

High-resolution seismic data were used in combination with core data to map transgressive deposits. All elevations relate to N.A.P., i.e. the Dutch ordnance datum (O.D.) that nearly equals current mean sea level. Several seismic datasets were used (Fig. 4.1). The largest dataset forms a 1 km x 0.25 km grid (Fig. 4.3) that was acquired in 2000 and 2001 using an X-star chirp-pulse system with a frequency of 2-8 kHz. Some isolated pre-2000 seismic lines were also gathered using the X-star system, but with frequencies of 1-6 kHz. In addition, a database of several hundred descriptions of both undisturbed and disturbed cores facilitated the interpretation of the seismic facies in terms of lithology and depositional environments. Additional vibracores were collected from key locations identified after the first analysis of the seismic-data. They were especially used to describe channel fill characteristics. Shell content was a clear discriminating parameter between fresh (e.g. *Valvata piscinalis),* back-barrier (*Cerastoderma lamarcki, Hydrobia ulvae, Mytilus edulis and Littorina littorea* assemblages) and open-marine (*Spisula sp., Donax vittatus, Polinices catena*) palaeoenvironments. Mixed shell assemblages exist near tidal inlets and on the seaward side of barrier islands (Van Straaten, 1956).

To establish a chronological framework, samples for ^{14}C-dating were collected and existing pollen spectra of cored material were used (Beets et al., 1995). To further constrain the time-frame of activity, the elevation of the present top of truncated channel fills was compared with Holocene sea-level data. Channel fills are deposited below contemporary sea level. Because their upper parts were truncated by subsequent wave erosion, this comparison yields maximum ages. We furthermore stratigraphically linked undated offshore units to dated onshore units.
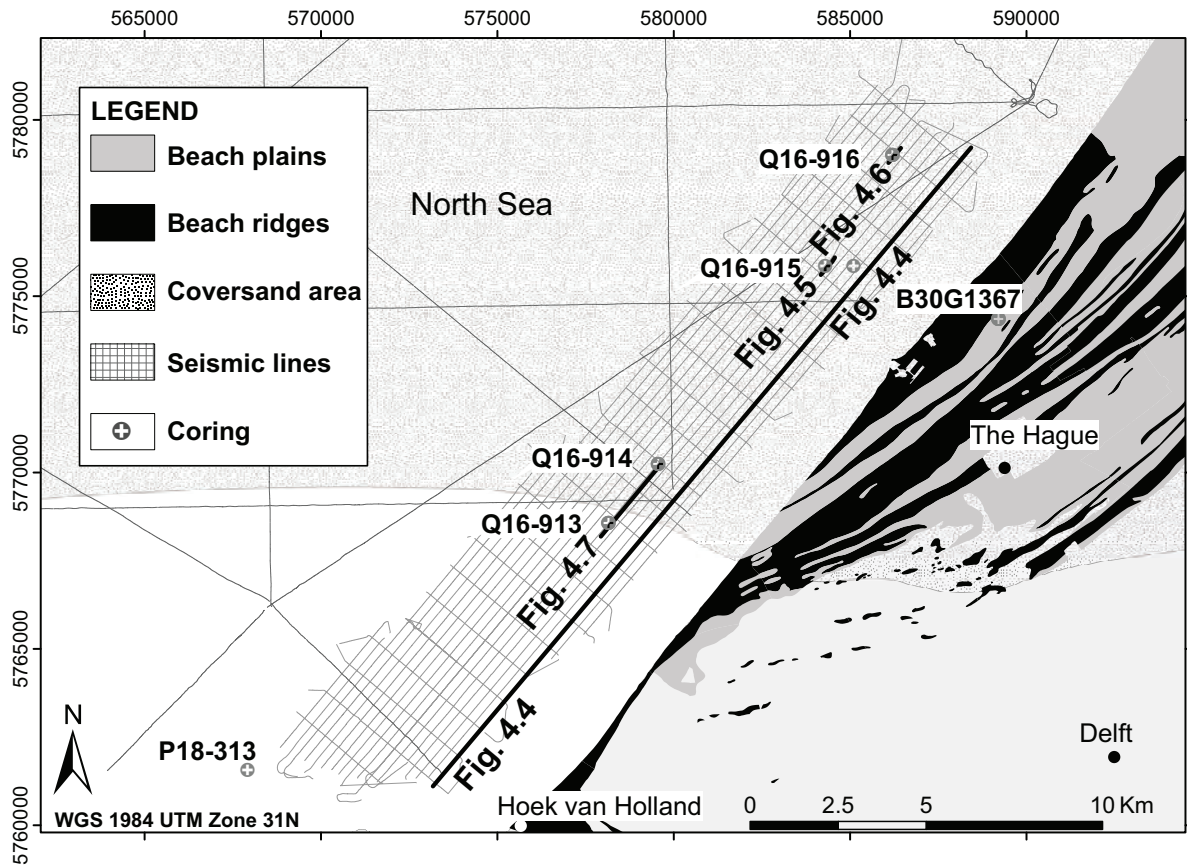
Figure 4.3 The study area with the seismic grid, the locations of the cross sections in Figures 4.4-4.7 and the position of the described cores.

4.3 Results: depositional units

We have divided the offshore sediments into nine depositional units based on their seismic reflection and lithological characteristics. They have been grouped into terrestrial and shallow marine deposits. For clarity, firstly the genetic interpretation of the units is given based on their lithology along a cross section (Fig. 4.4; see Fig. 4.3 for location). Secondly, their geometry, age and linkage to onshore sediments will be presented.

4.3.1   Lithological description and genetic interpretation

Terrestrial deposits: channel, aeolian and flood-basin deposits
Five terrestrial units were recognised in the seismic data and the cores (Fig. 4.4):

Unit 1: Below 20/19 m –O.D., a nearly transparent seismic facies is visible (Figs. 4.5-4.7; see Fig. 4.3 for location). The transparency may partly be due to attenuation of the seismic signal with increasing depth. The unit consists of fine to coarse sands (median: 150-600 μm) with dispersed gravel beds and loam/silt layers. Organic material is found only within the loams. Cores in a similar unit with respect to depth and lithology indicate unidirectional high-angle cross-bedding and the presence of reworked last interglacial shells (Beets et al., 1995). Based on their characteristics, these sands are interpreted as fluvial-channel deposits.

Unit 2: North of km 3.5 (Fig. 4.4), fine-grained and well-sorted sands (105-210 μm) lie concordantly on top of *Unit 1* (Figs. 4.4, 4.7). The top rises from 19 m –O.D. in the south to 16 m –O.D. in the north, and in the seismic data, the unit has a near-transparent reflection. *Unit 2* has a maximum thickness of 1-2 m. It is distinguished mainly on the basis of its pronounced undulating relief, especially south of km 11 where relief differences reach 3.5 m. North of km 13, the top of the unit is locally eroded. In most cases, root remains can still be observed in the top of the sand, indicating modest erosion of an overlying surface. If not eroded, a soil profile underlying a peat layer (*Unit 4*) is present in the top (Fig. A4.13). Considering the fine, well-sorted sands and the undulating relief, we interpret the sands as aeolian deposits.
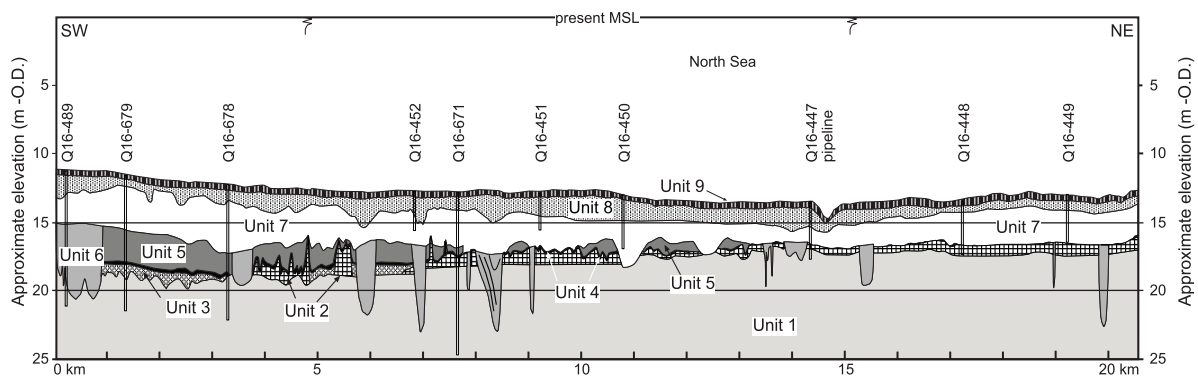
Figure 4.4 Shoreparallel cross section showing the seismic units and the cores used for interpreting the seismic data along this line. *Unit 1* is a complex of fluvial channel deposits, *Unit 2* is an aeolian deposit, *Unit 3* is a loamy overbank deposit, *Unit 4* is a peat layer, *Unit 5* consists predominantly of freshwater clay, *Unit 6* consists of back-barrier channel fills and *Units 7-9* are lower shoreface deposits. See text for detailed information.

Unit 3: South of km 11 (Fig. 4.4), a slightly less transparent unit covers *Units 1/2.* Only a few, poorly described old cores penetrate the unit and indicate the presence of a thin loam layer.

Unit 4: South of km 13 (Fig. 4.4), a peat layer caps *Units 2-3.* To the north, most of this unit has been removed by erosion (Figs. 4.4, 4.7, A4.13; see Fig. 4.3 for locations). The peat layer is 10-20 cm thick (Fig. A4.13), and marked by a single, continuous high-amplitude reflection on the seismic profiles. No plant remains were recognised in the cores. We interpret this unit as the basal peat which formed as a consequence of SLR-induced rise in groundwater level.

Unit 5: Where *Unit 4* has not been eroded, it is covered by an up to 2 m thick package of clay that contains some peat clasts, detritus and few shell fragments (Fig. A4.13). The boundaries of the unit are visible as high-amplitude reflections in the seismic data (the lower one being *Unit 4*), but internally the unit is transparent. In core Q16-914 (Fig. A4.13), remains of the freshwater mollusc *Valvata piscinalis* are present. In a similar unit, Beets et al. (1995) found an abundance of *Typha* pollen in one core (Q16-444) and high values (> 5%) for *Ulmus*, reliable indicators for a predominance of freshwater. The clay is laminated, and interpreted to have formed in a low-energy, upper estuarine environment with some tidal influence.

Shallow marine deposits; tidal channel fills and shoreface deposits
We recognised 4 back-barrier and open-marine units (Fig. 4.4):

Unit 6: This unit is mainly distinguished on the basis of very clear channel-shaped features in the seismic data (Figs. 4.5-4.7). These channels show up as dark patches with alternations of subparallel to oblique high- and low-amplitude reflections that are laterally continuous. Maximum scour depths reach 30 m -O.D. and the channels are hundreds of metres wide. Three undisturbed cores (Q16-913/915/916; Fig. A4.14; see Fig. 4.3 for locations) were used to describe the sedimentology and depositional environment of the channel fills. The alternating reflections are caused by lithological alternations between fine to medium sand (105-300 µm) and mud (Fig. A4.14). Seaward the reflection becomes more blurry suggesting a sandier infill. From bottom to top, the sand content of the fills shows no systematic decrease or increase. The mollusc shell assemblage consists of *Macoma balthica, Mytilus edulis, Cerastoderma sp., Scrobicularia plana* and *Peringia ulvae (Hydrobia ulvae)*, which is typical for back-barrier environments. Two channel systems (G and H) in the northern part of the study were previously recognised in seismic data by Rieu et al. (2005). They report an increase in the open-marine faunal component to the top of the fills, especially near the seaward terminus of the fills, which indicates landward migration of the channel network.

Unit 7: This unit truncates various older deposits (Figs. 4.4-4.7, A4.13, A4.14). The associated deposits consist of grey, fine to medium sand (150-300 μm) with low- and high-angle cross-stratification and horizontal parallel lamination. Clay is absent or scarce and organic detritus is occasionally present. Reworked shells occur in lags, but are also
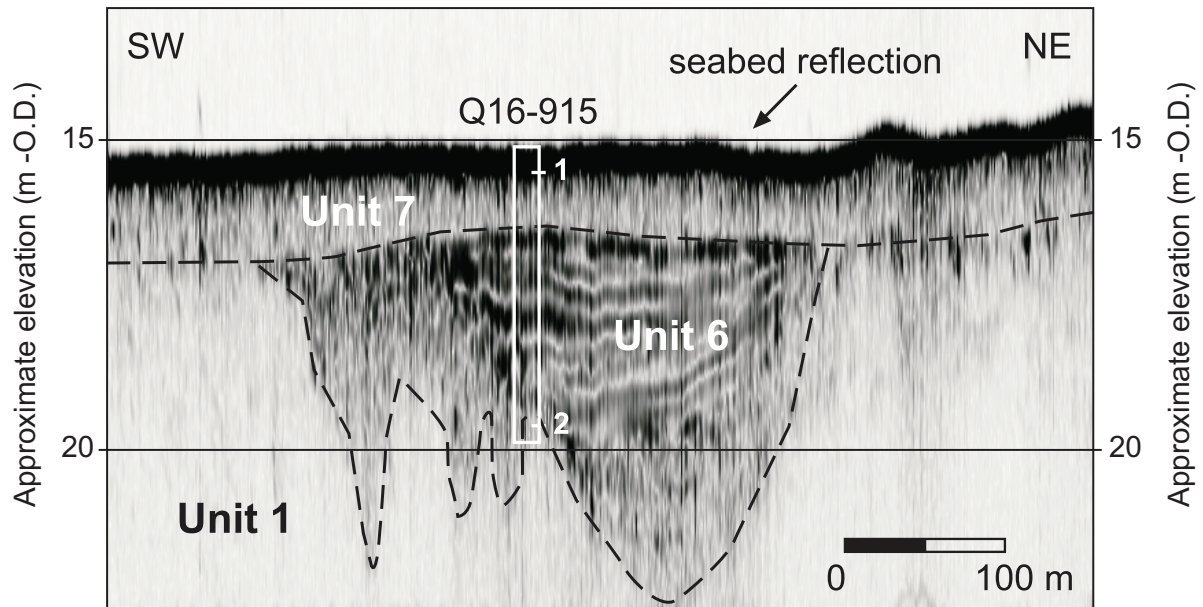
Figure 4.5 Seismic record of tidal-channel system G (*Unit 6*) with the positions of the dated shells (Tab. 4.1; see also Fig. A4.14). The concentric pattern of reflections indicating channel infilling and consisting of sand-clay alternations, is truncated by *Unit 7*.
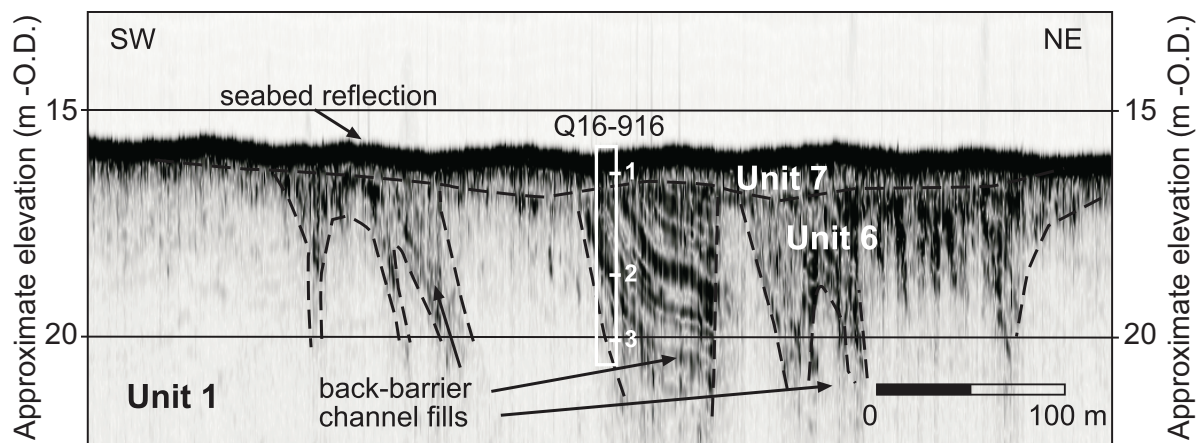
Figure 4.6 Seismic record of tidal-channel system F (three channel fills) with the position of dated shells (Tab. 4.1). The infill shows high-angle clinoform bedding, indicating limited lateral channel migration in combination with infilling.
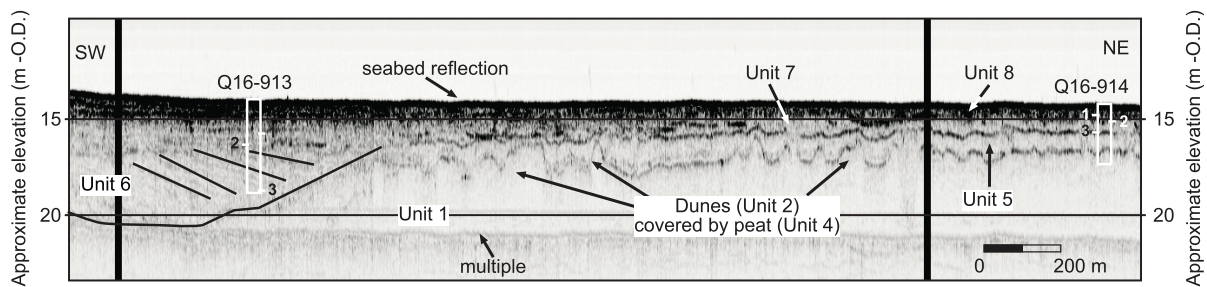
Figure 4.7 Seismic records of tidal-channel system I (at far left) and the preserved terrestrial deposits with pronounced dune topography. Also shown are the positions of dated shells (Tab. 4.1; see also Fig. A4.13). The peat layer on top of the dunes and the coversand is clearly visible as a dark band. A distinct dark reflection marks the boundary between *Units 5 and 7*.

The lags can often be seen in the seismic data as horizontal continuous high-amplitude reflections, especially at the base of the unit (Figs. 4.7, A4.13). Internally, the unit is transparent. *Spisula subtruncata* is abundant and *Polinices catena, Chamelea striatula* and *Tellina tenuis* are common as well. In addition, *Cerastoderma edulis* and *Macoma balthica* can be observed. The echinid *Echinocyamus pussilus* is also present and the total association indicates open-marine conditions. Beets et al. (1995) suggested the shell lags to be formed during storms and that the relative scarceness of infauna and mud are indicative of regular reworking by unidirectional tidal currents. Near km 11-12 (Fig. 4.4), *Unit 7* reaches the basal peat. Overall, the unit was formed on the lower shoreface.

Unit 8: To the top of *Unit 7* the reflections become blurry with a sharp transition (Figs. 4.4, 4.7), but core descriptions (Fig. A4.13) indicate no lithological difference to explain the change in reflection. It was also formed on the lower shoreface.

Unit 9: The upper 0-0.5 m of the *seafloor* falls within the dark seabed reflection (Fig. 4.4) and can therefore not be distinguished as a separate unit in the seismic data. It is the present active layer that can be recognised in cores as coarse, (300-600 μm), yellow or brown sands rich in shells (Fig. A4.13). *Spisula subtruncata* is still the dominant species, but many other open-marine North Sea pelecypod species are present.

4.3.2   Geometry, age and onshore linkage

Terrestrial deposits: channel, aeolian and flood-basin deposits
Our *Unit 1* is a thick fluvial deposit below 20/19 m –O.D. (see Fig. 4.8 for an overview of the off- and onshore units). Its stratigraphic position and lithological characteristics match two onshore units described by Busschers et al. (2007; their units B4 and B6ab). Onshore, the older unit B4 consists of medium-grained sandy fluvial channel-belt deposits from the middle Weichselian that are predominantly overlain by aeolian coversands. Unit B4 is dissected by younger, late Weichselian units B6ab. The latter floodplains lie 1-2 m lower

than the top of unit B4 and form the Rhine-Meuse palaeovalley. In the palaeovalley aeolian deposits are more scattered and at most locations a loam layer blankets units B6ab. The channel system of units B6ab was active until ~9 ka BP (Busschers et al., 2007; Hijma et al., 2009: Chap. 2). In our study area, aeolian deposits are widespread north of km 7. There, the top of *Unit 1* lies higher on average than south of km 7 where the top of *Unit 1* is mostly covered by a thin loam layer (*Unit 3*) instead of aeolian deposits (Figs. 4.3, 4.4). We therefore place the terrace scarp between units B4 and B6ab near km 7.

Unit 2 consists of aeolian deposits, locally with clear dune relief, especially around km 4-5. The sheet-like aeolian deposits north of km 7 are similar in lithology and undulating topography to coversand deposits onshore. The coversand dates mainly from the Late Glacial period (Van der Hammen et al., 1967; Van Huissteden et al., 2001; Schokker et al., 2005) and was deposited in a polar-desert periglacial environment.

The higher dunes around km 4-5 (Fig. 4.4) fringe the late Weichselian palaeovalley (see above) and mark the transition from this valley to the terrace/coversand area. Onshore, a few dunes have been found near the coversand boundary as well (Busschers et al., 2007; Hijma et al., 2009: Chap. 2), but the larger dune complexes developed in the central part of the Rhine-Meuse palaeovalley (Berendsen and Stouthamer, 2000). In general they consist of coarser sand than the coversand as they were deflated from nearby, seasonally dry river beds instead of being transported over longer distances. Too few corings exist offshore to confirm a distinction in grain size in our study area. Onshore ages range between Younger Dryas and late Boreal (Pons and Bennema, 1958; Van der Woude, 1983; Hijma et al., 2009: Chap. 2). The palaeo-dunes in the study area are dissected by channels of channel complex I (*Unit 6,* see below*)* and show an irregular pattern (Fig. 4.9).

The loam layer (*Unit 3*) south of km 7 occurs widespread onshore within the palaeovalley and is interpreted as an overbank deposit (Törnqvist et al., 1994). Just east of the study area, the loam is mainly of early Holocene age (Busschers et al., 2005; 2007; Hijma et al., 2009: Chap. 2).

Units 1-3 are capped by a peat layer (*Unit 4*) throughout the study area. However, it has been locally eroded north of km 7 due to shallower depth and hence vulnerability to later shoreface erosion. In core P18-313 the top of the peat has been dated at 8.5 ka BP (Tab. 4.1). Three km to the south of the study area, but still offshore, the top of the basal peat around 20 m –O.D. has also been dated at 8.5 ka BP, whereas the base was dated at ~8.8 ka BP (Hijma and Cohen, In press: Chap. 3). Farther south, at depths of 24 m –O.D., peat formation started at 11-10.5 ka BP (Van Heteren et al., 2002). Onshore, the unit is widespread and only absent in places of fluvial activity during peat formation or due to subsequent erosion.
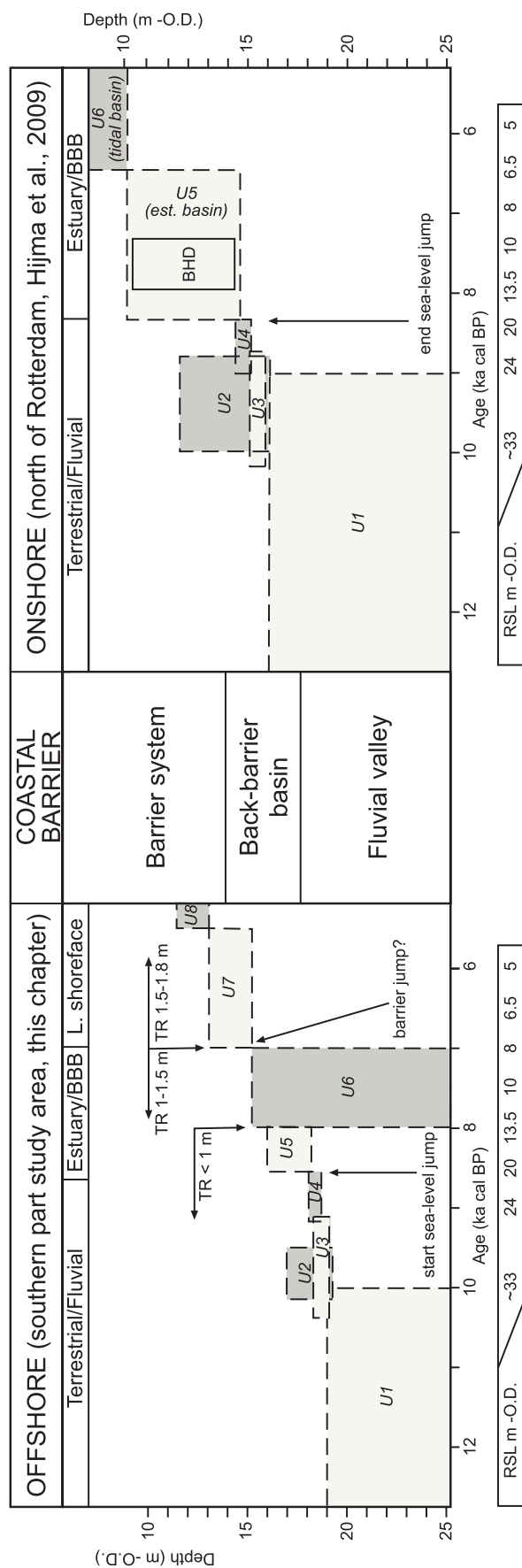
Figure 4.8 Schematic overview of the off- and onshore position of the units, both in time and current depth. For the onshore part, we labelled the deposits to match the named offshore units. Offshore, drowning occurred during the start of the sea-level jump, onshore predominantly during the final stage of the sea-level jump. The timing of barrier overstepping is not well constrained, but offshore it resulted in a change from a back-barrier basin (BBB) environment to a lower shoreface environment. In the depicted onshore area, no large tidal channels were active. (TR=Tidal range; BHD=Bay-head delta).

93

Table 4.1 Radiocarbon-dates from the study area. The dates were calibrated using Oxcal 4.0.5 software (Bronk Ramsey, 1995; 2001) with the Marine04-curve (Hughen et al., 2004) for shells and the INTCAL04-curve for terrestrial material (Reimer et al., 2004).

Core number (Units Fig. 4.4)	Lab. nr.	Coord.[1] (X, Y)	Sample depth (m -O.D.[2])	^{14}C age (uncorr.)	Std. dev.	Max. cal yr BP (2σ)	Min. cal yr BP (2σ)	Mean[3] cal BP	Std. dev. (1σ)	δ^{13}C (p.mil)	Dated material
Q16-913/1 (8)	UtC-13001	578157 5768560	-15.9	4390	40	4689	4412	4543	72	-2	Juvenile *Tellina tenuis* 1/2 doublet
Q16-913/2 (8)	UtC-13002	578157 5768560	-16.5	4566	47	4883	4607	4764	68	-0.2	Juvenile *Macoma balthica* 1 doublet
Q16-913/3 (6)	UtC-13003	578157 5768560	-18.6	7022	42	7585	7426	7511	40	-5.1	Juvenile *Macoma balthica* 1 doublet
Q16-914/1 (8)	UtC-13004	579562 5770245	-14.9	4042	33	4190	3950	4063	60	-0.9	5 Juvenile *Spisula sp.*
Q16-914/2 (7)	UtC-13005	579562 5770245	-15.2	5103	47	5570	5325	5463	66	-1.7	2 Juvenile *Spisula sp.*
Q16-914/3 (7)	UtC-13006	579562 5770245	-15.8	6094	36	6627	6421	6521	54	-1.4	6 Juvenile *Spisula sp.*
Q16-915/1 (7)	UtC-13007	584294 5775859	-15.5	5231	39	5685	5485	5594	45	-2.3	*Spisula sp.* 1 doublet
Q16-915/2 (6)	UtC-13008	584294 5775859	-19.6	7747	42	8332	8119	8222	54	-8.3	1 *Cerastoderma sp.*
Q16-916/1 (7)	UtC-13009	586201 5778991	-16.3	6148	38	6687	6468	6579	55	-3.1	2 Juvenile *Spisula sp.*
Q16-916/2 (6)	UtC-13010	586201 5778991	-18.6	7383	40	7940	7745	7849	49	-4.6	*Mytilus edulis* fragment
Q16-916/3 (6)	UtC-13011	586201 5778991	-20	7315	42	7895	7671	7777	55	-5.4	1 Juvenile *Cerastoderma sp.*
B30G1367/1 (7)	UtC-15527	589210 5774355	-13.25	4500	60	4828	4520	4686	84	-1.7	*Spisula subtruncata*
B30G1367/2 (7)	UtC-15528	589210 5774355	-15.25	5230	70	5754	5435	5594	80	-3	*Spisula subtruncata*
B30G1367/3 (6)	UtC-15529	589210 5774355	-17.08	6530	50	7169	6900	7045	70	-6.6	*Mytilus edulis*
B30G1367/4 (6)	UtC-15530	589210 5774355	-18.22	6670	70	7356	7015	7195	82	-4.3	*Mytilus edulis*
P18-313/1 (4)	GrN-21460	567915 5761568	-20.7	7720	40	8584	8422	8498	43		Top basal peat

1 - WGS 1984, UTM 31N

2 - O.D. = Dutch Ordnance Datum ~ mean sea level

3 - Mean as calculated by OxCal 4.0.5

Where the peat has not been partially eroded, it is covered by a clay layer that is several meters thick (*Unit 5*). South of core Q16-914 (Fig. A4.13), microfossil analysis shows that the clay was deposited in a low-energy freshwater environment (Beets et al., 1995; their core 92DW1) at the northern fringe of the Rhine-Meuse system. This evidence fits with onshore information indicating that freshwater conditions lasted for a long time during the transgression of the palaeovalley (Hijma et al., 2009: Chap. 2). North of core Q16-914 there are no offshore environmental data, but onshore, brackish lagoons were present in the former coversand area (Hijma et al., 2009: Chap. 2). No direct time control exists for *Unit 5*, but dated channel fills that clearly dissect this unit have oldest ages of ~ 8.2 ka BP

(this chapter), and the unit overlies basal peat that was flooded ~8.5 ka BP. *Unit 5* must therefore be early Atlantic, a fact that is corroborated by pollen data (Beets et al., 1995). South of the study area, closer to the Rhine-Meuse system, the clay deposits reach thicknesses of several metres, occur deeper and started to form in the Boreal (Van Heteren et al., 2002).

Shallow marine deposits; tidal channel fills and shoreface deposits
We identified 6 offshore channel systems within *Unit 6* (Systems F-K, Fig. 4.9). Channel widths and scour depths vary considerably, even within the same channel (Tab. 4.2). Some channels were more than 500 m wide and scouring reached 30 m –O.D. Considering palaeo-MSL during formation (Fig. 4.2), water depths must have been 15-20 m in the axis of the channels. Vertical and lateral dimensions are similar to those observed today in the Dutch Wadden Sea. All channels seem to show very little lateral migration (tens of metres only) as hardly any lateral-accretion units are visible in the seismic data (e.g. Figs. 4.5-4.7). In the present highstand situation, typical lateral migration rates of tidal channels can vary from a minimum of 0.1-0.2 m/yr in cohesive banks (McClennen and Housley, 2006) to a maximum of 25-100 m/yr in non-cohesive banks (Lüders, 1934, op. cit. Reineck, 1978; Ginsberg and Perillo, 2004). In the study area the back-barrier channels lay embedded within clayey deposits. The maximum period of activity is 800-1000 yr (see below) meaning the channels could have laterally migrated 80-160 m. This is more than the tens of metres we observed. Although channel system G and H show some signs of landward migration, in general the channel systems show no evidence for landward migration forced by coastal retrogradation. This is in agreement with Rieu et al. (2005) who infer a period of barrier overstepping based on similar observations.

The channel geometries show no clear shore-parallel diversions at the most landward parts. This is unlike similar features described to the north, where the distal parts of the channel features diverge to the north (Rieu et al., 2005). In the south-western part of the study area, the position of channel fills is obscured by the presence of shallow gas, which causes blanking of the seismic signal. Only the deepest channel fills have been preserved as the erosional base of *Unit 7* truncated the channel features, leaving a discontinuous pattern of channel systems numbered F to K (Fig. 4.9). Channel-fill system I is an exception since it consists of connected multiple channels (Fig. 4.9). Its position just north of the Rotterdam palaeo-estuary suggests a relationship between the observed anomalous pattern and fluvial influence. Possibly, avulsing fluvial distributaries connected to system I, resulting in the anomalous geometry. The anomaly is most pronounced in the area with the aeolian dunes. The channels seem curved around the peat-covered dunes and antecedent control on channel pattern may be inferred.

Especially channel systems H and I, but also systems G and F (Fig. 4.9) converge into a seaward direction, indicating the location of tidal inlets. The wave climate, sand

availability (submerged sandy deposits) and the low gradient of the shoreface must have led to the formation of barrier islands in between the inlets (see also Beets and Van der Spek, 2000). From three channel fills, shells were selected for radiocarbon dating (Figs. 4.5-4.7, A4.13, A4.14; Tab. 4.1). Ages corrected for the reservoir effect range between 8.3 and 7.4 ka BP. This corresponds to maximum ages estimated by comparing the depth of fill truncation to the sea-level curve (Tab. 4.2) and the ages show that the channels were active in roughly the same time period. Between 8.3-7.4 ka BP, sea level rose from ~15 m to 10 m below MSL (Van de Plassche, 1982; Vink et al., 2007), so on average 5-6 mm/yr. Considering a gradient of 20-25 cm/km for the top of *Unit 1* (Törnqvist, 1998) and ~20 cm/km for the top of *Unit 2* (based on Hijma et al., 2009: Chap. 2), this implies coastal retrogradation rates of ~25 m/yr. Onshore, mapped tidal basins inland of the oldest preserved beach ridges are >20 km in cross-shore width (Hijma et al., 2009: Chap. 2). If the tidal systems of *Unit 6* had similar widths and using a rate of retreat of 25 m/yr, the maximum period of activity of the observed tidal-channel systems is estimated to be ~800 yr.
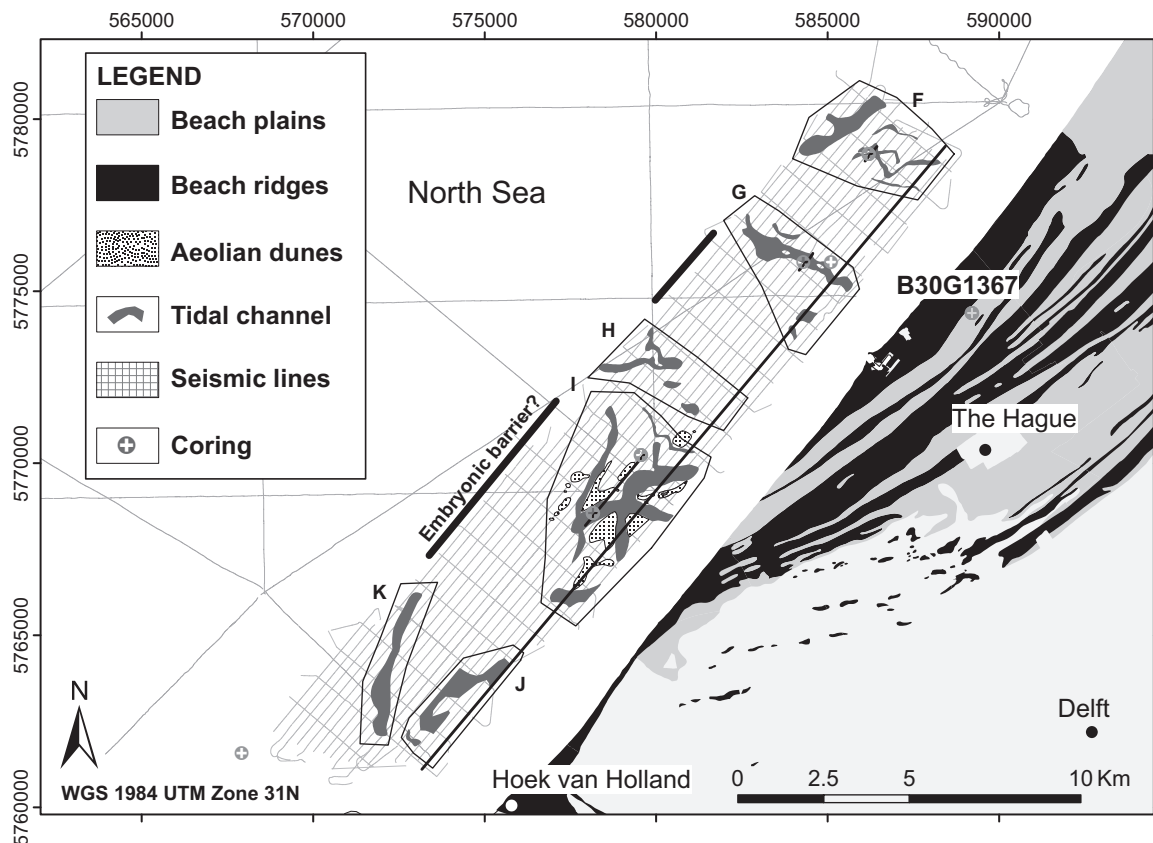
Figure 4.9 Pattern of the back-barrier channel fills and the aeolian dunes. The channel fills have been grouped in tidal systems F-K. The position of two inferred barriers is given.

This order of magnitude is in line with the established time-frame for the channel fills (8.3-7.4 ka BP). Onshore, core B30G1367 (Fig. 4.3, 4.9), was taken in a back-barrier channel fill that lies directly east of channel system G. The oldest obtained shell dates are ~7.2 ka BP (Tab. 4.1), so 1000 yr younger than the shells dated in core Q16-915 in channel system G, indicating that the channels were not active at the same time.

The large tidal-channel system I is positioned near the northern border of the palaeovalley at the transition to the northern coversand area (see Figs. 4.3 and 4.9). It is potentially in relation with the position of incised river channels that have been described onshore near the northern fringe of the palaeovalley (Busschers et al., 2007; Hijma et al., 2009: Chap. 2). The position of channel systems J and K are possibly linked to the incised, onshore fluvial systems at this latitude (Hijma et al., 2009: Chap. 2). Tidal-channel systems F-G are situated in the northern coversand area. The ages of systems F-G (Tab. 4.2) exclude the possibility of inherited fluvial channels as there were no such fluvial channels present in the coversand area until ~7.5 ka BP (Hijma et al., 2009: Chap. 2). The initial position of these systems is most likely inherited from small, local streams draining the coversand area.

The channel fills are truncated by the lower shoreface deposits of *Unit 7*. Ages of dated shells range from 6.7 to 5.4 ka BP (late Atlantic to early Subboreal). The oldest dates match the age of the oldest preserved progradational barrier onshore (Van der Valk, 1996b; Cleveringa, 2000) yielding 6.3-6 ka BP at a location ~8-10 km landward of the study area (Fig. 4.1). Considering the minimum average migration rate of the coastline (25 m/yr), the barrier system had passed the study area no later than 6.8-6.7 ka BP, which corresponds well with the age of *Unit 7*. *Unit 8*, which resembles *Unit 7* lithologically and genetically but has a more blurry reflection characteristic in the seismic data, has an age of 4.9-4 ka BP in the study area. It was formed during a period of coastal progradation, in contrast with *Unit 7* that was formed on a retreating shoreface. *Unit 9* is the present active layer, which is uniformly present offshore and is of subrecent age (Van Heteren et al., 2002).

4.4   Discussion

4.4.1   Tidal-channel infilling: river-mouth shifting as a driving mechanism?

Radiocarbon-dated juvenile shells indicate that the back-barrier channels started to fill in between 8.3-7.4 ka BP (Tabs. 4.1-2). Directly north of the present study area, channel infill started at the same time, attributed by Rieu et al. (2005) to a decrease of tidal prism that followed an extended period of tidal-prism increase. They hypothesized that tidal-prism decrease was governed by the gradually decreasing rate of both sea-level rise and tidal-amplitude increase. At that time, sea-level rise was 0.6 m/100 yr (Fig. 4.2) and tidal

amplitudes increased with 0.02-0.04 m/100 yr (based on Van der Molen and De Swart, 2001a). These numbers show that both parameters still increased at the time the back-barrier channels filled. Nevertheless, the rates of increase had reduced to a point where the newly created accommodation space (and associated potential tidal-prism increase) could locally be compensated by sedimentation. Areas that received the largest quantities of sediment, closest to the source, would have experienced reduced accommodation space and tidal prism first. The vicinity of the study area to the Rotterdam Rhine-Meuse estuary makes that a third mechanism leading to tidal prism reduction should be considered. Before 8 ka BP the main Rhine distributary was located to the south of the study area, near Hoek van Holland, debouching through the combined Rhine-Meuse estuary that extended more than 15 km seaward of the present coastline (Van Heteren et al., 2002). Due to northward shifting, the main distributary became connected to the estuarine basin of the study area after 8 ka BP. The presence of a sizable bay-head delta (Hijma et al., 2009: Chap. 2; Figs. 4.1, 4.9) at the location where the distributary entered the basin is testament to the fact that the Rhine dumped large volumes of sediment into the estuarine basin. Part of this sediment was deposited in the intertidal zone and thus had a direct influence on tidal prism. The dimensions of the bay-head delta can be used for a first-order assessment of the relevance of the fluvial sediment supply to the study area. The bay-head delta occupies an area of 24 million m^2 (based on Hijma et al., 2009: Chap. 2). Multiplication with an average thickness of 5 m gives 120 million m^3 of sediment, of which only about 25% could have been deposited in the intertidal zone (assuming a tidal range of 1.25 m following Van der Molen and De Swart, 2001a). Assuming a relatively small estuarine basin (10x10 km or 100 million m^2), tidal prism volume is maximum 125 million m^3. When compared to the intertidal volume of the sand unit (30 million m^3), it is clear that the maximum reduction of the intertidal area over 700 years is no more than about 25%. If the basin was wider (most likely as the basins described in this paper are ~20 km wide) and thus bigger, this percentage becomes smaller. Since the reduction in intertidal area is a proxy for the reduction in tidal prism, this calculation shows that fluvial sand input can only partly explain the reduction in tidal prism. The supply of fluvial mud however, may have contributed to the decrease of intertidal accommodation space as well, in addition to filling subtidal parts of the basins. The significance of that contribution cannot be determined at present, but it could be very substantial considering the widespread occurrence of Atlantic fluvial-tidal mud deposits onshore (Hijma et al., 2009: Chap. 2). To establish the preserved volume and distribution (intertidal *versus* subtidal) of fluvial mud in the former tidal basins, the riverine fines need to be distinguished from offshore-derived fines that entered the basins through the tidal inlets. The degree of mixing of silt-lutum populations is a possible key, as the flocculation behaviour of the lutum fraction differs with salinity.

To summarize, the impact of distributary shifting within the Rotterdam Rhine-Meuse estuary contributed to the decrease of tidal prism. Together with the decreasing rates of tidal amplitude rise and sea-level rise, this will have triggered channel filling. Most likely, the sandy sediments that filled in the channels in reaction to the tidal-prism decrease were coming from offshore as sandy fluvial sediments were for the larger part trapped in the bay-head delta (Hijma et al., 2009: Chap. 2). More muddy infills could have been supplied by both marine and fluvial sources. A nearby, offshore source was the promontory to the south near Hoek van Holland. The northward directed wave-driven longshore currents and the tide transported the eroded sediments from this promontory into the back-barrier basins.

4.4.2 Barrier overstepping: sea-level rise as a driving mechanism

During SLR, barrier-back-barrier systems can adapt to the changing conditions in two ways: either they continuously migrate landward (e.g. Swift, 1968; Swift and Moslow, 1982) or the barriers remain in place and are finally overstepped (Swift, 1968; Rampino and Sanders, 1980; 1982; Leatherman et al., 1983). A modelling study by Storms et al. (2002) showed that during rapid SLR (in their case 33 cm/100 yr) barrier overstepping occurs after a period of 4000 yr. Their boundary conditions were similar to present-day conditions along the Dutch coast. When SLR was less rapid, continuous retreat of the systems was predicted. This corroborated the hypothesis by Rieu et al. (2005) that coastal retrogradation directly north of our study area was punctuated by at least one period of barrier overstepping. Also the sequence in the present study area suggests overstepping to have occurred, because both back-barrier channels and tidal inlets show limited landward migration and seem 'frozen' in time. If the coastline did continuously migrate landward, the only explanation for the absence of evidence for landward tidal-inlet migration is the presence of very shallow tidal inlets around 8.3-7.4 ka BP. The remains of such shallow systems would then not have survived later shoreface erosion. Other evidence for overstepping is that offshore and onshore channels cannot be linked in time and space, which would be expected if channels migrated continuously landward.

Using the chronology obtained for our units, the timeframe for the overstepping is constrained to 7.5-6.6 ka BP. Truncation of *Unit 7* yielded maximum ages of 6.6-6.5 ka BP (Tab. 4.1), whereas the youngest channel-fill deposits of *Unit 6* date to ~7.5 ka BP (Q16-914/3; Tab. 4.1).

Within the possible timeframe of overstepping, sea level rose from 10 to 7 m –O.D. (33 cm/100 yr, the same as the threshold rate of Storms et al., 2002). The top of the truncated channel fills is located at an average depth of 16 m –O.D. (Tab. 4.2). This means that after overstepping occurred, a maximum of 6-9 m of sediment was eroded on the lower shoreface. This is a maximum value, because the typical elevation of the top of channel sediments in a back-barrier basin is below mean sea level.

Table 4.2 Characteristics of the tidal-channel systems. Incision depths are minimum depths as the seismic signal not always penetrates the entire channel fill. Maximum ages are obtained by comparing the depth of the top of the fill, assuming nil erosion, with the sea-level curve (Fig. 4.2). The minimum age is based on dates of the overlying *Unit 7*.

Channel system	Width (m)	Incision depth (m –O.D.)	Top of fill (m –O.D.)	Max. age (cal BP)	Min. age (cal BP)	Dated fill (cal BP)
F (main)	400-500	21-31	16	8500-8000	6700-6500	~7900-7700
G	300-700	18.5-22.7	14.5	8200-7700	6700-6500	~8300-8100
H	100-500	23	18	9000-8500	6700-6500	-
I	250-600	23	16	8500-8000	6700-6500	~7600-7400
J	500-900	20	14	8000-7500	6700-6500	-
K	200-400	23	16	8500-8000	6700-6500	-

Steady eustatic SLR was the most important governing factor in enabling overstepping to occur. An additional control was the gentle gradient of the submerged landscape (20-25 cm/km, see above). With the associated rapid rate of transgression of at least 25 m/yr, equally rapid barrier rollover was necessary to maintain a stable back-barrier basin configuration. Evidently, barrier-rollover speed was insufficient and eventually the barrier was overstepped.

4.4.3   Factors controlling channel migration and orientation

Lateral migration of the tidal channels was not only limited due to rapid landward migration of the system (see above), but in the study area also due to the thickness of the fine-grained, erosion-resistant back-barrier deposits on top of the Pleistocene substrate. Prior to the development of back-barrier channels in the study area, a clay unit of several metres thick (*Unit 5*) had already accumulated forming cohesive banks. Most likely, the fluvial(-tidal) channels that deposited the clay were transformed into the tidal channels visible in the seismic data. These tidal channels hence inherited the cohesive banks that hindered lateral migration. To the north, in the coversand area, *Unit 5* is less thick and channels show more lateral migration.

In the study area northward diversions of the most landward part of the channel fills are absent. This is in contrast to the study area of Rieu et al. (2005) where they describe such diversions and link it to strongly asymmetric back-barrier drainage basins as a result of a northward propagating tidal wave in the southern North Sea. This is indeed an important factor, but many more factors influence the geometry of back-barrier tidal channels, as well as that of the associated ebb- and flood-tidal deltas (e.g. tidal range, wave direction, the interaction of offshore and inlet tidal currents) leading to strong variations over relatively short distance (Sha and Van den Berg, 1993, concerning ebb-tidal deltas).

In the study area, the estuarine setting plays an additional role. In tidal basins such as the study area of Rieu et al. (2005) or the Wadden Sea, channel pattern is reminiscent of a low apple tree (main channel) with many branches. In wider (in a cross-shore direction) estuarine basins (our study area), channel pattern lies more parallel to the estuary and is more reminiscent of a poplar tree (main channel) with less and shorter branches (Van Veen et al., 2005). This notion could well explain the difference in channel pattern between our study area and those of Rieu et al. (2005).

4.5   Conclusions

Well preserved late Weichselian-early Holocene terrestrial and middle Holocene back-barrier deposits have been recognised in seismic data offshore the western Netherlands between Hoek van Holland and Leiden. They are overlain by lower shoreface deposits from the late Holocene. The terrestrial deposits consist of fluvial deposits that are covered by aeolian deposits, peat and estuarine clays. The deposits can be linked to similar onshore deposits. They are dissected by back-barrier tidal channel fills that have been dated 8.3-7.4 ka BP. The channel fills and occasionally the terrestrial deposits were truncated by wave-action during the landward migration of the coastline through the study area. This happened before 6.6 ka BP.

The nearby presence of the Rhine-Meuse estuary had a significant influence on the development of the back-barrier basin and especially the back-barrier tidal channels. The back-barrier channels started to fill in between 8.3-7.4 ka BP during a period of decreasing rates of both sea-level rise and tidal-amplitude increase. They were both still increasing, but the increase had reduced to a point where the newly created accommodation space in the tidal basin could locally be compensated by sediment supply. Also during this time, the main Rhine distributary shifted north to a position directly east of the study area and started to dump sediment into the estuary. This could have led to a maximum reduction of 25% of the tidal prism. Most likely, the sandy sediments that filled in the channels in reaction to the tidal-prism decrease were coming from offshore as sandy fluvial sediments were for the larger part trapped in a bay-head delta. More muddy infills could have been supplied by both marine and fluvial sources. Together with the ongoing decrease in both the rate of sea-level rise and tidal amplitude increase, the arrival of avulsed Rhine sediment caused tidal prism decrease and channel infilling.

We observe a period of barrier overstepping. Overstepping occurred between 7.5 and 6.6 ka BP. Rapid SLR in combination with a gentle subsurface gradient and an insufficient sediment supply governed the overstepping. Barrier rollover could not keep up with back-barrier basin widening on the landward side and at a certain moment the barrier was overstepped. An additional factor which possibly led to variations in migration rate could have been differences in the gradient of the transgressed surface.

Lateral migration of the tidal channels was limited, not only by rapid landward migration of the system, but also due to the thickness of the cohesive freshwater back-barrier deposits on top of the Pleistocene substrate that hindered meandering. To the north, lateral migration rates increase as the thickness of the back-barrier deposits is less.

The development of the study area shows that shifting of sediment sources, substrate gradient and substrate type are important governing factors in the behaviour of back-barrier systems.

Acknowledgments

5 Holocene transgression of the Rhine river-mouth area, The Netherlands: palaeogeography and sequence stratigraphy

Will be submitted as:

Hijma, M.P. & K.M. Cohen, *Holocene transgression of the Rhine river-mouth area, The Netherlands: palaeogeography and sequence stratigraphy.*

Abstract

We reconstructed the palaeogeography of the Rhine-valley (western Netherlands) during the early-middle Holocene transgression. The results are used to discuss the land-sea interactions during that time and to describe the incised-valley fill in sequence stratigraphic context. We show that the coastal prism formed in three stages: (1) Before 8.5/8.3 ka BP, when the area was dominated by fluvial environments with extensive wetlands; (2) After 8.5/8.3 ka, when coastal retrogradation occurred less strongly in the Rhine river-mouth area than along adjacent coastlines, creating a temporary promontory. Extensive back-barrier basins formed in which a bay-head delta developed. Tidal amplitudes and currents increased rapidly when the southern and northern North Sea became fully connected leading to wider and deeper tidal inlets; (3) Between 7.5-6.3 ka BP, when a northward avulsion of the Rhine river mouth resulted in severe erosion of the promontory sediments, which were stored in the back-barrier area hereby reducing retrogradation – setting the stage for the production of a maximum flooding surface. The location of the Rhine river-mouth area along a wide, low-gradient continental shelf meant that base-level changes were dominant for a relatively short period of the last glacial cycle. This resulted in a sequence that does not fit standard sequence models: the sequence boundary was formed ~60 ka before the LGM and lowstand system tract deposition lasted until 15-13 ka BP after the LGM. Deposits of such systems are therefore more representative of changes in the balance between river discharge and sediment load and could hold excellent records of climatic changes or other catchment-scale changes. The transgressive surface is diachronous, but the diachroneity is suppressed in those parts of the study area that drowned during a period of accelerating sea-level rise. In rapidly drowning areas such as the early Holocene Rhine river-mouth area, offshore preservation potential of the fluvial onlap at the top of the lowstand systems tract is higher than generally realised.

5.1 Introduction

The initiation of delta formation and the burial of incised valleys in the early-middle Holocene have been studied intensively around the world (e.g. Allen, 1990; Allen and Posamentier, 1993; Stanley and Warne, 1994; or recently Tanabe et al., 2006; Vis et al., 2008; Tamura et al., 2009; Hijma et al., 2009: Chap. 2). Most studies use thoroughly researched cores and cross sections to unravel and date developments, and scale this info up using conceptual models to arrive at a description of sedimentary architecture. In few deltas and estuaries, subsurface information is sufficient to map and trace architectural elements and reconstruct palaeogeography independent of conceptual models. An exception-to-the-rule example is the fluvially dominated part of the Rhine-Meuse delta in The Netherlands (Berendsen and Stouthamer, 2000). Such a palaeogeographic reconstruction helps to identify between allogenic and autogenic controls involved in the evolution of an area and can highlight those events that cannot otherwise be explained than by allogenic forcing. However, a detailed palaeogeographic reconstruction spanning the fluvial-to-marine transition for an early Holocene major river system is not yet available – despite the global significance of this time period (Stanley and Warne, 1994) in the evolution of today's coastal plains and major deltas – and the strong bearings of the Holocene analogue on the geological interpretations of ancient successions. This is due to common lack of appropriate resolution of geological datasets towards the base of Holocene coastal prisms. One issue is the depth of the deposits of interest (typically more than 10 m below the surface) which makes data gathering slow. Equally important is the complexity of environment in which basal coastal prism deposits accumulated, i.e. the fluvial-to-marine transition zone (Dalrymple and Choi, 2007), which demands denser data collection than simpler environments. When based on a dense set of observational data, a palaeogeographical reconstruction can validate and refine sedimentary-evolution and sequence-stratigraphical concepts. This approach is beneficial for the characterisation of Quaternary deltas/estuaries (many host important groundwater reserves) and ancient deltas/estuaries (many host significant hydrocarbon reserves) by projecting modern analogues on more ancient settings. As deltas and estuaries are vulnerable areas with regard to sea-level rise and erosion, adequate knowledge of the natural system is also essential for coastal management (protection, flood control).

This paper presents a detailed palaeogeographical reconstruction of the development of the Rhine-Meuse river-mouth area during transgression in the early-middle Holocene (9-6 ka cal BP). This was possible now that new datasets have been scrutinized and integrated (Hijma et al., 2009: Chap. 2; Hijma et al., Subm.: Chap. 4) and the local sea-level history of the study area has been resolved (Hijma and Cohen, In press: Chap. 3). The reconstruction comprises six maps and a schematic cross section along the valley axis. The work is principally based on mapped facies distributions, compiled from abundant core, borehole, seismic, microfossil and geochronological data collected by many workers. From

these maps, land-sea interactions are identified and discussed. The detailed reconstructed developments are then generalised by describing them in terms of sequence stratigraphical concepts for fourth-fifth order cycles (orders cf. Vail et al., 1977; Miall, 2000). Our division in systems tracts is primarily based on facies analysis and independent dating and only then contrasted with local sea-level history for the western Netherlands. The derived sequence model is then compared to the standard sequence model.

5.2   Setting

5.2.1   Regional setting

The Rhine-Meuse delta (~2,600 km^2) is fed by a catchment of ~220,000 km^2 and is part of the southern North Sea coastal plain (Fig. 5.1). The river Rhine is 1320 km long and has an average discharge of 2,260 m^3/s at the Dutch border (extreme peak discharge ~12,500 m^3/s), while the river Meuse is 925 km long with an average discharge of 230 m^3/s at the Dutch border (extreme peak discharge ~3000 m^3/s). All the active channels within the maximum ~50 km wide delta are fully embanked and channel widths and depths are regulated. Present-day gradients decrease from ~15 cm/km near the border to 2 cm/km near Rotterdam (Berendsen, 1998). Today, the apex of the delta coincides roughly with the Dutch-German border and is situated at 12 m O.D. (Dutch Ordnance Datum ~mean sea level). During the Holocene however (Fig. 2.2), the apex shifted over large distances (mainly upstream) due to sea-level rise and river response to climate changes (Pons, 1957; Törnqvist, 1998; Berendsen and Stouthamer, 2000) leading to fluvial onlap.

The present river mouth is characterised by an ebb-dominated regime, with maximum ebb velocities of 1.2 m/s and a mean tidal amplitude of ~1.8 m (Terwindt et al., 1963). Geological observations and modelling studies suggest the tidal amplitude to have been fairly constant in the last 6.3 ka (Roep and Beets, 1988; Van der Molen and De Swart, 2001a). For the early and middle Holocene, tidal amplitudes were modelled to be significantly lower due to shallower water depths in the southern North Sea (<1 m; Gerritsen and Berentsen, 1998; Van der Molen and De Swart, 2001a). Before 8.5/8.3 ka BP tidal amplitudes were especially low, because the connection between the Strait of Dover and the northern North Sea was not yet fully established (Conradsen and Heier-Nielsen, 1995; Lambeck, 1995; Jiang et al., 1997; Van der Molen and Van Dijck, 2000). Mean significant wave height at present is 1.1 m. For the middle Holocene mean significant wave height was modeled to be ~0.75 m (Van der Molen and De Swart, 2001b). Based on the tidal amplitude and the mean significant wave height, the present coast is classified as a mixed-energy, wave-dominated coast (Davis and Hayes, 1984). Palaeosalinity and palaeo-wave directions are not well established.

5.2.2 Geological setting

The study area is for the larger part located within the West Netherlands Basin (WNB), an active depocentre of the tectonic North Sea Basin (e.g. Ziegler, 1994). The southwest of the study area is situated on a relatively stable shoulder block of the London-Brabant massif, the Campine High (Figs. 2.1, 5.1; Kooi et al., 1998). A fault zone separates this block from the WNB (Fig. 2.1; Van Balen et al., 2000) with indications of displacement activity during the Late Glacial and Early Holocene (Van Balen et al., 2000; Cohen, 2005; Hijma et al., 2009: Chap. 2). During the Last Glacial Maximum (LGM; ~22 ka BP) sea level stood
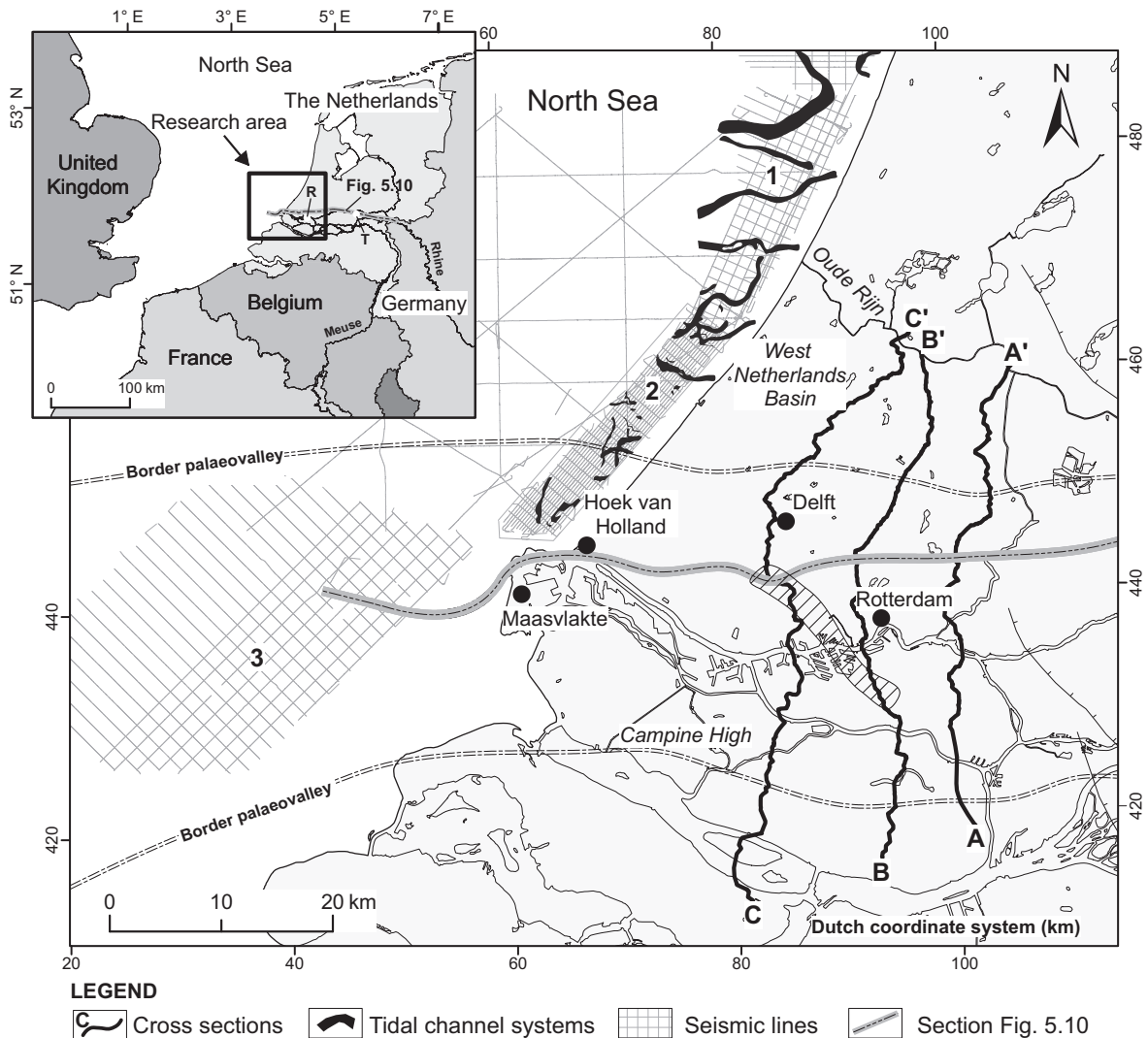
Figure 5.1 Location map of the study area. Cross sections were published by Hijma et al. (2009: Chap. 2). Offshore study areas: 1) Rieu et al. (2005); 2) Hijma et al. (Subm.: Chap. 4); 3) Van Heteren et al. (2002). The inset shows the full length of the section in Fig. 5.10 and the position of Rotterdam (R) and Tiel (T). The border of the palaeovalley is indicated and coincides with the border of the coversand areas north and south of the palaeovalley.

ca. 120 m lower (Fairbanks, 1989) and the mouth of the then combined northwest European rivers, including the Rhine-Meuse system, was located well south of the Strait of Dover (Bridgland and D'Ollier, 1995; Toucanne et al., 2009). During the last glacial, the Rhine-Meuse system had formed a wide palaeovalley traversing The Netherlands (Pons, 1954; Verbraeck, 1984; Cohen et al., 2002) through a periglacial landscape, some hundreds of kilometres south of the Fennoscandian Ice Sheet. Towards and during the LGM, the study area was uplifted due to peripheral glacio-isostatic adjustment (GIA) and consequently the area experienced accelerated subsidence ('forebulge collapse') in Late Glacial, early and middle Holocene times (Kiden et al., 2002; Vink et al., 2007). The GIA-induced uplift-subsidence events left a well developed incised-valley system (Busschers et al., 2007). The accelerated subsidence resulted in high rates of relative sea-level rise (SLR; Fig. 5.2). From 10 to 8 ka sea level in the southern North Sea rose from ~34 to 13.5 m –O.D. (Jelgersma, 1961; Vink et al., 2007; Hijma and Cohen, In press: Chap. 3), an average rate of 1 m/100 yr. In the two centuries after 8.45 ka the rate doubled due to drainage events near the Hudson Bay (Hijma and Cohen, In press: Chap. 3). After 8 ka SLR slowed down, with average rates of 55 cm/100 yr and 30 cm/100 yr between 8-7 ka and 7-6 ka, respectively (Jelgersma, 1961; Van de Plassche, 1982; 1995; Hijma and Cohen, In press: Chap. 3).

The glacial to interglacial transition resulted in a climate-driven change in river style from fully braided during the Late Pleniglacial to eventually meandering in the Holocene (Pons, 1957; Berendsen et al., 1995; Vandenberghe, 1995; Cohen, 2003). This change resulted in a lowering of the active riverbed with 1-2 m (e.g. Pons, 1957; Törnqvist, 1998; Hijma et al., 2009: Chap. 2), i.e. a climate-driven incision despite regionally ongoing GIA-accelerated subsidence. During the Holocene transgression, the modern coastal prism started to form which onlaps palaeovalley topography (valley gradient 25-20 cm/km). It is ~25 m thick in the western and <10 m in the eastern part of the study area. The prism is made up of an intercalation of tidal, estuarine and fluvial deposits including many organic beds, whereas the palaeovalley substrate consists mainly of fluvial channel sands overlain by a clayey loam bed, on average ~1 m thick and predominantly of early Holocene age (Busschers et al., 2005; Hijma et al., 2009: Chap. 2). North and south of the palaeovalley (Fig. 5.1), flanking older terraces are capped by a sheet of aeolian coversands (cf. Van der Hammen et al., 1967). In the central part of the palaeovalley complexes of aeolian dunes are present that bordered river courses of equal age. Most of them were formed during the Younger Dryas and earliest Holocene (Preboreal) in a period with seasonally-dry riverbeds and low groundwater levels (De Groot and De Gans, 1996; Berendsen and Stouthamer, 2001; Bohncke and Hoek, 2007). Dunes of slightly younger early Holocene age (Boreal) have also been encountered locally (Pons and Bennema, 1958; Hijma et al., 2009: Chap. 2). Most of the early Holocene depositional 'pre-transgression valley surface' is capped by a basal peat layer marking regional groundwater-level rise that is well datable

using ^{14}C dating and is traditionally mapped as the 'base Holocene coastal prism'. It in turn is covered by freshwater deposits that increasingly show a tidal signature to the top. Especially in former upper estuarine environments, these fluvial-tidal deposits consist of thick layers of organic-rich mud (Hijma et al., 2009: Chap. 2). Eventually, the transgression led to higher salinities and the formation of subtidal deposits indicating continued submergence of the terrestrial landscape (Pons et al., 1963; De Groot and De Gans, 1996; Hijma et al., 2009: Chap. 2). Within the coastal prism many organic layers are present, some of which are of regional extent and stratigraphic significance (Hijma et al., 2009: Chap. 2; Hijma and Cohen, In press: Chap. 3). The latter are mostly detrital peat/gyttja layers, whereas in-situ peats are of more local occurrence.
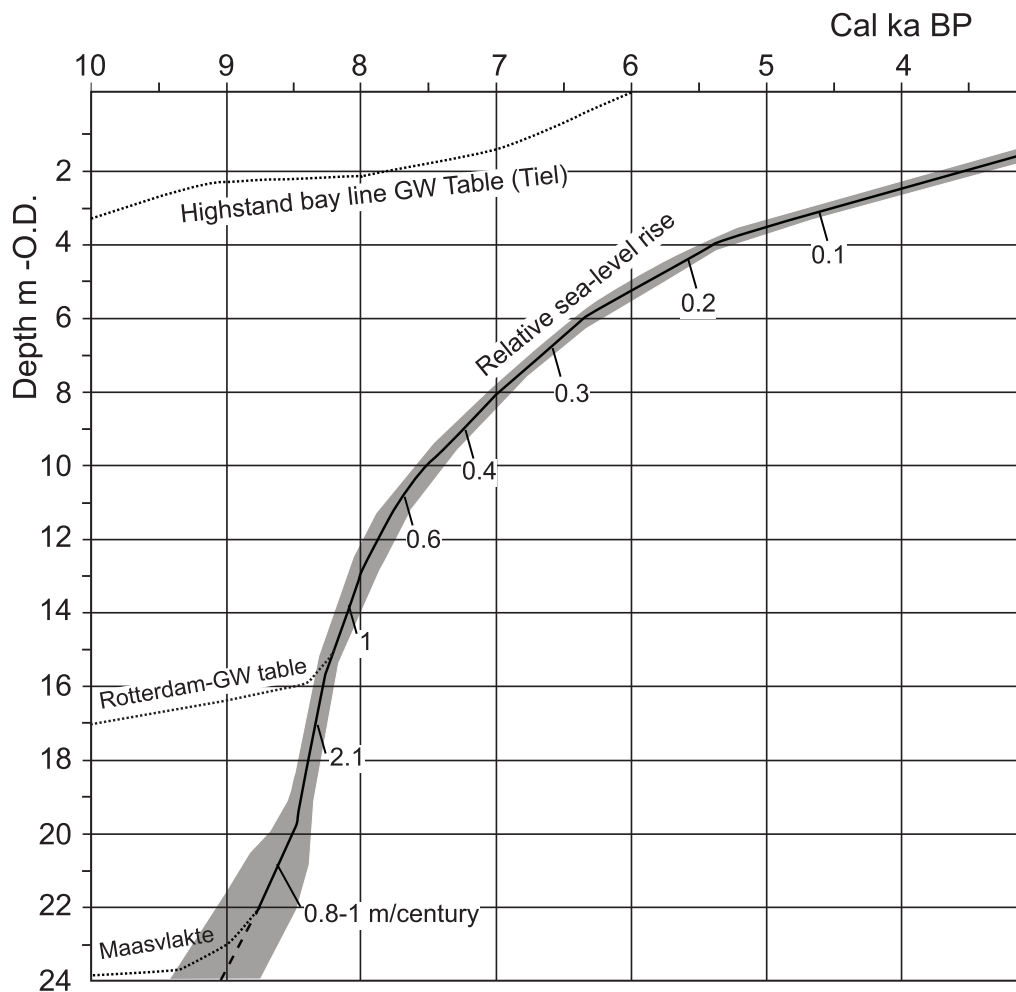
Figure 5.2 Relative sea-level curve and inland groundwater-level rise for the Rhine river-mouth area in The Netherlands. Based on Jelgersma (1961); Van de Plassche (1982; 1995); Cohen (2005) and Hijma and Cohen (Hijma and Cohen, In press: Chap. 3).

108

In the study area, a series of beach ridges is situated along the present coast that becomes progressively older in a landward direction. The oldest preserved beach ridge dates from 6.3-6 ka BP (Van der Valk, 1996b; Beets and Van der Spek, 2000; Cleveringa, 2000). It was formed during the turnaround from a retrogradational to a progradational coast. In the study area this occurred relatively early in comparison to other parts of the Dutch coast.

5.3   Methods

5.3.1   Data inventory

The onshore palaeogeographic reconstruction of the Holocene lower Rhine-Meuse delta is based on a synthesis of previously published data, which were confronted with materials in a large database consisting of tens of thousands of core descriptions, cone penetration test results, hundreds of radiocarbon dates, tens of OSL dates as well as pollen and diatom analyses. The bulk of the data comes from the Geological Survey (TNO, 2009), Utrecht University (Berendsen, 2005) and the municipalities of Rotterdam and Zoetermeer (See Hijma et al. (2009: Chap. 2) for full background on the various materials). A wealth of information also exists in published form, e.g in papers predominantly addressing coastal evolution (Pons et al., 1963; Van Straaten, 1965; Beets et al., 1992; Van der Valk, 1996a; b; Beets and Van der Spek, 2000; Cleveringa, 2000), addressing back-barrier (fluvial) development (Van der Woude, 1983; Berendsen and Stouthamer, 2000; Busschers et al., 2007) or a combination (De Groot and De Gans, 1996; Vos and Van Heeringen, 1997; Hijma et al., 2009: Chap. 2). A framework for temporal and spatial changes in back-barrier lithofacies, based on three 50 km long N-S cross sections, was provided by Hijma et al. (2009: Chap. 2) and is used as a starting point for drawing palaeogeographic maps of the back-barrier environment. In addition, published geological maps were used (Hageman, 1964; Van Rummelen, 1970; Verbraeck and Bisschops, 1971; Van Staalduinen, 1979; Kok, 1987; Bosch and Kok, 1994). Due to topographic inversion (differential compaction), sandy channel systems down to 4 m below the surface could be traced using high-resolution laser-altimetric-surface elevation data (Rijkswaterstaat-AGI, 2005; Berendsen and Volleberg, 2007). Where possible, these data were used to map (tidal-)channel belts with great precision. For the present-day offshore area, reconstruction relies heavily on published seismic data (Van Heteren et al., 2002; Rieu et al., 2005; Hijma et al., Subm.: Chap. 4). The original seismic data was re-analyzed when constructing the maps.

Selections of the data (e.g. borehole databases, seismic data, old maps) were converted to be used in a GIS-environment, which also served to digitize the palaeogeographic maps. Obviously, the amount of detail in the maps varies along with variations in data density.

5.3.2 Independent chronology

From the study area, hundreds of radiocarbon and tens of optically stimulated luminescence (OSL) dates were available. New-collected data within the project are documented in Hijma et al. (2009: Chap. 2). All radiocarbon dates have been calibrated using OxCal 4.0.5 software (Bronk Ramsey, 1995; 2001) with the INTCAL04-curve (Reimer et al., 2004) for terrestrial, botanical samples and the MARINE04-curve (Hughen et al., 2004) for marine shells. Details of most radiocarbon samples can be found online in a database that exists for the Rhine-Meuse delta: http://www.geo.uu.nl/fg/ palaeogeography/data/avulsions/radiocarbon_dates_Berendsen_&_Stouthamer_2001.pdf.

Details of many OSL-dates in The Netherlands can be found at: www.lumid.nl. Furthermore, a well established pollenstratigraphy (Van Geel et al., 1980/1981; Hoek, 2001) exists for The Netherlands, allowing to pinpoint pollen assemblages fairly accurate in time. The age-depth relation of organic layers, especially the basal peat, has been geostatistically modelled resulting in a 3D-stack of palaeo-groundwater tables for the Holocene (Cohen, 2005). This dataset is used for age constraints of organic layers where no direct chronological data are available (see also Hijma et al., 2009: Chap. 2).

5.3.3 Distinguished units and palaeoenvironments

The presented palaeogeography of the western Netherlands follows from detailed mapping of the distribution of facies units which are diagnostic for palaeoenvironments. Schemes that subdivide and classify these units are available for the study area, both onshore (Van Straaten, 1965; Cleveringa, 2000; Van den Berg et al., 2007; Hijma et al., 2009: Chap. 2) and offshore (Beets et al., 1995; Van Heteren et al., 2002; Rieu et al., 2005; Hijma et al., Subm.: Chap. 4). The facies units were translated into eleven sedimentary environments (Tab. 5.1) to construct the palaeogeographic maps. The palaeo-environments in the maps feature aeolian (coversand and inland dunes), fluvial (distal former floodplains and active overbank deposition), fluvial-tidal (upper estuary and basin), back-barrier tidal (basin), and further barrier (coastal dunes, beach plain), wetland (coastal/lagoonal peats), active channel (tidal, fluvial-tidal and fluvial) and open sea (North Sea) environments. The presence and position of the beach barriers on the maps before 6.3 ka BP are inferred, but the tidal inlets between 8-7.5 ka BP are based on seismic data. All wetland types, whether coastal or fluvial, have been grouped in a single environment. Maps for six specific time intervals are presented here, that bracket time intervals of differing duration (Figs. 5.3-8). The chosen intervals intent to separate the most important changes (next section). Dating resolution of the facies units and the temporal accuracy associated to our paleogeographical maps is ~200 calibrated years.

Table 5.1 Description of the mapped palaeoenvironments. Listed characteristics are: 1. lithology and stratigraphic position; 2. vegetation cover and soil and 3. salinity.

	Palaeoenvironment	Characteristics
Antecedent landscape elements (Late Glacial - early Holocene)	*Coversand area* Inactive, 2-4 m above palaeovalley flood plain	1. Fine and well-sorted, non-calcareous sands, with a palaeosol at the top. Overlies Rhine-Meuse terrace sands, undulating topography (1-2 m relief); 2. In the earliest Holocene covered by forest (e.g. *Pinus, Betula, Quercus*), podzolic palaeosols; 3. Freshwater environment.
	Abandoned floodplain	1. Variable, mostly thin, calcareous fluvial loams with vegetation horizon at the top. Overlies Rhine-Meuse palaeovalley channel deposits; 2. Semi-open landscape with many *Salix* trees, several semi-mature vegetation horizons (fluvisols); 3. Freshwater environment.
	Inland aeolian dune Mostly inactive and vegetated	1. Medium-coarse, well sorted sands with a decalcified top and local palaeosol. Overlies thin loam bed and Rhine-Meuse palaeovalley channel deposits, irregular micro topography with heights up to 15 m; 2. Initially vegetated by mixed forest, podzolic palaeosols; 3. Freshwater environment.
Active systems (early-middle Holocene)	*Active channel system* (fluvial, fluvial-tidal, tidal)	1. Very fine to coarse, calcareous sand, usually poorly sorted and slightly angular. In the (fluvial-)tidal zone also with clay laminae and shell fragments. Subtidal areas included in tidal-channel system; 2. None; 3. Fresh to brackish to marine.
	Fluvial overbank (natural levee, distal)	1. Proximal to channels: silty clay loam, sandy loam. Distal to channels: (silty) clay or humic clay; 2. Trees, grasses, scattered poorly developed vegetation horizons; 3. Freshwater environment.
	Upper estuary, fluvial-tidal basin	1. Silty to sandy clay with abundant woody debris. Permanently flooded, tidal signature; 2. Sparsely vegetated/non-vegetated, subaqueous, no soil formation; 3. Fresh to slightly brackish.
	Fluvial-tidal basin	1. Silty to sandy clay with locally fine sand laminations. Permanently flooded, tidal signature; 2. Sparsely vegetated/non-vegetated, subaqueous, no soil formation; 3. Fresh to slightly brackish.
	Tidal basin (inter/supra tidal flats; this includes all unmapped small tidal creeks and channels)	1. Rhythmic flaser-bedding and laminated grayish blue sandy clay. Higher parts are strongly rooted by *Phragmites*. Often strong bioturbation; 2. Intertidal: pioneering vegetation such as *Salicornia, Spartina* and *Limonium vulgare*. At the edges (fresher and higher) also dense *Phragmites* stands, immature soils; 3. Brackish to marine.
	Barrier	1. Fine to medium well sorted and rounded sand, with occasional clay layers and shells. Partly consisting of washover deposits and low aeolian dunes; 2. Pioneering, halophile vegetation withstanding occasional sand burial, scattered soil formation; 3. Brackish to salt, following progradation turning into freshwater environments (especially in upper parts).
	Wetlands (marshes, small lakes)	1. Peat and gyttja, often overlying semi-mature palaeosols (podzolic in coversand area, fluvisols in the palaeovalley); 2. Swamp forest and extensive *Phragmites-Carex* fields; 3. Mainly fresh, slightly brackish at the fringes of the tidal basins.
	Open sea	North Sea.

111

5.4   Palaeogeography: from river valley to estuary

In this section, a description of the sequential palaeogeographic development is given for the time-interval spanning the Holocene transgression with cross-reference (numbers) to features in the maps. The sections discuss the intervals between the time moments of each map.

5.4.1   Up to 9100 cal BP

Sea-level rise invoked diachronous back-filling of the palaeovalley and had reached 24 m –O.D. by 9.1 ka BP (Hijma and Cohen, In press: Chap. 3). The back-water effect caused river systems to change from incisive to aggradational in a certain stretch inland of the coastline. In the most western part of the study area (*1*; Fig. 5.3), aggradation started before 10 ka BP (Van Heteren et al., 2002), while near Rotterdam it started between 8.5-8 ka BP (De Groot and De Gans, 1996; Hijma et al., 2009: Chap. 2). East of Rotterdam (*2*), channels in incised position meandered within the palaeovalley, on both sides bordered by coversand-capped terraces (*3*). Within the valley floodplain, earlier formed inland-aeolian-dune complexes (*4*) were prominent features that influenced the course of the channels. West of Rotterdam, groundwater levels had already risen to floodplain surface and extensive wetlands had formed (*5*; Jelgersma, 1961). The Rhine and Meuse channels merged east of the Maasvlakte (Fig. 5.1). Wetlands separated this probably microtidal estuary (*6*) from a similar estuary of the Scheldt (*7*) to the south. The position of the shoreline is not known exactly. Tidal channels initially inherited the position of fluvial channels and therefore lay embedded within clay and peat deposits that hindered lateral migration (Van Heteren et al., 2002). The tidal channels only started to migrate freely after significant aggradation. The coastal system was shifting landward owing to the steadily rising sea level and ongoing land subsidence. In the present-day offshore area, the width of the active Rhine-Meuse floodplain inland of the coast appears smaller than further east. This pattern correlates with the area's neotectonic structure. The differential subsidence across the active faultzone resulted in wider floodplain across the faster subsiding WNB than on the more stable block downstream. The Scheldt (*7*) in its lower reaches had incised relative deeply during the Late Glacial (Vos and Van Heeringen, 1997; Bos et al., 2005) and earliest Holocene – as had fluvial channels of the Rhine and Meuse west of faultzone (Hijma et al., 2009: Chap. 2). The Scheldt confluence with the Rhine-Meuse system was probably at the study area's western end. Downstream of the confluence, the joint estuary occupied nearly the full width of the palaeovalley (based on Van Heteren et al., 2002). Extensive freshwater wetlands were present in the coversand areas north and south of the estuary (*8*). Pollen-dated peat samples trawled from the North Sea floor (Jelgersma, 1961), indicate that the eastward boundary of the wetlands lay ~20 km west of the present coastline (*9*). The 9.1 ka BP estuary can be classified as fluvially dominated and
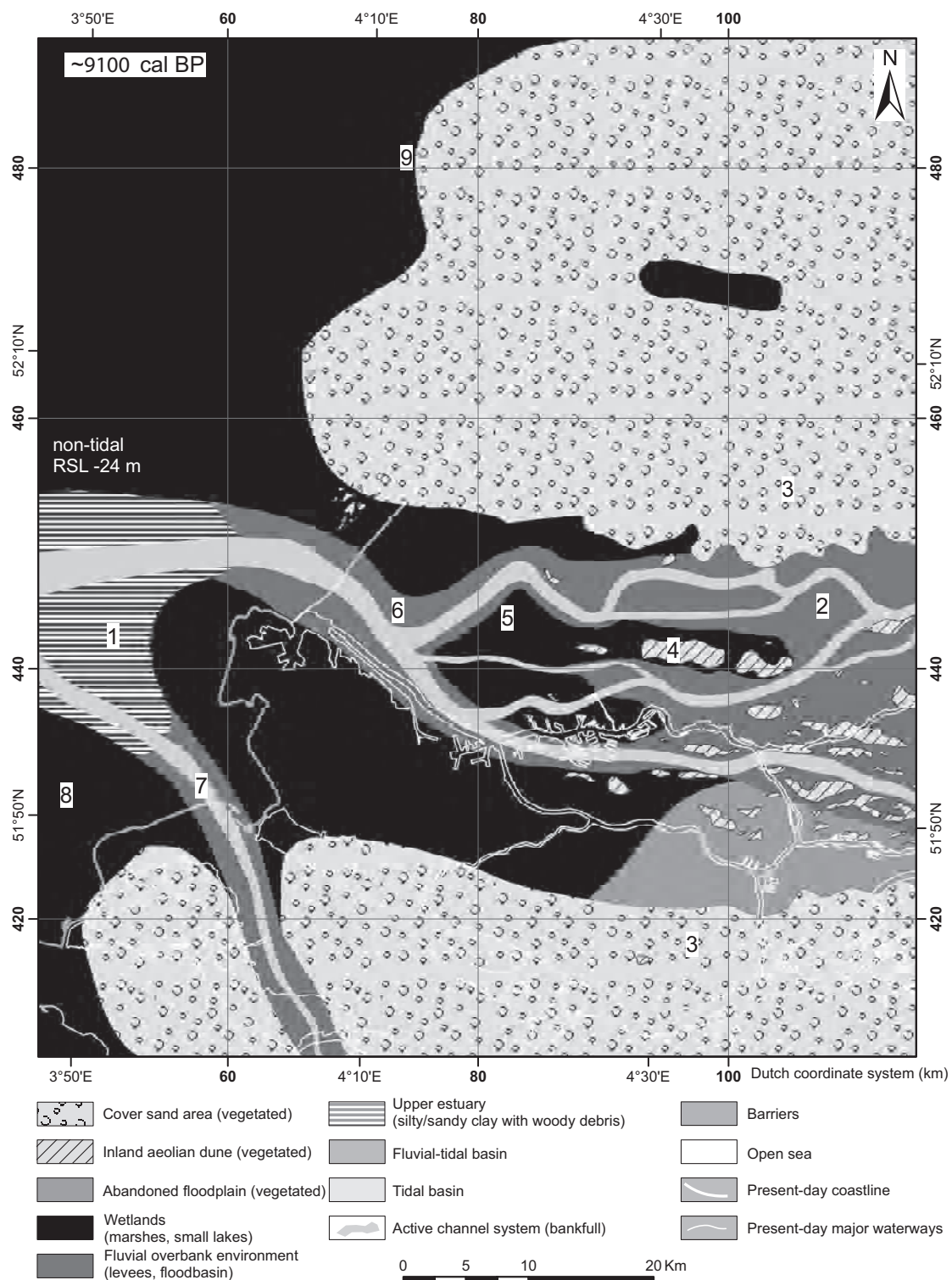
Figure 5.3 Palaeogeography around 9100 cal BP showing late Boreal channel belts within the palaeovalley. Widespread peat formation had already started. RSL=Relative sea level. See Fig. A5.15 for colour version.

the thick fresh, clayey deposits are characterised by an abundance of woody debris (Van Heteren et al., 2002), indicating that the wetlands upstream consisted for a significant part of swamp forest (see also Terbregge Member in Hijma et al., 2009: Chap. 2).

5.4.2   9100 – 8500 cal BP

This time interval is characterised by a gradual, but steady landward shift of the coastal and estuarine environments (Fig. 5.4). The first tidal-basin environments replace coversand wetlands (*10*). The presence of a wide estuary (*11*) with increasingly saline deposits is evident (Van Heteren et al., 2002). The estuary received the joint Rhine-Meuse and the Scheldt systems. As in the previous time slice, the estuary narrowed upstream (*12*) and then widened again into a wide fluvial floodplain (*13*). Around Rotterdam and in the southern part of the palaeovalley extensive wetlands with large *Salix* stands (*14*) fringed the channel belts (Hijma et al., 2009: Chap. 2).

5.4.3   8500 – 8000 cal BP

During this time interval sea level rose at accelerated pace from 19 to 13.5 m –O.D. due to a global sea-level jump preluding the 8.2 ka cold-climate event. The magnitude of the jump in the study area was 2.11 ± 0.89 m and the remaining ~4.5 m occurred as 'background' rise. The jump set on 8.45 ka BP and was completed by 8.2 ka BP (Hijma and Cohen, In press: Chap. 3). Accelerated SLR caused drowning of the area in less gradual fashion than before and the wide back-barrier basins show marked environmental change (Fig. 5.5). This was further enhanced by increasing tidal amplitudes along the coast and in the basins due to the establishment of a full connection between the southern and northern North Sea in this period (Conradsen and Heier-Nielsen, 1995; evident from Jiang et al., 1997; Van der Molen and De Swart, 2001a; also discussed in Hijma and Cohen, In press: Chap. 3). A coastline was now present in the western part of the area (*15*). The presence of back-barrier channels north of the main estuary is supported by seismic data, revealing tidal channel networks that were abandoned ~7.5 ka BP (Rieu et al., 2005; Hijma et al., Subm.: Chap. 4; see below). Assuming continuous, steady retreat of the coastline in the period before 7.5 ka BP, 3 m of SLR (Hijma and Cohen, In press: Chap. 3) and a gradient of 20 cm/km for the coversand area (based on Van de Plassche, 1982; Hijma et al., 2009: Chap. 2), the 8.0 ka BP back-barrier system has been projected ~15 km west of the 7.5 ka BP configuration.

The Meuse had avulsed to a more southerly course (*16*). Rhine, Meuse and Scheldt central-upper estuaries merged in a ~10 km-wide estuary (*17*). Tidal influence reached far inland, especially in the southern part of the Rhine-Meuse floodbasin (*18*), where thick stacks of layered silty clays, containing abundant woody debris accumulated (*19*; Hijma et al., 2009: Chap. 2). In contrast, in the north freshwater environments reached further
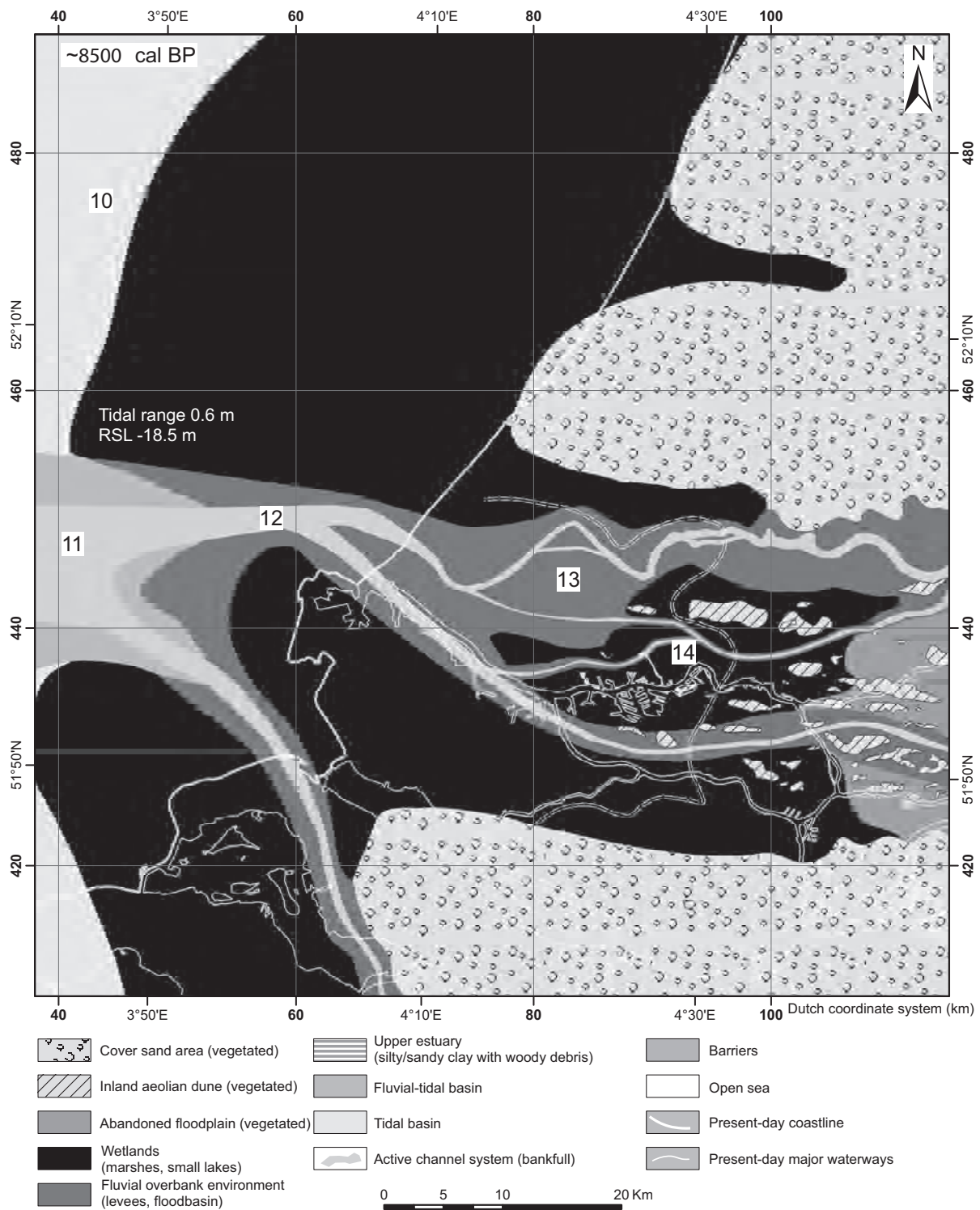
Figure 5.4 Palaeogeography around 8500 cal BP showing landward shifting of system, especially of the wetland area in the north. The landward limit of the drowned area in the Rhine-Meuse valley during the following sea-level jump is given (white double dashed line, based on Hijma and Cohen, In press: Chap. 3). RSL=Relative sea level. See Fig. A5.16 for colour version.

seaward (*20*) and a bay-head delta formed at the head of the estuary (*21*; Hijma et al., 2009: Chap. 2). This difference is explained by the larger discharge and sediment loads delivered by the Rhine in comparison to the Meuse. The central part of the palaeovalley,distal to main river branches, and the northern coversand area became covered by swamps and small lakes (*22*).

5.4.4   8000 – 7500 cal BP

Between 8-7.5 ka BP, sea level rose 3 m with a significantly lower rate (60 cm/100 yr) than in the preceding 500 years. As a result, the rate of retrogradation slowed down as sediment delivery started to keep up with accommodation space creation (Fig. 5.6). North and south of the main estuary, retrogradation of the coastline occurred at a faster rate than near the mouth, leading to the formation of a promontory. Differential retrogradation was caused by the presence of thick packages of especially clay and peat in the estuary mouth that are more resistant to erosion than the sandy coversand deposits, that were capped by a much thinner peat and clay layer (Beets et al., 1995; Hijma et al., Subm.: Chap. 4).

The existence of estuarine environments offshore the Maasvlakte (*23*) is evident from pollen/diatom and sedimentological interpretations: this stage is characterised by multiple, broad and generally shallow subtidal channels (Van Heteren et al., 2002). The estuary had widened due to increased tidal amplitudes that result in higher tidal velocities and an increase in the cross-sectional area *(24)*. The tidal-channel networks north of the estuary are based on seismics (Rieu et al., 2005; Hijma et al., Subm.: Chap. 4). Where these networks converge, tidal inlets are inferred with hypothetical barrier islands depicted in between. The rapid rate of retrogradation must have limited the width of the barrier islands. The position of the coastline south of the estuary mouth is uncertain. Bay-head delta formation continued at the termination of the main Rhine-distributaries (*25*; Hijma et al., 2009: Chap. 2). The Rhine channel network had changed into anastomosing style (cf. Makaske, 2001) in the back-barrier area *upstream* of the upper estuary (*26*). The position of the Meuse and the Scheldt estuaries was stable. The fluvial-tidal area had increased considerably in size, possibly explained by increasing tidal amplitudes. Most of the inland-aeolian dune complexes by now were covered with peat and clay. Only the large ones cropped out in the coastal plain forming important sites for human occupation.

The northern transition between the fluvial-tidal and the tidal-basin environment is based on pollen/diatom data (Beets et al., 1995; Hijma et al., 2009: Chap. 2; Hijma et al., Subm.: Chap. 4). The lateral transition was obviously gradual, but data resolution allows drawing a provisional, indicative boundary only. It is unknown to what extent fluvial-tidal and tidal outlets drained separate basins or if some of the basins were interconnected. The limit of the fluvial-tidal environment reaches well outside the palaeovalley across neighbouring coversand area (*27*). The formerly swampy northern rim of the palaeovalley had completely drowned by then, with no elevation differences remaining.
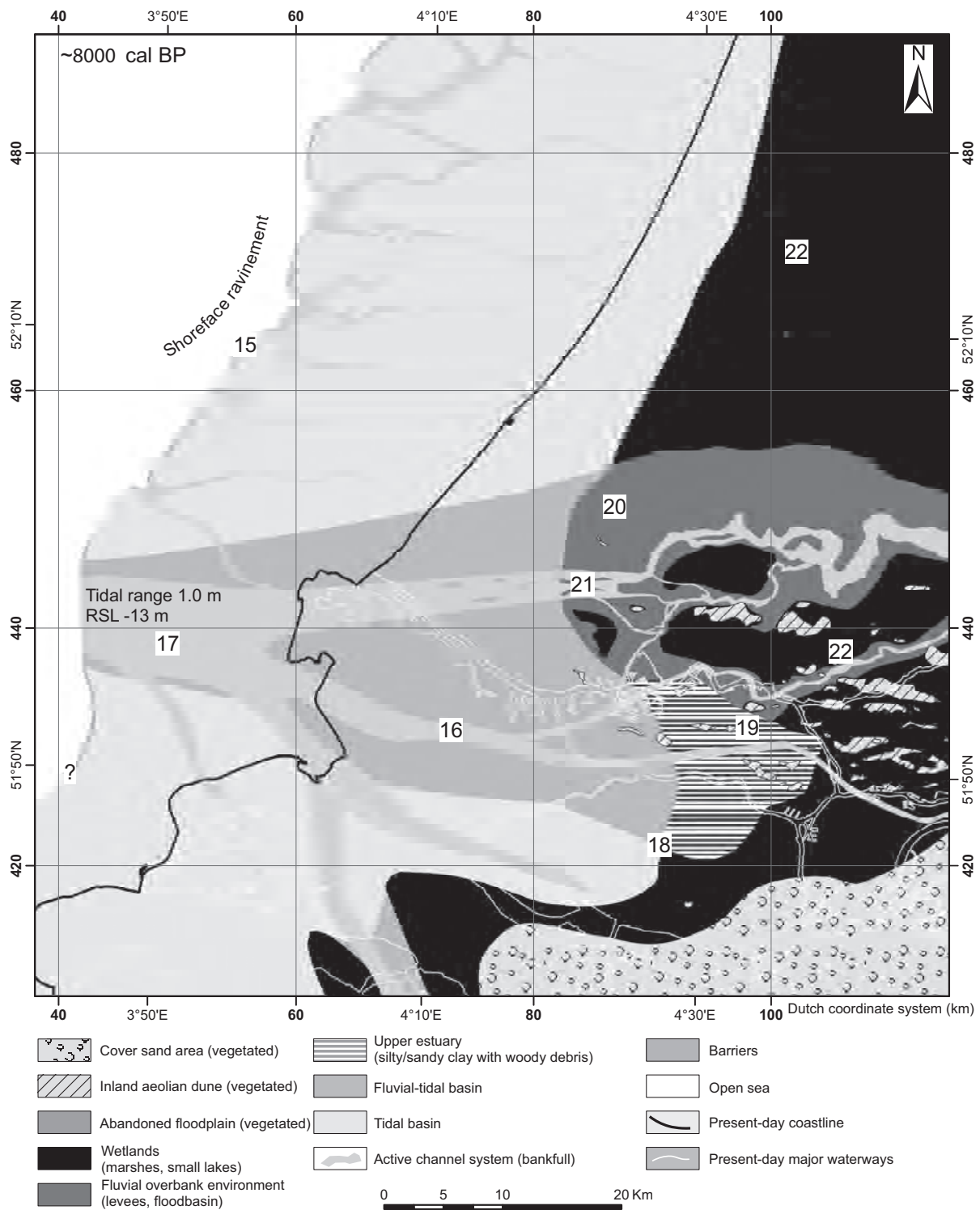
Figure 5.5 Palaeogeography around 8000 cal BP. During and immediately following the sea-level jump, rapid transgression and coastline retrogradation occurred. RSL=Relative sea level. See Fig. A4.17 for colour version.

5.4.5   7500 – 6800 cal BP

The rate of SLR decreased further to ~50 cm/100 yr and the overall rate of retrogradation further slowed down (Fig. 5.7), although during this period the barrier system north of the estuary mouth was probably overstepped (Rieu et al., 2005; Hijma et al., Subm.: Chap. 4). An upstream avulsion (Berendsen and Stouthamer, 2000; Hijma et al., 2009: Chap. 2) led to the formation of a new main Rhine-branch with its mouth near Leiden (*28*). Secondary distributary channels were probably connected to smaller tidal inlets (*29*). Dates of peat directly below overbank deposits and OSL-dates from bar deposits of the new branch indicate the avulsion to have occurred ~7.3 ka BP. This matches well with youngest ages of truncated estuarine deposits in the present-day offshore area (Van Heteren et al., 2002), indicating rapid transgression of the abandoned estuary (*23-24*). This resulted in strong erosion of the promontory (*30*). The large amount of available sediment was used to fill in the former Rhine-estuary with sand near the shoreline and mainly mud in the former upper estuary (*31*) where the environment remained essentially fresh, most likely due to input of several small and undetected Rhine-branches. In addition, the available sediment was transported north along the coast and then routed into the northern tidal basins by wave-driven, near-coastal longshore currents (Van Straaten, 1965; Van Heteren et al., 2002). The size and number of tidal inlets therefore decreased gradually, in turn leading to erosion of the ebb-tidal deltas (Beets et al., 1992) and a surplus of available sediment along the beach-barrier shores. Inland, Rhine-abandoned parts of the flood plain changed into wetlands (*32*) while in the northerly wetlands the new Rhine channel belt began to mature and prograde into tidal back-barrier area. The coastline north of Hoek van Holland had retreated to a position inland of the present coastline. The river Scheldt had switched to a new mouth in the south.

5.4.6   6800 – 6300 cal BP

A second avulsion along the Rhine further rerouted the main discharge to a northerly position (Berendsen and Stouthamer, 2000), but the outlet remained the same (Fig. 5.8). Most likely the new branch connected to an existing tidal channel (*33*). The former main Rhine branch was completely abandoned, leaving a basin that was rapidly transgressed and filled in by the wide Rijswijk-Zoetermeer system (*34*, Van der Valk 1996b). At present, deposits of this system lie at the surface as younger peat accumulations have been removed in the Medieval Times. As a result the system could be mapped in detail. Erosion of the wetlands occurred at the landward side of the Rijswijk-Zoetermeer basin and is characterised by a shell lag of *Hydrobia* and *Cerastoderma* species at the contact. The Rijswijk-Zoetermeer basin was filled in rapidly due to the surplus of available sediment (see previous interval) and by 6.1 ka BP the associated tidal inlet closed (Van der Valk, 1996b; Cleveringa, 2000; Van der Spek et al., 2007).

~7500 cal BP

Shoreface ravinement

Tidal range 1.5 m
RSL -10 m

Rhine-Meuse-Scheldt
promontory

27

?

25

24

23

26

N

Dutch coordinate system (km)

Cover sand area (vegetated)

Inland aeolian dune (vegetated)

Abandoned floodplain (vegetated)

Wetlands
(marshes, small lakes)

Fluvial overbank environment
(levees, floodbasin)

Upper estuary
(silty/sandy clay with woody debris)

Fluvial-tidal basin

Tidal basin

Active channel system (bankfull)

Barriers

Open sea

Present-day coastline

Present-day major waterways

0   5   10   20 Km

Figure 5.6 Palaeogeography around 7500 cal BP. Retrogradation slowed down due to a decreasing rate of sea-level rise. Longshore currents started to transport sediment from the eroding river mouth to the tidal basins to the north. RSL=Relative sea level. See Fig. A4.18 for colour version.
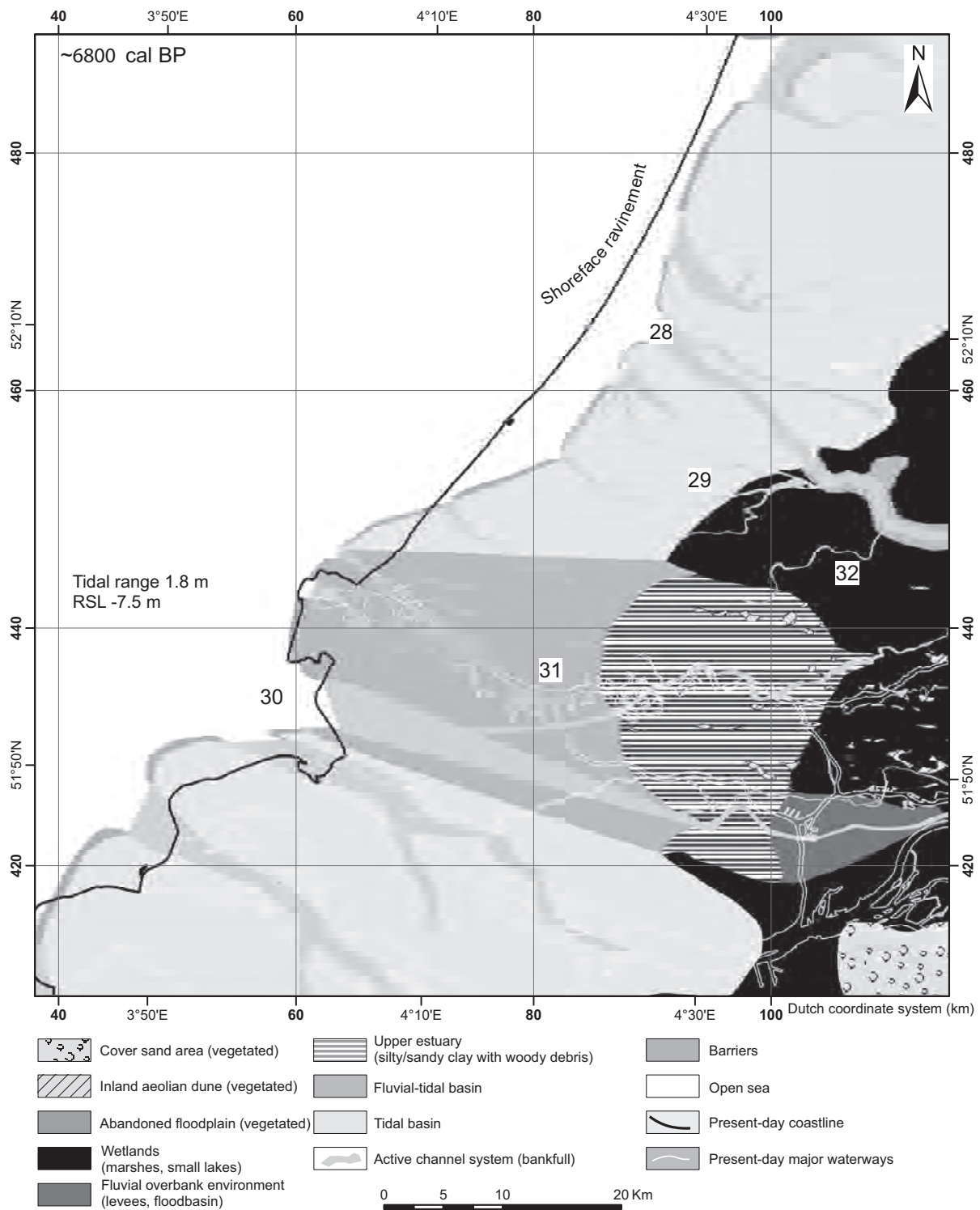
Figure 5.7 Palaeogeography around 6800 cal BP. The main Rhine river mouth had shifted north and outside the palaeovalley. RSL=Relative sea level. See Fig. A4.19 for colour version.

The map contains the following labels and annotations:

~6300 cal BP

Shoreface ravinement

Tidal range 1.8 m
RSL -6 m

Dutch coordinate system (km)

Legend:

Cover sand area (vegetated)

Inland aeolian dune (vegetated)

Abandoned floodplain (vegetated)

Wetlands
(marshes, small lakes)

Fluvial overbank environment
(levees, floodbasin)

Upper estuary
(silty/sandy clay with woody debris)

Fluvial-tidal basin

Tidal basin

Active channel system (bankfull)

Barriers

Open sea

Present-day coastline

Present-day major waterways

0   5   10   20 Km

Figure 5.8 Palaeogeography around 6300 cal BP. Retrogradation halted in the centre of the study area, but continued to the north. RSL=Relative sea level. See Fig. A4.20 for colour version.

121

The former Rhine-estuary near Rotterdam (*24-25, 31*) was completely filled with sediment. The disappearance of multiple Rhine channels and the closure of several tidal inlets resulted in poor drainage conditions and the wetland area increased rapidly. The coastline had reached its most eastward position (*35*) in this region shortly after the tidal inlets started to close (Van der Valk, 1996b; Cleveringa, 2000; Van der Spek et al., 2007). North of the active Rhine mouth (*35*), retrogradation of the coastline continued for several more centuries (Van der Valk, 1996a), although several tidal inlets closed (Van der Valk, 1996a; Cleveringa, 2000). Marine influence remained dominant in the Scheldt area (Vos and Van Heeringen, 1997). As the wave-driven longshore current was directed to north, the abundantly available Rhine-promontory sediment did not reach this area and retrogradation continued for several centuries more.

5.5 Discussion

5.5.1 Land-sea interactions

Based on changes in sediment delivery from the North Sea to the near-coastal zone, the studied period has been divided into three parts: 9.1-8.3 ka; 8.3-7.5 ka and 7.5-6.3 ka BP (Fig. 5.9). During this time significant changes occurred in tidal amplitudes, net sediment transport directions and magnitude due to deepening of the North Sea. The possible influence of these changes on the above described palaeogeographical development is discussed below.

9100 – 8300 cal BP: Disconnected southern and northern North Sea and weak, onshore net sediment transport

Before 8.5/8.3 ka, no full connection existed between the southern and northern North Sea (Fig. 5.9). The damped tidal wave (microtidal conditions) entered the shallow southern North Sea through the Strait of Dover, propagated parallel to the coast in the Deep Channel and then cross-shore towards the eastern shore, also transporting wave-induced suspended sediments (Van der Molen and Van Dijck, 2000; Van der Molen and De Swart, 2001a). Sediment supply to the near-coastal zone was therefore relatively high, especially near river mouths where fluvial sediment contributed to the sediment budget, although a great portion of the fluvial sediment was stored before it reached the sea (Erkens, 2009; Hijma et al., 2009: Chap. 2). The sediment was subsequently distributed in the coastal zone by especially wave-driven processes and slowed down overall retrogradation. High rates of sea-level rise however still led to rapid expansion of the North Sea over the low-gradient terrestrial surface. Wave action is thought to have been sufficient to form embryonic barrier systems along the shores (Beets and Van der Spek, 2000). Because of back-barrier storage of fluvial sediments, the formation of a promontory near the main

river mouth (Figs. 5.5-5.6) most likely was not caused by a relative excess of sediment. Instead, the presence of thick layers of clayey, fluvial and estuarine sediments from immediately preceding stages, occurring at shallow depths off the river mouth and being less susceptible to erosion than the sandy substrates to the north and south, promoted the differential retrogradation and promontory formation.

8300 – 7500 cal BP: Full connection, increased tidal amplitudes
Around 8.3 ka BP the southern and northern North Sea became connected after two centuries of increased rates of SLR. Had this jump not occurred, then the establishment of a full connection would have taken 1 or 2 centuries longer. The sedimentological fingerprint of the jump is clearly traceable in the subsurface as an upper-estuarine transgressive gyttjaic basal contact (Hijma et al., 2009: Chap. 2), but the influence of the jump on the eventual coastal configuration after transgression ended was relative limited. The connection resulted in major changes in the tidal configuration in front of the study area. Incoming tides from the northern North Sea formed an amphidromic point (Van der Molen and Van Dijck, 2000; Uehara et al., 2006). Tidal amplitudes and current velocities increased rapidly, while net sand transport remained cross-shore (Fig. 5.9). Modelling results suggest that large amounts of sediments, aided by wave suspension, were transported to the near-coastal zone and then distributed (Van der Molen and Van Dijck, 2000), but it was still insufficient to balance the accommodation space created by SLR. That modelling approach, however, does not include the presence of peat and clay at the bottom of part of the North Sea during this period. Especially the part of the North Sea floor that drowned near-instantaneously during the 8.5-8.3 sea level jump can be expected to have had a relative intact peat-and-clay cap initially. This cap progressively broke up and with some delay made the underlying sand available for wave and current transport towards the coast.

7500 – 6300 cal BP: Rhine mouth relocation, strong erosion of promontory, change to tidal-basin filling
During this period, two changes occurred: 1) stepwise northward avulsions by the Rhine occurring upstream led to a new course of the main distributary and subsequently the formation of a new main Rhine river mouth ~20 km to the north and 2) net fluxes of shoreface sand transport redirected from cross-shore to longshore, hereby reducing the sediment supply from deeper water to the near-coastal zone (Van der Molen and Van Dijck, 2000; Fig. 5.9). This reduction was enhanced by the deepening of the North Sea and the related reduction of wave-induced sediment suspension (Van der Molen and Van Dijck, 2000). Rates of SLR were decreasing, but still significant. Decelerating retrogradation indicates that a lot of sediment was still available for (re)distribution in the near-coastal zone.

The first mentioned change was the stepwise abandonment of the main Rhine mouth near Hoek van Holland after 7.5 ka BP. The Rhine avulsed out of the palaeovalley and started to debouch into a basin near Leiden. The former river mouth was transgressed and its promontory strongly eroded. The available sediment was initially mainly used to fill in the abandoned Rhine-estuary and the tidal basins directly north that started to fill in during this period (Rieu et al., 2005; Hijma et al., Subm.: Chap. 4). The resulting decrease in tidal prism led to shallower and narrower tidal inlets and erosion of the ebb-tidal deltas that further enhanced sediment availability. The shift of the Rhine mouth also resulted in a change of sedimentary regime.
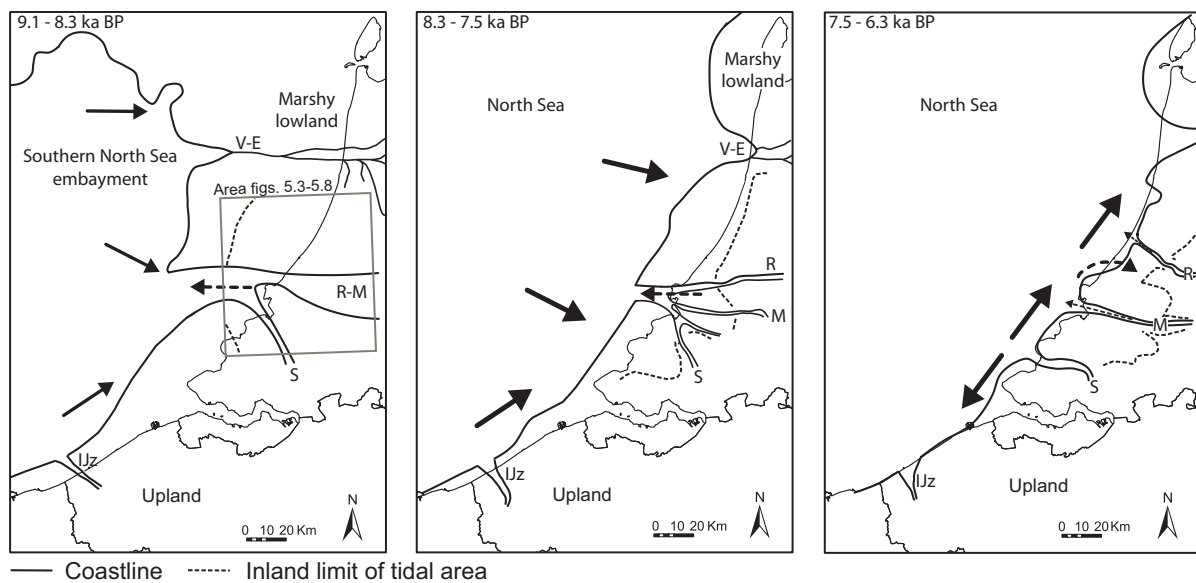
Figure 5.9 Schematic summary of the direction of net sand transport from the deeper North Sea to the coastal zone for the periods 9.1-8.3; 8.3-7.5 and 7.5-6.3 ka BP (thick solid lines: based on Van der Molen and Van Dijck, 2000). The net transport is dominated by tidal currents and before 7.5 ka BP was substantially aided by wave suspension. Fluvial-sand input to the coastal system is most likely limited as most sediment, especially bedload, was stored in the back-barrier basin (Hijma et al., 2009: Chap. 2). An important change occurred after 7.5 ka BP when a longshore current was established. Note that the modelled directions do not apply to the near-coastal zone as it was assumed that sediment dynamics in the near-coastal zone do not affect sediment exchange between the coastal zone and open sea, but only redistribute the sediment. Wave-driven currents, bedforms, the influence of tidal embayments and fluvial discharge that all strongly influence sediment transport in the near-coastal zone were not included. R=Rhine, M=Meuse, S=Scheldt, V-E=Vecht-Eem system and IJz=IJzer. The outline of the IJzer tidal basin is based on Baeteman (1999). The outline of the Vecht-Eem system is based on Pons and Wiggers (1959-1960) and De Gans and Van Gijssel (1996).

The abandoned estuary was large and wide and trapped all Rhine sediment before it could reach the North Sea (Hijma et al., 2009: Chap. 2).The newly formed estuary was much smaller and the Rhine soon started to prograde into the back-barrier basin in the next millennia, eventually forming a protruding delta in the North Sea (Van Heteren and Van der Spek, 2008).

5.5.2   Sequence stratigraphy: a lithofacies approach

During the early-middle Holocene the palaeovalley of the Rhine-Meuse system was filled in with fluvial, estuarine and marine deposits during a period of transgression. In the late Holocene, under conditions of slow SLR (Van de Plassche, 1982) the coastline was prograding. At the main Rhine outlet through the beach barrier a delta formed, in a position well north of the palaeovalley river mouth (Van Heteren and Van der Spek, 2008). This situation persisted until ~500 AD, after which the beach barrier experienced erosion (Pons et al., 1963). In Figure 5.10 a schematic longitudinal section along the palaeovalley axis is given, along with a subdivision into systems tracts and key stratigraphic surfaces. The section crosses the coastline at a point where *no* pronounced barrier system has evolved, i.e. where the coastal barrier never fully closed. As the valley was filled-in completely during one cycle, it can be classified as a 'simple fill' valley (Boyd et al., 2006), albeit that in lateral direction deposits wing out across valley-bordering coastal plain, well overfilling the palaeo-valley low.

At present many sequence-stratigraphy models have evolved with differences in naming and defining systems tracts and also in the placement of sequence boundaries (Catuneanu, 2002; 2007; Catuneanu et al., 2009). Here we use the terminology of the depositional-sequence-II model (cf. Haq et al., 1987; Posamentier et al., 1988). Our division in systems tracts is primarily based on facies analysis and independent dating and then contrasted with local sea-level history for the western Netherlands. In many other studies of post-LGM coastal sedimentary sequences, mostly in situations of limited spatial data coverage (see Introduction), tract-labels and boundaries are put on deposits based on global sea-level behaviour at the time of deposition. Our research differs from this practice by independently mapping and dating shifting palaeoenvironments in time and space first (above), and evaluating the options for drawing tract boundaries later (this section). In a perfect world without diachroneity in sedimentary response, trend breaks in global sea-level curves could be used to define boundaries between systems tracts. But because diachroneity exists and methods of boundary position based on high-resolution numerical dating can only be applied to the youngest geological time, we prefer a lithofacies approach to sequence stratigraphical division also for the youngest Holocene systems.

Sequence boundary positioning

We place the sequence boundary (SB) at the base of forced regressive deposits, i.e. it is

defined by the maximum erosion depth during sea-level fall after the last interglacial. In the western Netherlands this boundary was initiated during a period of pronounced sea-level fall shortly after 80 ka BP (Törnqvist et al., 2003) and associated to incision into the coastal prism of MIS 5a. This prism was likely smaller than the present prism (Wallinga et al., 2004) as only the Meuse had contributed fluvial sediment to the study area during the MIS-5 highstands (Van de Meene and Zagwijn, 1978; Busschers et al., 2007). It is important to note that the SB thus formed ~60 ka BP before the last sea-level lowstand of the LGM, during MIS 4 rather than MIS 2. The erosional contact of the boundary is typically marked by a gravel bed (Busschers et al., 2007; the base of their unit B3), separating MIS 4 from MIS 6 or older deposits. As several of such lags occur *within* the sequence and the MIS 4 and younger deposits look very similar, it can be hard to pinpoint the boundary exactly and the SB is described as a 'cryptic' sequence boundary (Miall and Arush, 2001). Based on the OSL-dated sedimentary-unit divisions in cross sections of Busschers et al. (2007), we have placed the sequence boundary at depths of 26-29 m –O.D. in the west; rising to 10 m –O.D. in the central part (Fig. 5.10). The period of incision during shelf emergence in MIS 4 was followed by net aggradation until MIS 2 (Busschers et al., 2007), while sea level fluctuated some 10 m around the 65 m –O.D. level (Waelbroeck et al., 2002).

Lowstand systems tract
The lowstand systems tract (LST) comprises all deposits since the onset of relative sea-level fall until the onset of the period where sediment supply is outpaced by accommodation space creation (Posamentier and Allen, 1999). It generally includes an earlier LST forming during sea-level fall and a later LST forming in between the sea-level lowstand and the start of transgression. In the study area the LST boundary was formed ~80 ka BP (see above). In upstream directions, LST-formation is diachronic: upstream reaches do not respond instantaneously to sea-level fall or rise and need time to adapt. Especially if sequence stratigraphy is applied to Quaternary cycles in areas with huge variations in sea-level and with very wide continental shelves (as in northwest Europe), the time-lag is significant.

In the study area, the distinction between early and late LST is fuzzy due to local subsidence depocentres and GIA differential subsidence complexities (Busschers et al., 2007) and they therefore have been lumped into one lowstand systems tract (Fig. 5.10). Between 35-24 ka BP and between 10-15 ka BP valley incision occurred due to glacio-isostatic uplift and climate change respectively (Kasse et al., 1995; Wallinga et al., 2004; Busschers et al., 2007). Scour depths occasionally reach below the 80-60 ka BP boundary, meaning that over limited areas the sequence boundary was formed as late as 10 ka BP. The aggradational phase between 24-15 ka was the result of increased sediment supply (climatic amelioration after LGM) during initial forebulge collapse (Busschers et al., 2007).

126
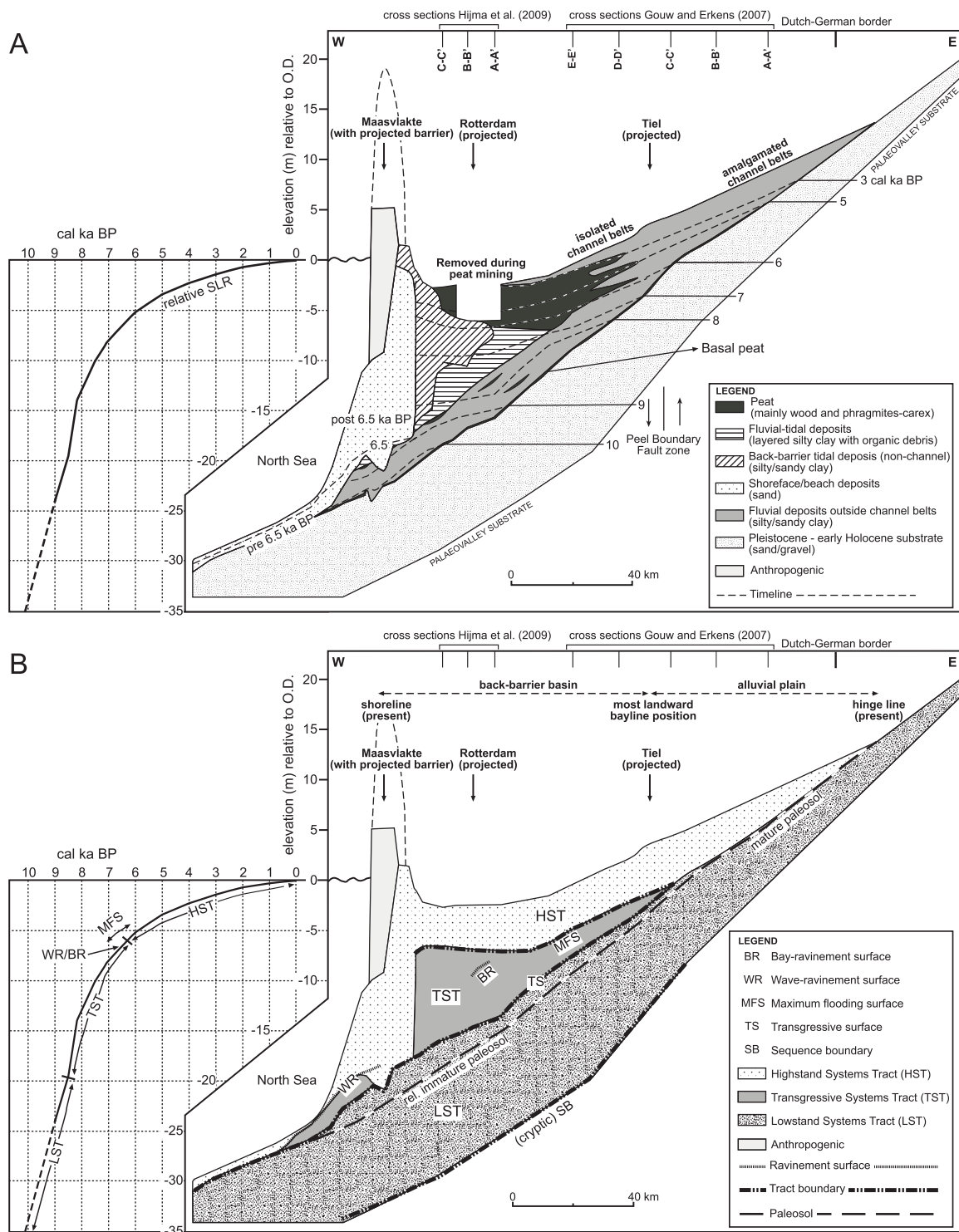
Figure 5.10 Chronometric and sequence stratigraphic subdivision of the Rhine-Meuse coastal prism. A: longitudinal section through the Rhine-Meuse coastal prism illustrating the infill of the basin in time (see Fig. 5.1 for position of section). B: Sequence stratigraphic interpretation of the Rhine-Meuse basin fill. Key stratigraphic surfaces are indicated. Note strong diachroneity of TS and TST. See text for discussion.

In the early Holocene overbank deposition increased due to rising base level (start of fluvial onlap) and flood-plain deposits (loamy overbanks) were covered by fluvial flood-basin deposits (sandy/silty clay loam and peat). This facies transition occurred ~10.5 ka BP (Van Heteren et al., 2002; Hijma et al., 2009: Chap. 2) in the west of our study area and as late as 5 ka BP in upstream parts of the Rhine delta (e.g. Berendsen and Stouthamer, 2000). Several, each weakly to well developed paleosols formed within these overbank deposits, reflecting periods of decreased sedimentation rates related to local depositional dynamics (nearby meander migration, crevassing, levee building). We place these early fluvial onlap deposits in the LST as sediment supply could still keep up with accommodation space creation in the study area. LST formation therefore ended between 10.5-5 ka BP, so 15-10 ka after the sea-level lowstand of the LGM. In modern deltas, the fluvial onlap is generally well preserved, except where younger tidal and fluvial channels have scoured into the LST. In now offshore areas of shallow shelf seas, preservation potential of the top of the LST is generally considered very low due to the erosive power of the lower shoreface environment (Catuneanu, 2007). However, west of the Maasvlakte metres-thick stacks of fluvial onlap (clay and peat) have been excellently preserved (deposits described by Van Heteren et al., 2002). This can be attributed to high rates of relative sea-level rise, marked by a period of increased rates that resulted in lowering of parts of the fluvial onlap deposits below the storm wave base.

Transgressive systems tract
This tract is bounded by the transgressive surface (TS; Posamentier and Vail, 1988) at its base and the maximum flooding surface (MFS; Posamentier et al., 1988) at the top. The transgressive surface (or maximum regressive surface; Helland-Hansen and Martinsen, 1996) is formed when creation of accommodation space starts to outpace sediment supply. By its nature it is therefore strongly diachronous over larger distances as basins are transgressed in a complex manner. In near-coastal settings it underlies the earliest estuarine deposits. It is generally conformable and not clearly traceable, except where waves or tidal channels formed wave-ravinement (Swift, 1975) or tidal-ravinement surfaces (Allen and Posamentier, 1993) respectively. In the study area, a bay-ravinement surface (Reynaud et al., 1999) is traceable over considerable area (Hijma et al., 2009: Chap. 2) near the top of the transgressive systems tract (TST; eastern shore of tidal basin). It consists of a lag deposit with *Cerastoderma* and *Hydrobia* shells erosively overlying a thin peat layer. In the palaeovalley between Rotterdam and some kilometres offshore, the TS separates fluvial from fluvial-tidal/estuarine deposits and is fairly synchronous (Fig. 5.10). The bounding contact was formed near-instantaneously over more than 30 km axially during a sea-level jump in the 150-200 yr after 8.45 ka BP (Hijma and Cohen, In press: Chap. 3). It is characterised by regional gyttja deposition on top of subregional floodbasin peats. Microfossil data indicate rapid deepening and increased salinity (freshwater

becomes brackish). Sedimentological structures show increasing tidal imprint (fluvial micro-intertidal becomes estuarine subtidal). Upstream and downstream of the Rotterdam area, the TS is more diachronous. Farther offshore, the transition occurred well before 8.45 ka BP. Later shoreface wave-erosion removed the oldest TST-deposits, especially outside the palaeovalley. In this area the TS is marked by a wave-ravinement surface that sometimes cuts into LST deposits and can be clearly traced in seismic data. Maximum 6-9 m was removed (Van Heteren et al., 2002; Rieu et al., 2005; Hijma et al., Subm.: Chap. 4).

East of Rotterdam, depositional environments remained essentially fresh during the transgression, but tidal influence reached further upriver than salinity. The earliest fluvial-tidal signatures are indicative for the TS 20-30 km east of Rotterdam. Beyond the limit of tidal influence until approximately the Peel Boundary Faultzone (Fig. 5.10), we continue tracing of the TS and use the base of subaqueous-deposited fluvial mud overlying subaerially matured flood-basin deposits as indicative. After 8.2-8 ka BP, the flood basins became permanently inundated and extensive swamps with numerous lakes formed (Van der Woude, 1983), indicating deepening of water due to water-level rise and insufficient sediment delivery. This continued until ~6 ka BP by which time the lakes had gradually filled and shallower flood basins came into existence with periodic instead of permanent flooding (Van der Woude, 1983).

As Figs. 5.5-5.6 and their description show, a bay-head delta existed at the termination of the main Rhine branches after 8 ka BP. In general, bay-head deltas are not formed during transgressive phases. Retrograding bay-head deltas develop when transgression of the open shoreline is faster than the rate of drowning of the river. This is associated to estuaries developing in shallow incised-valley systems that besides extending inland, consequently widen a lot with sea-level rise.

Highstand systems tract
The maximum flooding surface (MFS) marks the turnaround from retrogradation to progradation and it is generally linked to the most landward position of the shoreline. The MFS forms under conditions of decreasing rates of SLR when sedimentation rates can again balance (local) accommodation and excess sediment can be used for buildout. In the study area, as along any coast, the timing for the change is strongly variable as it depends on river-mouth positions, sediment-distribution processes and many other factors.

The first evidence for halted barrier rollover comes from preserved beach-barriers north of the transgressed Rhine-Meuse mouth that have been dated 6.3-6 ka BP (Cleveringa, 2000). The final switch to progradation is linked to strong erosion of the largely abandoned estuarine promontory south of the beach-barriers and a northward directed longshore current. Behind the barriers, tidal basin started to fill in and retrogradation gradually halted. Tidal-basin filling had in fact already started shortly after

8 ka BP (Rieu et al., 2005; Hijma et al., Subm.: Chap. 4) when the rate of SLR began to slow down, but the eroding promontory provided the additional sediment input that was needed to halt retrogradation. First locally, but then progressively from south to north, the tidal basins closed during a period of several millennia. When a tidal basin was closed, widespread peat formation started behind the barrier. This development indicates that the change from deepening to shallowing on tidal-basin scale already occurred after 8 ka BP, so well before retrogradation finally halted. This is in contrast to offshore areas, where the peak of deepest water is usually recorded in highstand deposits. To the west of the most landward barrier ridge, progradation resulted in the formation of several beach ridges separated by beach plains (Fig. 5.1). The ridges lie directly on lower shoreface deposits. Further offshore, lower shoreface deposits of the HST lie directly on lower shoreface deposits of the TST. Only dating can distinguish them.

In coastal settings, the MFS is often placed at the top of the youngest estuarine facies. In our study area, the surface is best characterised by the onset of widespread peat formation in the tidal basins (Holland Peat in Dutch stratigraphic terminology), even though the start of peat formation lags the end of coastal retrogradation most likely a few centuries. Fluvial deltaic channels lay encased in the peat with their base scouring into TST deposits. More landward, in the zone of inundated flood basins (see TST), we place the MFS at the base of peat accumulations or crevasse and lake delta deposits within these basins (halting of back-barrier retrogradation ~6.5-6 ka BP). Farther upstream, outside the reach of the TST, the HST lies directly on top of the LST as accommodation-space creation never outpaced sediment delivery. Sometimes a mature paleosol marks the transition; without a paleosol the contact can be difficult to recognize lithologically as it lies within aggrading flood-basin deposits.

Deviations from the standard sequence model
The timing of the formation of the SB well *before* the LGM and the start of TST formation well *after* the LGM during the very last phase of sea-level rise only indicate that the sequence of the Rhine coastal prism does not fit the standard base-level control sequence model, but that other factors influenced the extent of base-level control. Often these factors are related to the effect of climate conditions on the balance between river discharge and sediment load (e.g. Blum, 1994) leading to periods of incision with a timing and spatial expression independent of sea level fluctuations. For the Last Glacial, the very inland position on a wide, low-gradient continental shelf enabled the formation of SB at the MIS 5/4 transition (Törnqvist et al., 2003) but further base level lowering towards the LGM appears not to have been experienced *this far inland*. During the remainder of the Last Glacial, climate influence and GIA-effects dominated the processes of fluvial aggradation and incision (Busschers et al., 2007). Base-level control was thus limited and incision depth in the study area was little when compared to many other incised-valley

systems across the globe situated along shelves of smaller width. As a result, TST formation started relatively late and lasted only for 4-5 millennia. This means that for the last glacial cycle, the area near the highstand shoreline of the Rhine-Meuse system was only controlled by base-level changes during initial sea-level fall after the penultimate highstand and during a short period before the present highstand was reached. Most likely this is true for all highstand coastal areas situated along wide shelves (in the modern situation and in ancient precursors). Distinquishing last-cycle system-tract boundaries based on numerical dating alone should be avoided in such areas. Inner shelf LST-TST depositional systems are for the largest period of time representative of changes in the balance between river discharge and sediment load and could hold excellent records of climatic changes or other catchment-scale changes, but their stratigraphy may skip important beats of global sea-level variations.

5.6   Conclusions

The palaeogeography of the Rhine-Meuse river-mouth area during the early-mid Holocene transgression was reconstructed in detail. It illustrates and allows analysis of the transition from a river valley to an estuary during rapid rates of SLR. The early-mid Holocene coastal prism formed in three stages:

- Before 8.5/8.3 ka BP the southern North Sea was an isolated basin north of the Strait of Dover with microtidal conditions. Net sediment transport occurred from the deeper North Sea to the near-coastal zone where the sediment was distributed. This possibly slowed down retrogradation that nonetheless occurred at a rapid rate. Fluvial environments with extensive wetlands dominated the study area;

- When after 8.5/8.3 ka a full connection was established between the southern and northern North Sea tidal amplitudes and current velocities increased rapidly. The connection process was speeded up by the 8.5-8.3 ka BP sea-level jump. As a result strong retrogradation occurred and extensive back-barrier basins formed in which a bay-head delta developed after 8 ka BP. The transgressive sequence shows that retrogradation near the estuary occurred at a slower rate than at the adjacent coasts due to the presence of thick layers of clayey, fluvial and estuarine deposits near the mouth (differential erosion rates). As a consequence a promontory formed near the river mouth.

- Between 7.5-6.3 ka BP the rate of SLR slowed down significantly. Seismic data show the presence of extensive tidal-channel systems and indicate barrier overstepping. The relocation of the main Rhine-mouth 20 km to the north resulted in severe erosion of the promontory. The eroded sediments were deposited in upstream parts of the estuary, but were also used to progressively fill in tidal basins to the north. The tidal

inlets narrowed and their ebb-tidal deltas were strongly eroded which formed an additional sediment source. The relative abundance of sediments halted retrogradation ~6.3-6 ka BP, at first just north of the former river mouth then and progressively along the coast.

The Rhine coastal prism and buried incised valley of the Last Glacial and Holocene were divided into sequence stratigraphic tracts. Our division is primarily based on facies analysis and dating and then contrasted with local sea-level history of the western Netherlands. From the resulting sequence stratigraphic division, with the very detailed palaeogeographic reconstructions in mind, it is concluded that:

- The LST lower boundary was essentially formed early in MIS-4 during a first period of great sea-level fall. (Törnqvist et al., 2003). This is ~60 ka BP *before* the LGM-lowstand and the inner shelf remained exposed since.
- LST deposition in the study area lasted until 10.5-8 ka BP, this is 15-13 ka *after* the LGM-lowstand;
- In rapidly drowning areas such as the early Holocene Rhine river-mouth area, offshore preservation potential of the fluvial onlap marking the top of the LST is higher than generally realised;
- During the Holocene transgression, the palaeovalley became a sediment sink, trapping the TST. The transgressive surface is diachronous, but in the larger part of the study area was formed between 8.5-8.3 ka BP during a period of sea-level jumping. In the near-coastal part, the TST consists of tidal and estuarine deposits, while upstream it also consists of subaqeously deposited fluvial mud;
- In general, bay-head deltas are not formed during transgressive phases. Retrograding bay-head deltas seem to develop when transgression of the open shoreline is faster than the rate of drowning of the river. This is associated to estuaries developing in shallow incised-valley systems, such as the Rhine estuary, that besides extending inland, consequently widen a lot with sea-level rise;
- Retrogradation continued until 6.3-6 ka BP (and even longer to the north and south of the river mouths) after which widespread peat formation started in the former tidal basins, characterising the maximum flooding surface. The remaining deposits of the Holocene are merged into the HST;
- The change from deepening to shallowing already occurred shortly after 8 ka BP. This is in contrast to offshore areas, where the peak of deepest water is usually recorded in highstand deposits.
- The location of the Rhine river-mouth area along a wide, low-gradient continental shelf meant that base-level changes were dominant for a relatively short period. This resulted in a sequence that does not fit standard sequence models. Deposits of such

systems are therefore more representative of changes in the balance between river discharge and sediment load and could hold excellent records of climatic changes or other catchment-scale changes.

Acknowledgments

6 Synthesis and concluding remarks

The preceding chapters presented the results of several research tasks that were executed to meet the three objectives of this thesis, namely analyzing and explaining 1) *the early-mid Holocene sedimentary succession of the Rhine-Meuse river-mouth area, 2) the development of the river-mouth area in the early-mid Holocene in response to rapid sea-level rise* and 3) *the interaction of the fluvial and coastal systems during the early-mid Holocene transgression*. This final chapter first integrates and discusses the presented results in order to satisfy the main objectives. Partly, this was already initiated in chapter 5 that integrated the results of chapters 2-4. The second section gives suggestions how the results of the thesis can benefit ongoing and future research. The last section shows the relevance of the obtained results for several practical applications.

6.1   Synthesis

1. *The early-mid Holocene sedimentary succession of the Rhine-Meuse river-mouth area*

The Holocene sedimentary succession in the study area consists of a coastal prism of 10-25 m thick, resting on a sandy substrate formed by Late Glacial-early Holocene fluvial channel and aeolian deposits. At first, the lithology of the succession was described. Borehole descriptions, cone-penetration tests, seismic data and observations in construction pits were used to subdivide the succession in lithostratigraphic units (e.g. clay, sand) and subsequently in sedimentary facies (e.g. flood basin, tidal flat). Three onshore cross sections (Chapter 2) and one offshore cross section (Chapter 4) were constructed to illustrate the build-upl of the coastal prism. More than 100 published and 65 new radiocarbon and OSL-dates provide robust chronostratigraphic framework and pollen/diatom analysis give additional palaeo-environmental information. As the study area covers an entire river-mouth area, a highly complex zone, the succession varies widely across the study area. Nevertheless general trends can still be identified.

In the alluvial palaeovalley, the fluvial channels lay in slightly incised position until 10-8.5 ka BP. The contemporary widespread overbank deposits are characterised by a silty clay loam that contains mostly one or two vegetation horizons that formed during periods of limited overbank sedimentation. The upper vegetation horizon often grades into a basal peat layer indicating rising groundwater levels. Near active fluvial channels, the basal peat

is capped by clastic deposits. Farther away from the channels, basal peats grade into gyttja indicating that peat formation could not keep with groundwater-table rise and lakes formed. The change from peat formation to clastic sedimentation occurred before 10 ka BP in the most western part of the palaeovalley, while in the eastern part peat formation continued until 8.3 ka BP. The fluvial flood basins were inundated for large parts of the year and at a certain point became tidally influenced. The associated deposits, silty to sandy clay, show tidal lamination, can be metres thick, are found over large areas and characteristically contain large amounts of layered woody debris. The deposits are indicative for an estuarine environment and were deposited by tidally-influenced fluvial channels in the period well before 9 ka BP in the western part and until ~ 7 ka BP in the eastern part of the study area. The estuary was extensive, about 40 km long and 7-8 km wide. At the upstream end of the estuary near Delft, the main branches of the Rhine formed a bay-head delta between 8-7.3 ka BP. North and south of the estuary, tidal basins existed with less fluvial influence and hence more saline conditions. The tidal-basin deposits can be divided in sandy tidal-channel deposits, sand dominated sub- or intertidal flat deposits and mud dominated sub-, inter- or supratidal deposits. Brackish conditions are evident from pollen and diatom analysis and from the presence of brackish-water molluscs (e.g. e.g. *Hydrobia sp., Scrobicularia plana, Cerastoderma sp.*). In large parts of the study area, the estuarine and tidal deposits are capped by thick layers of peat that started to form 6.5 ka BP and illustrate the end of major clastic deposition: the basins were silted up. This was mainly the result of lower rates of sea-level rise and higher rates of sediment supply leading to narrower and fewer tidal inlets.

The sedimentary sequence in the study area enables a detailed analysis of the stratigraphic development in relation to sea-level rise and a detailed sequence-stratigraphic interpretation. The sequence stratigraphic approach focuses on the changes in depositional, rather than in lithological trends. First, a cross section was constructed along the axis of the palaeovalley (Chapter 5). The succession was then divided into three systems tract: a lowstand (LST), transgressive (TST) and highstand systems tract (HST). The LST comprises all deposits since the onset of relative sea-level fall until the onset of the period where sediment supply is outpaced by creation of accommodation space by the rising sea level (Posamentier and Allen, 1999). In the study area, this latter period began when widespread basal peat formation halted and gyttja accumulation and subaqueous clastic deposition started (formation of transgressive surface). In the palaeovalley between Rotterdam and some kilometres offshore, the transgressive surface was formed near-instantaneously during a sea-level jump of 2.11 ± 0.89 m in the 150-200 yr after 8.45 ka BP (Chapter 3). Farther offshore, the transition occurred well before 8.45 ka BP. The TST ends when sedimentation rates can again balance the rates of accommodation space creation. In the study area, as along any coast, the timing for the change is strongly variable as it depends on river-mouth positions, sediment-distribution processes and

many other factors (chapter 5). For the Rhine-Meuse river-mouth area this change is best characterised by the onset of widespread peat formation in the tidal basins after 6.5 ka BP.

The above systems tract division is primarily based on detailed facies analysis and dating and then contrasted with local sea-level history of the western Netherlands. In general, studies of coastal sedimentary sequence that were formed after the Last Glacial Maximum (~22 ka BP) have limited spatial data coverage. Sequence stratigraphic tract-labels and boundaries are therefore put on deposits based on global sea-level behaviour at the time of deposition. The method used in this thesis differs from this practice by independently mapping and dating shifting palaeoenvironments in time and space first, and evaluating the various options for drawing tract boundaries later. This more detailed analysis resulted in a TST that started relatively late, 10.5-8 ka BP, so 15-13 ka after the lowstand of the Last Glacial. This is in contrast to many other studies where the TST is started shortly after the lowstand. A late start of the TST is most likely typical for river-mouth areas along wide, low-gradient continental shelves where because of the wide shelf, base-level changes were only dominant for a relatively short period. This resulted in a sequence that does not fit standard large-scale sequence models. Deposits of such systems are therefore representative of changes in the balance between river discharge and alluvial sediment load and could hold excellent records of climatic changes or other catchment-scale changes (Chapter 5).

2. *The development of the Rhine-Meuse river-mouth area in the early-mid Holocene in response to rapid sea-level rise*

Before sea-level rise started to affect the study area, the Rhine and the Meuse formed a river system situated in a few meters deep palaeovalley that was bordered by higher, vegetated coversand areas. Flooding of the valley occurred regularly, but during large parts of the year the flood basins lay dry as is clear from the matured deposits. Between 10.5-8 ka BP, progressively in time from west to east, the effects of rapid post-glacial sea-level rise started to influence the study area: groundwater rise resulted in the formation of extensive wetlands, flood basins became more frequently flooded, sediment aggradation rates increased and finally the river valley started to change into an estuary (Chapter 2). Sea-level rise reached rates of 1 m/100 yr before 8 ka BP with a period of 2 m/100 yr between 8.5-8.3 ka BP as a result of sea-level jumping (Chapter 3). Accelerated SLR caused drowning of the area in a less gradual fashion than before and the wide estuary and adjacent back-barrier basins show marked environmental change. This was further enhanced by increasing tidal amplitudes along the coast and presumably also in the basins due to the establishment of a full connection between the southern and northern North Sea in this period (Chapter 5). Between 8-7.5 ka BP, sea level rose 3 m with a significantly lower rate (60 cm/100 yr) than in the preceding 500 years. As a result, the rate of

retrogradation slowed down as sediment delivery (from both marine and fluvial sources) started to keep up with accommodation space creation. North and south of the main estuary, retrogradation of the coastline occurred at a faster rate than near the mouth, leading to the formation of a promontory. Differential retrogradation was caused by the presence of thick packages of especially clay and peat in the estuary mouth. These are more resistant to erosion than the sandy coversand deposits, that were capped by a much thinner peat and clay layer. North of the estuary mouth, tidal-channel networks are found in seismic sections. Tidal inlets are inferred where these networks converge. In between the inlets, barrier islands could easily form due to the availability of sand, shallow coastal waters and wave action. An upstream avulsion (Chapters 2, 5) led to the formation of a new main Rhine-branch with its mouth near Leiden. This resulted in strong erosion of the largely abandoned mouth of the promontory. Partly, the available sediment was used to fill in the former Rhine-estuary. Another large part of the available sediment was transported north along the coast and then routed into the northern tidal basins (Chapter 4, 5). The size and number of tidal inlets therefore decreased gradually and the accompanying erosion of the ebb-tidal deltas (Beets et al., 1992), further added to the surplus of available sediment along the beach-barrier shores. The shift of the Rhine mouth also resulted in a change of sedimentary regime. The now abandoned estuary was large and wide and trapped all Rhine sediments before they could reach the North Sea. The newly formed estuary was much smaller and the Rhine soon started to prograde into the back-barrier basin in the next millennia, eventually forming a protruding delta in the North Sea (Van Heteren and Van der Spek, 2008). A second avulsion upstream along the Rhine ~6.5 ka BP resulted in a new main distributary that was situated more to the north (Berendsen and Stouthamer, 2000), but the outlet remained the same. The Rhine branch that was active before the second avulsion was completely abandoned, leaving a basin that was rapidly transgressed and filled in by the wide Rijswijk-Zoetermeer tidal-inlet system (Fig. 5.8). The closure of several tidal inlets (and fluvial outlets) resulted in poor drainage conditions and the wetland area increased rapidly. Around 6.5-6 ka BP, the coastline reached its most eastward position (Van der Valk, 1996b; Cleveringa, 2000; Van der Spek et al., 2007) and the early-mid Holocene transgression of the Rhine-Meuse valley was completed. The above developments are visualized in three onshore cross sections (Chapter 2), one offshore cross-section (Chapter 4) and six palaeogeographic maps (Chapter 5).

3. *The interaction of the fluvial and coastal systems during the early-mid Holocene transgression*

The above illustrated the impact of rapidly rising sea levels (part of the coastal system) on the fluvial system. Initially, as the palaeovalley flooded during rapid SLR, the most

important influence of the fluvial system on the development of the coastal system was that the coastal system inherited a fluvial landscape. As was already known, the morphology of the drowning landscape defined the sources and the sinks and the way in which the southern North Sea expanded during SLR. The location of the estuary and the first tidal basins were therefore all defined by the drowned fluvial drainage pattern. On a smaller scale, several other interactions between the two systems can be identified.

Before the study area was transgressed, the Rhine-Meuse-Scheldt system had a joint palaeovalley in the present offshore area. When sea-level rise started to influence the area, water levels rose in the palaeovalley and an estuary formed flanked by higher elevated, sandy areas. When the sea approached the study area, the early fluvial and estuarine deposits within the palaeovalley were less susceptible for erosion than the sandy substrates to the north and south, resulting in differential retrogradation and promontory formation.

After 7.5 ka BP the main branch of river Rhine relocated its mouth 20 km to the north. The cross sections (Chapter 2) show that it connected to an existing tidal inlet. Before ~8 ka BP, at the start of the transgression, the inherited fluvial morphology defined the location of the tidal inlets. Around 7.5 ka BP, halfway the transgression and with the palaeovalley filled in, it is the other way around: the position of tidal inlets starts to influence the location of river mouths.

There are several factors or a combination of factors imaginable that could have influenced the avulsion of the Rhine to the north. The new route of the Rhine to sea was much shorter than the previous one that directed the Rhine to the promontory. Gradient advantage therefore seems to have been important. Possibly in addition, northward tilting of the flood plain due to forebulge collapse played a role. This mechanism has been used to explain northward migration of Rhine and Meuse channel in areas more upstream (Cohen, 2003).

Around 6.5 ka BP the Rhine avulsed ~70 km upstream at Wijk bij Duurstede (Berendsen and Stouthamer, 2001), kept the same outlet, but between the avulsion point and the outlet shifted 7-10 km north. In both cases when the Rhine avulsed, the sea quickly transgressed the former course. Reconstructions show that soon after the promontory-outlet was abandoned, the promontory was strongly eroded and large amounts of sediment became available. After the second avulsion, the abandoned area just upstream of the outlet near Leiden was transgressed and a tidal inlet system formed (Rijswijk-Zoetermeer system). The above developments thus show that the location of tidal inlets, river avulsions and location of marine ingressions are strongly interlinked.

6.2   Concluding remarks: scientific challenges

The information on the magnitude, duration and timing of the multi-staged sea-level jump preluding the 8200 yr event (Chapter 3) is crucial as input in palaeoclimate models

hindcasting the cooling event. For realistic modelling, the total volume of freshwater release and the number of drainage events is essential (Wiersma, 2008). The derived rates of sea-level rise and the time-depth position of the extended sea-level curve relative to other published curves around the North Sea basin contribute to our understanding of spatial differences in glacio- and hydro-isostatic adjustments during the Holocene. The data can be used for geophysical modelling of Holocene crustal movements in the North Sea basin (e.g. Kiden et al., 2002; Vink et al., 2007). The movements are used to decipher the radial viscosity structure of the Earth (lithosphere thickness, upper- and lower-mantle viscosity) as well as the spatial trends in the drowning of the North Sea basin during post-glacial sea-level rise. Existing geophysical sea-level rise solutions for the North Sea can be greatly improved now that the eustatic step of the 8.5-8.3 ka sea-level jump is quantified. Past solutions used relative crude synthesised global eustatic curves. Palaeo sea-level data furthermore provide perspective for contemporary sea-level rise (Siddall et al., 2009) and constraints on future sea-level rise predictions. To extend the sea-level curve for various parts of the southern North Sea basin further in time, it is crucial to obtain high-quality index points from the North Sea. Recent offshore archaeological findings in the basin have stimulated interest and research in this area (Hublin et al., In press). Upcoming research in the North Sea will have to include the gathering of sea-level index points to reconstruct the drowning of the palaeolandscape. Besides offshore data, it is needed to collect sea-level data from the northern Netherlands, the zone where the last-glacial forebulge was probably most pronounced (Kiden et al., 2002; Cohen, 2003; Busschers et al., 2007; Vink et al., 2007). As yet, insufficient data exist to reconstruct an early-mid Holocene sea-level curve for these areas. Constructing this curve and comparing it to nearby curves would provide very valuable information on glacio/hydro isostatic adjustments that resulted from forebulge updoming/downwarping and loading/unloading of the North Sea basin. And not to forget, the sea-level jump (Chapter 3) could be confirmed and/or further constrained. Considering the fact that the 8.2 ka event is now so often used in the global-climate debate and used as a warning sign for possible future analogue developments, strong efforts should be made in reconstructing sea-level curves for several estuarine/deltaic systems for this crucial period. Preferably, study sites should be located in those parts of the world where the eustatic signal of the jump would be fully recorded, such as in the Asian mega deltas (see Kendall et al., 2008). Proper knowledge of background rates of sea-level rise in those areas is needed to define the 8.5-8.3 ka sea-level jump fingerprint accurately.

Around 8 ka BP a major tsunami was created by a underwater slide near the west coast of Norway (Bugge et al., 1987). The deposits of the tsunami (Second Storegga Slide tsunami) have been preserved as part of raised beach sequences in the United Kingdom (Smith et al., 2004) and Norway (e.g. Bondevik et al., 1997). The tsunami must also have impacted former North Sea coastlines at depth below or offshore The Netherlands (e.g.

Weninger et al., 2008), but no clear tsunami deposits have been recovered. An important question is whether the Storegga-tsunami had sufficient force to create a distinct deposit where it dissipated on the southern North Sea shores – which were of markedly different coastal geomorphology and lithology than the fjords of Norway and firths of Scotland. It may well be that most of the energy had already dissipated by wave breaking and rolling out across the shallowest part of the contemporary North Sea: the former land bridge between Texel and England that had been transgressed in the centuries to millennium before. During this study some indications for rapid, short-lived environmental change around ~8 ka BP have been obtained – a few meters above the 8.5-8.3 sea-level jump contact of chapter 3. In specific parts of the study area, a short-lived brackish pulse seems present at this level, followed by a period of rapid detrital-gyttjaic sedimentation. At several locations this organic layer has been dated at ~8 ka BP (this thesis), suggesting a link with the Storegga tsunami (Cohen and Hijma, 2008). Preliminary results of this work were picked up by the popular press, followed by a modelling exercise by WL|Delft Hydraulics (now Deltares) that did not exclude the possibility that the tsunami reached the Rotterdam area (Twigt and Blaas, 2007; Vatvani, 2007), although modest wave heights (max 1.5 m) were predicted. Further research, aimed specifically at this interval, is needed to conclude whether the tsunami had a significant impact in The Netherlands or not, and if it impacted The Netherlands, how it can be distinguished from storm-surge deposits. This research could easily be combined with sea-level research in the northwestern Netherlands (notably the MIS-4/3 Rhine palaeovalley, e.g. Velsen) and the northern Netherlands (notably below the Wadden Sea). In both regions possible tsunami impact would have been larger than in the Rotterdam area. The research on early-mid Holocene sea levels and glacio-isostatic adjustments would help to identify the depth at which the tsunami deposits would be expected. Vice versa, once identified, the Storegga-event layer becomes a stratigraphic marker that can improve sea-level and GIA/landsubsidence studies.

6.3   Concluding remarks: practical applications

Ancient estuarine and incised-valley deposits host significant hydrocarbon reservoirs and petroleum explorationists have focused on these deposits (Boyd et al., 2006). As subsurface data is often scarce, three-dimensional models are generally used to reconstruct the facies distribution of the ancient estuarine and incised-valley systems. Quantitative field data is still urgently needed to test the models. Recently, these data have been published for the fluvially dominated upper Rhine-Meuse delta and lower Mississippi Valley (Gouw, 2007b). With the results of the present study, parameters describing the architecture of the estuarine/incised-valley fill deposits of the Holocene Rhine-Meuse system can be

quantified and used for improving architecture models and hence the prediction of hydrocarbon reservoirs.

In The Netherlands the substrate is and will be intensively used, especially in the study area that is densely populated and also includes the Rotterdam harbour. The detailed cross sections and palaeogeographic maps can be used in planning infrastructural works and groundwater extraction and defining archaeological expectancy maps. During the project, provisional results and integrated interpretations were exchanged with the Bureau Oudheidkundig Onderzoek Rotterdam (BOOR; Bureau of Archaeological Research Rotterdam). Amongst others, this aided the documentation of archaeological prospections of building sites for underground stations of the RandstadRail (BOOR-reports 265, 318, 421).

Another project in which the results are used is started by the Hoogheemraadschap of Rijnland (regional water board). In a low-lying polderarea near Zoetermeer (< 4 m –O.D.), increasingly brackish seepage negatively influences water quality. Seepage is strongest where Holocene channel belts are in contact with the sandy Pleistocene substrate. The cross sections and palaeogeographic maps identify such areas, benefitting plans for closing the strongest seepage sources.

Currently, Deltares/TNO Geological Survey of The Netherlands is building a 3D geological model for the upper 30 m based on core descriptions and incorporating the results of this study. This model will be beneficial for all sorts of practical applications, but also for scientific research. The 3D-view on the sedimentary succession and the possibility to work with huge amounts of data will open doors for new ways of research.

This study incorporated significant amounts of cone-penetration-test data and illustrated their usefulness for obtaining relatively quick and cheap lithological data, especially when used in combination with core descriptions. However, tens of thousands of CPT results (as well as core descriptions) from the study area have not been used for this study as they were not readily available. The importance and potential of this unexplored dataset is very large for both scientific and more directly applied usage. This notion fortunately takes hold and plans exist to create one national database. Integration of the scattered databases, preferably directed by the government in cooperation with (applied) scientific partners, will undoubtedly prove very valuable.

Finally, I hope this thesis will be a valuable contribution to the global scientific effort to understand the post-glacial transgression of river valleys and their transformation into estuaries and deltas. Future, modelled predictions for sea-level rise and estuarine/deltaic developments are frequently in the news. Without understanding previous developments that occurred during periods in which climate changed more rapidly than at present, upper and lower limits for future scenarios are not well defined and the predictions must be handled with care.

Samenvatting

Van riviervallei naar estuarium

De vroeg-midden Holocene transgressie van de Rijn-Maas vallei, Nederland

Een estuarium is het meest zeewaartse deel van een rivier en ontvangt sediment dat zowel vanuit zee als door de rivier aangevoerd wordt. De meeste hedendaagse estuaria zijn ontstaan in rivierdalen uit de laatste ijstijd. Deze eindigde 12 duizend jaar geleden toen de huidige warme periode aanbrak die het Holoceen genoemd wordt (Fig. 1.2). De dalen verdronken toen het ijs smolt en de zeespiegel snel begon te stijgen. Het sedimentpakket in dergelijke dalen bevat belangrijke informatie over hoe rivier- en kustsystemen reageren op zeespiegelstijging. Door dit pakket te bestuderen neemt onze kennis toe van de natuurlijke langetermijnontwikkeling van dergelijke systemen. Deze kennis kan bijvoorbeeld toegepast worden in beheer- en beleidsplannen, zeker gezien de verwachte zeespiegelstijging in de komende eeuw. Daarnaast zijn olie- en gasvoorraden vaak aanwezig in miljoenen jaren geleden opgevulde rivierdalen en een beter begrip van de opvulling kan helpen de olie en het gas te winnen. Het sediment dat het ondiepe dal van het Rijn-Maas systeem heeft opgevuld is uitermate geschikt om te bestuderen, aangezien er veel gegevens beschikbaar zijn (boorbeschrijvingen, dateringen, seismiek e.d.). Dit proefschrift presenteert de resultaten van de studie naar de ontwikkeling van de Rijn-Maasmond na de laatste ijstijd en laat zien hoe de riviervallei verdronk en een estuarium werd. De hoofddoelen van het onderzoek waren het analyseren en verklaren van:

1. de vroeg-midden Holocene, ofwel de 12-6 duizend jaar oude opeenstapeling van sediment in de Rijn-Maasmond;
2. de vroeg-midden Holocene ontwikkeling van het Rijn-Maasmond gebied in reactie op de zeer snelle zeespiegelstijging;
3. de interactie tussen de rivier- en kustsystemen tijdens de vroeg-midden Holocene verdrinking.

Om deze doelen te halen zijn de volgende onderzoekstaken uitgevoerd:

- Het samenvoegen van de grote hoeveelheid data (boorbeschrijvingen, dateringen, pollen analyses, seismische data, etc.) tot een database (Hfst. 2);
- Deze database gebruiken om de sedimentologische opbouw van het Rijn-Maasmondgebied te documenteren en de ruimtelijke en temporele veranderingen in afzettingstype te begrijpen (Hfst. 2 en 4);
- Het reconstrueren van Holocene zeespiegelstanden vóór 7500 jaar geleden (Hfst. 3);
- Het reconstrueren van de vroeg-midden Holocene geografische ontwikkeling van het studiegebied, het ontrafelen van land-zee interacties en de ontwikkeling beschrijven volgens sequentie stratigrafische concepten (Hfst. 5).

De Holocene ontwikkeling van de Rijn-Maasmond in profielen en woorden (Hfst. 2)

Er is een grote hoeveelheid data (boringen, dateringen, etc.) van de ondergrond van het Rijn-Maasmondgebied beschikbaar, maar deze zijn verspreid over instituten en gemeentes. Tijdens deze studie zijn veel van deze data samengevoegd tot een database; daarnaast zijn ook veel nieuwe gegevens verzameld. In hoofdstuk 2 zijn deze data gebruikt om drie 25 m diepe noord-zuid doorsneden te maken die de bodemopbouw tonen vanaf de Oude Rijn tot aan het Haringvliet (Addendum 1). Afzettingen van ongeveer 9-6 duizend jaar oud zijn goed bewaard gebleven en liggen op zandige afzettingen uit de laatste ijstijd. Kort na 9000 jaar geleden begonnen de rivieren meer te overstromen als gevolg van de zeespiegelstijging. Hiermee begon de opvulling van het rivierdal. Tussen de rivieren in vond grootschalige veenvorming plaats door stijgende grondwaterstanden. Rond 8000 jaar geleden stonden grote delen van het onderzoeksgebied permanent onder water en begon de invloed van het getij goed merkbaar te worden. Het meeste rivierzand bereikte de zee niet, maar werd opgevangen in het ontstane estuarium dat toen tussen Delft en Hoek van Holland lag. Vanaf 7300 jaar geleden verlegde de hoofdmonding van de Rijn zich naar Leiden. In het voormalige mondingsgebied brak de zee snel binnen en werd een getijdebekken gevormd. Kort voor 6000 jaar geleden stopte de kusterosie en begonnen de getijdengeulen te verzanden. Dit betekende het einde van de vroeg-midden Holocene verdrinking.

De tijdspanne en de grootte van de zeespiegelsprong die het 8.2 event inluidde (Hfst. 3)

De periode van sterke afkoeling rond 8200 jaar geleden (8.2 event) is de meest uitgesproken abrupte klimaatsverandering in het Holoceen. Vaak wordt het plotselinge leeglopen van twee grote ijsrandmeren in Noord-Amerika daarvoor verantwoordelijk gehouden. De landijsdam in de Hudson Baai waarachter de meren gevormd waren brak door en de meren liepen leeg in de Noord-Atlantische Oceaan. Behalve meerwater kwam er ook veel landijs in zee terecht. Deze gebeurtenis zorgde voor verzoeting van de oceaan. Dit leidde tot een verzwakking van de warme Golfstroom en daardoor met name op het noordelijk halfrond tot een duidelijke afkoeling. De grootte hoeveelheid water die in de oceaan terecht kwam leidde daarnaast tot een bovenmatig snelle stijging van de zeespiegel. Tot nog toe was de grootte van deze zeespiegelsprong slechts geschat met behulp van modelreconstructies, maar nog niet door middel van een directe en nauwkeurige bepaling van vroegere zeespiegelstanden. De modelschattingen liepen uiteen van 0.4 tot 1.4 m wereldwijde stijging. Ook het moment waarop de meren leegliepen was niet goed bekend. Door het dateren van snel verdronken veenlagen in het gebied Hoek van Holland-Rotterdam wordt in dit proefschrift (Hoofdstuk 3) aangetoond dat de zeespiegelsprong 8450 ± 44 jaar geleden begon. De periode van snelle zeespiegelstijging duurde ongeveer 200 jaar. Hierin steeg de zee bij Nederland 4.06 ± 0.5 m. Deze stijging is onderverdeeld in een zeespiegelsprong van 2.11 ± 0.89 m (door de Hudson Baai gebeurtenissen) en een

stijging van 1.95 ± 0.74 m die sowieso had plaatsgevonden in die 200 jaar. De gemiddelde, wereldwijde zeespiegelsprong was zeer waarschijnlijk nog een stuk groter dan de 2.11 m in Nederland. Dit komt doordat Nederland relatief dicht bij de Hudson Baai ligt. De massa van de meren en het landijs eromheen was dermate groot dat zeewater richting de Hudson Baai aangetrokken werd. De zeespiegel rond de Hudson Baai stond daarom relatief hoog. Toen de meren leegliepen en veel landijs afsmolt, verdween de aantrekkingskracht en vloeide zeewater weg van de Hudson Baai. Dit effect was zo groot dat rond de Hudson Baai de zeespiegel niet steeg toen de meren leegliepen, maar juist daalde! Hoe verder van de Hudson Baai vandaan, hoe kleiner de invloed was van het verdwijnen van de aantrekkingskracht. Op enige afstand van de Hudson Baai wogen het verdwijnen van de aantrekkingskracht en het toevoegen van water aan de oceaan tegen elkaar op. Modeluitkomsten geven aan dat in Nederland de zeespiegelsprong ongeveer 70% van de wereldwijde zeespiegelsprong was. Als dit klopt, betekent dit dat de wereldwijde zeespiegelsprong 3 ± 1.25 m was. Dit is dus aanzienlijk hoger dan eerder geschatte waardes van 0.4 tot 1.4 m. Deze discrepantie suggereert dat ofwel uit een andere bron, bijvoorbeeld Antarctica, ook veel smeltwater aan de oceaan toegevoegd werd of, meer waarschijnlijker, dat het volume van de meren en het opgebroken ijs samen groter was dan vermoed.

De midden-Holocene ontwikkeling van een waddengebied (Hfst. 4)
In hoofdstuk 4 wordt de reactie van een waddengebied met rivierinvloed (estuarien bekken) op zeer snelle zeespiegelstijging beschreven. Hoge resolutie seismiek, lithologische informatie en koolstofdateringen zijn verzameld voor de kust van Den Haag. Zij tonen aan dat landafzettingen uit het einde van de ijstijd en het begin van het Holoceen goed bewaard zijn gebleven. Deze landafzettingen liggen begraven onder midden-Holocene estuariene sedimenten die afgezet zijn in een Waddenzee-achtig gebied. Geulen in dit waddengebied begonnen tussen 8300 en 7400 jaar geleden op te vullen. In deze periode verlegde de Rijnmonding zich naar het waddengebied, waardoor veel sediment in het gebied terecht kwam. Mede hierdoor, maar ook doordat de zee minder snel was gaan stijgen en de getijamplitude niet sterk meer toenam, kon er bij elke vloed steeds minder water het bekken instromen. Dit leidde tot het versmallen en opvullen van de getijgeulen. De onderzochte afzettingen liggen tegenwoordig buitengaats. Dit betekent dat op een zeker moment de kustlijn door het onderzoeksgebied is geschoven. Golferosie heeft daarbij het bovenste deel van de eerdere afzettingen verwijderd. Dateringen tonen aan dat dit al vóór 6600 jaar geleden gebeurde. Tussen 7400 (toen er nog getijgeulen waren) en 6600 jaar geleden moet de kustlijn daarom door het onderzoeksgebied heen zijn geschoven. Dit ging grotendeels zeer geleidelijk, maar er zijn sterke aanwijzingen dat in ieder geval eenmalig de waddeneilanden snel een flink stuk landwaarts sprongen. De snelheid van landwaartse verplaatsing van de waddeneilanden was niet groot genoeg om het snelle landwaartse uitbreiden van het estuariene bekken bij te benen, kortom de

afstanden tussen de eilanden en het vaste land werd groter. Op een zeker moment, mogelijk na een grote storm, verdwenen de eilanden om een heel stuk landwaarts weer opgebouwd te worden.

De getijgeulen in het estuariene bekken verplaatsten zich slechts enkele tientallen meters in honderden jaren. Ook vertonen zij geen typisch kronkelend stelsel, maar zijn ze behoorlijk recht. Dit werd veroorzaakt doordat ze ingebed lagen in een dikke laag estuariene klei die zijwaartse verplaatsing verhinderde en doordat ze het patroon van een ouder, estuarien riviersysteem overgenomen hadden die vaak rechter zijn dan getijdengeulen. Deze ontwikkeling van het studiegebied laat zien dat naast riviermondverleggingen en verandering van de zeespiegel, ook het materiaal waaruit de ondergrond bestaat sterk van invloed is op de ontwikkeling van achter eilanden gelegen estuariene bekkens.

De Holocene verdrinking van de Rijnmond: kaarten en opeenstapeling (Hfst. 5)
De paleogeografie van de Rijn-Maas vallei tijdens de vroeg-midden Holocene verdrinking wordt in hoofdstuk 5 beschreven. De paleogeografische kaarten worden gebruikt om land-zee interacties gedurende de verdrinking te bespreken. De kaarten laten zien dat de afzettingen in de vallei gevormd zijn gedurende drie fasen: (1) voor 8500/8300 jaar geleden, toen het onderzoeksgebied bestond uit een riviervlakte met veel moerassen; (2) na 8500/8300 maar voor 7500 jaar geleden, toen de terugschrijding van de kust minder snel verliep rondom de Rijn-Maasmond dan in de naastgelegen gebieden en de Rijn-Maasmond een uitstulping werd. Achter kleine eilanden vormden zich grote bekkens waarin bij Delft de Rijn een delta vormde. Getijamplitude en de snelheid van getijstromingen namen sterk toe door het steeds groter worden van de Noordzee. Dit leidde tot bredere en diepere zeegaten; (3) tussen 7500 en 6300 jaar geleden, toen een noordwaartse verplaatsing van de Rijnmond resulteerde in sterke erosie van de verlaten uitstulping. Het hierdoor beschikbaar gekomen sediment werd opgeslagen in de bekkens, waardoor de snelheid van kustterugschrijding afnam (Fig. A4.15-A4.20).

De hierboven beschreven ontwikkeling is gebruikt om standaard concepten voor grootschalige landschappelijke veranderingen (sequentie stratigrafie) te toetsen. Deze veranderingen worden vaak gekoppeld aan een dalende of stijgende zeespiegel. De ligging van het mondingsgebied van de Rijn en de Maas aan de rand van een breed continentaal plat (de Noordzee) betekent echter dat gedurende een cyclus van zeespiegeldaling (ijstijd) en zeespiegelstijging (warme tijd) veranderingen in het zeeniveau (ofwel de erosiebasis) slechts kort bepalend zijn voor het riviergedrag. Dit resulteert in een sedimentaire opeenvolging die niet past binnen standaard concepten. Als de zeespiegel daalt, verlaagt het kustnabije deel van een rivier zijn bedding om dezelfde gradiënt te behouden. Omdat de Noordzee zo breed en plat is, zorgt een behoorlijke zeespiegeldaling er al snel voor dat de kustlijn zeer ver van de huidige kustlijn afligt. Zo ver, dat een verdere daling van het

zeeniveau weinig invloed meer heeft op het riviergedrag in Nederland. Andere factoren, zoals klimaat, zijn dan belangrijker. De diepste rivierinsnijding tijdens de laatste ijstijd vond bijvoorbeeld 80.000 jaar geleden plaats, ongeveer 60.000 jaar voordat de zeespiegel haar diepste punt bereikte. Afzettingen van kustnabije delen van riviersystemen zoals de Rijn- en Maas registeren en potentieel archiveren daarom vooral veranderingen van afvoer en sedimentlast in het stroomgebied.

Synthese (Hfst. 6)
Het laatste hoofdstuk integreert en bediscussieert de resultaten om aan de hoofddoelen te kunnen voldoen. Voor hoofddoelen 1 en 2 is dit reeds grotendeels gedaan in hoofdstuk 5. Hoofddoel 3, betreffende de interactie tussen de kust- en riviersystemen, komt uitgebreid aan bod in de synthese.

Tijdens het begin van de verdrinking overerfde het kustsysteem een rivierlandschap en werd het daarmee, weliswaar indirect, sterk beïnvloed door het riviersysteem. De vorm van het verdrinkende landschap bepaalde waar erosie en waar sedimentatie plaatsvond en hoe de Noordzee zich uitbreidde. De positie van het Rijn-Maas estuarium en de getijbekkens werd dan in het begin ook volledig bepaald door het verdrinkende rivierlandschap. Ook op een kleinere schaal was er een wisselwerking tussen de twee systemen. Voordat het landschap verdronk, deelden de Rijn, Maas en Schelde een vallei in het nu buitengaats gelegen deel. Door de zeespiegelstijging veranderde de vallei in een estuarium met aan beide zijden hogere, zandige gebieden. Toen de kustlijn dichterbij kwam bleken de rivier- en estuariumafzettingen beter bestand tegen erosie dan de zandige gebieden. Dit had tot gevolg dat rond de riviermonding een uitstulping ontstond die dus niet het gevolg was van een uitbouwende delta, maar van differentiële erosie.

Voor 8000 jaar geleden bepaalde de vorm van het verdrinkende rivierlandschap de positie van zeegaten. Rond 7500 jaar geleden is dit omgedraaid: nu beïnvloedt de ligging van zeegaten de positie van riviermondingen. Kort na 7500 jaar geleden kreeg de hoofdgeul van de Rijn een verbinding met een zeegat 20 km ten noorden (bij Katwijk). Rond 6500 jaar geleden vond er 70 km bovenstrooms een rivierverlegging plaats bij Wijk bij Duurstede. De Rijn behield dezelfde monding, maar tussen de monding en Wijk bij Duurstede verplaatste de Rijn zich 5-7 km naar het noorden. Zowel bij de verlegging van 7500 jaar als die van 6500 jaar geleden vond er sterke erosie plaats in de door de Rijn verlaten gebieden. Reconstructies laten zien dat de uitstulping bij Hoek van Holland sterk geërodeerd werd toen de hoofdtak van de Rijn zich verlegde naar Katwijk. Ook na de verlegging van 6500 jaar geleden vond er sterke erosie plaats van het door de Rijn verlaten gebied waarin zich snel het Rijswijk-Zoetermeer getijsysteem ontwikkelde. De hierboven beschreven ontwikkelingen laten zien dat de posities van zeegaten, rivierverleggingen en zee-inbraken elkaar sterk beïnvloeden, maar dat de manier waarop afhankelijk is van de voorgeschiedenis van het gebied en dus varieert door de tijd heen.

Author and contribution declaration

The contributions of each co-author to chapters 2-5 are indicated below, declaring most of the work to have been carried out by the Ph.D.-candidate. Authors are identified by their initials. All authors contributed through discussion and commenting with the principal author during data collection, analysis and manuscript preparation. All figures are by the first author. Chapters 2 and 3, besides internal reviews by members from the supervising committee, benefitted from external peer review.

For chapter 2, all new fieldwork was planned and executed by MPH; for the northern part of the study area (Oude Rijn and surroundings) in close collaboration with GH. All cross sections were constructed by MPH. KMC and AJFvdS reviewed the cross sections and first draft manuscripts, and contributed earlier collected datings and palaeoenvironmental information. Sampling new data was done by MPH and GH, supervised by KMC, AJFvdS and ES.

For chapter 3, MPH and KMC collaborated in collecting and sampling basal-peat data. MPH constructed the sea-level curve, calculated the timing of the event and performed the OxCal-routines. MPH and KMC each contributed to calculating the magnitude of the sea-level jump and the background rate, including error propagation.

For chapter 4, initial screening of the seismic data was executed by SvH, and handed over to MPH. Sampling of shell material was done by AJFvdS. SvH and AJFvdS provided access to earlier collected offshore seismic data sets at Deltares / TNO DINO / Geological Survey of The Netherlands. MPH carried out detailed seismic interpretation, onshore-offshore correlation and chronostratigraphic positioning. The text contains contributions by SvH.

Chapter 5 was entirely constructed by MPH with textual contributions by KMC.

References

Allen, G.P. & H.W. Posamentier (1993), Sequence Stratigraphy and facies model of an incised valley fill: the Gironde estuary, France. Journal of Sedimentary Petrology 63 (3), 378-391.

Allen, J.R.L. (1990), The Severn Estuary in southwest Britain: its retreat under marine ingression, and fine-sediment regime. Sedimentary Geology 66, 13-28.

Alley, R.B. & A.M. Ágústsdóttir (2005), The 8k event: cause and consequences of a major Holocene abrupt climate change. Quaternary Science Reviews 24 (10-11), 1123-1149.

Autin, W.J. (2008), Stratigraphic analysis and paleoenvironmental implications of the Wijchen Member in the lower Rhine-Meuse valley of the Netherlands. Netherlands Journal of Geosciences - Geologie en Mijnbouw 87 (4), 291-307.

Baeteman, C. (1999), The Holocene depositional history of the IJzer palaeovalley (western Belgian coastal plain) with reference to the factors controlling the formation of intercalated peat beds. Geologica Belgica 2 (3-4), 39-72.

Ballarini, M., J. Wallinga, A.G. Wintle & A.J.J. Bos (2007), A modified SAR protocol for optical dating of individual grains from young quartz samples. Radiation Measurements 42 (3), 360-369.

Barber, D.C., A. Dyke, C. Hillaire-Marcel, A.E. Jennings, J.T. Andrews, M.T. Kerwin, G. Bilodeau, G. McNeely, J. Southon, M.D. Morehead & J.-M. Gagnon (1999), Forcing of the cold event of 8,200 years ago by catastrophic drainage of Laurentide lake. Nature 400, 344-348.

Bard, E., B. Hamelin, M. Arnold, L. Montaggioni, G. Cabioch, G. Faure & F. Rougerie (1996), Deglacial sea-level record from Tahiti corals and the timing of global meltwater discharge. Nature 382 (6588), 241-244.

Bauer, E., A. Ganopolski & M. Montoya (2004), Simulation of the cold climate event 8200 years ago by meltwater outburst from Lake Agassiz. Paleoceanography 19, PA3014.

Beets, D.J. & A.J.F. Van der Spek (2000), The Holocene evolution of the barrier and the back-barrier basins of the Belgium and the Netherlands as a function of late Weichselian morphology, relative sea-level rise and sediment supply. Netherlands Journal of Geosciences - Geologie en Mijnbouw 79, 3-16.

Beets, D.J., L. Van der Valk & M.J. Stive (1992), Holocene evolution of the coast of Holland. Marine Geology 103, 423-444.

Beets, D.J., P. Cleveringa, C. Laban & P. Battegazore (1995), Evolution of the lower coast of Holland between Monster and Noordwijk. Med. Rijks. Geol. Dienst 52, 235-247.

Belknap, D.F. & J.C. Kraft (1981), Preservation potential of transgressive coastal lithosomes on the U.S. Atlantic shelf. Marine Geology 42 (1-4), 429-442.

Bennema, J. (1954a), Bodem- en zeespiegelbewegingen in het Nederlandse kustgebied. Ph.D.-thesis, University of Wageningen: 187 pp.

Bennema, J. (1954b), Holocene movements of land and sea-level in the coastal area of The Netherlands. Geologie en Mijnbouw 16, 254-264.

Berendsen, H.J.A. (1982), De genese van het landschap in het zuiden van de provincie Utrecht, een fysisch-geografische studie. Ph.D.-thesis, Universiteit Utrecht, Utrecht: 256 pp.

Berendsen, H.J.A. (1998), Birds-eye view of the Rhine-Meuse delta (The Netherlands). Journal of coastal research 14 (3), 740-752.

Berendsen, H.J.A. (2005). De Laaglandgenese Databank. Department of Physical Geography, Faculty of Geosciences, Utrecht University.

Berendsen, H.J.A. & E. Stouthamer (2000), Late Weichselian and Holocene palaeogeography of the Rhine-Meuse delta, The Netherlands. Palaeogeography, Palaeoclimatology, Palaeoecology 161 (3-4), 311-335.

Berendsen, H.J.A. & E. Stouthamer (2001), Palaeogeographic development of the Rhine-Meuse delta, The Netherlands. Assen: Koninklijke van Gorcum, 268 pp.

Berendsen, H.J.A. & E. Stouthamer (2002), Paleogeographic evolution and avulsion history of the Holocene Rhine-Meuse delta, The Netherlands. Netherlands Journal of Geosciences - Geologie en Mijnbouw 81 (1), 97-112.

Berendsen, H.J.A. & K.P. Volleberg (2007), New prospects in geomorphological and geological mapping of the Rhine-Meuse Delta – Application of detailed digital elevation maps based on laser altimetry. Netherlands Journal of Geosciences - Geologie en Mijnbouw 86 (1), 15-22.

Berendsen, H.J.A., W.Z. Hoek & E.A. Schorn (1995), Late Weichselian and Holocene river channel changes of the rivers Rhine and Meuse in the central Netherlands (Land van Maas en Waal). In: B. Frenzel, ed., European river activity and climate change during the Lateglacial and Early Holocene ESF Project European Paläoklimaforschung / Paleoclimate Research. 151-171.

Berendsen, H.J.A., K.M. Cohen & E. Stouthamer (2007a), The use of GIS in reconstructing the Holocene palaeogeography of the Rhine–Meuse delta, The Netherlands. International Journal of Geographical Information Science 21 (5), 589-602.

Berendsen, H.J.A., B. Makaske, O. Van de Plassche, M.H.M. Van Ree, S. Das, M. Van Dongen, S. Ploumen & W. Schoenmakers (2007b), New groundwater-level rise data from the Rhine-Meuse delta - implications for the reconstruction of Holocene relative mean sea-level rise and differential land-level movements. Netherlands Journal of Geosciences - Geologie en Mijnbouw 86 (4), 333-354.

Blum, M.D. (1994), Genesis and architecture of incised valley fill sequences: a Late Quaternary example from the Colorado River, Gulf Coastal Plain of Texas. In: P. Weimer and H.W. Posamentier, eds., Siliclastic sequence stratigraphy: recent developments and applications. American Association of Petroleum Geologists Memoir 58, 259-283.

Bohncke, S.J.P. & W.Z. Hoek (2007), Multiple oscillations during the Preboreal as recorded in a calcareous gyttja, Kingbeekdal, The Netherlands. Quaternary Science Reviews 26 (15-16), 1965-1974.

Bondevik, S., J.I. Svendsen, G. Johnsen, J. Mangerud & P.E. Kaland (1997), The Storegga tsunami along the Norwegian coast, its age and run up. Boreas 26 (1), 29-53.

Bos, J.A.A., D.J. Huisman, P. Kiden, W.Z. Hoek & B. van Geel (2005), Early Holocene environmental change in the Kreekrak area (Zeeland, SW-Netherlands): A multi-proxy analysis. Palaeogeography, Palaeoclimatology, Palaeoecology 227 (4), 259-289.

Bosch, J.H.A. & H. Kok (1994), Toelichting bij de geologische kaart van Nederland 1:50.000, Blad Gorinchem West (38 W). Rijks Geologische Dienst, Haarlem: 159 pp.

Boyd, R., R.W. Dalrymple & B.A. Zaitlin (2006), Estuarine and incised-valley facies models. In: H.W. Posamentier and R.G. Walker, eds., Facies models revisited SEPM Special Publication. Tulsa, Oklahoma, USA: SEPM, 171-235.

Bridgland, D.R. & B. D'Ollier (1995), The Pleistocene evolution of the Thames and Rhine drainage systems in the southern North Sea Basin. In: R.C. Preece, ed., Island Britain: a Quaternary Perspective. Geol. Soc. Spec. Publ. 96, 27-45.

Bronk Ramsey, C. (1995), Radiocarbon calibration and analysis of stratigraphy: The OxCal program. Radiocarbon 37 (2), 425-430.

Bronk Ramsey, C. (2001), Development of the radiocarbon calibration program OxCal. Radiocarbon 43 (2A), 355-363.

Bugge, T., S. Befring, R. Belderson, T. Eidvin, E. Jansen, N. Kenyon, H. Holtedahl & H. Sejrup (1987), A giant three-stage submarine slide off Norway. Geo-Marine Letters 7 (4), 191-198.

Bunnik, F.P.M. (2008), Palynologisch onderzoek van boringen Benthuizen (07.09.034), Bergschenhoek (07.09.036), Nieuwendijk (07.09.038), Rotterdam Houtlaan (07.09.201) en een ontsluiting te Rotterdam Blijdorp (M4). 2008-U-R0196/A, TNO - Geological Survey of The Netherlands, Utrecht: 16 pp.

Bunnik, F.P.M. & H. Cremer (2008), De fossiele diatomeeënflora en palynomorfen in boringen 31C1166 (Boskoop) en 38A1846 (Waddinxveen). 2007-U-R1215/A, TNO - Geological Survey of The Netherlands, Utrecht: 28 pp.

Busschers, F.S., H.J.T. Weerts, J. Wallinga, P. Cleveringa, C. Kasse, H. De Wolf & K.M. Cohen (2005), Sedimentary architecture and optical dating of Middle and Late Pleistocene Rhine-Meuse deposits - fluvial response to climate change, sea-level fluctuation and glaciation. Netherlands Journal of Geosciences - Geologie en Mijnbouw 84, 25-41.

Busschers, F.S., R.T. Van Balen, K.M. Cohen, C. Kasse, H.J.T. Weerts, J. Wallinga & F.P.M. Bunnik (2008), Response of the Rhine-Meuse fluvial system to Saalian ice-sheet dynamics. Boreas 37 (3), 377-398.

Busschers, F.S., C. Kasse, R.T. van Balen, J. Vandenberghe, K.M. Cohen, H.J.T. Weerts, J. Wallinga, C. Johns, P. Cleveringa & F.P.M. Bunnik (2007), Late Pleistocene evolution of the Rhine-Meuse system in the southern North Sea basin: imprints of climate change, sea-level oscillation and glacio-isostacy. Quaternary Science Reviews 26 (25-28), 3216-3248.

Cattaneo, A. & R.J. Steel (2003), Transgressive deposits: a review of their variability. Earth-Science Reviews 62, 187-228.

Catuneanu, O. (2002), Sequence stratigraphy of clastic systems: concepts, merits and pitfalls. Journal of African Earth Sciences 35 (1), 1-43.

Catuneanu, O. (2007), Principles of sequence stratigraphy. Oxford, Great Britain: Elsevier, 375 pp.

Catuneanu, O., V. Abreu, J.P. Bhattacharya, M.D. Blum, R.W. Dalrymple, P.G. Eriksson, C.R. Fielding, W.L. Fisher, W.E. Galloway, M.R. Gibling, K.A. Giles, J.M. Holbrook, R. Jordan, C.G.S.C. Kendall, B. Macurda, O.J. Martinsen, A.D. Miall, J.E. Neal, D. Nummedal, L. Pomar, H.W. Posamentier, B.R. Pratt, J.F. Sarg, K.W. Shanley, R.J. Steel, A. Strasser, M.E. Tucker & C. Winker (2009), Towards the standardization of sequence stratigraphy. Earth-Science Reviews 92 (1-2), 1-33.

Chambers, R.M., L.A. Meyerson & K. Saltonstall (1999), Expansion of Phragmites australis into tidal wetlands of North America. Aquatic Botany 64 (3-4), 261-273.

Chappell, J. & H. Polach (1991), Post-glacial sea-level rise from a coral record at Huon Peninsula, Papua New Guinea. Nature 349 (6305), 147-149.

Clarke, G.K.C., D.W. Leverington, J.T. Teller & A.S. Dyke (2004), Paleohydraulics of the last outburst flood from glacial Lake Agassiz and the 8200 BP cold event. Quaternary Science Reviews 23, 389-407.

Cleveringa, J. (2000), Reconstruction and modelling of Holocene coastal evolution of the western Netherlands. Ph.D.-thesis, Utrecht University: 197 pp.

Cleveringa, P. (1985), Uitkomsten van pollenanalytisch onderzoek aan monsters afkomstig uit een ontsluiting te Rijswijk (Plaspoelpolder). Palaeobotanie Kenozoïcum 975a, Rijks Geologische Dienst, Haarlem: 5 pp.

Cleveringa, P. & M.A. Veldkamp (1996), Pollenanalytische en C14-dateringen van de boring Maassluis 37B/226. Palaeobotanie Kenozoïcum, 1255A, Rijks Geologische Dienst, Haarlem: 3 pp.

Coerts, A. (1996), Analysis of static cone penetration test data for subsurface modelling - a methodology. Ph.D.-thesis, Utrecht University, Utrecht: 263 pp.

Cohen, K.M. (2003), Differential subsidence within a coastal prism. Late-Glacial – Holocene tectonics in the Rhine-Meuse delta, The Netherlands. Ph.D.-thesis, Utrecht University: 176 pp.

Cohen, K.M. (2005), 3D geostatistical interpolation and geological interpolation of palaeo-groundwaterrise within the coastal prism in the Netherlands. In: L. Giosan and J.P. Bhattacharaya, eds., River Deltas: Concepts, models, and examples SEPM Special Publication 83. Tulsa, Oklahoma, USA: SEPM (Society for Sedimentary Geology), 341-364.

Cohen, K.M. & M.P. Hijma (2008), Het Rijnmond gebied in het vroeg-Holoceen: inzichten uit een diepe put bij Blijdorp (Rotterdam). Grondboor en Hamer 3/4, 64-71.

Cohen, K.M., H.J.A. Berendsen & E. Stouthamer (2002), Fluvial deposits as a record for Late Quaternary neotectonic activity in the Rhine-Meuse delta, The Netherlands. Netherlands Journal of Geosciences - Geologie en Mijnbouw 81 (3-4), 389-405.

Conradsen, K. & S. Heier-Nielsen (1995), Holocene paleoceanography and paleoenvironments of the Skagerrak-Kattegat, Scandinavia. Paleoceanography 10 (4), 801-813.

Cremer, H. (2008), Paleoecologisch diatomeeënonderzoek van boringen Benthuizen (07.09.034), Bergschenhoek (07.09.036), Nieuwendijk (07.09.038), Rotterdam Houtlaan (07.09.201) en Rotterdam Blijdorp (M4). 2008-U-R0124/B, TNO - Geological Survey of The Netherlands, Utrecht: 38 pp.

Cronin, L.E. (1975, ed.), Estuarine research, II: Geology and Engineering. New York: Academic Press, 757 pp.

Dalrymple, R.W., ed., (1992), Tidal depositional systems. Facies Models - Response to Sea Level Change, Reprint Series 4: 195-218. St. John's, Newfoundland: Geological Association of Canada.

Dalrymple, R.W. & K. Choi (2007), Morphologic and facies trends through the fluvial-marine transition in tide-dominated depositional systems: A schematic framework for environmental and sequence-stratigraphic interpretation. Earth-Science Reviews 81 (3-4), 135-174.

Dalrymple, R.W., B.A. Zaitlin & R. Boyd (1992), Estuarine facies models: conceptual basis and stratigraphic implications. Journal of Sedimentary Research 62, 1130-1146.

Dalrymple, R.W., R. Boyd & B.A. Zaitlin, eds. (1994), Incised-valley systems: origin and sedimentary sequences. SEPM Special Publication 51. Tulsa, Oklahoma, USA: SEPM (Society for Sedimentary Geology), 391 pp.

Davis, R.A., Jr. & M.O. Hayes (1984), What is a wave-dominated coast? Marine Geology 60 (1-4), 313-329.

De Gans, W. & K. Van Gijssel (1996), The Late Weichselian morphology of the Netherlands and its influence on Holocene coastal development. In: D.J. Beets, M.M. Fischer and W. De Gans, eds., Coastal studies on the Holocene of the Netherlands Mededelingen Rijks Geologische Dienst. Haarlem: Rijks Geologische Dienst, 11-25.

De Groot, T.A.M. & W. De Gans (1996), Facies variations and sea-level response in the lower Rhine-Meuse area during the last 15000 years (the Netherlands). In: D.J. Beets, M.M. Fischer and W. De Gans, eds., Coastal studies on the Holocene of the Netherlands Med. Rijks. Geol. Dienst. Haarlem: Rijks Geologische Dienst, 229-250.

De Jong, J. (1970), Voorlopige uitkomsten van C14-onderzoek, verricht aan boringen uit de Hoeksewaard. Palaeobotanie Kenozoïcum 535A, Rijks Geologische Dienst, Haarlem: 1 pp.

De Jong, J. (1973a), Uitkomsten van C14-bepaling aan twee boringen bij Schipluiden. Palaeobotanie Kenozoïcum 702, Rijks Geologische Dienst, Haarlem: 4 pp.

De Jong, J. (1973b), Wijzigingen C14-uitkomsten van boringen bij Schipluiden. Palaeobotanie Kenozoïcum 702a, Rijks Geologische Dienst, Haarlem: 1 pp.

De Jong, J. (1977), Uitkomsten C14-ouderdomsbepalingen aan boringen uit het Oude Rijn-gebied. Palaeobotanie Kenozoïcum 800, Rijks Geologische Dienst, Haarlem: 3 pp.

De Jong, J. (1979a), Uitkomsten C14-bepalingen van een boring te Wilsveen. Palaeobotanie Kenozoïcum 855A, Rijks Geologische Dienst, Haarlem: 2 pp.

De Jong, J. (1979b), Uitkomsten C14-ouderdomsbepalingen aan materiaal afkomstig uit de boringen Zuid Plaspolder en Waddinxveen. Palaeobotanie Kenozoïcum 838, Rijks Geologische Dienst, Haarlem: 5 pp.

De Jong, J. (1979c), Uitkomsten C14-ouderdomsbepalingen aan materiaal verkregen uit de boringen Zuid Plaspolder en Waddinxveen. Palaeobotanie Kenozoïcum 838a, Rijks Geologische Dienst, Haarlem: 2 pp.

De Jong, J. (1984), Uitkomsten C14-ouderdomsbepalingen aan boringen bij Berkel en Bleiswijk. Palaeobotanie Kenozoïcum 934, Rijks Geologische Dienst, Haarlem: 2 pp.

De Jong, J. (1985), Uitkomsten C14-bepalingen aan monsters afkomstig uit een ontsluiting te Rijswijk (Plaspoelpolder). Palaeobotanie Kenozoïcum 975, Rijks Geologische Dienst, Haarlem: 5 pp.

De Jong, J. (1986), Nagekomen C14-ouderdomsbepalingen aan schelpen afkomstig uit een ontsluiting te Rijswijk (Plaspoelpolder). Palaeobotanie Kenozoïcum 975b, Rijks Geologische Dienst, Haarlem: 2 pp.

De Jong, J. (1987a), Uitkomsten C14-ouderdomsbepalingen van boring Schipluiden III. Palaeobotanie Kenozoïcum 1003a, Rijks Geologische Dienst, Haarlem: 3 pp.

De Jong, J. (1987b), Uitkomsten van C14-ouderdomsbepalingen in een boring te Delft. Palaeobotanie Kenozoïcum 1004a, Rijks Geologische Dienst, Haarlem: 5 pp.

De Jong, J. (1988), Uitkomsten C14-ouderdomsbepalingen aan materiaal, verkregen uit de boring Smitshoek 37H/549. Palaeobotanie Kenozoïcum 1061, Rijks Geologische Dienst, Haarlem: 3 pp.

De Jong, J. (1989a), Basisgegevens en uitkomsten van C14-ouderdomsbepalingen in betrekking tot een tweetal oost-west gerichte profielen in het Maasmondgebied. Palaeobotanie Kenozoïcum 1086, Rijks Geologische Dienst, Haarlem: 31 pp.

De Jong, J. (1989b), Pollenanalytisch onderzoek van een traject uit boring Rotterdam 37F/371 (LGM). Palaeobotanie Kenozoïcum 1075, Rijks Geologische Dienst, Haarlem: 6 pp.

De Jong, J. (1991a), Uitkomsten C14-ouderdomsbepalingen van boring Schipluiden III. Palaeobotanie Kenozoïcum 1003b, Rijks Geologische Dienst, Haarlem: 3 pp.

De Jong, J. (1991b), Uitkomsten van C14-ouderdomsbepalingen in een boring te Delft. Palaeobotanie Kenozoïcum 1004b, Rijks Geologische Dienst, Haarlem: 3 pp.

De Jong, J. (1992), Pollenanalytisch onderzoek van boring Schiedam 37 E/549. Palaeobotanie Kenozoïcum 1143, Rijks Geologische Dienst, Haarlem: 2 pp.

De Wolf, H. (1979), Diatomeeënonderzoek van enkele monsters van de boringen Zoeterwoude, Moerkapelle en Stompwijk. Afdeling Diatomeeën, report 420, Rijks Geologische Dienst, Haarlem: 1 pp.

De Wolf, H. (1981a), Diatomeeënonderzoek van de boring Groenendijk. Afdeling Diatomeeën, report 424, Rijks Geologische Dienst, Haarlem: 2 pp.

De Wolf, H. (1981b), Diatomeeënonderzoek van de boring Waddinxveen. Afdeling Diatomeeën, report 426, Rijks Geologische Dienst, Haarlem: 2 pp.

De Wolf, H. (1981c), Diatomeeënonderzoek van de boring Zuid Plaspolder. Afdeling Diatomeeën, report 425, Rijks Geologische Dienst, Haarlem: 2 pp.

De Wolf, H. (1986a), Diatomeeënonderzoek van de boring Schipluiden I. Afdeling Diatomeeën, report 480, Rijks Geologische Dienst, Haarlem: 4 pp.

De Wolf, H. (1986b), Diatomeeënonderzoek van de boring Schipluiden II. Afdeling Diatomeeën, report 481, Rijks Geologische Dienst, Haarlem: 4 pp.

De Wolf, H. (1989a), Diatomeeënonderzoek van de boring Hoogvliet 37G432. Afdeling Diatomeeën, report 513, Rijks Geologische Dienst, Haarlem: 4 pp.

De Wolf, H. (1989b), Diatomeeënonderzoek van de boring Schipluiden 37E546 (IV). Afdeling Diatomeeën, report 517, Rijks Geologische Dienst, Haarlem: 3 pp.

De Wolf, H. (1990), Diatomeeënonderzoek van de boring Terbregge 37F370. Afdeling Diatomeeën, report 516, Rijks Geologische Dienst, Haarlem: 6 pp.

De Wolf, H. (1995), Diatomeeënonderzoek van de Noordzeeboringen: 88AS126, 72H39, 92DW135, 79D006, 91.034, 78H19, 93DW93, 88AS19, 93DW68, 93DW175, 94DW186, 94DW187, 94DW188, 94DW189, 94DW191, 94DW194, 94DW01, 92DW69, 93DW09. Afdeling Diatomeeën, report 597, Rijks Geologische Dienst, Haarlem: 10 pp.

De Wolf, H. (2004), Palaeo-ecologisch diatomeeënonderzoek van monsters van de boringen 38F0622, 31H0813, 39G0306, 44F0247, 38H0256, 39G037, 43E0345, 37G058, 39E0319, 45E0437, 39F0755. NITG 04-198/B, TNO Bouw en Ondergrond, Utrecht: 7 pp.

De Wolf, H. (2006), Paleo-ecologisch diatomeeënonderzoek van monsters van de boring Nesselanden 38A0349. TNO 2006-U-R0042/B, TNO Bouw en Ondergrond, Utrecht: 3 pp.

De Wolf, H. (Unpublished), Diatomeeënonderzoek van enige boringen ten behoeve van het EPOCH III project. Afdeling Diatomeeën, preliminary report 602, Rijks Geologische Dienst, Haarlem: 5 pp.

De Wolf, H. & P. Cleveringa (2006), Palaeo-ecologisch diatomeeënonderzoek van monsters van de boring Stompwijk 30H0369. 2006-U-R0151/B, TNO Bouw en Ondergrond, Utrecht: 12 pp.

Den Held, A., M. Schmitz & G. Van Wirdum (1992), Types of terrestrializing fen vegetation in the Netherlands. In: J.T.A. Verhoeven, ed., Fens and bogs in the Netherlands: vegetation, history, nutrient dynamics and conservation Geobotany. Dordrecht: Kluwer Academics Publishers, 237-321.

Ellison, C.R.W., M.R. Chapman & I.R. Hall (2006), Surface and deep ocean interactions during the cold climate event 8200 years ago. Science 312 (5782), 1929-1932.

Erkens, G. (2009), Sediment dynamics in the Rhine catchment: quantification of fluvial response to climate change and human impact. Ph.D.-thesis, Utrecht University.

Fagel, N., L.Y. Alleman, L. Granina, F. Hatert, E. Thamo-Bozso, R. Cloots & L. Andre (2005), Vivianite formation and distribution in Lake Baikal sediments. Global and Planetary Change 46 (1-4), 315-336.

Fairbanks, R.G. (1989), A 17,000-year glacio-eustatic sea level record: influence of glacial melting rates on the Younger Dryas event and deep-ocean circulation. Nature 342, 637-642.

Fairbridge, R.W. (1961), Eustatic changes in sea level. Physics and Chemistry of The Earth 4, 99-185.

FitzGerald, D. & J. Knight, eds. (2005), High-resolution morphodynamics and sedimentary evolution of estuaries. Coastal systems and continental margins, 8. Springer, 364 pp.

Fleming, K., P. Johnston, D. Zwartz, Y. Yokoyama, K. Lambeck & J. Chappell (1998), Refining the eustatic sea-level curve since the Last Glacial Maximum using far- and intermediate-field sites. Earth and Planetary Science Letters 163 (1-4), 327-342.

Frouin, M., D. Sebag, A. Durand, B. Laignel, J.-F. Saliege, B.J. Mahler & C. Fauchard (2007), Influence of paleotopography, base level and sedimentation rate on estuarine system response to the Holocene sea-level rise: The example of the Marais Vernier, Seine estuary, France. Sedimentary Geology 200 (1-2), 15-29.

Galbraith, R.F. & P.F. Green (1990), Estimating the component ages in a finite mixture. Nuclear Tracks and Radiation Measurements 17, 197-206.

Gerritsen, H. & C.W.J. Berentsen (1998), A modelling study of tidally induced equilibrium sand balances in the North Sea during the Holocene. Continental Shelf Research 18, 151-200.

Gibbard, P.L., J. Rose & D.R. Bridgland (1988), The history of the great northwest European rivers during the past three million years (and discussion). Philosophical Transactions of the Royal Society of London. Series B, Biological Sciences 318 (1191), 559-602.

Gilbert, G.K. (1880), Land, sculpture, geology of the Henry Mountains. USA. Geographical and Geological Survey, Rocky Mountain Region, 160 pp.

Ginsberg, S.S. & G.M.E. Perillo (2004), Characteristics of tidal channels in a mesotidal estuary of Argentina. Journal of coastal research 20 (2), 489-497.

Gotjé, W. (1993), De Holocene laagveenontwikkeling in de randzone van de Nederlandse kustvlakte (Noordoostpolder). Ph.D.-thesis, Vrije Universiteit, Amsterdam: 182 pp.

Gouw, M.J.P. (2002), Toelichting op het geologisch profiel Zwijndrechtse Waard en Hoekse Waard. Projectgroep Archeologie HSL-Zuid/A16, RWS/RACM, Amersfoort: 29 (in Dutch) pp.

Gouw, M.J.P. (2007a), Alluvial architecture of fluvio-deltaic successions: a review with special reference to Holocene settings. Netherlands Journal of Geosciences - Geologie en Mijnbouw 86 (3), 211-228.

Gouw, M.J.P. (2007b), Alluvial architecture of the Holocene Rhine-Meuse delta (The Netherlands) and the Lower Mississippi Valley (U.S.A.). Ph.D.-thesis, Utrecht University, Utrecht: 192 pp.

Gouw, M.J.P. & G. Erkens (2007), Architecture of the Holocene Rhine-Meuse delta (the Netherlands) - A result of changing external controls. Netherlands Journal of Geosciences - Geologie en Mijnbouw 86 (1), 23-54.

Gupta, S., J.S. Collier, A. Palmer-Felgate & G. Potter (2007), Catastrophic flooding origin of shelf valley systems in the English Channel. Nature 448 (7151), 342-345.

Hageman, B.P. (1964), Toelichting bij de geologische kaart van Nederland 1:50.000, Blad Goeree en Overflakkee. Rijks Geologische Dienst, Haarlem (with English summary): 89 pp.

Hanebuth, T., K. Stattegger & P.M. Grootes (2000), Rapid flooding of the Sunda Shelf: A Late-Glacial sea-level record. Science 288 (5468), 1033-1035.

Hanebuth, T.J.J., K. Stattegger & A. Bojanowski (2009), Termination of the Last Glacial Maximum sea-level lowstand: The Sunda-Shelf data revisited. Global and Planetary Change 66 (1-2), 76-84.

Haq, B.U., J. Hardenbol & P.R. Vail (1987), Chronology of fluctuating sea levels since the Triassic (250 millions years ago to present). Science 235, 1156-1166.

Hedberg, H.D. (1976), International stratigraphic guide: A guide to stratigraphical classification, terminology, and procedure. International Union of Geological Sciences, Commission on stratigraphy, International on Stratigraphic Classification. New York: Wiley, 200 pp.

Helland-Hansen, W. & O.J. Martinsen (1996), Shoreline trajectories and sequences: description of variable depositional-dip scenarios. Journal of Sedimentary Research 66 (4), 670-688.

Hijma, M.P. & K.M. Cohen (In press), Timing and magnitude of the sea-level jump preluding the 8,200 yr event. Geology.

Hijma, M.P., A.J.F. Van der Spek & S. Van Heteren (Subm.), Development of a mid-Holocene estuarine basin, Rhine-Meuse mouth area, offshore the Netherlands. Conditionally accepted for publication by Marine Geology.

Hijma, M.P., K.M. Cohen, G. Hoffmann, A.J.F. Van der Spek & E. Stouthamer (2009), From river valley to estuary: the evolution of the Rhine mouth in the early to middle Holocene (western Netherlands, Rhine-Meuse delta). Netherlands Journal of Geosciences - Geologie en Mijnbouw 88 (1), 13-53.

Hillaire-Marcel, C., A. De Vernal & D.J.W. Piper (2007), Lake Agassiz final drainage event in the northwest North Atlantic. Geophysical Research Letters 34, L15601.

Hoek, W.Z. (2001), Vegetation response to the ~14.7 and ~11.5 ka cal. BP climate transitions: is vegetation lagging climate? Global and Planetary Change 30 (1-2), 103-115.

Hoek, W.Z. (2008), The Last Glacial-Interglacial transition. Episodes 31 (2), 226-229.

Hori, K. & Y. Saito (2007), An early Holocene sea-level jump and delta initiation. Geophysical Research Letters 34, L18401.

Hublin, J.-J., D. Weston, P. Gunz, M. Richards, W. Roebroeks, J. Glimmerveen & L. Anthonis (In press), Out of the North Sea: the Zeeland Ridges Neandertal. Journal of Human Evolution.

Hughen, K.A., M.G.L. Baillie, E. Bard, J. Warren Beck, C.J.H. Bertrand, P.G. Blackwell, C.E. Buck, G.S. Burr, K.B. Cutler, P.E. Damon, R.L. Edwards, R.G. Fairbanks, M. Friedrich, T.P. Guilderson, B. Kromer, G. McCormac, S. Manning, C. Bronk Ramsey, P.J. Reimer, R.W. Reimer, S. Remmele, J.R. Southon, M. Stuiver, S. Talamo, F.W. Taylor, J. Van der Plicht & C.E. Weyhenmeyer (2004), Marine04 marine radiocarbon age calibration, 0-26 kyr BP. Radiocarbon 46 (3), 1059-1086.

Hutton, J. (1788), Theory of the earth; or an investigation of the laws observable in the composition, dissolution, and restoration of land upon the globe. Transactions of the Royal Society of Edinburgh I (part II). 209-304. Taken from http://records.viu.ca/~johnstoi/.

Jay, T., 2004. Water spear: language as estuary, Pacific Estuarine Research Society, Port Townsend.

Jelgersma, S. (1961), Holocene sea-level changes in The Netherlands. Mededelingen Geologische Stichting 7, 1-101.

Jelgersma, S., 1966. Sea-level changes during the last 10,000 years, Proc. Intern. Symp. World climates from 8000 BC to 0 BC. Royal Meteor. Soc., London: 54-71.

Jelgersma, S. (1979), Sea-level changes in the North Sea basin. In: E. Oele, R. Schüttenhelm and A.J. Wiggers, eds., Acta Univ. Ups. Symp. Univ. Ups. Annum Quingentesimum Celebrantis, vol. 2. 233-248.

Jiang, H., S. Björck & K.L. Knudsen (1997), A palaeoclimatic and palaeoceanographic record of the last 11000 14C years from the Skagerrak-Kattegat, northeastern Atlantic margin. The Holocene 7 (3), 301-310.

Kasse, C., S.J.P. Bohncke & J. Vandenberghe (1995), Climatic change and fluvial dynamics of the Maas during the late Weichselian and early Holocene. Paläoklimaforschung/Palaeoclimate Research 14, 123-150.

Kendall, R.A., J.X. Mitrovica, G.A. Milne, T.E. Törnqvist & Y. Li (2008), The sea-level fingerprint of the 8.2 ka climate event. Geology 36 (5), 423-426.

Kiden, P. (1995), Holocene relative sea-level change and crustal movement in the southwestern Netherlands. Marine Geology 124, 21-41.

Kiden, P., L. Denys & P. Johnston (2002), Late Quaternary sea-level change and isostatic and tectonic land movement along the Belgian-Dutch North Sea coast: geological data and model results. Journal of Quaternary Science 17, 535-546.

Kok, H. (1987), Korte toelichting bij de geologische kaart van Nederland 1:50.000, Blad Rotterdam Oost (37W). Rijks Geologische Dienst, Haarlem: 89 pp.

Kooi, H., P. Johnston, K. Lambeck, C. Smither & M. Ronald (1998), Geological causes of recent (~100 yr) vertical land movement in the Netherlands. Tectonophysics 299 (4), 297-316.

Laban, C. (1995), The Pleistocene glaciations in the Dutch sector of the North Sea: A synthesis of sedimentary and seismic data. Ph.D.-thesis, University of Amsterdam.

Lambeck, K. (1995), Late Devensian and Holocene shorelines of the British Isles and North Sea from models of glacio-hydro-isostatic rebound. Journal of the Geological Society 152, 437-448.

Lambeck, K., S. Smither & P. Johnston (1998), Sea-level change, glacial rebound and mantle viscosity for Northern Europe. Geophys. J. Int. 134, 102-144.

Lambeck, K., Y. Yokoyama & T. Purcell (2002), Into and out of the Last Glacial Maximum: sea-level change during Oxygen Isotope Stages 3 and 2. Quaternary Science Reviews 21 (1-3), 343-360.

Lauff, G.H. (1967, ed.), Estuaries, Publication 83. American Association for the Advancement of Science, 757 pp.

Leatherman, S.P., M.R. Rampino & J.E. Sanders (1983), Barrier island evolution in response to sea level rise; discussion and reply. Journal of Sedimentary Petrology 53 (3), 1026-1033.

Leverington, D.W., J.D. Mann & J.T. Teller (2002), Changes in the Bathymetry and Volume of Glacial Lake Agassiz between 9200 and 7700 14C yr BP. Quaternary Research 57 (2), 244-252.

Liu, J., Y. Saito, H. Wang, Z. Yang & R. Nakashima (2007), Sedimentary evolution of the Holocene subaqueous clinoform off the Shandong Peninsula in the Yellow Sea. Marine Geology 236 (3-4), 165-187.

Louwe Kooijmans, L.P. (1974), The Rhine/Meuse Delta: four studies on its prehistoric occupation and Holocene geology. Ph.D.-thesis, Leiden University, Leiden: 421 pp.

Lüders, K. (1934), Über das Wandern der Priele. Abh. naturwiss. Verein Bremen 29, 19-32.

Lyell, C. (1830), Principles of Geology. London: Murray.

MacLaren, C. (1842), The glacial theory of Professor Agassiz of Neuchatel. American Journal of Science 42, 346-365.

Makaske, B. (1998), Anastomosing rivers. Forms, processes and sediments. Ph.D.-thesis, Utrecht University: 298 pp.

Makaske, B. (2001), Anastomosing rivers: a review of their classification, origin and sedimentary products. Earth-Science Reviews 53 (3-4), 149-196.

Marshall, J.D., B. Lang, S.F. Crowley, G.P. Weedon, P. van Calsteren, E.H. Fisher, R. Holme, J.A. Holmes, R.T. Jones, A. Bedford, S.J. Brooks, J. Bloemendal, K. Kiriakoulakis & J.D. Ball (2007), Terrestrial impact of abrupt changes in the North Atlantic thermohaline circulation: Early Holocene, UK. Geology 35 (7), 639-642.

McClennen, C.E. & R.A. Housley (2006), Late-Holocene channel meander migration and mudflat accumulation rates, Lagoon of Venice, Italy. Journal of coastal research 22 (4), 930-945.

Miall, A.D. (1995), Whither stratigraphy? Sedimentary Geology 100, 5-20.

Miall, A.D. (2000), Principles of Sedimentary Basin Analysis. Springer, 616 pp.

Miall, A.D. & M. Arush (2001), Cryptic sequence boundaries in braided fluvial successions. Sedimentology 48 (971-985).

Murray, A.S. & A.G. Wintle (2003), The single aliquot regenerative dose protocol: potential for improvements in reliability. Radiation Measurements 37 (4-5), 377-381.

Neal, A. (2004), Ground-penetrating radar and its use in sedimentology: principles, problems and progress. Earth-Science Reviews 66 (3-4), 261-330.

Oele, E., W. Apon, M.M. Fischer, R. Hoogendoorn, C.S. Mesdag, E.F.J. De Mulder, B. Overzee, A. Sesören & W.E. Westerhoff (1983), Surveying The Netherlands, Sampling Techniques, Maps and their application. Geologie en Mijnbouw 62, 355-372.

Oomkens, E. & J.H.J. Terwindt (1960), Inshore estuarine sediments in the Haringvliet (Netherlands). Geologie en Mijnbouw 39, 701-710.

Peltier, W.R. (2002), On eustatic sea level history: Last Glacial Maximum to Holocene. Quaternary Science Reviews 21 (1-3), 377-396.

Peltier, W.R. (2004), Global glacial isostasy and the surface of the ice-age earth: the ICE-5G (VM2) model and grace. Annual Review of Earth and Planetary Science 32, 111-149.

Peltier, W.R. & R.G. Fairbanks (2006), Global glacial ice volume and Last Glacial Maximum duration from an extended Barbados sea level record. Quaternary Science Reviews 25 (23-24), 3322-3337.

Perillo, G.M.E., ed., (1995), Geomorphology and sedimentology of estuaries. Developments in sedimentology, 53. Elsevier, 471 pp.

Pons, L.J. (1954), Het fluviatiele laagterras van Rijn en Maas. Boor en Spade 7, 97-110.

Pons, L.J. (1957), De geologie, bodemvorming en de waterstaatkundige ontwikkeling van het Land van Maas en Waal en een gedeelte van het Rijk van Nijmegen. Ph.D.-thesis, Wageningen University, Wageningen: 156 pp.

Pons, L.J. & J. Bennema (1958), De morfologie van het Pleistocene oppervlak in westelijk Midden-Nederland, voor zover gelegen beneden gemiddeld zeeniveau (N.A.P.). Tijdschrift van het Koninklijk Nederlandsch Aardrijkskundig Genootschap 75 (2), 121-138.

Pons, L.J. & A.J. Wiggers (1959-1960), De holocene wordingsgeschiedenis van Noordholland en het Zuiderzeegebied. Tijdschrift van het Koninklijk Nederlandsch Aardrijkskundig Genootschap LXXVI-LXXVII, 104-152;3-57.

Pons, L.J., S. Jelgersma, A.J. Wiggers & J.D. De Jong (1963), Evolution of the Netherlands coastal area during the Holocene. In: J.D. De Jong, ed., Verhandelingen van het KNGMG: Transactions of the jubilee convention - part two 21. 's Gravenhage: N.V. Boek- Kunstdrukkerij v/h Mouton & Co., 197-207.

Posamentier, H.W. & P.R. Vail (1988), Eustatic controls on clastic deposition II - sequence and system tract models. In: C.K. Wilgus et al., eds., Sea-level changes - An integrated approach. Tulsa: Spec. Publ. Soc. Econ. Paleontol. Mineral. 42, 125-154.

Posamentier, H.W. & G.P. Allen (1999), Siliciclastic Sequence Stratigraphy - Concepts and Applications. SEPM Concepts in Sedimentology and Paleontology 7. Tulsa, 204 pp.

Posamentier, H.W., M.T. Jervey & P.R. Vail (1988), Eustatic controls on clastic deposition I - conceptual framework. In: C.K. Wilgus et al., eds., Sea-level changes - An integrated approach. Tulsa: Spec. Publ. Soc. Econ. Paleontol. Mineral. 42, 110-124.

Rampino, M.R. & J.E. Sanders (1980), Holocene transgression in south-central Long Island, New York. Journal of Sedimentary Petrology 50 (4), 1063-1079.

Rampino, M.R. & J.E. Sanders (1982), Holocene transgression in South-central Long Island, New York; reply. Journal of Sedimentary Petrology 52 (3), 1020-1025.

Rasmussen, S.O., B.M. Vinther, H.B. Clausen & K.K. Andersen (2007), Early Holocene climate oscillations recorded in three Greenland ice cores. Quaternary Science Reviews 26 (15-16), 1907-1914.

Rasmussen, S.O., K.K. Andersen, A.M. Svensson, J.P. Steffensen, B.M. Vinther, H.B. Clausen, M.-L. Siggaard-Andersen, S.J. Johnsen, L.B. Larsen, D. Dahl-Jensen, M. Bigler, R. Röthlisberger, H. Fischer, K. Goto-Azuma, M.E. Hansson & U. Ruth (2006), A new Greenland ice core chronology for the last glacial termination. Journal of Geophysical Research 111, D06102.

Raven, J.G.M. & W.J. Kuijper (1981), Calais deposits (Holocene) near Benthuizen (Province of Zuid-Holland, The Netherlands), with a palaeoecological reconstruction. Meded. Werkgr. Tert. en Kwart. Geol. 18, 11-28.

Reimer, P.J., M.G.L. Baillie, E. Bard, A. Bayliss, J.W. Beck, C.J.H. Bertrand, P.G. Blackwell, C.E. Buck, G.S. Burr, K.B. Cutler, P.E. Damon, R.L. Edwards, R.G. Fairbanks, M. Friedrich, T.P. Guilderson, A.G. Hogg, K.A. Hughen, B. Kromer, G. McCormac, S. Manning, C. Bronk Ramsey, R.W. Reimer, S. Remmele, J.R. Southon, M. Stuiver, S. Talamo, F.W. Taylor, J. Van der Plicht & C.E. Weyhenmeyer (2004), INTCAL04 Terrestrial radiocarbon age calibration, 0-26 cal kyr BP. Radiocarbon 46 (3), 1029-1058.

Reineck, H.E. (1978, ed.), Das Watt, Ablagerungs- und Lebensraum. Frankfurt am Main: Waldemar Kramer, 185 pp.

Reinson, G.E., ed., (1992), Transgressive barrier island and estuarine systems. Facies models - response to sea level change, Reprint Series 4: 179-194. St. John's, Newfoundland: Geological Association of Canada.

Renssen, H., H. Goosse, T. Fichefet & J.-M. Camping (2001), The 8.2 kyr BP event simulated by a global atmosphere-sea-ice-ocean model. Geophysical Research Letters 28, 1567-1570.

Reynaud, J.-Y., B. Tessier, J.-N. Proust, R.W. Dalrymple, J.-F. Bourillet, M. De Batist, G. Lericolais, S. Berné & T. Marsset (1999), Architecture and sequence stratigraphy of a Late Neogene incised valley at the shelf margin, southern Celtic Sea. Journal of Sedimentary Research 69 (2), 351-364.

Richter, J.P. (1939), The literary works of Leonardo da Vinci (Volumes 1 and 2). London: Oxford University Press.

Rieu, R., S. Van Heteren, A.J.F. Van der Spek & P.L. De Boer (2005), Development and preservation of a mid-Holocene tidal-channel network offshore the western Netherlands. Journal of Sedimentary Research 75 (3), 409-419.

Rijkswaterstaat-AGI (2005), Actueel Hoogtebestand Nederland (AHN). Revised version. Rijkswaterstaat, Adviesdienst Geo-informatie en ICT, Delft.

Rodnight, H., G.A.T. Duller, A.G. Wintle & S. Tooth (2006), Assessing the reproducibility and accuracy of optical dating of fluvial deposits. Quaternary Geochronology 1 (2), 109-120.

Roep, T.B. & D.J. Beets (1988), Sea level rise and paleotidal levels from sedimentary structures in the coastal barriers in the western Netherlands since 5600 BP. Geologie en Mijnbouw 67, 53-60.

Roep, T.B., H. Holst, R.L.M. Vissers, H. Pagnier & D. Postma (1975), Deposits of southward-flowing, pleistocene rivers in the channel region, near Wissant, NW France. Palaeogeography, Palaeoclimatology, Palaeoecology 17 (4), 289-308.

Schirmer, W. (1995), Valley bottoms in the Late Quaternary - der Talgrund in im jüngeren Quartär. Zeitschrift für Geomorphologie N.F. Supplement 100, 27-51.

Schokker, J., P. Cleveringa, A.S. Murray, J. Wallinga & W.E. Westerhoff (2005), An OSL dated Middle and Late Quaternary sedimentary record in the Roer Valley Graben (southeastern Netherlands). Quaternary Science Reviews 24 (20-21), 2243-2264.

Sha, L.P. & J.H. Van den Berg (1993), Variation in ebb-tidal delta geometry along the coast of the Netherlands and the German Bight. Journal of coastal research 9 (3), 730-746.

Siddall, M., W.G. Thompson, C. Waelbroeck & L. Newman (2009), Understanding sea level: ways forward from the past (Edited). Pages News 17 (2), 1-88.

Silberhorn, G.M. (1999), Common plants of the Mid-Atlantic coast: a field guide. Revised edition. Baltimore: The John Hopkins University Press, 294 pp.

Smith, A.J. (1985), A catastrophic origin for the palaeovalley system of the eastern English Channel. Marine Geology 64 (1-2), 65-75.

Smith, D.E., S. Shi, C.L. Brooks, R.A. Cullingford, A.G. Dawson, S. Dawson, C.R. Firth, I.D.L. Foster, P.T. Fretwell, B.A. Haggart, L.K. Holloway & D. Long (2004), The Holocene Storegga Slide tsunami in the United Kingdom. Quaternary Science Reviews 23/24, 2295-2325.

Stanley, D.J. & A.G. Warne (1994), Worldwide initiation of Holocene marine deltas by deceleration of sea-level rise. Science 265, 228-231.

Steffen, H. (2006), Determination of a consistent viscosity distribution in the earth's mantle beneath Northern and Central Europe. Ph.D.-thesis, Institut für Geologische Wissenschaften der Freie Universität Berlin, Berlin, Germany.

Stocker, T.F. (1998), Climate change: The seesaw effect. Science 282 (5386), 61-62.

Storms, J.E.A., G.J. Weltje, J.J. van Dijke, C.R. Geel & S.B. Kroonenberg (2002), Process-response modeling of wave-dominated coastal systems: simulating evolution and stratigraphy on geological timescales. Journal of Sedimentary Research 72 (2), 226-239.

Stortelder, A.H.F., P.W.F.M. Hommel, R.W. De Waal, K.W. Van Dort, J.G. Vrielink & R.J.A.M. Wolf (1998), Broekbossen. Natuurhistorische bibliotheek 66. Utrecht: Stichting Uitgeverij van Koninklijke Nederlandse Natuurhistorische Vereniging.

Stouthamer, E. (2001), Holocene avulsions on the Rhine-Meuse delta, the Netherlands. Ph.D.-thesis, Utrecht University: 224 pp.

Swift, D.J.P. (1968), Coastal erosion and transgressive stratigraphy. Journal of geology 126, 235-248.

Swift, D.J.P. (1975), Barrier island genesis: evidence from the central Atlantic shelf of North America. Sedimentary Geology 14, 1-43.

Swift, D.J.P. & T.F. Moslow (1982), Holocene transgression in South-central Long Island, New York; discussion. Journal of Sedimentary Petrology 52 (3), 1014-1019.

Tamura, T., Y. Saito, S. Sieng, B. Ben, M. Kong, I. Sim, S. Choup & F. Akiba (2009), Initiation of the Mekong River delta at 8 ka: evidence from the sedimentary succession in the Cambodian lowland. Quaternary Science Reviews 28 (3-4), 327-344.

Tanabe, S., Y. Saito, Q. Lan Vu, T.J.J. Hanebuth, Q. Lan Ngo & A. Kitamura (2006), Holocene evolution of the Song Hong (Red River) delta system, northern Vietnam. Sedimentary Geology 187 (1-2), 29-61.

Teller, J.T., D.W. Leverington & J.D. Mann (2002), Freshwater outbursts to the oceans from glacial Lake Agassiz and their role in climate change during the last deglaciation. Quaternary Science Reviews 21 (8-9), 879-887.

Terwindt, J.H.J., J.D. De Jong & E. Van der Wilk (1963), Sediment movement and sediment properties in the tidal area of the Lower Rhine (Rotterdam Waterway). Verhandelingen KNGMG 21 (2), 243-258.

Thomas, E.R., E.W. Wolff, R. Mulvaney, J.P. Steffensen, S.J. Johnsen, C. Arrowsmith, J.W.C. White, B. Vaughn & T. Popp (2007), The 8.2 ka event from Greenland ice cores. Quaternary Science Reviews 26 (1-2), 70-81.

TNO (2009), DINOloket (Internet Portal for Geo-Information), http://www.dinoloket.nl/nl/DINOLoket.html.

Törnqvist, T.E. (1993), Fluvial sedimentary geology and chronology of the Holocene Rhine-Meuse delta, the Netherlands. Ph.D.-thesis, Utrecht University: 169 pp.

Törnqvist, T.E. (1998), Longitudinal profile evolution of the Rhine-Meuse system during the last deglaciation: interplay of climate change and glacio-eustasy? Terra Nova 10 (1), 11-15.

Törnqvist, T.E., H.J.T. Weerts & H.J.A. Berendsen (1994), Definition of two new members in the upper Kreftenheye and Twente Formations (Quaternary, the Netherlands): a final solution to persistent confusion? Geologie en Mijnbouw 72, 251-264.

Törnqvist, T.E., J. Wallinga & F.S. Busschers (2003), Timing of the last sequence boundary in a fluvial setting near the highstand shoreline-Insights from optical dating. Geology 31 (3), 279-282.

Törnqvist, T.E., A.F.M. De Jong, W.A. Oosterbaan & K. Van der Borg (1992), Accurate dating of organic deposits by AMS ^{14}C measurement of macrofossils. Radiocarbon 34 (3), 566-577.

Törnqvist, T.E., S.J. Bick, J.L. González, K. Van der Borg & A.F.M. De Jong (2004), Tracking the sea-level signature of the 8.2 ka cooling event: New constraints from the Mississippi Delta. Geophysical Research Letters 31, L23309.

Törnqvist, T.E., S.R. Wortman, Z.R.P. Mateo, G.A. Milne & J.B. Swenson (2006), Did the last sea level lowstand always lead to cross-shelf valley formation and source-to-sink sediment flux? Journal of Geophysical Research 111.

Toucanne, S., S. Zaragosi, J.F. Bourillet, M. Cremer, F. Eynaud, B. Van Vliet-Lanoë, A. Penaud, C. Fontanier, J.L. Turon, E. Cortijo & P.L. Gibbard (2009), Timing of massive `Fleuve Manche' discharges over the last 350 kyr: insights into the European ice-sheet oscillations and the European drainage network from MIS 10 to 2. Quaternary Science Reviews 28 (13-14), 1238-1256.

Twigt, D. & M. Blaas (2007), Storegga tsunami simulations. Report Z3929, WL-Delft Hydraulics: pp.

Uehara, K., J.D. Scourse, K.J. Horsburgh, K. Lambeck & A.P. Purcell (2006), Tidal evolution of the northwest European shelf areas from the Last Glacial Maximum to the present. Journal of Geophysical Research 111, C09025.

Vail, P.R. (1975), Eustatic cycles from seismic data for global stratigraphic analysis (abstract). American Association of Petroleum Geologists Bulletin 59, 2198-2199.

Vail, P.R., R.M.J. Mitchum & S.I. Thompson (1977), Seismic stratigraphy and global changes of sea level, part four: global cycles of relative changes of sea level. American Association of Petroleum Geologists Memoir 26, 83-98.

Van Balen, R.T., F. Van Bergen, C. De Leeuw, H. Pagnier, H. Simmelink, J.D. Van Wees & J.M. Verweij (2000), Modelling the hydrocarbon generation and migration in the West Netherlands Basin, the Netherlands. Netherlands Journal of Geosciences - Geologie en Mijnbouw 79 (1), 29-44.

Van de Meene, E.A. (1977), Toelichting bij de geologische kaart van Nederland 1:50.000, Blad Arnhem Oost (40 O). Rijks Geologische Dienst, Haarlem (with English summary).

Van de Meene, E.A. & W.H. Zagwijn (1978), Die Rheinläufe im deutsch-niederländischen Grenzgebiet seit der Saale-Kaltzeit. Überblick neuer geologischer und pollenanalytischer untersuchingen, 28, 345^359. Forthschr.Geol. Rheinl.Westfalen 28, 245-359.

Van de Plassche, O. (1982), Sea-level change and water-level movements in The Netherlands during the Holocene. Ph.D.-thesis, Vrije Universiteit, Amsterdam: 93 pp.

Van de Plassche, O. (1995), Evolution of the intra-coastal tidal range in the Rhine-Meuse delta and Flevo Lagoon, 5700-3000 yrs cal B.C. Marine Geology 124 (1-4), 113-128.

Van de Plassche, O. & T.B. Roep (1989), Sea-level changes in the Netherlands during the last 6500 years: basal peat vs. coastal barrier data. In: D.B. Scott, P.A. Pirazzoli and C.A. Honig, eds., Late Quaternary sea-level correlation and applications. Dordrecht: Kluwer, 41-56.

Van de Plassche, O., S.J.P. Bohncke, B. Makaske & J. van der Plicht (2005), Water-level changes in the Flevo area, central Netherlands (5300-1500 BC): implications for relative mean sea-level rise in the Western Netherlands. Quaternary International 133-134, 77-93.

Van den Berg, J.H., J.R. Boersma & A. Van Gelder (2007), Diagnostic sedimentary structures of the fluvial-tidal transition zone – Evidence from deposits of the Rhine and Meuse. Netherlands Journal of Geosciences - Geologie en Mijnbouw 86 (3), 287-306.

Van der Hammen, T., G.C. Maarleveld, J.C. Vogel & W.H. Zagwijn (1967), Stratigraphy, climatic succession and radiocarbon dating of the Last Glacial in the Netherlands. Geologie en Mijnbouw 46 (3), 79-95.

Van der Molen, J. (2002), The influence of tides, wind and waves on the net sand transport in the North Sea. Continental Shelf Research 22 (18-19), 2739-2762.

Van der Molen, J. & B. Van Dijck (2000), The evolution of the Dutch and Belgian coasts and the role of sand supply from the North Sea. Global and Planetary Change 27 (1-4), 223-244.

Van der Molen, J. & H.E. De Swart (2001a), Holocene tidal conditions and tide-induced sand transport in the southern North Sea. Journal of Geophysical Research C 106, C5, 9339-9362.

Van der Molen, J. & H.E. De Swart (2001b), Holocene wave conditions and wave-induced sand transport in the southern North Sea. Continental Shelf Research 21 (16-17), 1723-1749.

Van der Spek, A.J.F. & D.J. Beets (1992), Mid-Holocene evolution of a tidal basin in the western Netherlands: a model for future changes in the northern Netherlands under conditions of accelerated sea-level rise? Sedimentary Geology 80 (3-4), 185-197.

Van der Spek, A.J.F., J. Cleveringa & S. Van Heteren, 2007. From transgression to regression: coastal evolution near The Hague, The Netherlands, around 5000 BP. In: N.C. Kraus and J. Dean Rosati (Editors), Coastal sediments '07, Proceedings of the 6th International Symposium on Coastal Engineering and Science of Coastal Sediments Processes, New Orleans, Louisiana: 1129-1141.

Van der Valk, L. (1996a), Coastal barrier deposits in the central Dutch coastal plain. In: D.J. Beets, M.M. Fischer and W. De Gans, eds., Coastal studies on the Holocene of the Netherlands Med. Rijks. Geol. Dienst. Haarlem: Rijks Geologische Dienst, 133-200.

Van der Valk, L. (1996b), Geology and sedimentology of Late-Atlantic sandy, wave-dominated deposits near The Hague (South-Holland, the Netherlands): a reconstruction of an early prograding coastal sequence. In: D.J. Beets, M.M. Fischer and W. De Gans, eds., Coastal studies on the Holocene of the Netherlands Med. Rijks. Geol. Dienst. Haarlem: Rijks Geologische Dienst, 201-228.

Van der Woude, J.D. (1983), Holocene paleoenvironmental evolution of a perimarine fluviatile area - Geology and paleobotany of the area surrounding the archeological excavation at the Hazendonk river dune (western Netherlands). Analecta Praehistorica Leidensia XVI, 1-124. Earlier appeared as Ph.D.-thesis (1981), Vrije Universiteit, Amsterdam.

Van Dijk, G.J., H.J.A. Berendsen & W. Roeleveld (1991), Holocene water level development in the Netherlands' river area; implications for sea-level reconstruction. Geologie en Mijnbouw 70 (4), 311-326.

Van Geel, B., S.J.P. Bohncke & H. Dee (1980/1981), A palaeoecological study of an upper late glacial and holocene sequence from "de borchert", The Netherlands. Review of Palaeobotany and Palynology 31, 367-392.

Van Heteren, S. & A.J.F. Van der Spek (2008), Waar is de delta van de Oude Rijn? Grondboor en Hamer 3/4, 72-76 (in Dutch).

Van Heteren, S., A.J.F. Van der Spek & T.A.M. De Groot (2002), Architecture of a preserved Holocene tidal complex offshore the Rhine-Meuse mouth, the Netherlands. NITG 01-27-A, Netherlands Institute of Applied Geoscience TNO - National Geological Survey: 40 pp.

Van Huissteden, J. & C. Kasse (2001), Detection of rapid climate change in Last Glacial fluvial successions in The Netherlands. Global and Planetary Change 28 (1-4), 319-339.

Van Huissteden, J., J.C.G. Schwan & M.D. Bateman (2001), Environmental conditions and paleowind directions at the end of the Weichselian Late Pleniglacial recorded in aeolian sediments and geomorphology (Twente, Eastern Netherlands). Netherlands Journal of Geosciences - Geologie en Mijnbouw 80 (2), 1-18.

Van Rummelen, F.F.F.E. (1970), Toelichting bij de geologische kaart van Nederland 1:50.000, Blad Schouwen-Duiveland. Rijks Geologische Dienst, Haarlem (with English summary): 116 pp.

Van Staalduinen, C.J. (1979), Toelichting bij de geologische kaart van Nederland 1:50.000, Blad Rotterdam West (37 W). Rijks Geologische Dienst, Haarlem (with English summary): 140 pp.

Van Straaten, L.M.J.U. (1954), Radiocarbon datings and changes of sea level at Velzen. Geologie en Mijnbouw 16, 247-253.

Van Straaten, L.M.J.U. (1956), Composition of shell beds formed in tidal flat environment in the Netherlands and in the Bay of Arcachon (France). Geologie en Mijnbouw 18, 209-226.

Van Straaten, L.M.J.U. (1965), Coastal barrier deposits in South and North Holland - in particular in the area around Scheveningen and IJmuiden. Meded. Geol. St. Nieuwe Ser. 17, 41-75.

Van Veen, J., 1936. Transport des sables par des courants dans les cours inférieurs des rivières, dans les estuaires néerlandais et dans la Mer du Nord, VI Assemblé générale de l'Ass. Int. d'hydrologie Scientifique, Edinburgh.

Van Veen, J., A.J.F. Van der Spek, M.J. Stive & T. Zitman (2005), Ebb and flood channel systems in the Netherlands tidal waters. Journal of coastal research 21 (6), 1107-1120.

Vandenberghe, J. (1985), Paleoenvironment and stratigraphy during the last glacial in the Belgian-Dutch border region. Quaternary Research 24 (1), 23-38.

Vandenberghe, J. (1995), Timescales, climate and river development. Quaternary Science Reviews 14 (6), 631-638.

Vatvani, A. (2007), Storegga tsunami simulations for the Dutch coasts. In: WL-Delft Hydraulics, R&D Annual Report 2006; Sect. Hydrodynamics, 8-22. pp.

Veldkamp, M.A. (1996), Pollenanalytische en C14-dateringen van de boring Maassluis 37B/226. Palaeobotanie Kenozoïcum 1255A, Rijks Geologische Dienst, Haarlem: 3 pp.

Verbraeck, A. (1970), Toelichting bij de geologische kaart van Nederland 1:50.000, Blad Gorinchem Oost (38 O). Rijks Geologische Dienst, Haarlem (with English summary).

Verbraeck, A. (1984), Toelichting bij de geologische kaart van Nederland 1:50.000, Blad Tiel West (39 W) en Blad Tiel Oost (39 O). Rijks Geologische Dienst, Haarlem (with English summary): 335 pp.

Verbraeck, A. & J.H. Bisschops (1971), Toelichting bij de geologische kaart van Nederland 1:50.000, Blad Willemstad Oost (43 O). Rijks Geologische Dienst, Haarlem (with English summary): 112 pp.

Vermeer-Louman, G.G. (1934), Pollen-analytisch onderzoek van den West-Nederlandschen bodem. Ph.D.-thesis, Universiteit van Amsterdam, Amsterdam: 184 pp.

Vink, A., H. Steffen, L. Reinhardt & G. Kaufmann (2007), Holocene relative sea-level change, isostatic subsidence and the radial viscosity structure of the mantle of northwest Europe (Belgium, the Netherlands, Germany, southern North Sea). Quaternary Science Reviews 26 (25-28), 3249-3275.

Vis, G.-J., C. Kasse & J. Vandenberghe (2008), Late Pleistocene and Holocene palaeogeography of the Lower Tagus Valley (Portugal): effects of relative sea level, valley morphology and sediment supply. Quaternary Science Reviews 27 (17-18), 1682-1709.

Von Grafenstein, U., H. Erlenkeuser, J. Müller, J. Jouzel & S. Johnsen (1998), The cold event 8200 years ago documented in oxygen isotope records of precipitation in Europa and Greenland. Climate Dynamics 14, 73-81.

Von Grafenstein, U., H. Erlenkeuser, A. Brauer, J. Jouzel & S.J. Johnsen (1999), A mid-European decadal isotope-climate record from 15,500 to 5000 years BP. Science 284 (5420), 1654-1657.

Vos, P.C. & R.M. Van Heeringen (1997), Holocene geology and occupation history of the Province of Zeeland. In: M.M. Fischer, ed., Holocene evolution of Zeeland (SW Netherlands) Mededelingen Rijks Geologische Dienst. Haarlem: Rijks Geologische Dienst, 5-110.

Waelbroeck, C., L. Labeyrie, E. Michel, J.C. Duplessy, J.F. McManus, K. Lambeck, E. Balbon & M. Labracherie (2002), Sea-level and deep water temperature changes derived from benthic foraminifera isotopic records. Quaternary Science Reviews 21 (1-3), 295-305.

Wallinga, J. (2002), Optically stimulated luminescence dating of fluvial deposits: a review. Boreas 31 (4), 303 - 322.

Wallinga, J., T.E. Törnqvist, F.S. Busschers & H.J.T. Weerts (2004), Allogenic forcing of the late Quaternary Rhine-Meuse fluvial record: the interplay of sea-level change, climate change and crustal movements. Basin Research 16, 535-547.

Weerts, H.J.T. (1996), Complex confining layers. Architecture and hydraulic properties of Holocene and Late Weichselian deposits in the fluvial Rhine-Meuse delta, the Netherlands. Ph.D.-thesis, Utrecht University: 189 pp.

Weninger, B., R. Schulting, M. Bradtmöller, L. Clare, M. Collard, K. Edinborough, J. Hilpert, O. Jöris, M.J.L.T. Niekus, E.J. Rohling & B. Wagner (2008), The catastrophic final flooding of Doggerland by the Storegga Slide tsunami. Documenta Praehistorica XXXV (Neolithic studies 15), 1-24.

Westerhoff, W.E., T.E. Wong & E.F.J. De Mulder (2003), Opbouw van de ondergrond - Opbouw van het Neogeen en Kwartair. In: E.F.J. De Mulder, M.C. Geluk, I.L. Ritsema, W.E. Westerhoff and T.E. Wong, eds., De ondergrond van Nederland. Groningen/Houten: Wolters Noordhoff, 295-352.

Wiersma, A.P. (2008), Character and causes of the 8.2 ka climate event - comparing coupled climate model results and palaeoclimate reconstructions. Ph.D.-thesis, Faculty of Earth and Life Sciences, Vrije Universiteit, Amsterdam: 159 pp.

Wiersma, A.P., H. Renssen, H. Goosse & T. Fichefet (2006), Evaluation of different freshwater forcing scenarios for the 8.2 ka BP event in a coupled climate model. Climate Dynamics 27 (7-8), 831-849.

Woldstedt, P. (1954), Das Eiszeitalter, Grundlinien einer Geologie des Quartärs. Stuttgart.

Zagwijn, W.H. (1955), Palaeobotanisch onderzoek van een viertal veenprofielen van Voorne-Putten. Palaeobotanie Kenozoïcum 109, Rijks Geologische Dienst: 19 pp.

Zagwijn, W.H. (1974), The palaeogeographic evolution of The Netherlands during the Quaternary. Geologie en Mijnbouw 53 (6), 369-385.

Ziegler, P.A. (1994), Cenozoic rift system of western and central Europe: an overview. Geologie en Mijnbouw 73, 99-127.

Zonneveld, I.S. (1960), De Brabantse Biesbosch. Een studie van bodem en vegetatie van een zoetwatergetijdendelta. Ph.D.-thesis, Wageningen Universiteit, Wageningen: 210 pp.

Appendix 1 - Pollen, diatom and radiocarbon-dating reports

Report number	Author(s)	Year	Content[1]	Code in chapter 2
Reports TNO Built Environment and Geosciences				
NITG 04-U-198/B	De Wolf, H.	2004	D	H-1
2006-U-R0042/B	De Wolf, H.	2006	D	H-2
2006-U-R0151/B	De Wolf, H., Cleveringa, P.	2006	D	H-3
2007-U-R1215/A	Bunnik, F.P.M., Cremer, H.	2007	D/P	H-4
2008-U-R0124/B	Cremer, H.	2008	D	H-5
2008-U-R0196/A	Bunnik, F.P.M.	2008	P	H-6
Paleobotany Reports Geological Survey of The Netherlands				
109	Zagwijn, W.H.	1955	C/P	H-7
535a	De Jong, J.	1970	C	H-8
702/702a	De Jong, J.	1973ab	C	H-9
800	De Jong, J.	1977	C	H-10
838a	De Jong, J.	1979bc	C	H-11
855a	De Jong, J.	1979a	C	H-12
934	De Jong, J.	1984	C	H-13
975	De Jong, J.	1985	C	H-14
1003a	De Jong, J.	1987a	C	H-17
1004a	De Jong, J.	1987a	C	H-19
1061	De Jong, J.	1988	C	H-21
1075	De Jong, J.	1989b	P	H-22
1086	De Jong, J.	1989a	C	H-23
1143	De Jong, J.	1992	P	H-24
1255A	Veldkamp, M.A.	1996	C/P	H-25
Diatom Reports Geological Survey of The Netherlands				
420	De Wolf, H.	1979	D	H-26
424	De Wolf, H.	1981a	D	H-27
425	De Wolf, H.	1981c	D	H-28
426	De Wolf, H.	1981b	D	H-29
480	De Wolf, H.	1986a	D	H-30
481	De Wolf, H.	1986b	D	H-31
513	De Wolf, H.	1989a	D	H-32
516	De Wolf, H.	1990	D	H-33
517	De Wolf, H.	1989b	D	H-34

1 - D = Diatom analysis, P = Pollen analysis, C = Radiocarbon date

Appendix 2 - Details of radiocarbon dates

Nr. (Add. 1)	Lab. nr.[1]	14C age (yr)	1σ (yr)	δ13C (p.mil)	Cal. Age (2σ, yr BP)[2]	Coord. (X-Y)[3]	Core or sample name	Depth sample top (m O.D.)[4]	Depth sample base (m O.D.)	Dated or parent material	Reference
1	UtC-13825	6800	80		7826-7509	100045-420826	02.05.001	-9.62	-9.65	Terr. botan. macrofos. (base peat)	Hijma et al., 2009
2	UtC-13818	6229	47		7258-7005	99861-421423	02.05.002	-10.05	-10.10	Terr. botan. macrofos. (silty gyttja)	Hijma et al., 2009
3	UtC-13819	6740	50		7678-7510	99861-421423	02.05.002	-11.51	-11.51	Terr. botan. macrofos. (silty gyttja)	Hijma et al., 2009
4	UtC-13820	7000	50		7938-7711	99861-421423	02.05.002	-12.10	-12.10	Terr. botan. macrofos. (silty gyttja)	Hijma et al., 2009
5	UtC-13821	7120	80		8160-7787	99861-421423	02.05.002	-12.20	-12.22	Terr. botan. macrofos. (silty gyttja)	Hijma et al., 2009
6	UtC-13822	7050	50		7972-7760	99861-421423	02.05.002	-12.20	-12.22	Terr. botan. macrofos. (silty gyttja)	Hijma et al., 2009
7	UtC-13823	7050	50		7981-7787	99861-421423	02.05.002	-12.40	-12.42	Terr. botan. macrofos. (fen-wood peat)	Hijma et al., 2009
8	UtC-13824	7143	49		8045-7850	99861-421423	02.05.002	-12.65	-12.65	Terr. botan. macrofos. (wood peat)	Hijma et al., 2009
9	UtC-13817	7390	60		8347-8045	99861-421423	02.05.002	-12.85	-12.88	Terr. botan. macrofos. (wood peat)	Hijma et al., 2009
10	UtC-13816	7670	60		8582-8382	99861-421423	02.05.002	-13.10	-13.10	Wood	Hijma et al., 2009
11	GrN-10862	3770	60		4406-3975	100459-428793	Rijsoord I	-4.14	-4.18	Peat	Van Dijk, unpublished
12	GrN-10863	3730	70		4349-3880	100459-428793	Rijsoord II	-4.39	-4.43	Peat	Van Dijk, unpublished
13	GrN-10864	4280	70		5044-4584	100459-428793	Rijsoord III	-5.14	-5.18	Peat	Van Dijk, unpublished
14	GrN-10865	5120	60		5993-5725	100459-428793	Rijsoord IV	-6.98	-7.03	Gyttja on clay	Van Dijk, unpublished
15	GrN-10866	6700	70		7673-7442	100459-428793	Rijsoord V	-11.08	-11.13	Alnus fruit	Van Dijk, unpublished
16	UtC-15340	7420	70	-27.4	8382-8049	99670-428378	07.09.007	-13.91	-13.96	(base fen-wood peat)	Hijma et al., 2009
17	GrN-2829	5885	70		6885-6504	99625-431100	B37H0274	-7.35	-7.45	Wood peat	De Jong, 1989b
18	GrN-2354	6555	100		7589-7264	99625-431100	B37H0274	-9.53	-9.60	Gyttja	De Jong, 1989b
19	GrN-2832	7240	90		8303-7870	99625-431100	B37H0274	-12.27	-12.34	Gyttja	De Jong, 1989b
20	UtC-15338	7400	60	-26.3	8363-8047	99632-431481	07.09.016	-14.05	-14.10	Terr. botan. macrofos. (wood peat)	Hijma et al., 2009
21	GrN-8433	3510	90		4078-3565	98475-433775	Bolnes 6	-2.35	-2.38	Wood peat	Van de Plassche, 1982
22	GrN-8434	3820	90		4509-3933	98475-433775	Bolnes 7	-2.60	-2.62	Wood peat	Van de Plassche, 1982
23	GrN-8921	5280	60		6208-5921	98450-433300	Bolnes 17	-6.83	-6.86	Peat	Van de Plassche, 1982
24	GrN-8931	6320	35		7316-7168	98450-433450	Bolnes 8	-7.80	-7.83	Wood peat	Van de Plassche, 1982
25	GrN-8916	6245	35		7260-7022	98450-433300	Bolnes 14	-7.94	-7.98	Wood peat	Van de Plassche, 1982
26	GrN-8917	6325	45		7414-7163	98450-433300	Bolnes 15	-8.34	-8.36	Peat	Van de Plassche, 1982
27	GrN-8930	6550	40		7564-7417	98450-433450	Bolnes 9	-8.51	-8.54	Wood peat	Van de Plassche, 1982
28	GrN-8929	6495	40		7481-7318	98450-433450	Bolnes 10.1	-9.04	-9.06	Wood peat	Van de Plassche, 1982
29	GrN-8928	6670	35		7606-7476	98450-433450	Bolnes 10.2	-9.06	-9.10	Wood peat	Van de Plassche, 1982
30	GrN-8927	6670	70		7656-7434	98450-433450	Bolnes 11	-9.55	-9.57	Wood peat	Van de Plassche, 1982
31	UtC-14226	6470	70	-25.1	7507-7260	100560-442745	B38A0349	-12.00	-12.16	Terr. botan. macrofos. (base peat)	Hijma et al., 2009
32	UtC-14227	6620	70	-26.0	7616-7421	100560-442745	B38A0349	-12.55	-12.63	Terr. botan. macrofos. (top peat)	Hijma et al., 2009
33	UtC-14228	6900	80	-26.6	7928-7594	100560-442745	B38A0349	-12.80	-12.90	Terr. botan. macrofos. (base peat)	Hijma et al., 2009

Nr. (Add. 1)	Lab. nr. [1]	¹⁴C age (yr)	1σ (yr)	δ¹³C (p.mil)	Cal. Age (2σ, yr BP) [2]	Coord. (X-Y) [3]	Core or sample name	Depth sample top (m O.D.) [4]	Depth sample base (m O.D.)	Dated or parent material	Reference
34	UtC-14229	7490	80	-27.9	8432-8066	100560-442745	B38A0349	-14.68	-14.73	Terr. botan. macrofos. (top peat)	Hijma et al., 2009
35	UtC-14230	8330	70	-31.0	9486-9129	100560-442745	B38A0349	-15.10	-15.17	Terr. botan. macrofos. (gyttja)	Hijma et al., 2009
36	UtC-14231	8250	70	-27.1	9423-9031	100560-442745	B38A0349	-15.10	-15.17	Terr. botan. macrofos. (gyttja)	Hijma et al., 2009
37	UtC-14232	8380	70	-28.3	9531-9143	100560-442745	B38A0349	-15.10	-15.17	Terr. botan. macrofos. (gyttja)	Hijma et al., 2009
38	GrN-8656	5615	45		6484-6305	101610-446440	446-101-0021	-7.71	-7.74	Top clayey gyttja	De Jong, 1979bc
39	GrN-8732	5860	40		6780-6561	101610-446440	446-101-0021	-8.22	-8.25	Base fen peat	De Jong, 1979bc
40	UtC-14949	6441	40	-26.8	7428-7279	103534-446343	06.09.011	-9.06	-9.07	Terr. botan. macrofos. (fen peat)	Hijma et al., 2009
41	UtC-14951	6560	49	-25.6	7569-7340	103534-446343	06.09.011	-9.13	-9.16	Terr. botan. macrofos. (fen peat)	Hijma et al., 2009
42	UtC-14957	7909	43	-24.0	8977-8598	103479-446968	06.09.002	-16.25	-16.25	Charcoal	Hijma et al., 2009
43	UtC-15284	5768	45	-7.4	6288-6056*	103523-447586	B38A1846 (Waddinxveen)	-9.60	-9.60	Shell (*Cerastoderma lamarcki*)	Hijma et al., 2009
44	UtC-15285	5950	60	-6.0	6507-6250*	103523-447586	B38A1846 (Waddinxveen)	-9.25	-9.27	Shell (*Cerastoderma lamarcki*)	Hijma et al., 2009
45	UtC-15286	5972	44	-4.9	6485-6282*	103523-447586	B38A1846 (Waddinxveen)	-9.18	-9.20	Shell (*Cerastoderma lamarcki*)	Hijma et al., 2009
46	UtC-15287	5899	42	-5.9	6406-6220*	103523-447586	B38A1846 (Waddinxveen)	-8.38	-8.38	Shell (*Cerastoderma lamarcki*)	Hijma et al., 2009
47	UtC-15341	6450	50	-30.5	7435-7269	103523-447586	B38A1846 (Waddinxveen)	-10.50	-10.51	Terr. botan. macrofos. (base fen peat)	Hijma et al., 2009
48	UtC-15334	5390	70	-30.1	6300-5995	103792-452948	B31C1166 (Boskoop)	-7.70	-7.71	Terr. botan. macrofos. (top fen peat)	Hijma et al., 2009
49	UtC-15335	5800	70	-32.0	6750-6440	103792-452948	B31C1166 (Boskoop)	-7.90	-7.91	Terr. botan. macrofos. (base fen peat)	Hijma et al., 2009
50	GrN-8914	7035	45		7960-7759	104250-457750	Alphen a/d Rijn	-10.64	-10.65	Peat	Van de Plassche, 1982
51	GrN-15934	3980	40		4567-4296	93650-429360	B37H0350 (Smitshoek)	-4.38	-4.45	Peat with gyttja	De Jong, 1988
52	GrN-2823	5770	75		6737-6408	92310-432625	B37H0273	-7.73	-7.80	Gyttja	De Jong, 1989b
53	GrN-2949	7410	65		8375-8048	92310-432625	B37H0273	-12.85	-12.95	*Phragmites* peat	De Jong, 1989b
54	GrN-2347	7900	75		8993-8559	92310-432625	B37H0273	-13.42	-13.48	*Phragmites* peat	De Jong, 1989b
55	GrN-2177	8130	70		9299-8779	92310-432625	B37H0273	-15.93	-15.96	Clayey *Phragmites* peat	De Jong, 1989b
56	UtC-15339	7710	70	-26.8	8608-8385	92615-436111	07.09.201	-15.93	-15.96	*Linum usitatissimum* (top fen peat)	Hijma et al., 2009
57	UtC-14941	7211	40	-26.1	8159-7955	91671-437648	Construction Pit Rdames-M12A	-14.30	-14.30	Terr. botan. macrofos. (base peat)	Hijma et al., 2009
58	UtC-14940	7486	41	-25.4	8382-8198	91671-437648	Construction Pit Rdames-M11B	-16.30	-16.30	Terr. botan. macrofos. (top peat)	Hijma et al., 2009
59	UtC-14939	7817	43	-26.4	8723-8475	91671-437648	Construction Pit Rdames-M10B	-16.60	-16.60	Terr. botan. macrofos. (base peat)	Hijma et al., 2009
60	UtC-14942	8243	43	-29.8	9401-9033	91671-437648	Construction Pit Rdames-M13	-17.50	-17.50	Terr. botan. macrofos. (org. mat. in x-bedding)	Hijma et al., 2009
61	GrA-30061	5625	45		6490-6309	91858-437635	Rotterdam-Stationsplein	-7.38	-7.38	Peat	BOOR, internal reports

Nr. (Add. 1)	Lab. nr.[1]	[14]C age (yr)	1σ (yr)	δ^{13}C (p.mil)	Cal. Age (2σ, yr BP)[2]	Coord. (X-Y)[3]	Core or sample name	Depth sample top (m O.D.)[4]	Depth sample base (m O.D.)	Dated or parent material	Reference
62	GrN-28993	5420	35		6295-6123	91508-437669	Rdam CS-1	-10.28	-10.28	Peat	Guiran and Brinkkemper, 2007
63	GrN-28991	4730	40		5585-5325	91473-437657	Rdam CS-4	-7.16	-7.16	Peat	Guiran and Brinkkemper, 2007
64	GrA-32037	7180	45		8156-7882	91078-438453	2e Pollenbak BOOR Blijdorp	-13.39	-13.39	Top clayey peat	BOOR, internal reports
65	GrA-32101	7160	45		8150-7868	91078-438453	2e Pollenbak BOOR Blijdorp	-13.61	-13.61	Bottom clayey peat	BOOR, internal reports
66	GrN-30066	7560	40		8428-8224	91058-438530	1e Pollenbak BOOR Blijdorp	-15.17	-15.17	Peat/Gytja	BOOR, internal reports
67	GrN-30067	7560	40		8428-8224	91058-438530	1e Pollenbak BOOR Blijdorp	-15.21	-15.21	Peat/Gytja	BOOR, internal reports
68	GrN-30068	7740	40		8591-8431	91058-438530	1e Pollenbak BOOR Blijdorp	-15.26	-15.26	Peat/Gytja	BOOR, internal reports
69	UtC-14953	7610	60	-28.6	8544-8326	91087-438458	Construction Pit Blijdorp-4C	-15.05	-15.09	Terr. botan. macrofos. (peat)	Hijma et al., 2009
70	UtC-14952	7730	42	-28.0	8589-8425	91087-438458	Construction Pit Blijdorp-4AB	-15.12	-15.14	Terr. botan. macrofos. (peat)	Hijma et al., 2009
71	UtC-14954	8210	50	-27.8	9395-9020	91087-438458	Construction Pit Blijdorp-5A	-16.50	-16.50	Terr. botan. macrofos. (strongly humic clay)	Hijma et al., 2009
72	UtC-14955	8300	50	-28.6	9441-9132	91064-438522	Construction Pit Blijdorp-6	-19.00	-19.00	Terr. botan. Macrofos. (org. mat in x-bedding)	Hijma et al., 2009
73	GrN-30404	11350	80		13368-13090	90897-439042	Ring 560 westtube	-23.00	-29.00	*Pinus*	Guiran, 2006
74	GrN-30405	11320	80		13349-13062	90897-439042	Ring 560 westtube	-23.00	-29.00	*Pinus*	Guiran, 2006
75	GrN-30406	11380	80		13390-13109	90897-439042	Ring 560 westtube	-23.00	-29.00	*Pinus*	Guiran, 2006
76	GrN-11311	5915	45		6877-6642	94270-446860	446-094-0015	-11.78	-11.80	Fen peat	De Jong, 1984
77	GrN-11312	7225	45		8161-7965	94270-446860	446-094-0015	-12.76	-12.79	Fen peat	De Jong, 1984
78	GrN-11313	8490	80		9606-9296	94270-446860	446-094-0015	-15.55	-15.58	Humic clay	De Jong, 1984
79	GrN-8915	7020	70		7965-7695	99475-457375	Hazerswoude	-11.50	-11.51	*Phragmites* peat	Van de Plassche, 1982
80	GrN-8084	3435	35		3829-3590	97990-459730	N. Groenendijk I	-3.32	-3.35	Wood peat	De Jong, 1977
81	GrN-8085	3730	60		4283-3898	97990-459730	N. Groenendijk II	-4.13	-4.15	*Phragmites* peat	De Jong, 1977
82	GrN-8086	4250	60		4967-4584	97990-459730	N. Groenendijk III	-4.41	-4.43	*Phragmites* peat	De Jong, 1977
83	GrN-8087	4350	60		5271-4827	97990-459730	N. Groenendijk IV	-4.73	-4.75	*Phragmites* peat	De Jong, 1977
84	GrN-8088	4780	60		5609-5324	97990-459730	N. Groenendijk V	-4.98	-5.00	*Phragmites* peat	De Jong, 1977
85	GrN-8093	4405	40		5271-4860	98150-460450	Groenendijk	-3.62	-3.65	Clayey peat	De Jong, 1977
86	UtC-14956	6877	42	-29.0	7821-7616	81167-412558	B43E0245	-11.07	-11.08	Terr. botan. macrofos.	Hijma et al., 2009
87	GrN-5918	5435	60		6393-6005	82125-418600	Zuid-Beijerland	-5.05	-5.19	Gytja	De Jong, 1970
88	GrN-289	3100	200		3822-2793	82025-426850	Hekelingen II	-2.87	-2.91	Fen peat	Zagwijn, 1955
89	GrN-296	3325	110		3845-3346	82025-426850	Hekelingen II	-3.29	-3.32	Clay peat	Zagwijn, 1955
90	GrN-286	3820	180		4813-3724	82025-426850	Hekelingen II	-3.87	-3.91	Wood peat	Zagwijn, 1955
91	GrN-2825	5740	65		6715-6400	86300-430800	B37G0309	-7.82	-7.90	Fen peat	De Jong, 1989b
92	GrN-2180	7940	75		8997-8601	86300-430800	B37G0309	-17.42	-17.48	Base wood peat	De Jong, 1989b
93	UtC-14224	7880	70	-26.2	8982-8548	86218-430764	B37G0548	-16.71	-16.89	Terr. botan. macrofos. (base wood peat)	Busschers et al., 2007
94	UtC-11763	8420	80		9545-9150	85686-439887	B37E0549	-21.61	-21.61	Terr. botan. macrofos. (humic clay)	Hijma et al., 2009
95	UtC-11764	9200	60		10516-10237	85686-439887	B37E0549	-24.86	-24.86	Terr. botan. macrofos. (humic clay)	Hijma et al., 2009

Nr. (Add. 1)	Lab. nr.[1]	^{14}C age (yr)	1σ (yr)	δ^{13}C (p.mil)	Cal. Age (2σ, yr BP)[2]	Coord. (X-Y)[3]	Core or sample name	Depth sample top (m O.D.)[4]	Depth sample base (m O.D.)	Dated or parent material	Reference
96	UtC-15342	7290	60	-30.6	8282-7971	85205-440796	07.09.033	-15.03	-15.07	Terr. botan. macrofos. (gyttja)	Hijma et al., 2009
97	UtC-15405	7030	130	-23.1	8156-7616	85205-440796	07.09.033	-15.46	-15.57	Terr. botan. macrofos. (gyttja)	Hijma et al., 2009
98	UtC-10757	8220	60		9401-9021	86817-442257	B37E0586	-16.30	-16.30	Terr. botan. macrofos. (top Wijchen Member)	Busschers et al., 2005
99	GrN-13471	4395	40		5262-4855	83710-441165	B37E0562 (Schipluiden III)	-4.99	-5.03	Base fen peat	De Jong, 1987a, 1991a
100	GrN-13472	4965	40		5875-5601	83710-441165	B37E0562 (Schipluiden III)	-6.22	-6.26	Fen peat	De Jong, 1987a, 1991a
101	GrN-13473	5730	40		6638-6414	83710-441165	B37E0562 (Schipluiden III)	-7.66	-7.70	Fen peat	De Jong, 1987a, 1991a
102	GrN-13474	6335	45		7415-7166	83710-441165	B37E0562 (Schipluiden III)	-11.15	-11.24	Central part wood peat layer	De Jong, 1987a, 1991a
103	GrN-14445	7265	45		8176-7998	83710-441165	B37E0562 (Schipluiden III)	-14.14	-14.18	Clayey fen peat	De Jong, 1987a, 1991a
104	GrN-6494	4290	60		5042-4645	81775-443775	Schipluiden I	-4.12	-4.15	Top fen peat	De Jong, 1973ab
105	GrN-6495	4685	60		5583-5310	81775-443775	Schipluiden I	-4.92	-4.94	Top fen peat	De Jong, 1973ab
106	GrN-6496	4995	60		5894-5609	81775-443775	Schipluiden I	-5.33	-5.35	Fen Peat	De Jong, 1973ab
107	GrN-6497	5470	60		6405-6061	81775-443775	Schipluiden I	-6.40	-6.43	Top fen peat	De Jong, 1973ab
108	GrN-14443	4270	60		5033-4618	83445-444715	B37E570	-4.71	-4.74	Fen peat	De Jong, 1987b, 1991b
109	GrN-14444	4710	40		5582-5321	83445-444715	B37E570	-6.77	-6.80	Fen peat	De Jong, 1987b, 1991b
110	GrN-13478	6040	45		7004-6749	83445-444715	B37E570	-8.84	-8.88	Fen peat	De Jong, 1987b, 1991b
111	GrN-13479	8250	50		9409-9032	83445-444715	B37E570	-18.44	-18.48	Peat	De Jong, 1987b, 1991b
112	GrN-12847	4580	35		5448-5057	82200-449500	Rijswijk Plaspoelpolder	-3.93	-3.95	Base fen peat	De Jong, 1985,1986
113	GrN-12846	5350	80		6290-5942	82200-449500	Rijswijk Plaspoelpolder	-5.05	-5.05	*Scrobicularia plana* (in viva, doublet)	De Jong, 1985,1986
114	GrN-12848	5610	70		6556-6283	82200-449500	Rijswijk Plaspoelpolder	-5.45	-5.45	*Macoma balthica* (hinged, not in viva)	De Jong, 1985,1986
115	GrN-12849	5560	60		6475-6221	82200-449500	Rijswijk Plaspoelpolder	-5.45	-5.45	*Mac. Balt., Zirfea crispata* (not in viva)	De Jong, 1985,1986
116	GrN-13490	5390	80		6293-6001	82200-449500	Rijswijk Plaspoelpolder	-7.50	-7.50	*Macoma Balthica* (hinged, not in viva)	De Jong, 1985,1986
117	UtC-9900	5834	40		6345-6170*	85230-450623	B30G0862	-5.06	-5.06	*Scrobicularia plana* (transported, doublet)	Cleveringa, 2000
118	UtC-9899	6089	36		6622-6415*	85230-450623	B30G0862	-7.79	-7.79	*Scrobicularia plana* (transported, doublet)	Cleveringa, 2000
119	UtC-9894	6205	47		6773-6515*	84963-450825	B30G0861	-9.35	-9.35	*Scrobicularia plana* (transported, single)	Cleveringa, 2000
120	UtC-9892	6327	44		6910-6668*	84860-450974	B30G0860	-10.00	-10.00	*Scrobicularia plana* (in viva, doublet)	Cleveringa, 2000
121	GrN-2268	5890	80		6903-6497	88400-452150	Quarry Nootdorp	-8.05	-8.05	Peat	Zagwijn, 1965
122	GrN-9428	4400	40		5270-4857	89135-454475	B30G0627	-5.02	-5.04	Fen peat	De Jong, 1979a
123	GrN-9429	5045	40		5905-5663	89135-454475	B30G0627	-5.96	-5.98	Gytja with many *Phragmites* fragments	De Jong, 1979a

Appendix 2 (continued)

Nr. (Add. 1)	Lab. nr.[1]	14C age (yr)	1σ (yr)	δ13C (p.mil)	Cal. Age (2σ, yr BP)[2]	Coord. (X-Y)[3]	Core or sample name	Depth sample top (m O.D.)[4]	Depth sample base (m O.D.)	Dated or parent material	Reference
124	GrN-9807	5625	45		6490-6309	89135-454475	B30G0627	-6.97	-6.99	Fen peat	De Jong, 1979a
125	GrN-9808	6345	40		7415-7170	89135-454475	B30G0627	-11.27	-11.29	Gytja with wood and Phragmites remains	De Jong, 1979a
126	UtC-14456	5570	60		6160-5839*	91762-457067	B30H0369	-6.10	-6.10	Scrobicularia plana (one valve)	Hijma et al., 2009
127	UtC-14455	5630	60		6178-5899*	91762-457067	B30H0369	-6.22	-6.22	Scrobicularia plana (one valve)	Hijma et al., 2009
128	UtC-14454	5500	90		6114-5657*	91762-457067	B30H0369	-6.67	-6.67	Scrobicularia plana (doublet)	Hijma et al., 2009
129	UtC-14453	5866	60		6415-6167*	91762-457067	B30H0369	-7.07	-7.07	Scrobicularia plana (one valve)	Hijma et al., 2009
130	UtC-14452	5935	56		6481-6244*	91762-457067	B30H0369	-7.45	-7.45	Scrobicularia plana (doublet)	Hijma et al., 2009
131	UtC-14451	5711	69		6268-5949*	91762-457067	B30H0369	-8.12	-8.12	Cerastastoderma doublet	Hijma et al., 2009
132	UtC-14458	6030	60		7154-6698	91762-457067	B30H0369	-9.36	-9.36	Fen peat	Hijma et al., 2009
133	UtC-14457	6210	60		7258-6960	91762-457067	B30H0369	-9.60	-9.60	Fen peat	Hijma et al., 2009
134	UtC-15536	5800	50	-24.7	6731-6488	94862-459157	07.09.013	-9.41	-9.51	Fen peat	Hijma et al., 2009
135	UtC-15337	6910	60	-25.6	7922-7622	94862-459157	07.09.013	-12.46	-12.51	Leaves (top basal peat)	Hijma et al., 2009
136	UtC-14221	7090	90	-29.3	8154-7698	95193-462131	B30H0277 (NM-1)	-12.35	-12.66	Terr. botan. macrofos. (base peat)	Hijma et al., 2009
137	UtC-14222	6840	70	-29.9	7830-7575	95752-462491	B30H0276 (NM-2)	-12.49	-12.84	Terr. botan. macrofos. (base peat)	Hijma et al., 2009
138	UtC-14223	6840	60	-29.1	7818-7578	96800-462988	B30F0518 (NM-10)	-11.97	-12.22	Terr. botan. macrofos. (base peat)	Hijma et al., 2009
139	GrN-8734	8020	70		9086-8639	106610-446440	446-101-0021	-12.68	-12.70	Humic clay (palaeosol in top WM)	De Jong, 1979b
140	UtC-14945	5547	40	-27.4	6406-6286	103227-447369	06.09.010	-9.81	-9.99	Fen peat	Hijma et al., 2009
141	UtC-14944	5771	35	-7.3	6277-6103*	103227-447369	06.09.010	-9.81	-9.99	Shell (Cerastoderma) in peat	Hijma et al., 2009
142	UtC-15139	5757	42	-25.3	6661-6447	106758-451937	07.09.132	-7.52	-7.54	Terr. botan. macrofos. (base phragmites peat)	Hoffmann, in prep.
143	UtC-15140	5795	36	-29.3	6674-6493	106758-451937	07.09.133	-8.27	-8.28	Terr. botan. macrofos. (base Phragmites peat)	Hoffmann, in prep.
144	UtC-15142	6411	39	-23.1	7421-7272	106962-453342	07.09.133	-9.54	-9.57	Terr. botan. macrofos. (top Phragmites peat)	Hoffmann, in prep.
145	UtC-15143	6436	38	-25.0	7426-7289	106962-453342	07.09.132	-8.91	-8.92	Terr. botan. macrofos. (top wood peat)	Hoffmann, in prep.
146	GrN-21606	8090	40		9233-8782	76955-438765	B37B0226	-19.07	-19.10	Peat on WM	Veldkamp, 1996
147	GrA-42323	7725	45	-25.4	8589-8421	85530-437565	B37E3412	-16.17	-16.17	Terr. botan. macrofos. (top wood peat)	Cohen, unpublished

1 - GrA- and GrN-samples were dated by the Centre for Isotopes, Groningen, the Netherlands; UtC-samples by R. van de Graaf-lab, Utrecht, the Netherlands

2 - 14C dates calibrated using OxCal 4.0 software (Bronk Ramsey, 1995;2001) with the INTCAL04-curve (Reimer et al., 2004), 2σ intervals

3 - Dutch coordinate system: Rijksdriehoekstelsel, position in metres

4 - O.D. = Dutch Ordnance Datum (N.A.P.) ~ mean sea level

* - Dates that were corrected for a marine reservoir effect using the Marine04-curve (Hughen et al., 2004). In Groningen, radiocarbon dates of shells are not corrected for the isotopic fractioning effect (in the North Atlantic: adding ~410 years). As this about equals the marine reservoir effect, no reservoir correction has been applied for shells dated in Groningen.

Appendix 3 - Details of OSL dates

Lett. (Add. 1)	NCL code	Age (ka BP)	1σ	Coord. (X-Y)[1]	Core or sample name	Sample depth (m O.D.)[2]	Dose rate (Gy/ka)	1σ	Equiv. Dose (Gy)	1σ	Poor bleaching	Reference
a	4207131	8.9	0.5	103523-447586	B38A1846	-15.73/-15.83	1.61	0.06	14.29	0.49		Hijma et al., 2009
b	4207132	8.1	0.4	103523-447586	B38A1846	-18.70/-18.80	1.25	0.05	10.16	0.36		Hijma et al., 2009
c	4207133	36.0	1.9	103523-447586	B38A1846	-21.65/-21.75	1.14	0.05	40.95	1.29		Hijma et al., 2009
d	4207129	7.1	0.5	103792-452948	B31C1166	-15.30/-15.40	1.68	0.06	11.85	0.75		Hijma et al., 2009
e	4207130	8.3	0.5	103792-452948	B31C1166	-18.20/-18.30	1.61	0.06	13.42	0.52		Hijma et al., 2009
f	4107127	10.0	0.6	91065-438514	Blijdorp OSL 6	-18.75	1.00	0.04	9.93	0.33		Hijma et al., 2009
g	4107126	8.7	0.8	91065-438514	Blijdorp OSL 3	-20.00	1.51	0.06	13.12	1.01		Hijma et al., 2009
h	4107128	9.1	0.5	91065-438514	Blijdorp OSL 7	-21.40	1.20	0.05	10.93	0.41		Hijma et al., 2009
i	603032	38.3	4.0	81167-412558	B43E0245	-14.11	1.33	0.07	51.00	4.70	some Pb	Busschers et al., 2007
j	603033	34.1	2.7	81167-412558	B43E0245	-16.30	1.40	0.06	47.60	3.20	some Pb	Busschers et al., 2007
k	603034	24.8	2.6	81167-412558	B43E0245	-18.42	1.39	0.06	34.60	3.20	some Pb	Busschers et al., 2007
l	603035	25.8	1.4	81167-412558	B43E0245	-20.32	1.59	0.06	40.90	1.60		Busschers et al., 2007
m	603036	58.2	6.1	81167-412558	B43E0245	-23.41	0.60	0.04	52.30	4.90	some Pb	Busschers et al., 2007
n	1104016	10.2	0.6	86218-430764	B37G0548	-20.17	1.13	0.05	11.60	0.50		Busschers et al., 2007
o	1104017	11.1	0.6	86218-430764	B37G0548	-23.25	1.12	0.05	12.40	0.50		Busschers et al., 2007
p	N/A; sample De1	11.1	0.6	99670-428378	B37E0586	-17.29	2.19	0.07	24.40	1.20		Busschers et al., 2007
q	N/A; sample De2	15.9	1.6	99625-431100	B37E0586	-18.29	1.05	0.03	16.70	1.60		Busschers et al., 2007
r	N/A; sample De3	22.9	1.9	99625-431100	B37E0586	-22.04	1.17	0.03	26.70	2.10		Busschers et al., 2007
s	N/A; sample De4	22.8	2.0	99625-431100	B37E0586	-25.09	1.12	0.03	25.50	2.10		Busschers et al., 2007
t	N/A; sample De5	60.5	5.3	99632-431481	B37E0586	-26.09	0.74	0.02	44.70	3.70	some Pb	Busschers et al., 2007
u	N/A; sample De6	73.8	4.6	98475-433775	B37E0586	-27.29	0.62	0.02	45.80	2.40	some Pb	Busschers et al., 2007
v	N/A; sample De7	196.0	21.0	98475-433775	B37E0586	-30.29	0.69	0.02	135.00	14.00		Busschers et al., 2007
w	N/A; sample De8	190.0	38.0	98450-433300	B37E0586	-31.29	0.84	0.03	159.00	31.00	some Pb	Busschers et al., 2007
x	N/A; sample Lei1	47.7	4.0	87540-454380	B30G0863	-19.12	1.11	0.06	53.00	3.40		Busschers et al., 2007
y	N/A; sample Lei2	52.7	4.6	87540-454380	B30G0863	-21.17	0.99	0.05	52.10	3.80		Busschers et al., 2007
z	N/A; sample Lei3	67.7	11.7	87540-454380	B30G0863	-23.62	0.78	0.05	52.80	8.50		Busschers et al., 2007

1 - Dutch coordinate system: Rijksdriehoekstelsel, position in metres

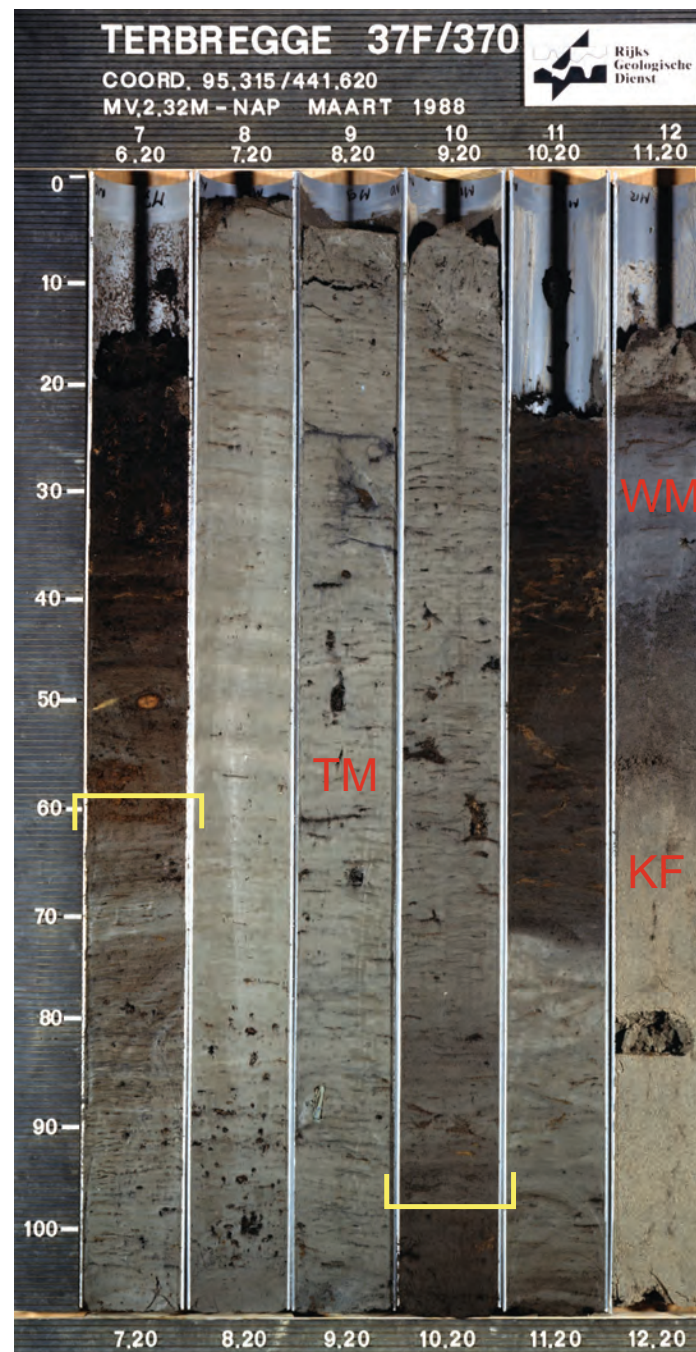2 - O.D. = Dutch Ordnance Datum (N.A.P.) ~ mean sea level

Figure A4.1 (Chapter 2) Core B37F0370 (see Fig. 2.1 for location). Between the yellow brackets a banded, laminated silty clay with woody debris (occasionally with rootlets) is visible. This facies marks shallow subaqueous deposition in freshwater fluvial-tidal flood basins in the upper estuary of the early Atlantic Rhine. The facies overlies basal peat and early Holocene deposits. TM=Terbregge Member; WM=Wijchen Member; KF=Kreftenheye Formation.
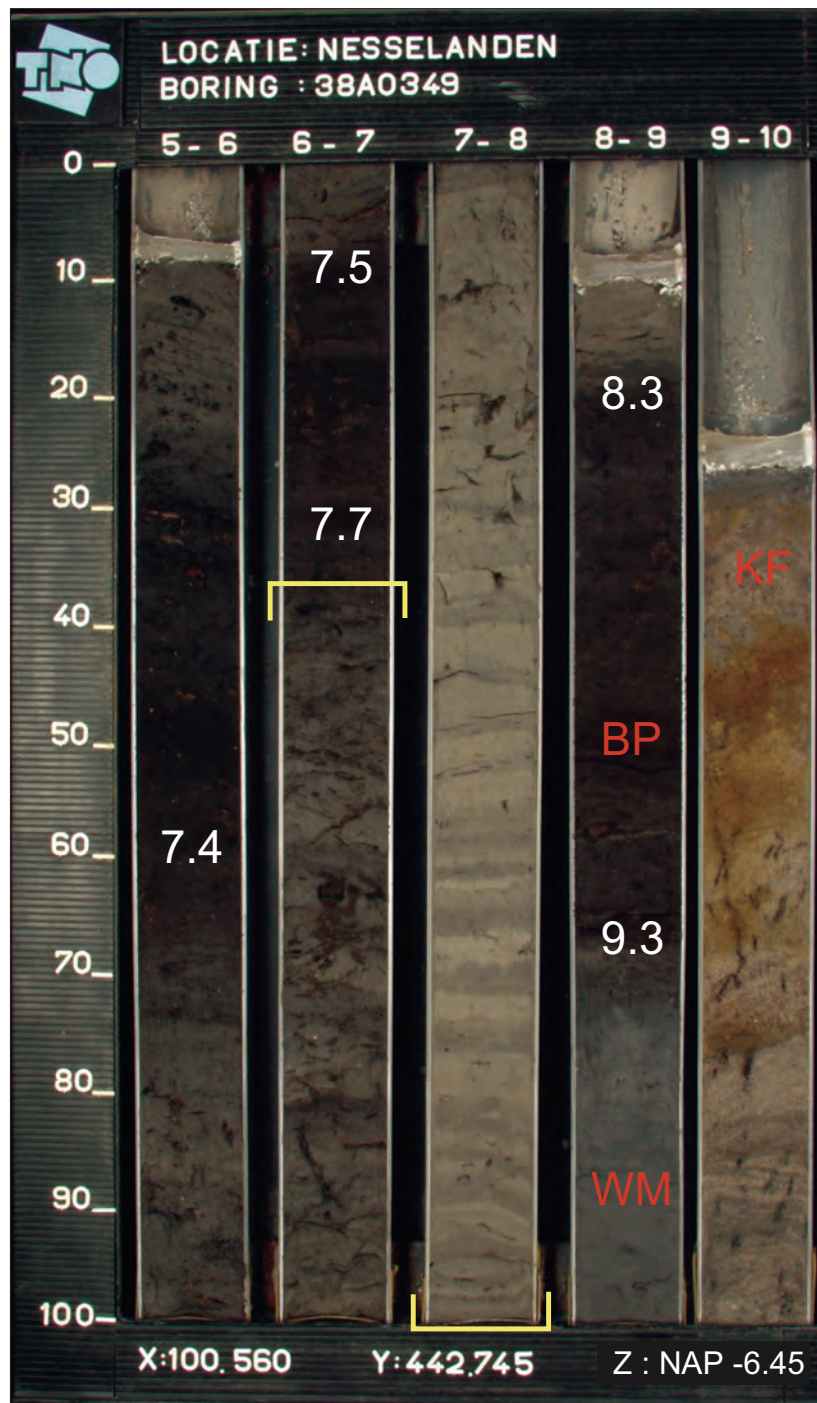
Figure A4.2 (Chapter 2) Core B38A0349 (Add. 1, section A-A', km 28). Between the yellow brackets, a light-dark banded clay is visible. This facies marks rapid deposition in fresh, shallow water. The dark bands mark seasonal diatom blooms, suggesting the interval 7-8 m to have accumulated within 24 years (App. 1, H-2). Calibrated ages (ka BP) are depicted in white; decimal dot indicates the sampling position for ^{14}C dating. Surface elevation was corrected from 5.7 to 6.45 m -O.D. BP=Basal Peat; WM=Wijchen Member; KF=Kreftenheye Formation.
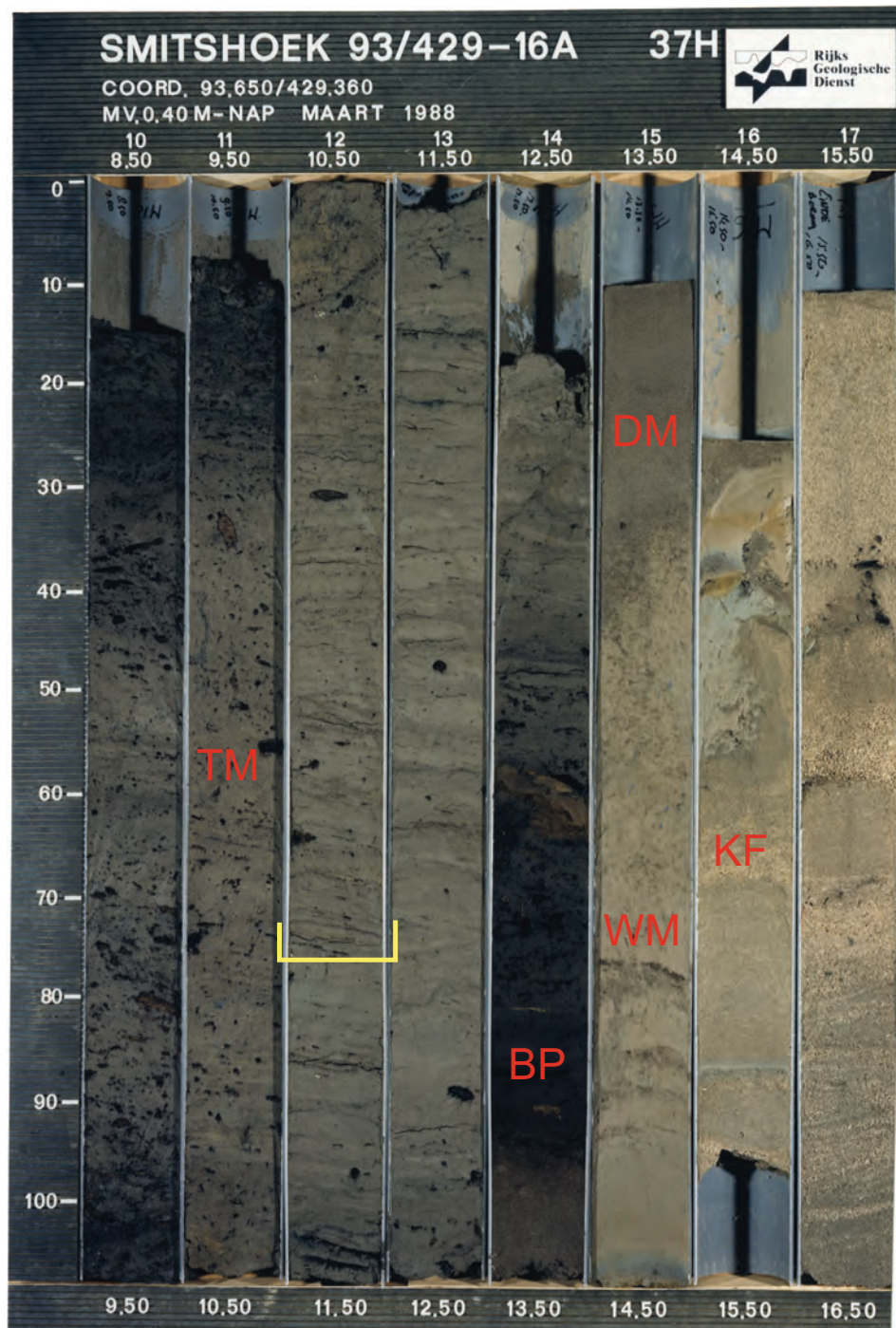
Figure A4.3 (Chapter 2) Core B37H0549 (Add. 1, section B-B', km 17). Above the yellow bracket, a banded, laminated silty clay with abundant woody debris is shown (Terbregge Member, TM). The facies is characteristic for fluvial-tidal flood basins ~7 cal ka BP. The clay overlies the basal peat (BP). DM=Delwijnen Member; M=Wijchen Member; KF=Kreftenheye Formation.
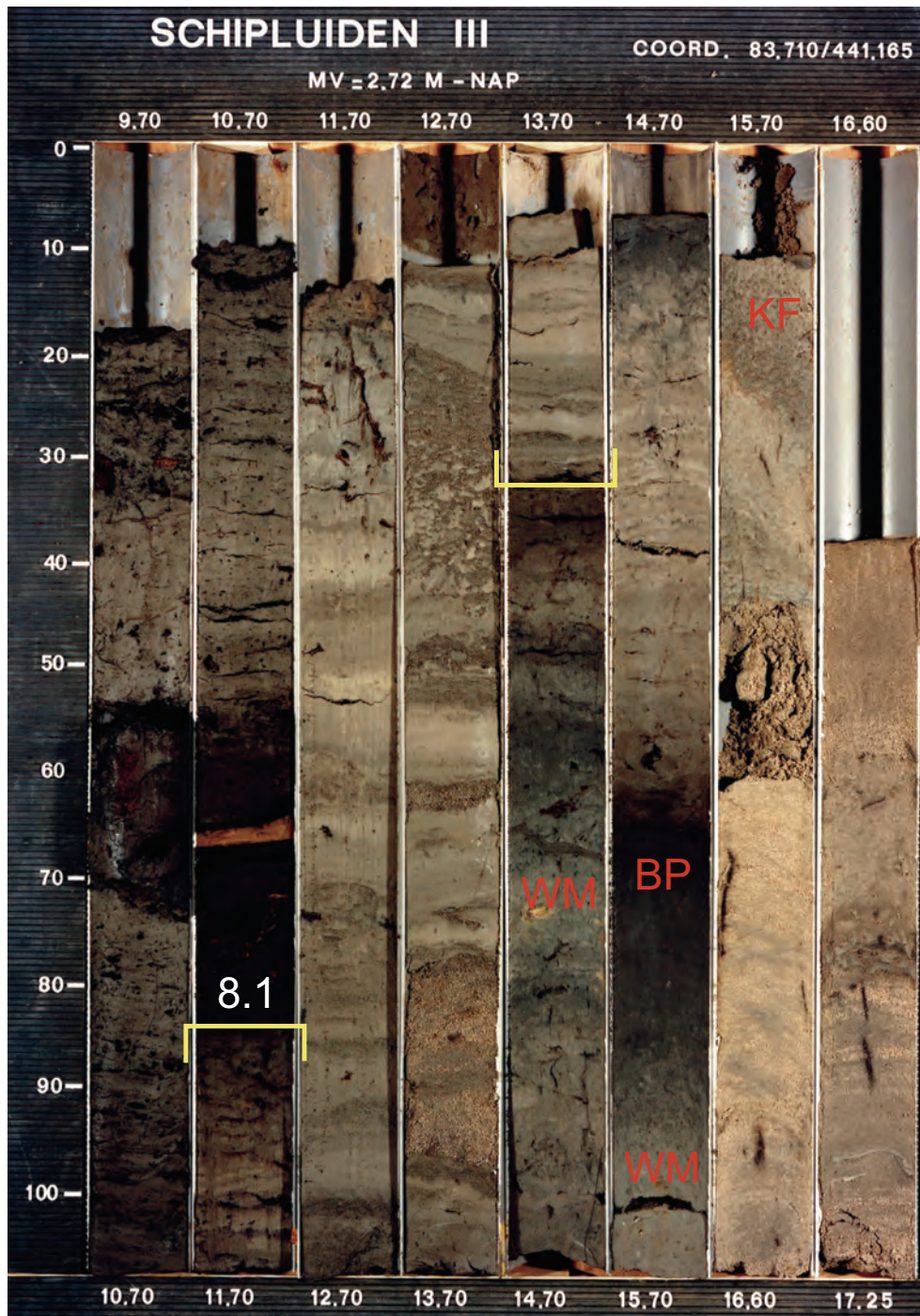
Figure A4.4 (Chapter 2) Core B37E0562 (Add. 1, section C-C', km 38). Between the yellow brackets early Holocene aggrading overbank deposits are shown, with many sand layers and clay pebbles. Note the thickness of the Wijchen Member (WM) and occurrence of organic horizons and a basal peat (BP) within it. Calibrated ages (ka) are depicted in white. KF=Kreftenheye Formation.
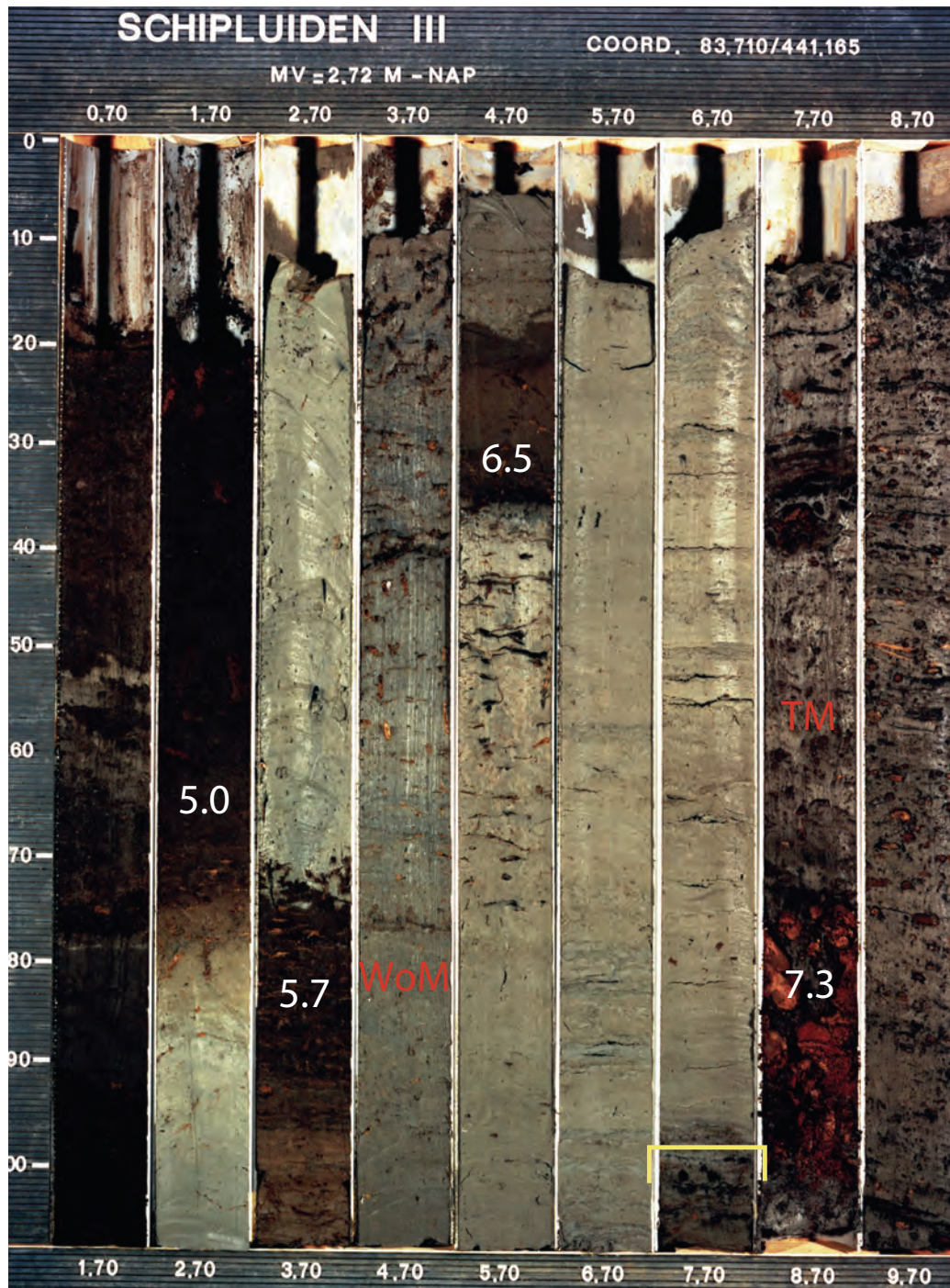
Figure A4.5 (Chapter 2) Core B37E0562 (Add. 1, section C-C', km 38). Below the yellow bracket the deposits directly south of the bay-head delta are shown, containing many wood fragments, indicative for the nearby presence of a river mouth. Above the yellow bracket brackish deposits occur (based on nearby diatoms counts, App. 4, H-31, H-34). Around 5 cal ka BP widespread peat formation starts. Calibrated ages (ka BP) are depicted in white. TM=Terbregge Member; WoM=Wormer Member.
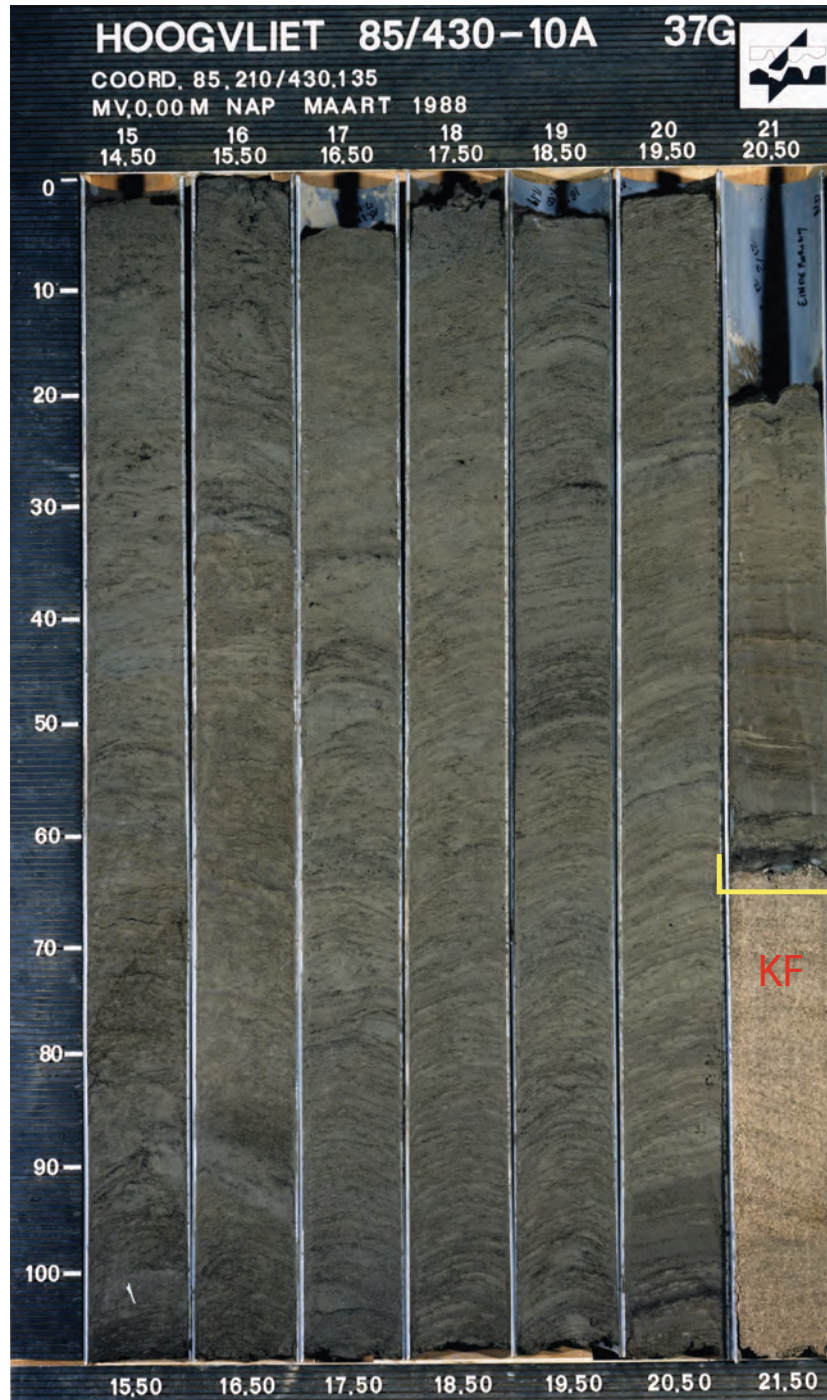
Figure A4.6 (Chapter 2) Core Hoogvliet (see Fig. 2.1 for location). Above the yellow bracket distinct parallel laminated heterolithic bedding is shown. The succession dates to 7.5-6.5 cal ka BP. The deposits erosively overly the Kreftenheye Formation (KF).
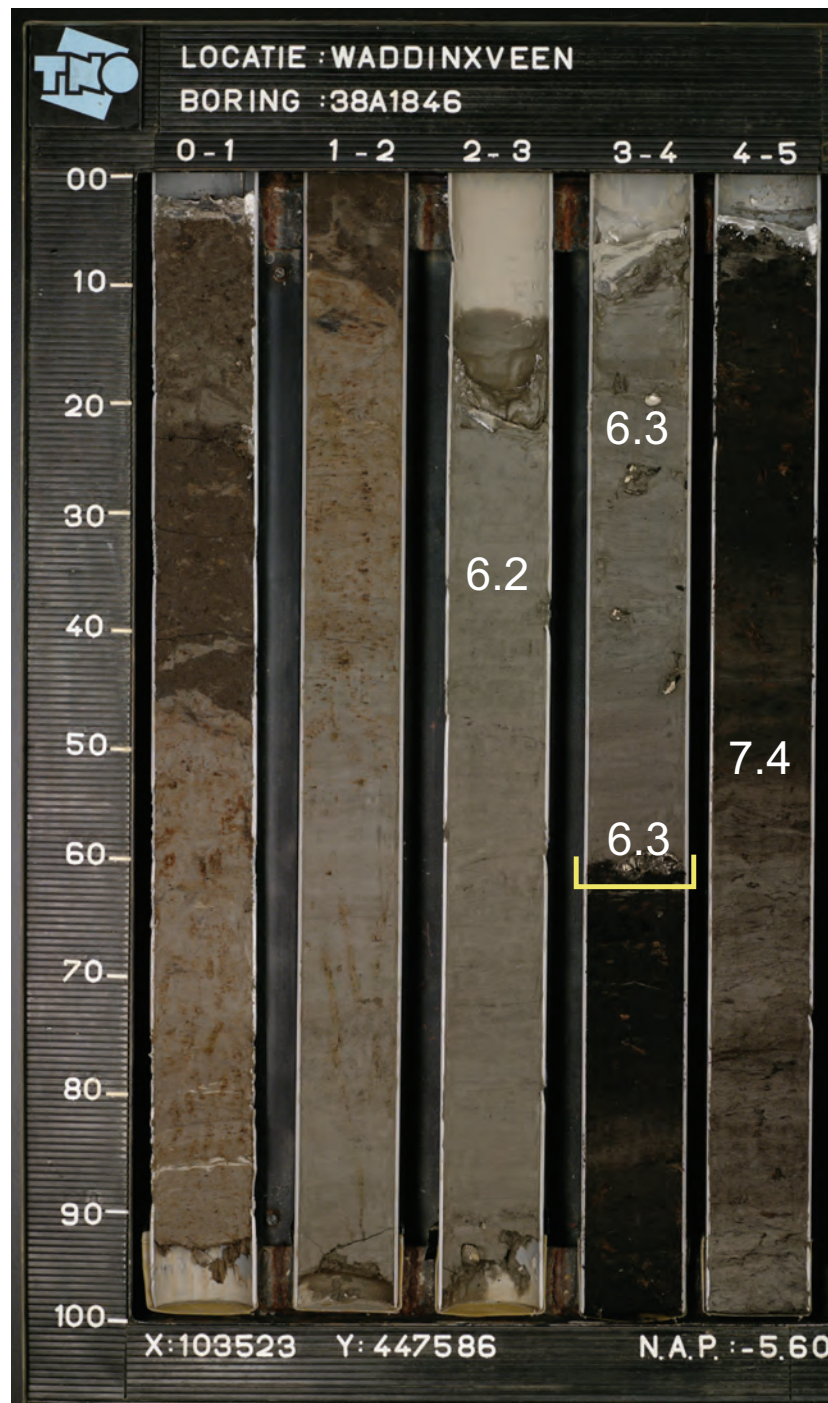
Figure A4.7 (Chapter 2) Core B38A1846 (Add. 1, section A-A', km 35.5). Above the yellow bracket, a shell lag is visible at the base of clayey tidal basin deposits overlying a freshwater peat. Note the homogeneous character of the marine deposits. Calibrated ages in ka BP are depicted in white (shell dates are corrected for the marine reservoir effect).
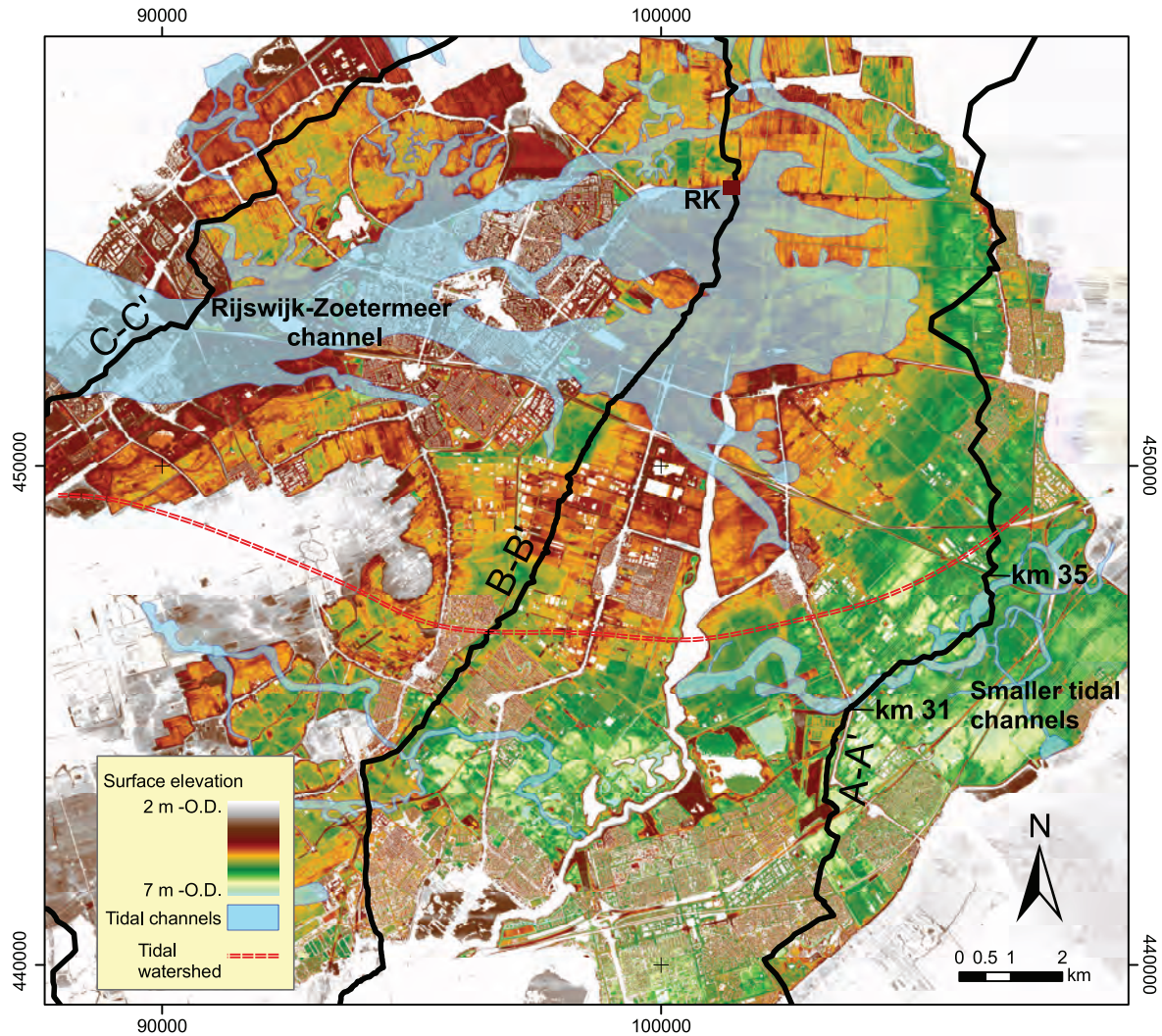
Figure A4.8 (Chapter 2) Annotated visualisation of AHN digital elevation data (Rijkswaterstaat-AGI, 2005) showing the estimated position of the tidal watershed between the Rijswijk-Zoetermeer tidal system (traceable in the image) and a coexisting tidal inlet system to the south (Hoek van Holland tidal system). Most channel patterns in the elevation model have a tidal nature and relate to architectural elements within a few metres below the surface. RK indicates the study area of Raven and Kuijper (1981). The position of parts of cross sections A-A', B-B' and C-C' are shown.
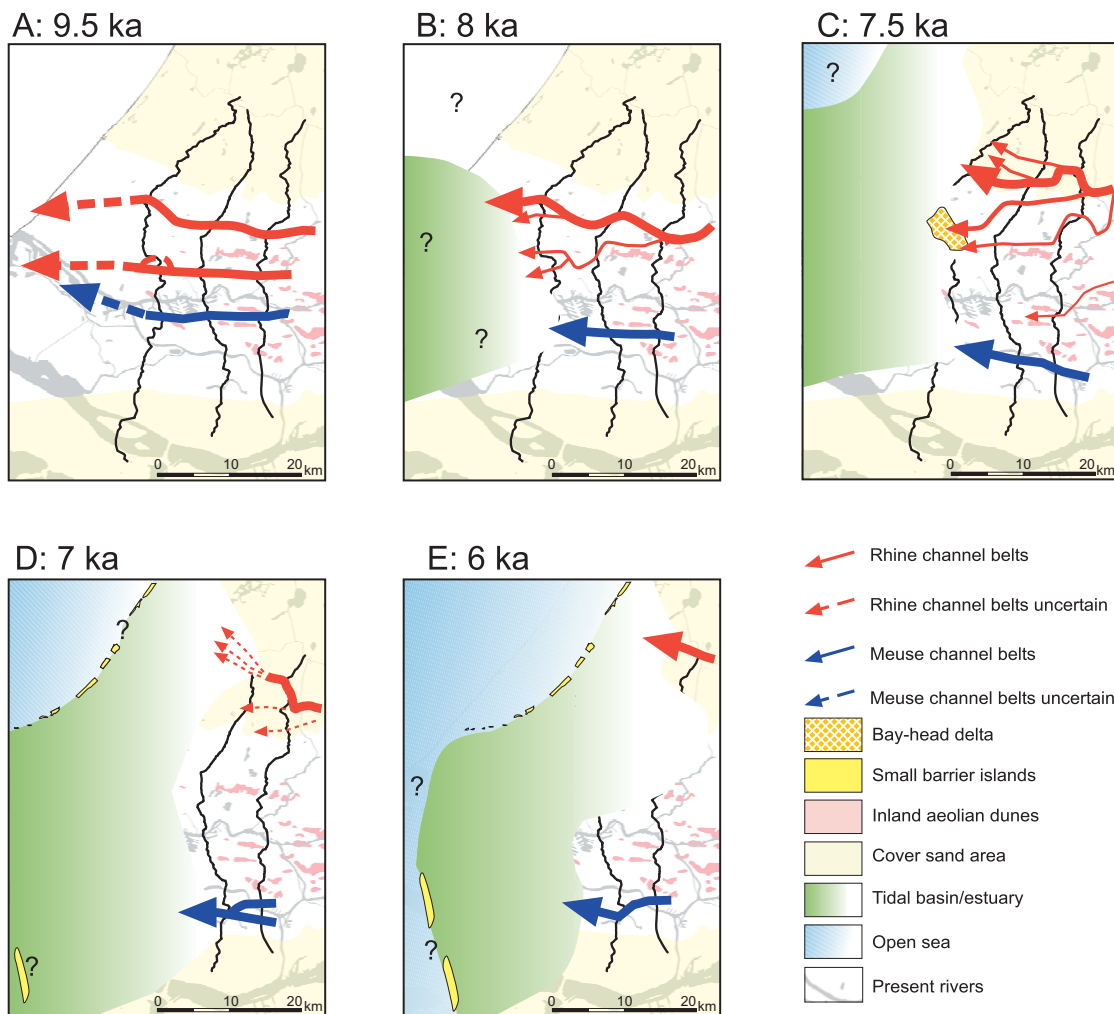
Figure A4.9 (Chapter 2) Schematic palaeogeographic evolution of the western Netherlands during the Holocene transgression. Rhine and Meuse channel belt positions are indicated for five time frames between 9.5 and 6.0 ka.

A: 9.5 cal ka BP (Boreal): Two Rhine branches and one Meuse branch flow parallel within Younger Dryas-Early Holocene inherited channel belts. Inland aeolian activity continued.

B: 8 cal ka BP (early Atlantic): Rivers had transformed to aggrading channel belts, still mainly restricted to the Younger Dryas-Early Holocene inherited incised channel belts. A small connection between the two Rhine branches was established and the southern branch was partially abandoned. The sea transgressed the palaeo-valley.

C: 7.5 cal ka BP (middle Atlantic): The Meuse shifted to the south, while the Rhine shifted north. Secondary Rhine branches remained active in central parts of the study area, feeding a bay-head delta (active 8-7.3 cal ka BP). Also the northern part of the study area was transgressed.

D: 7 cal ka BP (middle Atlantic): The Meuse remained active in the same area, with a landward migrating mouth. The Rhine discharge shifted further north, establishing the Oude Rijn outlet and abandoning former southerly outlets. Bay-head deltas most likely formed; they were possibly not recognized due to a lack of data and poor preservation. Offshore, embryonic barriers were presumably present.

E: 6 cal ka BP (late Atlantic): The Oude Rijn channel belt was formed in the north of the study area. The position of the Meuse did not alter. Transgression halted and the coastline started to prograde.

178
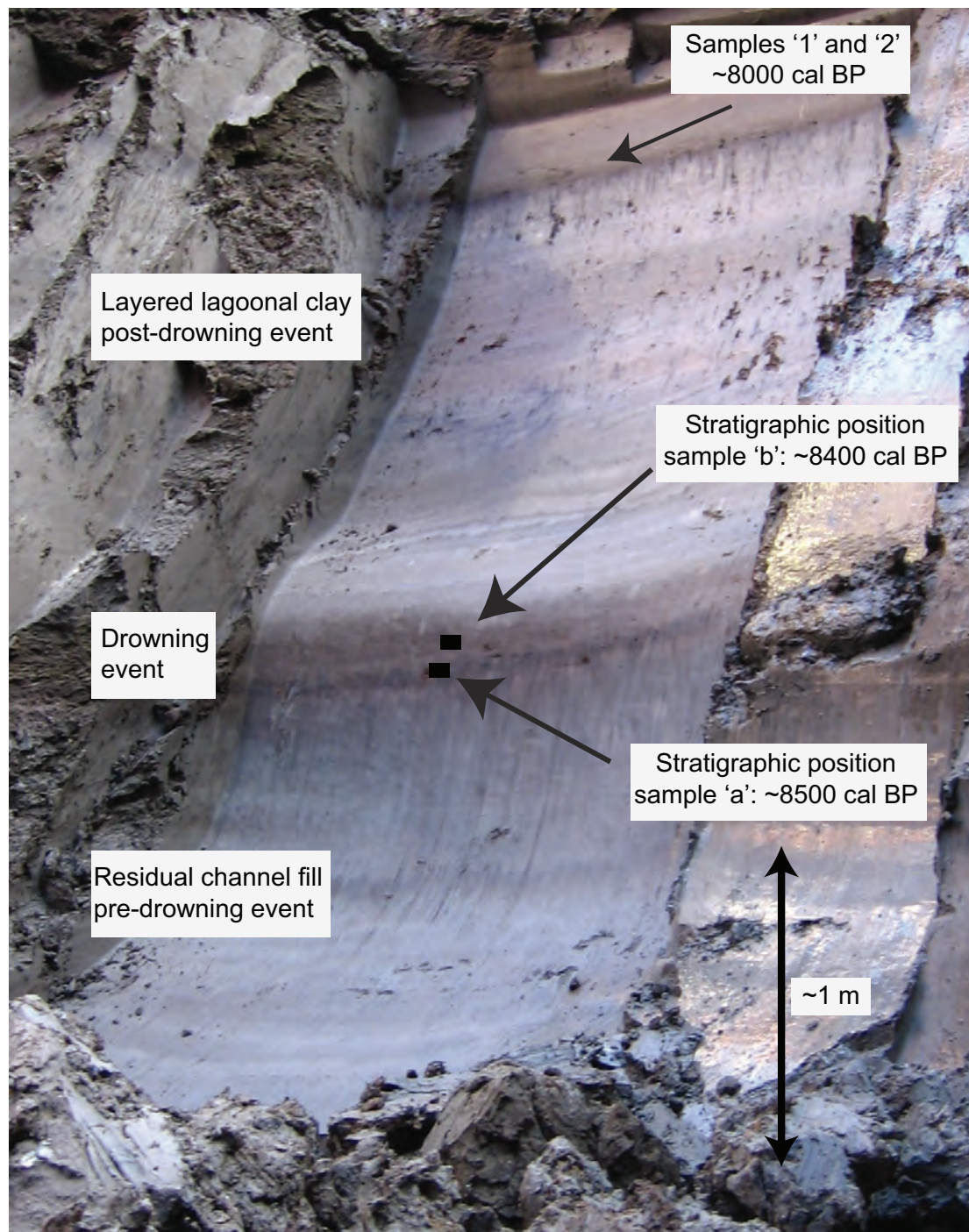
Figure A4.10 (Chapter 3) Stratigraphic position of samples 'a' and 'b' (Table S3.1) in construction pit ROT Blijdorp. The drowning event is encountered in a gyttja layer covering residual channel fill deposits, and overlain by layered upper estuarine/lagoonal clays. Samples were taken from the face in the left of the picture. Diatom assemblages in the gyttja layer suggest a slightly brackish environment, while the lagoonal clays show tidal lamination.
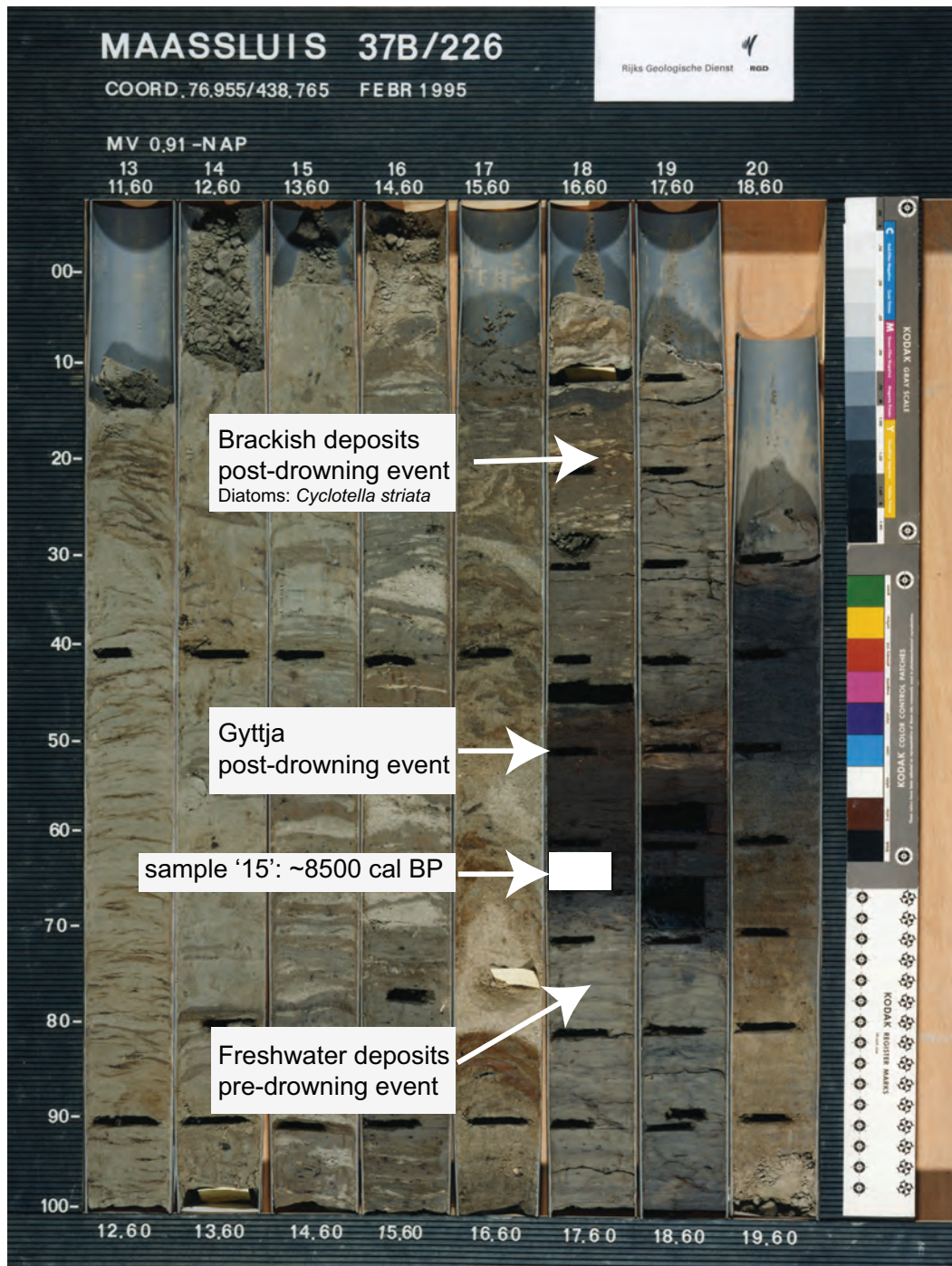
Figure A4.11 (Chapter 3) Core B37B0226 (MSS-site) with the position of sample '15' (Table S3.1). The dated freshwater peat layer is overlain by a gyttja layer that grades into brackish tidal deposits (clay with increasing sand content) as is evident from pollen and diatoms.
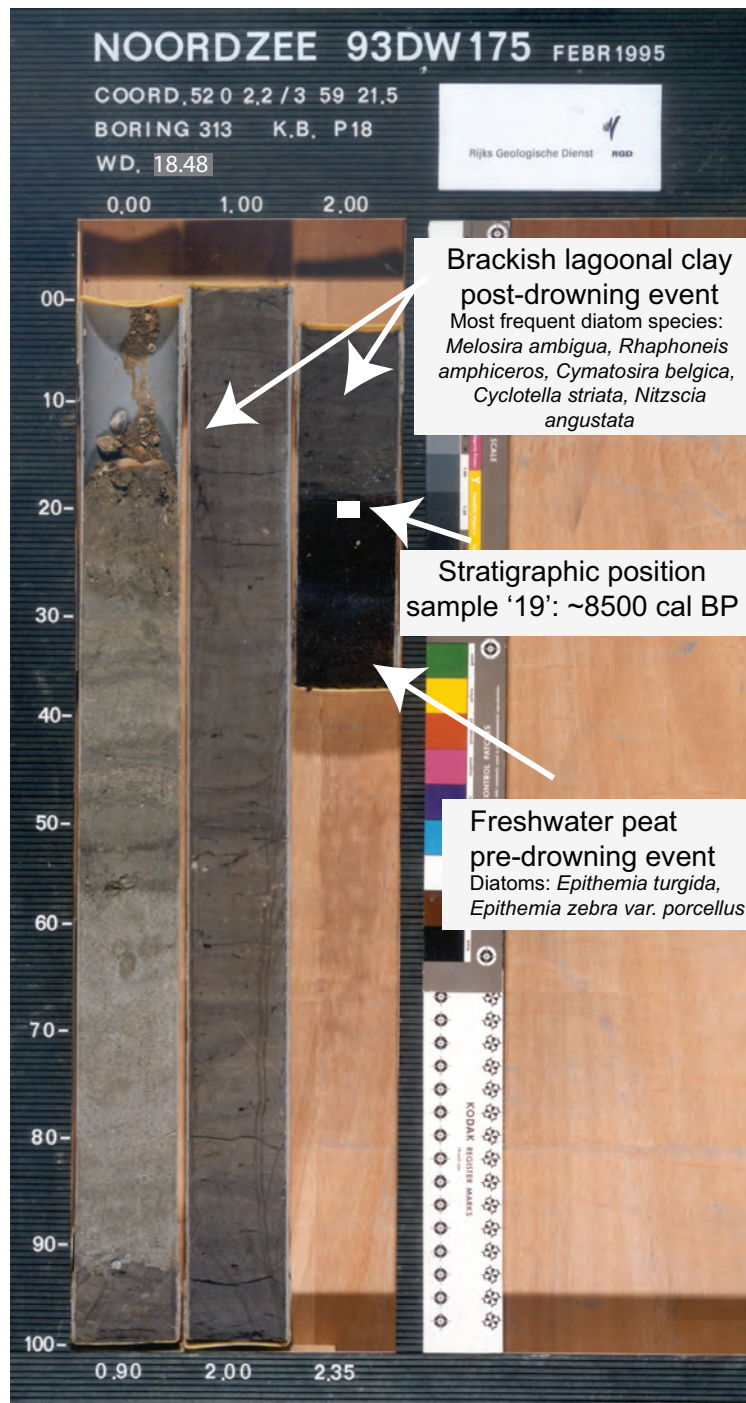
Figure A4.12 (Chapter 3) Core P18-313 (MVL-site) with the position of sample '19' (Table S3.1). The dated peat layer is directly overlain by brackish lagoonal clays (starting as a gyttjaic deposit) as is evident from diatoms.
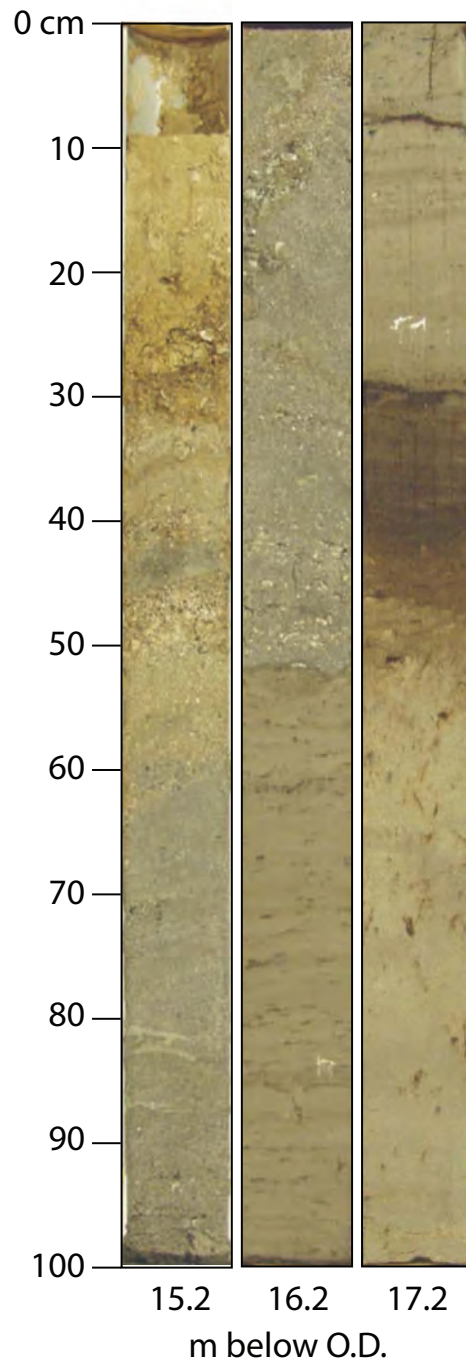
Figure A4.13 (Chapter 4) Core Q16-914 (see Fig. 4.3 for location, also Fig. 4.7) with the verticale scale in cm below seabed. Below 245 cm aeolian deposits are present (*Unit 2*) overlain by the basal peat (*Unit 4*). The clayey deposits of *Unit 5* lie between 150-230 cm. Truncation *Unit 7* (65-150 cm) is characterised by a shell lag at the base. Above 65 cm, younger lower shoreface deposits are situated (*Units 8* and *9*). Calibrated ages (ka BP) are depicted in white; decimal dot indicates the sampling position for ^{14}C dating.
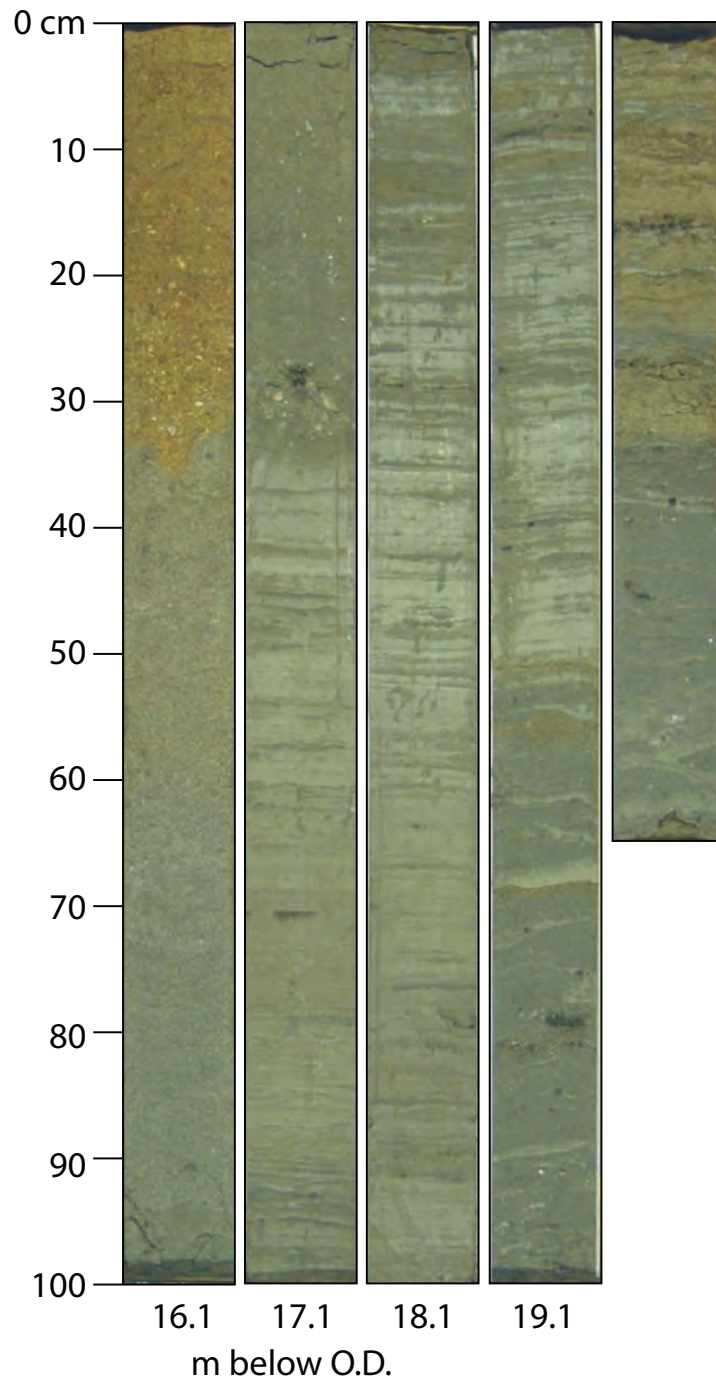
Figure A4.14 (Chapter 4) Core Q16-915 (see Fig. 4.3 for location, also Fig. 4.5) with the verticale scale in cm below seabed. Below 130 cm the channel fill facies of *Unit 6* is shown. Between 35 and 130 cm truncation *Unit 7* is present, in turn truncated by *Units 8* and *9*. The channel fill consists of sand-clay alternations. Calibrated ages (ka BP) are depicted in white; decimal dot indicates the sampling position for ^{14}C dating.
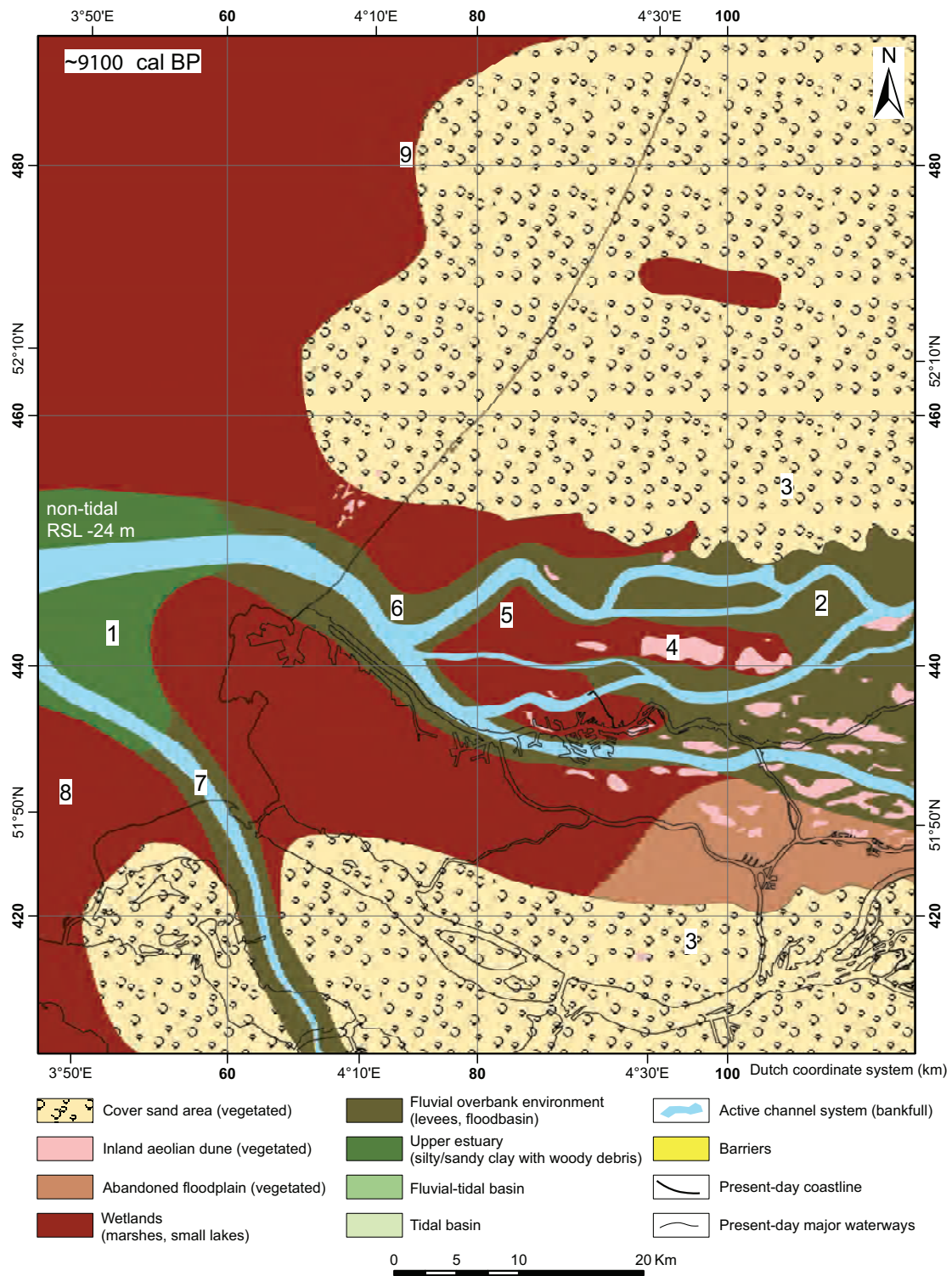
Figure A4.15 (Chapter 5) Palaeogeography around 9100 cal BP showing late Boreal channel belts within the palaeovalley. Widespread peat formation had already started. RSL=Relative sea level. Colour version of Fig. 5.3.
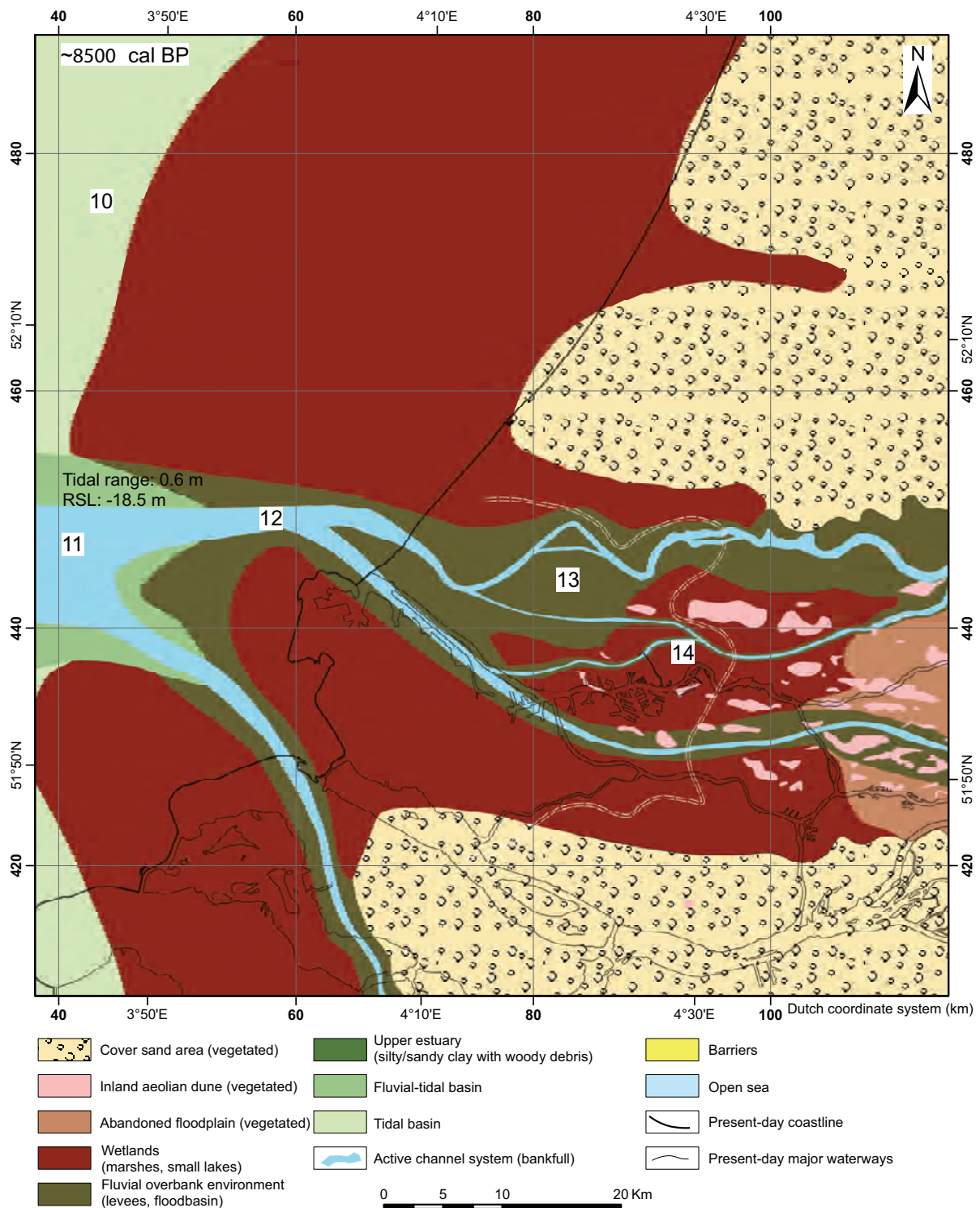
Figure A4.16 (Chapter 5) Palaeogeography around 8500 cal BP showing landward shifting of system, especially of the wetland area in the north. The landward limit of the drowned area in the Rhine-Meuse valley during the following sea-level jump is given (white double dashed line, based on Hijma and Cohen, In press: Chap. 3). RSL=Relative sea level. Colour version of Fig. 5.4.

185
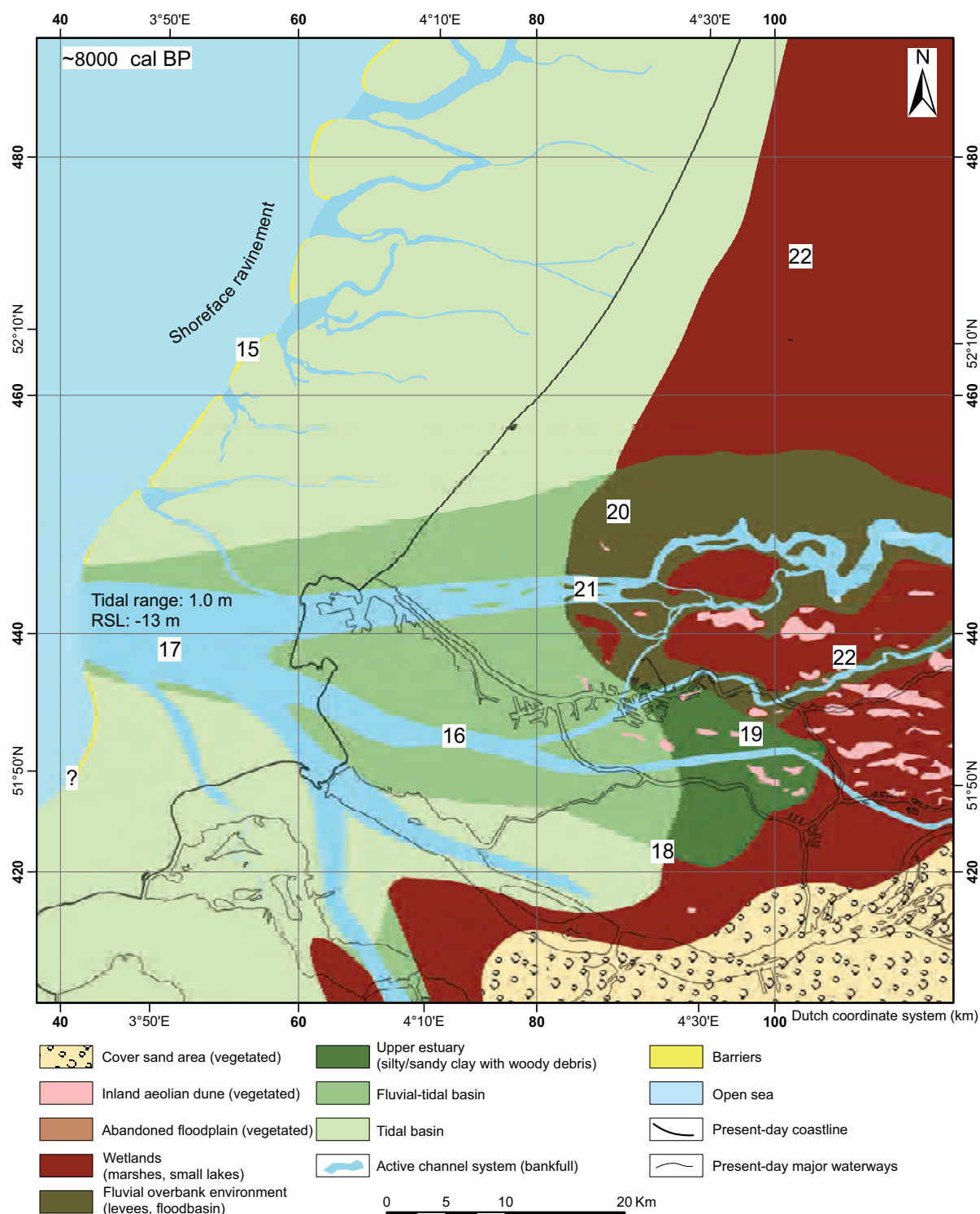
Figure A4.17 (Chapter 5) Palaeogeography around 8000 cal BP. During and immediately following the sea-level jump, rapid transgression and coastline retrogradation occurred. RSL=Relative sea level. Colour version of Fig. 5.5.
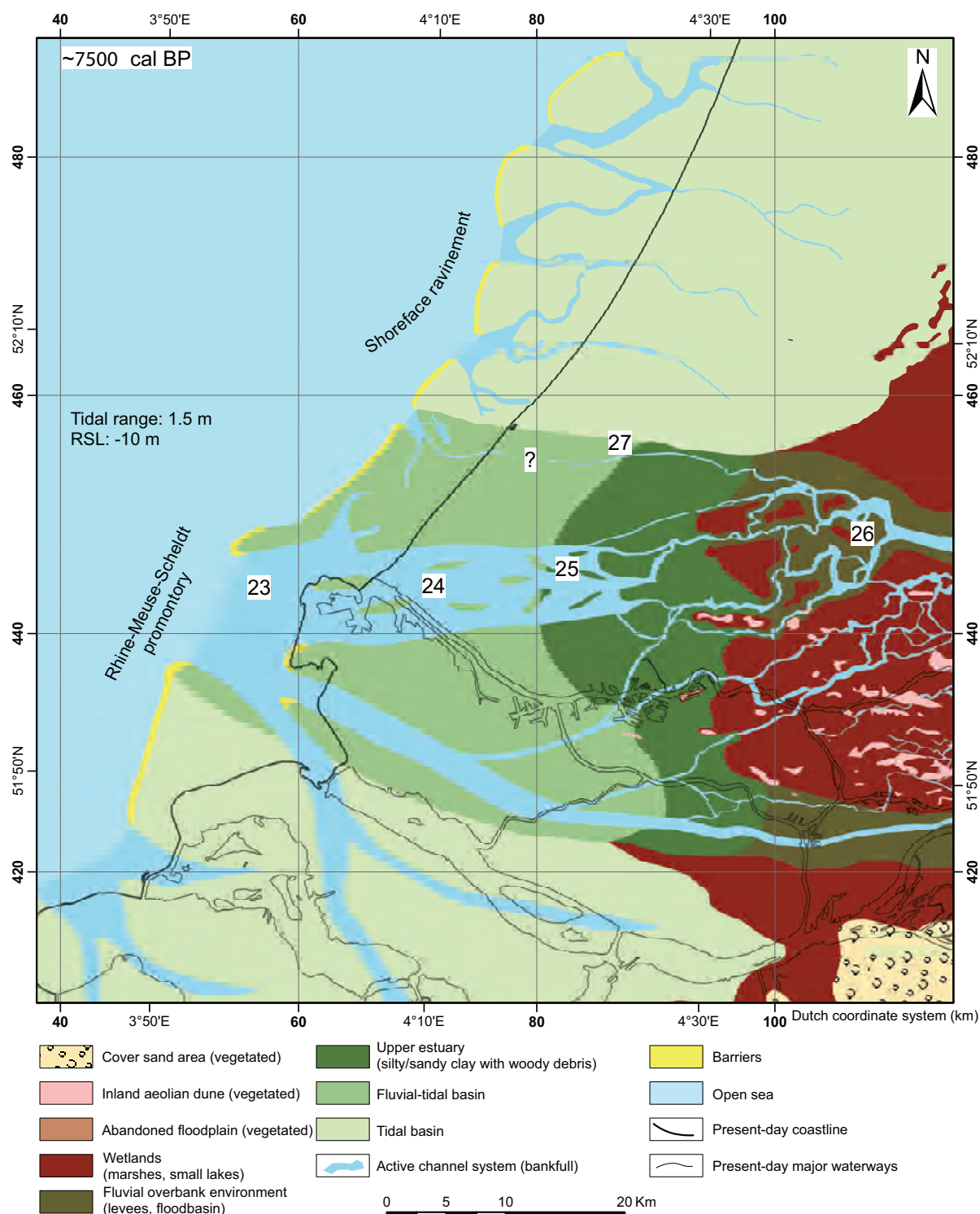
Figure A4.18 (Chapter 5) Palaeogeography around 7500 cal BP. Retrogradation slowed down due to a decreasing rate of sea-level rise. Longshore currents started to transport sediment from the eroding river mouth to the tidal basins to the north. RSL=Relative sea level. Colour version of Fig. 5.6.
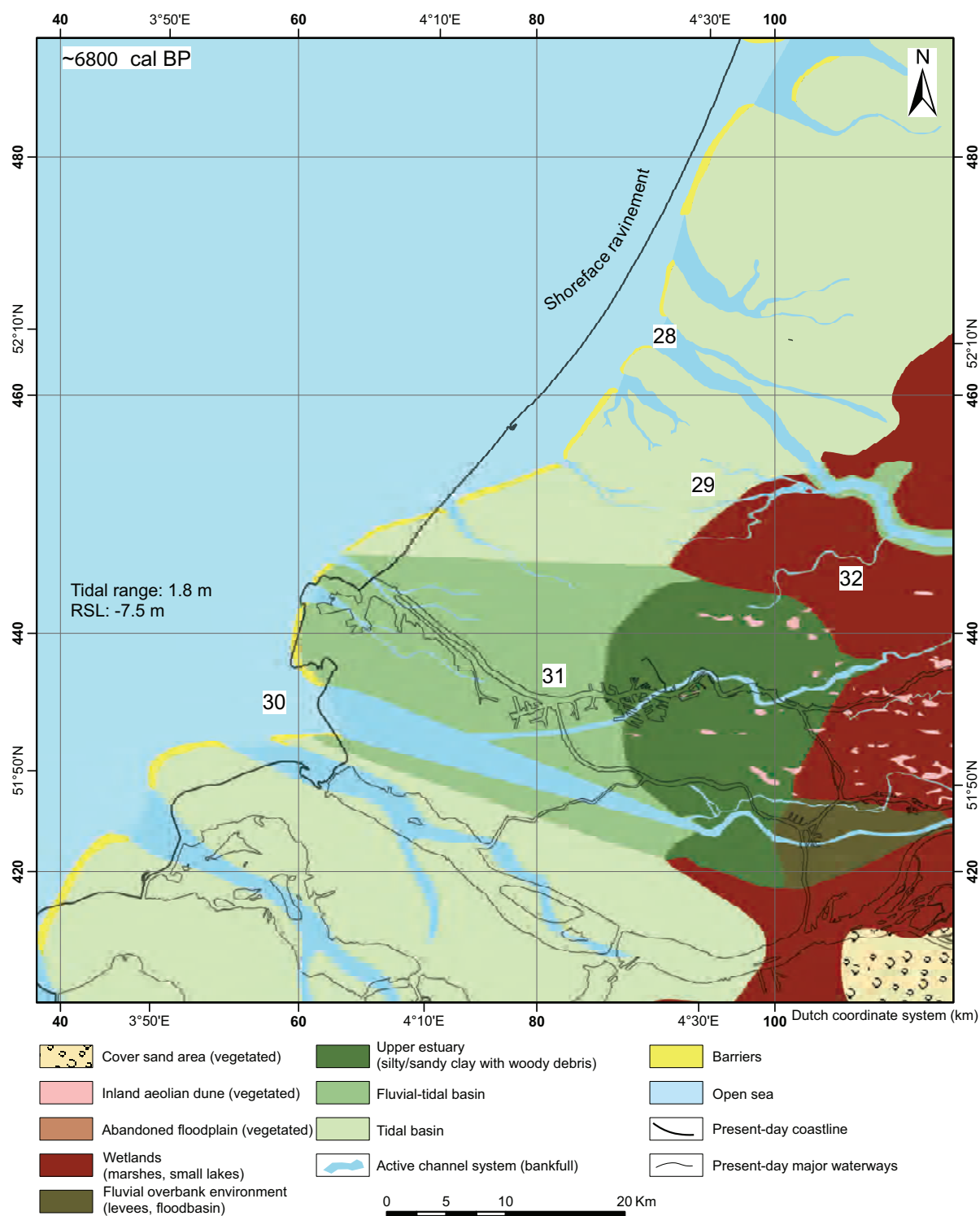
Figure A4.19 (Chapter 5) Palaeogeography around 6800 cal BP. The main Rhine river mouth had shifted north and outside the palaeovalley. RSL=Relative sea level. Colour version of Fig. 5.7.
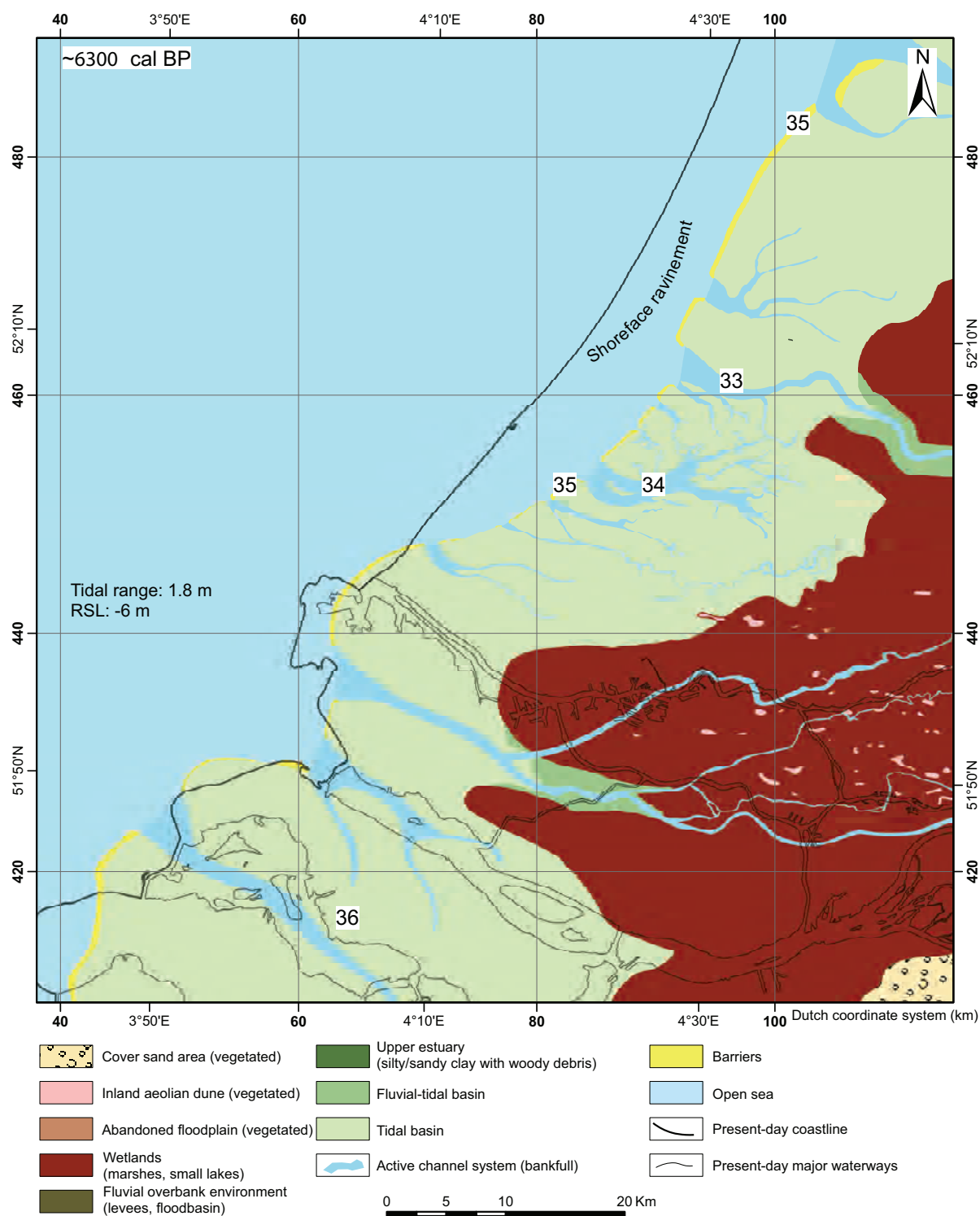
Figure A4.20 (Chapter 5) Palaeogeography around 6300 cal BP. Retrogradation halted in the centre of the study area, but continued to the north. RSL=Relative sea level. Colour version of Fig. 5.8.

Author's background

I grew up in my own study area. After being born in Pijnacker, I spend most of my youth in Zoetermeer at 5 m below mean sea level. There I enjoyed both my primary (Prins Mauritsschool) and secondary education (Oranje Nassau College). At that time, Zoetermeer was still surrounded by the 'green heart' of Holland. Although I understood its beauty and quietness, full appreciation followed during this research when I worked in many corners of the heart. I am still struggling whether to like or dislike the invasion of the area by infrastructural works in recent years. The relative emptiness is gone, but this thesis could and has been written.

The author at work in the Hoeksche Waard.

The many holidays with my parents, brother and sister to the mountains and the sea unearthed my interests and in 1997 I started studying Physical Geography at Utrecht University. In my first year, I executed many corings in the Rhine-Meuse delta during the field course led by Henk Berendsen. Not really interested in quaternary geology, I choose to study fluvial and coastal processes on shorter time scales. During an internship at Waikato University, New Zealand, I analysed the relation between sediment parameters and beach slope at the beaches of Coromandel Peninsula. My graduation concerned the evaluation of several aeolian sand transport models using four different sand traps at The Hors, Texel, The Netherlands.

After finishing my study in 2002, I worked six months for Rijkswaterstaat-RIZA studying the impact of vessel passages on the resuspension of sediment in groyne fields. Subsequently, I worked four months as a junior researcher at Utrecht University using hourly-averaged video images to define mean beach widths and beach-flood frequencies. After returning from travelling in South-America, I became seriously interested in quaternary geology at the archaeological company BAAC. In many different settings, from ice-pushed to beach ridge, I had to reconstruct palaeoenvironments and to estimate the probability that people lived there in the past.

During my Ph.D.-research, I could combine my interests in processes on both short and longer time scales. After all, every sand grain or clay flock in the geological record was once deposited during a short-lived event.

355 W BORREN Carbon exchange in Western Siberian watershed mires and implication for the greenhouse effect; A spatial temporal modeling approach -- Utrecht 2007: Knag/Faculteit Geowetenschappen Universiteit Utrecht. 125 pp, 36 figs, 17 tabs. ISBN: 978-90-6809-396-4, Euro 13,00

356 S O NEGRO Dynamics of technological innovation systems; The case of biomass energy -- Utrecht 2007: Knag/Copernicus Institute. 166 pp, 24 figs, 17 tabs. ISBN: 978-90-6809-397-1, Euro 18,00

357 R NAHUIS The politics of innovation in public transport; Issues, settings and displacements -- Utrecht 2007: Knag/Copernicus Institute. 184 pp, 9 figs, 40 tabs, 4 box. ISBN 978-90-6809-398-8, Euro 20,00

358 M STRAATSMA Hydrodynamic roughnesses of floodplain vegetation; Airborne parameterization and field validation -- Utrecht 2007: Knag/Faculteit Geowetenschappen Universiteit Utrecht. 180 pp, 55 figs, 28 tabs. ISBN: 978-90-6809-399-5, Euro 23,00

359 H KRUIZE On environmental equity; Exploring the distribution of environment quality among socio-economic categories in the Netherlands -- Utrecht 2007: Knag/Copernicus Institute. 219 pp, 76 figs, 25 tabs. ISBN: 978-90-6809-401-5, Euro 25,00

360 T VAN DER VALK Technology dynamics, network dynamics and partnering; The case of Dutch dedicated life sciences firms -- Utrecht 2007: Knag/Copernicus Institute. 143 pp, 23 figs, 25 tabs. ISBN: 978-90-6809-402-2, Euro 15,00

361 M A SCHOUTEN Patterns in biodiversity; Spatial organisation of biodiversity in the Netherlands -- Utrecht 2007: Knag/Copernicus Institute. 152 pp, 16 figs, 20 tabs. ISBN: 978-90-6809-403-9, Euro 20,00

362 M H J W VAN AMSTEL – VAN SAANE Twilight on self-regulation; A socio-legal evaluation of conservation and sustainable use of agrobiodiversity by industry self-regulation -- Utrecht 2007: Knag/Copernicus Institute. 167 pp, 15 figs, 13 tabs, 5 box. ISBN: 978-90-6809-404-6, Euro 20,00

363 S MUHAMMAD Future urbanization patterns in the Netherlands, under the influence of information and communication technologies -- Utrecht 2007: Knag/Faculteit Geowetenschappen Universiteit Utrecht. 187 pp, 82 figs, 20 tabs. ISBN: 978-90-6809-405-3, Euro 20,00

364 M GOUW Alluvial architecture of the Holocene Rhine-Meuse delta (The Netherlands) and the Lower Mississippi Valley (U.S.A.) -- Utrecht 2007: Knag/Faculteit Geowetenschappen Universiteit Utrecht. 192 pp, 55 figs, 14 tabs. ISBN: 978-90-6809-406-0, Euro 22,00

365 E HEERE & M STORMS Ormeling's cartography; Presented to Ferjan Ormeling on the occasion of his 65th birthday and his retirement as Professor of Cartography -- Utrecht 2007: Knag/Faculteit Geowetenschappen Universiteit Utrecht. ISBN: 978-90-6809-407-7, Euro 20,00

366 S QUARTEL Beachwatch; The effect of daily morphodynamics on seasonal beach evolution -- Utrecht 2007: Knag/Faculteit Geowetenschappen Universiteit Utrecht. 125 pp, 39 figs, 7 tabs. ISBN: 978-90-6809-408-4, Euro 12,50

367 R O VAN MERKERK Intervening in emerging nanotechnologies; A CTA of Lab-on-a-chip technology regulation -- Utrecht 2007: Knag/Copernicus Institute. 206 pp, 19 box, 35 figs, 12 tabs. ISBN: 978-90-6809-409-1, Euro 20,00

368 R M FRINGS From gravel to sand; Downstream fining of bed sediments in the lower river Rhine -- Utrecht 2007: Knag/Faculteit Geowetenschappen Universiteit Utrecht. ISBN: 978-90-6809-410-7, Euro 25,00

369 W IMMERZEEL Spatial modelling of the hydrological cycle, climate change and agriculture in mountainous basins -- Utrecht 2008: Knag/Faculteit Geowetenschappen Universiteit Utrecht. 147 pp, 54 figs, 12 tabs. ISBN: 978-90-6809-411-4, Euro 25,00

370 D S J MOURAD Patterns of nutrient transfer in lowland catchments; A case study from northeastern Europe -- Utrecht 2008: Knag/Faculteit Geowetenschappen Universiteit Utrecht. 176 pp, 44 figs, 19tabs. ISBN: 978-90-6809-412-1, Euro 20,00

371 M M H CHAPPIN Opening the black box of environmental innovation; Governmental policy and learning in the Dutch paper and board industry -- Utrecht 2008: Knag/Copernicus Institute. 202 pp, 41 figs, 30 tabs. ISBN: 978-90-6809-413-8, Euro 22,50

372 R P ODDENS & M VAN EGMOND Ormelings atlassen; Catalogus van atlassen geschonken aan de Universiteit Utrecht door de hoogleraren F.J. Ormeling sr. en jr. – Utrecht 2008: Knag/Faculteit Geowetenschappen Universiteit Utrechts. ISBN: 978-90-6809-415-2, Euro 15,00

373 R VAN MELIK Changing public space; The recent redevelopment of Dutch city squares – Utrecht 2008: Knag/Faculteit Geowetenschappen Universiteit Utrecht. 323 pp, 47 figs, 32 tabs. ISBN: 978-90-6809-416-9, Euro 20,00

374 E ANDRIESSE Institutions and regional development in Southeast Asia; A comparative analysis of Satun (Thailand) and Perlis (Malaysia) -- Utrecht 2008: Knag/Faculteit Geowetenschappen Universiteit Utrecht. 250 pp, 42 figs, 43 tabs, 18 box. ISBN: 978-90-6809-417-6, Euro 25,00

375 E HEERE GIS voor historisch landschapsonderzoek; Opzet en gebruik van een historisch GIS voor prekadastrale kaarten -- Utrecht 2008: Knag/Faculteit Geowetenschappen Universiteit Utrecht. 231 pp, 73 figs, 13 tabs. ISBN: 978-90-6809-418-3, Euro 30,00

376 V D MAMADOUH, S M DE JONG, J F C M THISSEN & J A VAN DER SCHEE Dutch windows on the Mediterranean; Dutch Geography 2004-2008 -- Utrecht 2008: Knag/International Geographical Union Section The Netherlands. 104 pp + cd-rom, 38 figs, 9 tabs. ISBN: 978-90-6809-419-0, Euro 10,00

377 E VAN MARISSING Buurten bij beleidsmakers; Stedelijke beleidsprocessen, bewonersparticipatie en sociale cohesie in vroeg-naoorlogse stadswijken in Nederland -- Utrecht 2008: Knag/Faculteit Geowetenschappen Universiteit Utrecht. 230 pp, 6 figs, 31 tabs. ISBN: 978-90-6809-420-6, Euro 25,00

378 M DE BEER, R C L BUITING, D J VAN DRUNEN & A J T GOORTS (Eds.) Water Wegen; Op zoek naar de balans in de ruimtelijke ordening -- Utrecht 2008: Knag/VUGS/Faculteit Geowetenschappen Universiteit Utrecht. 91 pp, 18 figs, 1 tab. ISBN: 978-90-6809-421-3, Euro 10,00

379 J M SCHUURMANS Hydrological now- and forecasting; Integration of operationally available remotely sensed and forecasted hydrometeorological variables into distributed hydrological models -- Utrecht 2008: Knag/Faculteit Geowetenschappen Universiteit Utrecht. 154 pp, 65 figs, 12 tabs. ISBN 978-90-6809-422-0, Euro 15,00

380 M VAN DEN BROECKE Ortelius' *Theatrum Orbis Terrarum* (1570-1641); Characteristics and development of a sample of *on verso* map texts -- Utrecht 2009: Knag/Faculteit Geowetenschappen Universiteit Utrecht. 304 pp + cd-rom, 9 figs, 65 tabs. ISBN 978-90-6809-423-7, Euro 30,00

381 J VAN DER KWAST Quantification of top soil moisture patterns; Evaluation of field methods, process-based modelling, remote sensing and an integrated approach -- Utrecht 2009: Knag/Faculteit Geowetenschappen Universiteit Utrecht. 313 pp, 108 figs, 47 tabs. ISBN 978-90-6809-424-4, Euro 30,00

382 T J ZANEN 'Actie, actie, actie…'; De vakbeweging in regio Noord-Nederland, 1960-1992 -- Utrecht/ Groningen 2009: Knag/Faculteit Ruimtelijke Wetenschappen Rijksuniversiteit Groningen. ISBN 978-90-6809-425-1, Euro 30,00

383 M PERMENTIER Reputation, neighbourhoods and behaviour -- Utrecht 2009: Knag/Faculteit Geowetenschappen Universiteit Utrecht. 146 pp, 10 figs, 19 tabs. ISBN 978-90-6809-426-8, Euro 15,00

384 A VISSER Trends in groundwater quality in relation to groundwater age -- Utrecht 2009: Knag/Faculteit Geowetenschappen Universiteit Utrecht. 188 pp, 47 figs, 24 tabs. ISBN 978-90-6809-427-5, Euro, 20,00

385 B A FURTADO Modeling social heterogeneity, neighborhoods and local influences on urban real estate prices; Spatial dynamic analyses in the Belo Horizonte metropolitan area, Brazil -- Utrecht 2009: Knag/Faculteit Geowetenschappen Universiteit Utrecht. 236 pp, 50 figs, 48 tabs. ISBN 978-90-6809-428-2, Euro 25,00

386 T DE NIJS Modelling land use change; Improving the prediction of future land use patterns -- Utrecht 2009: Knag/Faculteit Geowetenschappen Universiteit Utrecht. 206 pp, 59 figs, 32 tabs. ISBN 978-90-6809-429-9, Euro 25,00

387 I J VISSEREN-HAMAKERS Partnerships in biodiversity governance; An assessment of their contributions to halting biodiversity loss -- Utrecht 2009: Knag/Copernicus Institute. 177 pp, 4 figs, 4 tabs. ISBN 978-90-6809-430-5, Euro 20,00

388 G ERKENS Sediment dynamics in the Rhine catchment; Quantification of fluvial response to climate change and human impact -- Utrecht 2009: Knag/Faculteit Geowetenschappen Universiteit Utrecht. ISBN 978-90-6809-431-2, Euro 30,00

389 M P HIJMA From river valley to estuary; The early-mid Holocene transgression of the Rhine-Meuse valley, The Netherlands -- Utrecht 2009: Knag/Faculteit Geowetenschappen Universiteit Utrecht. ISBN 978-90-6809-432-9, Euro 25,00